

ECOLOGICAL AND EVOLUTIONARY IMPLICATIONS OF SHAPE DURING POPULATION EXPANSION

Submitted by

Christopher Lee Coles

to the University of Exeter as a thesis for the degree of

Doctor of Philosophy in Biological Sciences

January 2015

This thesis is available for library use on the understanding that it is copyright material and that no quotation from the thesis may be published without proper acknowledgement.

I certify that all material in this thesis which is not my own work has been identified and that no material has previously been submitted and approved for the award of a degree by this or any other University.

Signature:

In loving memory of
Laura Joan Coles

Abstract

The spatial spread of populations is one of the most visible and fundamental processes in population and community ecology. Due to the potential negative impacts of spatial spread of invasive populations, there has been intensive research into understanding the drivers of ecological spread, predicting spatial dynamics, and finding management strategies that best constrain or control population expansion. However, understanding the spread of populations has proved to be a formidable task and our ability to accurately predict the spread of these populations has to date been limited. Microbial populations, during their spread across agar plate environments, can exhibit a wide array of spatial patterns, ranging from relatively circular patterns to highly irregular, fractal-like patterns. Work analysing these patterns of spread has mainly focused on the underlying mechanistic processes responsible for these patterns, with relatively little investigation into the ecological and evolutionary drivers of these patterns. With the increased recognition of the links between microbial and macrobial species, it is possible that many of the ecological/evolutionary mechanisms responsible for these patterns of spread at a microbial level extrapolate to the spatial spread of populations in general.

Through an interdisciplinary approach, combining empirical, computational and analytical methods, the principal aim of this thesis was to investigate the ecological and evolutionary basis of microbial spatial dynamics. The first section of this thesis utilises the *Pseudomonas* microbial model system to show that the rate of microbial spatial spread across agar plate surfaces is affected by both intrinsic and extrinsic factors, thereby causing the exhibited rates of spread to deviate from the predictions made by the classical models in spatial ecology. We then show the spatial dynamics of microbial spread depends on important environmental factors, specifically environmental viscosity and food availability and that these spatial dynamics (particularly the shape of spread) has conflicting impacts on individual- and group-level fitness. From this, we used a geometric framework representing the frontier of a population, combined with an individual based model, to illustrate how individual-level competition along the leading edge of the population, driven by geometric factors and combined with simple life-history rules, can lead to patterns of population spread reminiscent of those produced by natural biofilms. The thesis finishes by establishing that the

spatial pattern of spread is not seemingly amenable to artificial selection, although based on other results in this thesis, we believe it remains likely that the patterns of spatial spread and the strategies responsible for them have evolved over time and will continue to evolve. Combined, the results of this thesis show that the array of evolutionary factors not accounted for by the simple ecological models used to help manage invasive species will often cause these models to fail when attempting to accurately predict spatial spread.

Acknowledgements

First, I would like to thank my supervisors Dave and Stuart for their unwavering support and guidance throughout the course of my PhD. Stuart first introduced me to mathematical ecology in my undergraduate degree and had enough confidence in me to recommend me for the PhD. Dave took me on and helped mould me from a mathematician into a hybrid mathematician/ecologist. Their support has managed to keep my spirits up, especially when I was my lowest. Without their enthusiasm, this thesis would surely have faltered and for that, I am deeply indebted.

I have made many friends during my time in Falmouth. In particular, I would like to thank Dom and Lou, who were great housemates and helped fuel a MasterChef addiction; Jenni and Neil, for their invitations to the pub and Barry Pepper/Rock films. I would also like to mention Katy and Sally for their support during the years.

Further thanks must go to my friends from further afield. To Rich and Francesca, thanks for the tea, biscuits and general good company. Donna and Keith, thanks for letting me be your 'adopted son', you've helped so much over these past few years and your invitations to spend Christmases at yours have been a treat. It has been great to meet the Vinecombe clan! May there be many more nights of Trivial Pursuit and Uno! From my Undergrad days, Jason you have been great over the years, distracting me from my thesis when I have almost certainly needed it. Mark and Sam, our NFL talk should be on the radio!

Of course, my thanks also go to my Dad and Theresa, both of whom have been influential on this thesis. I am happy that our bond has been repaired over the past few years and I hope it will continue to remain strong. Last of all, I would like to thank my Mum, to whom this thesis is dedicated. To lose you has hurt more than words can say, but I am so fortunate you were my mum. Your constant love and support carried me through to heights I do not think anyone ever expected. I am so sorry you could not be here to see it!

Contents

Chapter 1	General Introduction and Literature Review: The spread of species – Why is the rate of spread not always constant?	14
Chapter 2	The spatial dynamics of biological invasions: when and why do model systems defy model predictions?	61
Chapter 3	How does food and environmental viscosity affect the pattern of invasive microbial spread	95
Chapter 4	How does the geometry of the microbial colony affect the multi-level selection of social behaviour?	112
Chapter 5	Games with frontiers – Part 1: Competition intensifies as invasion waves expand	139
Chapter 6	Games with frontiers – Part 2: Dispersal games along an invasion front	151
Chapter 7	Games with frontiers – Part 3: An Individual Based Modelling Approach	178
Chapter 8	Getting into shape: Can the shape of spatial spread be selected for?	219
Chapter 9	General discussion	241
Appendix A	Image analysis protocol used in Chapter 2	264
Appendix B	Sensitivity analysis of numerical model used in Chapter 4	266
Appendix C	Calculating the overlap between two circles	271
Appendix D	Calculating the overlap between three circles	276
Appendix E	Calculate the asymptotic fitness of individuals along edge of a circular population	281
Appendix F	Proof of values in table 6.2	287
Appendix G	Collision detection algorithm used in IBM in Chapter 7	292
Appendix H	Sensitivity analysis of IBM model used in Chapter 7	294
Appendix I	Classification algorithm/criteria used in Chapter 7	301
	References	305

List of tables and figures

Chapter 1

Figure 1.1	The three phases during the spatial spread of a population	19
Figure 1.2	The three classifications for the rate of spread of a species	20
Figure 1.3	An illustration of stratified diffusion	23
Figure 1.4	The predicted propagation of a substance through a one-dimensional environment according to Fisher's equation	31
Figure 1.5	Gaussian and fat-tailed dispersal kernels	34
Figure 1.6	<i>Pseudomonas aeruginosa</i> grown on three different agar plates containing KB agar	51
Figure 1.7	The urban spread of London between the 17 th and 20 th century	53
Figure 1.8	The growth of the bacterium <i>Escherichia coli</i> and the predictive results of reaction-diffusion models	55
Figure 1.9	The growth of the bacterium <i>Paenibacillus dendritiformis</i> and the predictive results of reaction-diffusion models	56

Table 1.1	The four types of social behaviour defined by Hamilton	45
------------------	--	-----------

Chapter 2

Figure 2.1	The radial range of muskrat spread increases linearly with time during its invasion of central Europe	63
Figure 2.2	The areas of the static microcosm from which samples were taken in order to isolate WS and SM mutants	68
Figure 2.3	An overview of the experimental design	69
Figure 2.4	<i>A Pseudomonas fluorescens</i> WS biofilm exhibiting a non-circular pattern of spread and its resultant binary image after the process of image analysis	70
Figure 2.5	The three categories used to measure the rate of spread of each colony	72
Figure 2.6	The change of radial area against time for each colony categorised according to morphology and the agar concentration of the environment.	75
Figure 2.7	The average rate of dispersal for each combination of agar concentration and morphology	76
Figure 2.8	Reaction norm graph showing the extrinsic effect of agar concentration on the average rate of dispersal for each genotype	77
Figure 2.9	The probability of a significantly accelerating spread for the WS and SM morphologies in 0.5%, 0.75% and 1% agar concentrations (± 1 SE).	78
Figure 2.10	The aggregated circularity of each genotype through time on the three different agar environments.	79
Figure 2.11	The change in circularity between the start point and end point of each time series.	80
Figure 2.12	A WS morphology on 50% agar at hours 12, 18 and 30	84

Table 2.1	The overall proportion of the colonies exhibiting a constant,	74
------------------	---	-----------

significantly accelerating or significantly decelerating rates of spread

Chapter 3

Figure 3.1	The average area of spread across all ten <i>Pseudomonas aeruginosa</i> replicates for each of the environments tested.	102
Figure 3.2	The spatial spread after 24 hours of <i>Pseudomonas aeruginosa</i> in each of the 15 different environments.	103
Figure 3.3	The spatial spread after 48 hours of <i>Pseudomonas aeruginosa</i> in each of the 15 different environments.	104
Figure 3.4	The proportion of the ten inoculated <i>Pseudomonas aeruginosa</i> colonies exhibiting at least one tendrils for each environment treatment at hours 24, 30 and 48.	105
Figure 3.5	The average number of tendrils exhibited by the ten <i>Pseudomonas aeruginosa</i> colonies grown in each environment treatment at hours 24, 30 and 48.	106
Figure 3.6	The average length of tendrils exhibited by <i>Pseudomonas aeruginosa</i> colonies grown in each environment treatment at hours 24, 30 and 48.	107

Chapter 4

Figure 4.1	A <i>Pseudomonas aeruginosa</i> strain PAO1 colony grown on 0.5% KB agar with a distinctive siderophore halo	114
Figure 4.2	Plot showing the shapes produced by the geometric model and its siderophore halo.	120
Figure 4.3	The background environments based on the matern covariance function.	121
Figure 4.4	The area covered by a colony shape, a colony shape combined with it's siderophore halo or the siderophore halo for the scenarios where there is either a matching area and matching perimeter	125
Figure 4.5	The difference in size between a colony, which exhibits tendrils, and a circular colony with matching perimeter.	127
Figure 4.6	Diagram of the setup used to calculate the approximate optimum number of tendrils.	127
Figure 4.7	The resources acquired by a colony shape, a colony shape combined with it's siderophore halo or the siderophore halo for the scenarios where there is either a matching area and matching perimeter and the colony is situated on a randomly generated background.	129

Table 4.1	The parameters used for shapes in both the matching area and matching perimeter scenario.	119
Table 4.2	The parameters used in the auto-correlated environments	122

Chapter 5

Figure 5.1	An illustration of three neighbouring individuals situated on the leading edge of the population such that they intersect.	144
Figure 5.2	As the radius of the population increases, the curvature of the leading edge of the population tends towards zero.	147
Figure 5.3	The effect of the radius (curvature) of the main population on the fitness of a focal individual neighbored by two individuals on the edge of the population.	149
Figure 5.4	The effect of the colonies radius on the fitness of a non-dispersing individual neighbored by non-dispersing individuals(case 1) on the edge of the population.	149

Table 5.1	The parameters and values used in this chapter	147
------------------	--	------------

Chapter 6

Figure 6.1	The six cases possible for three neighbouring individuals situated on the leading edge of the population.	158
Figure 6.2	Illustration of the overlaps between neighbouring individuals	160
Figure 6.3	How the dispersal distance of those individuals actively dispersing in each of the six cases affect the fitness of the focal individual when the cost of dispersal is set to zero.	161
Figure 6.4	How the dispersal distance of those individuals actively dispersing in each of the six cases affect the fitness of the focal individual when there exists a cost of dispersal.	163
Figure 6.5	The effect of the main population radius on the distance an actively dispersing individual has to move before a non-dispersing neighbour gains an advantage and the movement an individual must move in order to achieve optimum movement based on the dispersal cost.	164
Figure 6.6	The resultant social behaviour between an actively dispersing individual and a neighbouring non-actively dispersing individual.	165
Figure 6.7	The resultant interaction between two neighbouring dispersing individuals whom can move distinct dispersal distances for radius = 0.025.	169
Figure 6.8	The resultant interaction between two neighbouring dispersing individuals whom can move distinct dispersal distances for radius = 0.5.	170

Table 6.1	The parameters and values used as part of this study	157
------------------	--	------------

Table 6.2	The movement required by an actively dispersing individual to eliminate overlap with neighbouring individuals in the various scenarios detailed	161
------------------	---	------------

Chapter 7

Figure 7.1	In the figure, the region representing an individual is shown by the dark grey circle whilst the circle of influence is shown by the light grey circle.	185
-------------------	---	------------

Figure 7.2	The life history process each individual in the model goes through for each iterative time step	186
Figure 7.3	An illustration of how the direction of movement by the focal individual	186
Figure 7.4	An illustration of the simplified 'hinge' calculation vs. the mathematical calculation	192
Figure 7.5	A flowchart of the calculations involved for each individual's energy budget during each time step.	196
Figure 7.6	The results of the null model	198
Figure 7.7	The proportion of actively dispersing individuals versus non-actively dispersing individuals for the Mostly Dispersing, Irregular, Small/Large Tendrils, Circle consisting of non-disperser cases in table 3 for $p(\text{mutate})=0.1$.	204
Figure 7.8	A colour code chart of the classifications for the model	205
Figure 7.9	The derived fitness measurement for actively and non-actively dispersing individuals at different costs of dispersal for $p(\text{mutate})=0.1$. Also shown is the total food acquired by individuals along the leading edge of the colony at 1000 iterations.	206
Figure 7.10	A close up view of the tip of a tendril	207
Figure 7.11	Pictures of <i>Pseudomonas aeruginosa</i> colonies spreading on an agar plate surface.	209

Table 7.1	Overview of the parameters and default values of the parameters utilised.	185
Table 7.2	Describing the advantages and disadvantages of both dispersal phenotypes within the system	190
Table 7.3	The first part of the categorisation for those scenarios involving mutation.	199
Table 7.4	The second part of the categorisation for those scenarios involving mutation.	201

Chapter 8

Figure 8.1	An illustration of the sampling region for experiment 1	224
Figure 8.2	A diagram of the experimental design used in experiment 1.	225
Figure 8.3	An illustration of the sampling region for experiment 2	227
Figure 8.4	A diagram of the experimental design used in experiment 2.	228
Figure 8.5	The circularity and tendril score measurement for each selection line through each selection point.	230
Figure 8.6	The results of the assays taken after 10 and 20 selection points for both the circularity and tendril score measurements.	231
Figure 8.7	The circularity and tendril score measurements at each selection point for those colonies sampled from the centre.	232
Figure 8.8	The circularity and tendril score measurements at each selection point for those colonies sampled from one of the knuckles of the colony.	233
Figure 8.9	The circularity and tendril score measurements at each	234

	selection point for those colonies sampled from one of the tendril tips of the colony.	
Figure 8.10	The circularity and tendril score measurements at each selection point for those colonies sampled from one of the webbing sites in-between tendrils of the colony.	235
Figure 8.11	The circularity and tendril score measurements from the assay of the colonies after 10 selections points.	236

Appendix A

Table A.1	A description of the six different thresholds used in the image-analysis algorithm.	265
------------------	---	------------

Appendix B

Figure B.1	These plots show the effect of the halo length parameter upon the various fitness measurements used in Chapter 4.	267
Figure B.2	These plots show the effect of the tendril length parameter upon the various fitness measurements used in Chapter 4.	269
Figure B.3	These plots show the effect of the inner circle radius parameter upon the various fitness measurements used in Chapter 4.	270

Table B.1	The parameters used in this appendix for shapes in both the matching area and matching perimeter scenarios	266
------------------	--	------------

Appendix C

Figure C.1	An illustration of two circles situated a set distance from each other such that they overlap	271
Figure C.2	Diagram defining the parameters of the calculation between two overlapping circles	272
Figure C.3	Another diagram defining the parameters of the calculation between two overlapping circles	274

Appendix D

Figure D.1	An illustration of three circles situated a set distance from each other such that they overlap	276
Figure D.2	A diagram defining the parameters of the area calculation for a circular triangle	277
Figure D.3	A situation with 3 overlapping circles which do not form a compatible circular triangle	279

Appendix E

Figure E.1	An illustration that for 3 individuals along the leading edge of the population, the leading edge connecting their origins can be approximated as a straight line	282
Figure E.2	An illustration of the chords and intersection points for the overlapping area between tree circles.	284

Appendix F

Figure F.1	The main population with two individuals situated along the leading edge	287
-------------------	--	------------

Appendix H

Figure H.1	The total number of individuals, the number of non-actively and the number actively dispersing individuals situated along leading edge after 1000 iterations for various dispersal cost coefficients and initial parameter sets.	295
Figure H.2	Same as figure H.1 but for the initial population radius parameter value used in Chapter 7.	297
Figure H.3	Same as figure H.1 but for the parameter representing the distance moved by an active disperser.	299
Figure H.4	Same as figure H.1 but for the system parameter representing the distance moved by a non- active disperser.	300
Figure H.5	Same as figure H.1 but for the allowed overlap parameter	301

Table H.1	The parameters used in this appendix to examine the sensitivity of results produced by the individual based model shown in Chapter 7 on initial parameters	294
------------------	--	------------

Appendix I

Table I.1	The algorithm used for each classification of pattern produced by the model	303
------------------	---	------------

Author's Declaration

All chapters in this thesis were written by Christopher Lee Coles under the guidance and supervision of David Hodgson and Stuart Townley. C. L. Coles carried out all lab work, coding and statistical analysis unless otherwise stated below. This thesis was made possible by funding from the Biotechnology & Biological Sciences Research Council (BBSRC). All work was conducted at the Centre for Ecology and Conservation at the University of Exeter based in Cornwall. Individual contributions to this thesis are detailed below for each chapter.

Chapter 2

A pilot experiment for this chapter was part of Aoife Parsons' Msc project in 2011; this project also had the same title as Chapter 2. Results of this experiment helped to suggest improvements to our original experimental design. *Pseudomonas fluorescens* strain SBW25 originally supplied by Angus Buckling from his lab at the University of Oxford. Laboratory training was supplied by Michelle Hares. A. Buckling, M. Hares and D. J. Hodgson offered advice to help solve some of the initial set-up problems. D.J. Hodgson assisted with the statistical analysis and experimental design in the original Msc project.

Chapter 3

Strains of *Pseudomonas aeruginosa* PAO1 were originally supplied by A. Buckling from the lab at University of Oxford.

Chapter 4

D.J Hodgson and C. L. Coles co-created the initial foundation code in R from which this study was built upon.

Chapter 5/6

S.B. Townley helped to conceive the initial geometric observations of microbial growth from which the mathematical formulation was built upon

Chapter 7

D. J. Hodgson provided some assistance with the formulation of the model.

Chapter 8

D.J. Hodgson assisted with the statistical analysis and experimental design.

It is noted that in the cases where the term 'we' is used, the research was carried out by C. L. Coles unless otherwise stated here.

Chapter 1 – Literature review

General Introduction

The spatial spread of a population is one of the most visible and central factors in ecology. The spread of a population through space is a key component of a population's life history strategy (Kokko and Lopez-Sepulcre, 2006), affecting characteristics of not only the population itself but the characteristics of those populations it interacts with (Comins et al., 1980). Indeed, the spatial spread of a population of a given species can have a significant effect upon the functioning of ecosystems, potentially leading to various negative outcomes. These outcomes include the destruction of habitats (Mack et al., 2000), the extinction of native species (Clavero and Garcia-Berthou, 2005) and various socio-economic problems (Pimentel et al., 2005). Consequently, the potential repercussions of spatial spread have received considerable interest from researchers and governments alike, with one of the ultimate aims being to understand and manage the spread of various species (Puth and Post, 2005). While the study of a species' movement is one of the most accessible areas of ecology, our understanding of how species spread through environments is still remarkably in its infancy (Holt, 2005).

Classically, researchers have studied the spatial spread of species using an interdisciplinary approach, in which empirical data from field studies and predictive modelling simulations have been analysed to help us to understand the processes underpinning the movement of a species across a landscape. However, in this classical theory, there is a growing disconnect between empirical evidence and modelling approaches (Kot et al., 1996). For example, while the classical theory of spatial spread suggests simple local diffusion processes (based on Fickian diffusion) as the key determinant behind the spatial spread of a species (Skellam, 1951), recent empirical evidence has increasingly showed this is not always the case (Phillips et al., 2006), with factors such as kin competition (Travis et al., 2009), resource limitation (Lubina and Levin, 1988) and climate variability (Urban et al., 2008) causing spread to deviate from Fickian diffusion. Such disconnects between theory and evidence can be critical, with the constant rates of spread predicted by Fickian diffusion shown to be erroneous for a number of invasive species (Hastings et al., 2005).

Therefore, while the process of spatial spread was once considered well understood, extensive research is now required to improve our understanding of the underlying intrinsic and extrinsic mechanisms in order to eliminate the disconnect between empirical evidence and modelling predictions.

While it is increasingly acknowledged that the spread of a species does not always follow the local diffusion processes described in the classical literature, our understanding of how intrinsic and extrinsic factors affect the spread of a species is hampered by the difficulty of conducting empirical case studies in the field (Verhulst et al., 1997). Current methods tracking the spread of a population can often fail to detect when individuals undergo long-distance dispersal events, subsequently us to underestimate the true rate of spread (Kokko and Lopez-Sepulcre, 2006). Therefore, in order to understand the underpinning processes driving spatial spread, new empirical studies utilising novel techniques and model systems are required. Such knowledge would help to improve the reliability of predictive models and therefore help us to manage the spread of various populations.

Throughout this thesis, we utilise an interdisciplinary approach based upon the microbial model system, to investigate the factors and processes underpinning the spatial dynamics of microbial spread across agar plate surfaces and the spread of populations in general. This is done not only with the aim of answering questions relating to the spatial ecology of microbial populations, but also with the aim of establishing microbes as an ideal model system for answering fundamental questions in spatial ecology. The thesis begins by discussing what the literature currently says about the spread of species through space. Specifically, this chapter focuses on the rate of spread and investigates how it can deviate from the constant rate of spread prediction made by the classical models of spatial spread. Following this, we discuss why understanding the processes behind the rate of spread is critical for the preservation of endangered species, before introducing the microbial model system and discussing why it is ideally suited for studies of spatial spread. After reviewing the known processes responsible for the spatial spread of bacteria, this chapter finishes with an outline of the thesis structure.

The spread of populations: Why is the rate of spread not always constant?

Dispersing across space is a natural process for members of a population, enabling individuals to escape density/environment-dependent factors associated with negative fitness consequences such as scarce food availability, competition and habitat loss. Subsequently, while dispersal can be a risky strategy, it offers a way to increase the long-term persistence of the population (Wenny, 2001, Kokko and Lopez-Sepulcre, 2006). With evidence of rapid climate change increasing the fragmentation and unpredictability of environments, the resulting increased likelihood of dispersal means understanding the processes behind dispersal and population spread is a critical topic for the study of invasive species (Pearson and Dawson, 2005).

There are three phases during the spread of a species (also termed invasion). These are establishment in the new habitat, range expansion and habitat saturation (Shigesada et al., 1995, Shigesada, 1997). Other phases may exist (Ricklefs, 2005, Reise et al., 2006) but these three stages are widely acknowledged to be the key stages of spread.

1. Establishment in the new habitat

The establishment phase begins once initial dispersal of a non-native species into its new patch has finished. When a species is introduced to an environment it has previously not colonised, the relatively low population density of the species during its introduction means it is at the greatest risk of extinction during this phase (Purvis et al., 2000). The pronounced effect of stochastic events upon the persistence of the population, combined with other factors such as resource availability, competition with native species and Allee effects means that the population initially faces an uphill struggle to establish itself in their new habitat (Taylor and Hastings, 2005, Liebhold and Tobin, 2008). As such, successful establishment in a new environment is reliant upon having the right combination of life history characteristics (Moyle and Marchetti, 2006). Our understanding of which combinations of these parameters provide the recipe for successful establishment is restricted due to limited number of available studies from which these parameters are measured (Kolar and Lodge, 2001). Moreover, the studies which do measure these characteristics, often only account for those invasive populations that successfully establish themselves in

an environment, ignoring those which fail (Versteirt et al., 2012). Consequently, while characteristics such as reproduction rate, body mass, reproduction strategy, time of maturation and initial starting density have all been found to significantly affect the success of specific populations, we do not know to what degree these characteristics improve the persistence of invasive populations overall (Kolar and Lodge, 2001, Williamson and Fitter, 1996). Better understanding of which life history traits favour invasive spread would enable us to ascertain which habitats, resources and conditions are least suitable for an invasive species thereby helping us eliminate invasive species while they are at their most vulnerable (Mack et al., 2000).

Because of the lower population density during the establishment phase, there is thought to be less pressure on the species to disperse (Lockwood et al., 2005). Consequently, the rate of expansion is usually slower than in the range expansion phase, giving rise to an apparent lag phase (Arim et al., 2006). The appearance of lag phases can be problematic in predictive models as they may occur during any of the three stages of spatial spread and can last for extraordinary lengths of time, disguising which stage the spread of the species is actually in (Crooks, 2005). However, some researchers believe the appearance of the establishment phase may be an anomaly arising due to the difficulty of detecting the maximum extent of a species' range (Kokko and Lopez-Sepulcre, 2006, Hastings et al., 2005, Carey, 1991). Subsequently, there is a requirement for better tracking and monitoring approaches to capture the spread of a population, in order to establish the causes and appearances of lag phases in populations.

2. Range expansion

It is assumed that once the density of the species has reached a sufficient threshold, depending on the characteristics of the population and its interactions with the surrounding ecosystem, the species may either remain relatively localised or begin to rapidly spread through the environment in order to prosper (Shigesada et al., 1995, Shigesada, 1997). This phase of rapid colonisation is called the range expansion phase. It is during this phase that a species is considered invasive if it begins to colonise space it has previously never occupied (Levine, 2000). Researchers classify the rate (note that we use the terminology rate of spread, more accurately this is the radial rate of spread)

at which the invasive population colonises the surrounding un-colonised environment during the range expansion phase, into three groups (figure 1.2).

1 – A constant rate of spread:

Empirical evidence suggests this is the most common rate of spread exhibited by invasive populations. Researchers believe that a constant rate of spread arises due to the combined effect of population growth and localised diffusion. Examples include the expansion of the sea otter in California (Lubina and Levin, 1988), muskrats in central Europe (Skellam, 1951, Andow et al., 1990) and the invasion of the bank vole across Ireland (White et al., 2012).

2 – A biphasic rate of spread:

A biphasic rate of spread occurs when populations appear to exhibit two distinct constant rates of spread sequentially. Examples include the spread of the European starling (Hengeveld, 1989) and the house sparrow (Okubo, 1988.) across the United States.

3 – An accelerating rate of spread:

A population may also exhibit a non-constant rate of spread. Typically these non-constant rates of spread are accelerating rates of spread (i.e. the rate of spread increases through time), although they may also exhibit a decelerating rate of spread. Examples include the introduction of the cane toad into north east Australia (Urban et al., 2008), the rice water weevil (Andow et al., 1993, Andow et al., 1990), and the invasion of house finches throughout North America (Veit and Lewis, 1996).

The rate of range expansion is affected by a range of biological constraints stemming from both extrinsic and intrinsic factors (Arim et al., 2006). However, there is no general consensus on which key factors determine the exhibited rate of spread classification of a population (Grosholz and Ruiz, 1996).

3. Habitat saturation

The range expansion phase continues until the population eventually covers all of the colonisable area. At this point the radial range of the spread plateaus and no further expansion can occur unless other suitable, yet to be colonized, habitat becomes available.

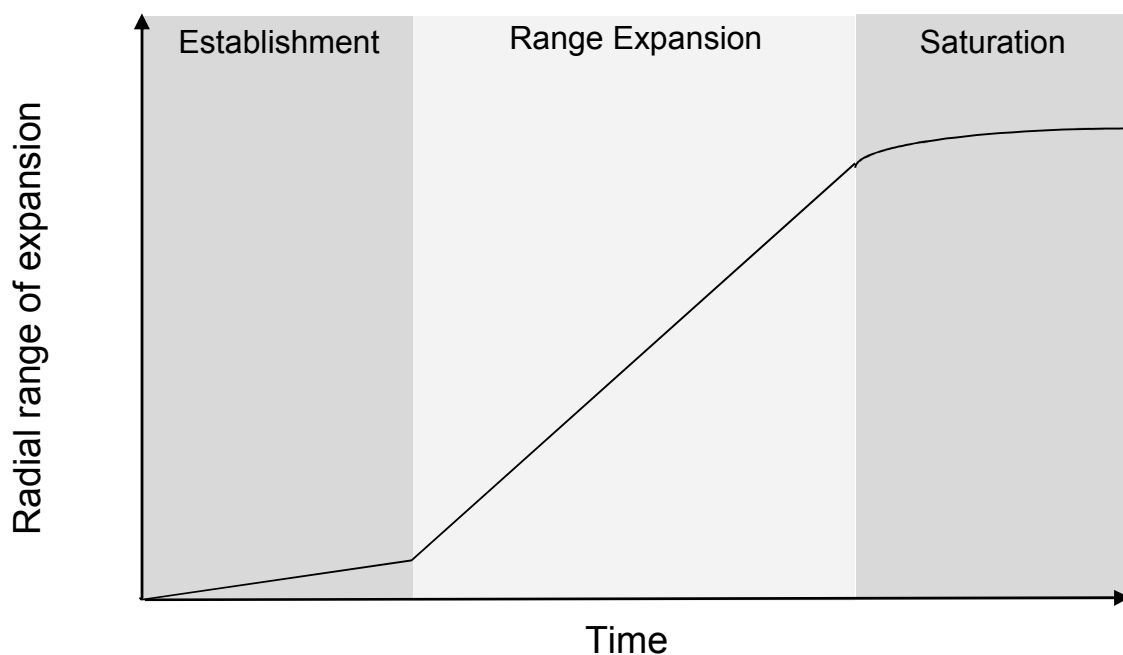


Figure 1.1: There are three phases during the spatial spread of a population. Initially populations start at low densities and require time to establish themselves in the environment, resulting in an apparent time lag. Once density has reached a threshold, the population can then rapidly colonise the surrounding environment. This phase continues until all unoccupied space suitable for the species has been colonised, at which point the radial range of the species plateaus. Note we assume a constant rate of spread in this figure during the range expansion phase.

Of these phases, there is a higher likelihood of manipulating the eventual outcome of the spread of a species in the establishment and range expansion phases, as the sooner conservation management strategies are implemented, the more effective they are (Mack et al., 2000). However, due to difficulties detecting the establishment phase empirically, conservation and management prevention strategies have typically focused on the range expansion phase (Kokko and Lopez-Sepulcre, 2006).

Note that we have defined three different phases of the rate of spread exhibited by a population. However, classical studies investigating the rate of a species spread have typically predicted the rate of spatial spread to be constant through time. This was based on the assumption that all individuals move according to a normal distribution and have an equal probability of dispersing in every direction (Skellam, 1951). While a number of empirical studies support the prediction of constant rate of spread, an increasing number of empirical studies have found non-constant rates of spread. Of particular note are those empirical cases classified as having an accelerating rate of spread through time. The next

section discusses some of the suggested theories for why the spread of a population might accelerate through time.

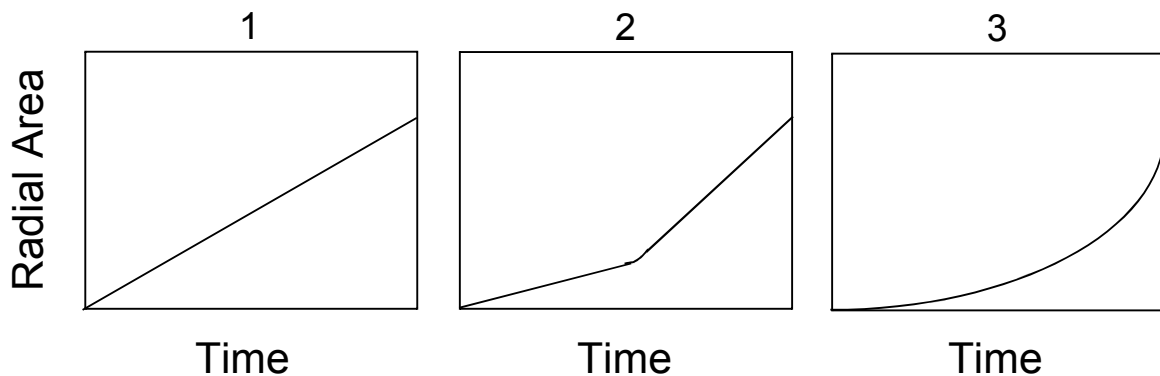


Figure 1.2: The three classifications for the rate of spread of a species: (1) a constant rate of rate, (2) a biphasic rate of spread and (3) an accelerating rate of spread.

Why are rates of spread not always constant?

Broadly, there are three proposed reasons as to why populations exhibit an accelerating (or non-constant) rate of spread during the range expansion phase. These are either effects arising because of ecological factors, evolutionary adaptations of dispersal mechanisms or the impact of human activity.

Ecological mechanisms

The rate at which a population spreads during the range expansion phase is thought to depend on interactions between individuals within the population and interactions outside of the population, either with individuals of other populations or with the local environment (Andow et al., 1990, Grosholz and Ruiz, 1996, Phillips et al., 2006, Urban et al., 2008, White et al., 2012). An example illustrating this can be seen in studies investigating the effect of climate change upon the rate of spread (Walther et al., 2009). Climate change can alter the local environment in such a way that it benefits the fitness of the spreading invasive population, possibly enhancing the competitive ability of invasive individuals against individuals of other populations (Walther et al., 2009). Moreover, changes to the landscape of the environment can create corridors that allow invasive species to reach other suitable habitats (Walther et al., 2009). These can affect the interactions individuals of one population have with individuals of other populations and is thought to increase the rate of spatial spread for the invasive population (Walther et al., 2009). Other ecological factors known to affect the interactions behind the rate of spread include allee

effects and temporal variation in dispersal rates (Perkins et al., 2013, Veit and Lewis, 1996, Ellner and Schreiber, 2012), highlighting that both intrinsic and extrinsic factors can affect the rate of spatial spread.

Emergent properties of spatial spread such as stratified diffusion can also affect the exhibited rate of spread. Stratified diffusion is the result of dispersal within a population occurring via different dispersal mechanisms, each operating at different speeds. With this in mind, consider a population with individuals, which locally diffuse by one mechanism, but also contains individuals, which undergo long distance dispersal events by another mechanism. Under this scenario, the main colony increases in size by local diffusion mechanisms emanating from its centre, while those individuals that undergo long distance dispersal events into unoccupied territory can begin to form a centre of a new colony, independent of the original colony (figure 1.3). The new colony will then begin to spread from this new focal point by the same local diffusion processes as the original colony, thereby increasing the possible area the population can spread into at each time step (Shigesada et al., 1995, Shigesada, 1997).

Assuming a homogeneous environment, each of the three classifications of spread can be exhibited by the process of stratified diffusion, depending on which of the diffusion mechanisms is the main source of spread (Shigesada et al., 1995, Shigesada, 1997). For instance, when only local diffusion contributes to the spread of a population, the population exhibits a constant rate of spread, while when only long-range dispersal mechanisms contribute to the spread of a population, the population exhibits an accelerating rate of spread. More intriguing cases arise when considering how combinations of local diffusion and long distance dispersal affect the rate of spread. The population can exhibit both biphasic and accelerating rates of spread, depending on the frequency and magnitude of long distance dispersal events. These results are consistent when dispersal rates are either constant or heterogeneous amongst individuals (Yamamura, 2002).

The process of stratified diffusion relies on the assumption that individuals undergo long distance dispersal events. This assumption is increasingly being verified, with empirical studies often showing the dispersal kernel of individuals (the probability density function of how far an individual travels in one time step)

is best fitted by leptokurtic functions, which incorporate long distance dispersal events (Chapman et al., 2007, Vinatier et al., 2011, Ronce, 2007). While it is difficult to verify the presence of stratified diffusion in empirical studies due to the relatively low resolution of current data capture methods, studies are increasingly finding evidence for its existence (Ciosi et al., 2011). Consequently, we must be aware of the effect ecological mechanisms can have upon the rate of spread.

Evolutionary mechanisms

The process of natural selection (Darwin, 1859) is considered the main driver behind the diversity of traits found within a population. However, emergent evolutionary properties arising from the spatial spread of a population may also play a significant part in a process known as spatial sorting (Travis et al., 2009, Shine et al., 2011a, Travis and Dytham, 2002). In a population recently introduced to a new environment, there is likely to be variation in the dispersal ability amongst individuals. This variation may arise from changes in multiple phenotypic traits e.g. changes in the speed of dispersal or a reduced investment in processes, which have a trade-off against dispersal (Shine et al., 2011a, Lee and Klasing, 2004). As individuals in the population disperse from the origin of their introduction, their dispersal ability sorts them through space, with those best adapted to dispersal occupying the leading edge of the population, and poorer dispersers occupying the intermediate space behind the leading edge. Therefore, individuals at the leading edge of the population are restricted in their choice of mate, as in general, the individuals surrounding them will also have a relatively strong dispersal ability compared to the average individual in the population (Cwynar and Macdonald, 1987). Consequently, dispersers along the leading edge will tend to mate with other dispersers, potentially resulting in offspring with even higher mean dispersal rate compared to the ancestral generation (Cwynar and Macdonald, 1987). Furthermore, lower population density at the range edge allows those at the range edge more room to reproduce. Combined, this creates a positive feedback at the leading edge of the range expansion, possibly resulting in an accelerating rate of spread because of the evolution of increased dispersal along the leading edge, across generations (Travis et al., 2009).

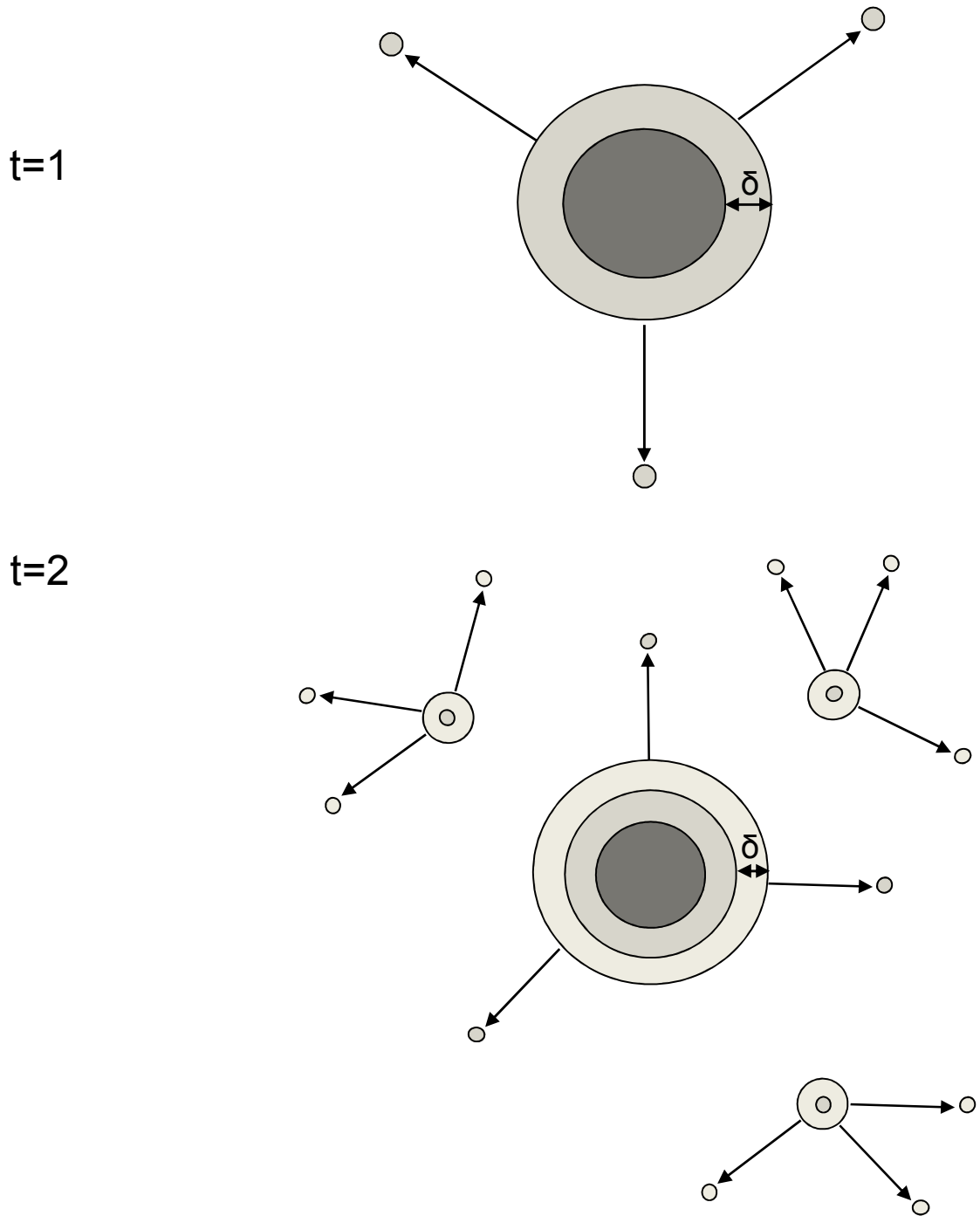


Figure 1.3: An illustration of stratified diffusion. At each localised colony origin within the population, dispersal can occur via local diffusion, causing the circular spread of the localised colony to increase by radius δ . Those individuals within these localised colonies, which undergo long distance dispersal events (as shown by each of the directed arrows), can form new origins from which local diffusion and future long distance dispersal events can emanate from. Parameters of such a mechanism can dictate the rate of spread exhibited by a population.

The process of spatial sorting is influential upon the development of dispersal in many organisms. Examples include birds (Berthouly-Salazar et al., 2012), insects (Leotard et al., 2009) and plants (Cwynar and Macdonald, 1987) amongst others. However, it is unknown whether spatial sorting necessarily increases the fitness of individuals in the population. For instance, it is thought spatial sorting has caused cane toads on the invasion front in northeast Australia to develop longer legs, enabling them to disperse 3-10 times faster than its originally introduced ancestor (Phillips et al., 2008, Alford et al., 2009). However, the development of this dispersal mechanism has resulted in a potential decrease in fitness, with toads exhibiting an increased onset of spinal arthritis (Brown et al., 2007, Shilton et al., 2008) and consequently higher mortality (Phillips et al., 2008). This is in contrast to natural selection, which favours individuals with a higher fitness. It is important to note here that spatial sorting is not a replacement for the theory of natural selection, but an additional process which affects a limited range of characteristics (i.e. dispersal) compared to the theory of natural selection (Shine et al., 2011a).

Spatial sorting is thought to occur over extremely fast time scales and can lead to the rapid evolution of both life-history traits and dispersal traits, with an apparent interaction between the two (Perkins et al., 2013). Furthermore, theoretical approaches have shown that spatial sorting does not require extreme selection and heritability parameters for it to arise (Travis et al., 2009, Perkins et al., 2013, Perkins, 2012). It is therefore a convincing explanation for why the rate of a species spread accelerates (Phillips et al., 2008). However, there is yet to be an established unequivocal link between empirical studies and theory due to the difficulty of separating the effects of natural selection from those of spatial selection (Shine et al., 2011a).

Human Impact

The rapid growth of the human species has affected ecosystems worldwide and has led to a massive displacement of populations. Processes associated with humans such as the development of agricultural processes, deforestation and building construction has resulted in habitat fragmentation, a decline in biological diversity and irreversible climate change (Ramankutty and Foley, 1999, Tilman et al., 2001, Malmqvist and Rundle, 2002, Hughes et al., 2003). Similarly, these processes have affected the dispersal of populations, leading to

an increasing number of individuals within populations undergoing long distance dispersal events (Tilman and Lehman, 2001). Indeed, the development of roads between cities is one example of human impact affecting the rate of spread of a population, as the surface of the road is often easier to traverse compared to the original terrain it was built upon (Urban et al., 2008). Additionally, with global trade increasing, species have been able to spread by hitchhiking onto travelling vehicles (Urban et al., 2008). One can consider this hitchhiking as a special case of stratified diffusion, with hitchhiking individuals becoming new population origins from which a population can spread (Urban et al., 2008). Hence, human induced disturbance upon ecosystems can affect the delicate balance of species, potentially decreasing the competition faced by an invasive species during its spread into non-native habitat (Tilman, 2004). Therefore, researchers must keep the effect of human growth under scrutiny in order to protect biodiversity and prevent negative consequences such as an increase in the rate of spread of dangerous invasive populations.

It is clear we require a deeper understanding of which processes cause an invasive species to colonise environments faster than we previously expected. By developing our understanding of these processes, we can create strategies in order to help control the spread of invasive species and prevent the extinction of endangered species. The next section briefly discusses some of the reasons why we believe it is important to control the spread of invasive species, their potential impact and the methods currently used to control their spread.

Why do we want to control the spread of a species?

Invasive species are one of the major problems faced by conservation managers due to their increasing numbers posing a great risk to biodiversity worldwide (D'Antonio et al., 2004). Biodiversity is considered to be important for a number of reasons (Hooper et al., 2005). First, biodiversity is a fundamental component behind a number of ecosystem goods (e.g. foods, genetic diversity and medicine) and services (e.g. pollution breakdown, nutrient storage and protection of water resources). Secondly, there are a number of ethical reasons, as some people consider allowing the extinction of a species morally wrong. Thirdly, there are a number of cultural reasons such as scientific pursuit and our own cultural heritage. While there is some argument about a number of these

reasons (i.e. invasions by species occur naturally all the time), there is enough of a consensus to agree the conservation of biodiversity is an important issue due to its potential for negative outcomes to these factors we consider important (Hector et al., 2001). Particularly as many believe that many of these invasions are because of human related causes (Urban et al., 2008) and thus are not born of entirely natural causes. However, to date, preserving global biodiversity is proving to be a formidable challenge with the limited resources available.

The increasing recognition of the negative impact caused by invasive species has caused governments and organisations to implement a number of rules to prevent the spread of non-native species. For instance, members of the World Trade Organisation have agreed to restrict the movement of species that may pose a threat to human, animal or plant life (World Trade Organisation, 6 December 1951). However, even with the best protocols in place, completely controlling the movement of species is not always possible. If a population manages to establish itself in an environment, then we have a limited number of choices at our disposal to control the spread. Two examples discussed here are eradication control methods and biological control agents.

Conservation managers can control a population either by mechanical means (e.g. hunting), or by the use of chemicals such as pesticides. The likelihood of successful control efforts depends on the control strategy/method used and the dispersal ability of the species (Mack et al., 2000). Unfortunately, many efforts to control expanding populations often only have transient benefits, which can potentially lead to a worsening of the problem. For instance, some eradication control efforts using hunting methods may ultimately cause the population of the species to boom as a response (Stott et al., 2010), possibly leading to an increase in the resultant rate of spread. Eradication control efforts via pesticides can also be problematic, as some control studies have found that these pesticides negatively affect non-target species. Moreover, pesticides may be effective for only short periods of time, as species can evolve pesticide resistance (Hemingway et al., 2002). Subsequently, management using eradication control methods must carefully consider the impact of these methods to avoid negative consequences.

An alternative method of controlling populations is the use of biological control agents. Biological control agents are natural enemies introduced to reduce the population size of a species, particularly invasive species. Researchers choose specific biological control agents because either they are natural predators from the origin of the invasive species or they are a species with developed predation methods, which the invasive species has not encountered before. They have been successfully used as an alternative to eradication control methods (Smith, 1996). For example, the spread of alligator weed in Florida has been controlled successfully by using the alligator weed flea beetle (*Agasicles hygrophila*) thereby resulting in the elimination of pesticide use (Coombs, 2004). However, biological control agents are not always successful and can significantly affect the non-target species. For example, the introduction of the cane toad (*Bufo marinus*), an amphibian native to Central and South America, into northeast Australia was originally utilised to control and eradicate cane beetles (*Dermolepida albohirtum*) which were detrimental to sugar cane crops. This was extremely unsuccessful as it not only failed to affect the population of the cane beetle, but it has also caused widespread biodiversity loss and socio-economic damage in Australia. Consequently, while control methods can be successful, it is clear they require extensive testing before their implementation.

Invasive species that exhibit an accelerating rate of spread are the most concerning to conservation managers as it leads to a reduction in the time taken for the spread to reach the saturation phase. Researchers have proposed a variety of methods to prevent an invasion from developing an accelerating rate of spread. For instance, targeted culling of the best-adapted invaders at the frontier of invasive spread may prevent the spatial selection process from choosing those individuals who spread fastest (Sih et al. 2010). Other methods of preventing accelerating rates of spread involve targeting the environment itself. For example, (Tingley et al., 2013) used the theory behind the spread of invasive populations to create a predictive model in order to predict how the closure of several artificial water bodies to create a buffer zone might affect the spread of the invasive cane toad across Australia. Through this knowledge, conservation managers have begun to implement procedures to carry these recommendations out, in order to slow down (i.e. prevent acceleration of) the threat of the cane toad and protect populations of numerous endemic

(e.g. *Varanus panoptes rubidus*, *Acan-thophis wellsii*) and endangered (e.g. *Dasyurus hallucatus*) species (Shine, 2010, Tingley et al., 2013), thereby highlighting how the understanding of invasive spread can help conservation efforts. Indeed, the use of predictive models helps us to ascertain whether these strategies work or may in fact increase the problem. The following discusses a number of the modelling approaches used to predict the spread of species.

How do we currently model the spatial spread of populations?

Formulating ecological systems as a set of mathematical equations in the form of a model is a fundamental tool in ecology. Models allow researchers to predict the outcome of a set of assumptions theorised to suitably represent a system (Nisbet, 1998). Often the parameterisation of these models is based upon evidence from empirical studies, but their true power lies in their ability to explore theories not easily tested by empirical studies (Jackson et al., 2000). Unfortunately, due to the complexity involved, mathematics cannot define many of the processes and interactions within ecological systems. Consequently, predictive models are often approximations of the truth based upon the assumptions made about the system. As such, their true purpose is to help us understand the key factors that underpin the development of complex phenomena seen in nature. Studies modelling of spatial spread have utilised a variety of different modelling approaches. In this review, we discuss five key modelling approaches commonly used to model spatial population distributions.

Reaction-diffusion equations utilise partial differential equations to describe the spread of a population according to population growth and the laws of diffusion (Fisher, 1930, Fisher, 1937, Kolmogorov et al., 1937, Turing, 1952).

Integro-difference equations describe the spread of a population by modelling the interaction between population growth and a probability distribution function representing the movement of individuals (Kot et al., 1996).

Individual based models utilise computational algorithms to investigate how local interactions gives rise to global phenomena (Grimm, 1999).

Metapopulation models analyse the dynamics between multiple spatially explicit populations bound together by dispersal (Hanski and Gilpin, 1991).

Statistical models utilise empirical data to define relationships between parameters of the system (Nelder, 1972).

There is little to no consensus on which of these modelling approaches is best as each approach has different strengths and weaknesses (Hastings et al., 2005). The following briefly describes the strengths and weaknesses of each approach.

Reaction-Diffusion equations

Reaction-Diffusion equations have traditionally been the modelling approach used in classical spatial ecology to predict the spatial spread of a population (Skellam, 1951). Reaction-Diffusion equations utilise partial differential equations to describe how processes, such as growth and diffusive movement, affect the distribution of a population through both time and space. Their popularity stems from their ability to describe the spatial dimension of a population via the use of continuous deterministic equations, making them amenable to classical mathematical analysis (Richardson and Pyšek, 2008). While they commonly focus on the spread of a population in one dimension, under the right conditions, reaction-diffusion equations in two (or more) dimensions can generate different spatial patterns of spread. Indeed, studies often use reaction-diffusion equations in two dimensions to represent a number of biological phenomena, including the spread of forest fires and the morphogenesis of animal skin patterns (Murray, 1993, Turing, 1952, Chetehouna et al., 2004).

The reaction-diffusion approach has been developed from the system of partial differential equations proposed by Fisher and Kolmogorov (Fisher, 1937, Kolmogorov et al., 1937). The classical model used by (Fisher, 1937) and (Skellam, 1951) to describe the spread dynamics of a population through a one dimensional environment is shown by equation 1.1 (also known as the KPP-Fisher equation – we refer to this as the classical reaction-diffusion equation system):

$$\frac{\partial n}{\partial t} = f(n) + D\nabla^2 n \quad (1.1)$$

where $f(n)$, D and n represents the population growth rate, the rate of diffusion and the population density respectively. It represents the spatial spread of a population as an interaction between two components. First, a reaction component $f(n)$ representing the population growth rate and a second component $D\nabla^2 n$ representing the movement (diffusion) of the population

through the spatial domain (figure 1.4). In (Fisher, 1937), density dependent spread is represented by the logistic growth function, $f(n) = Rn \left(1 - \frac{n}{K}\right)$, where K is the carrying capacity and R is the intrinsic growth rate, while in (Skellam, 1951), density independent spread is represented by the Malthusian growth function, $f(n) = Rn$, where R is also the intrinsic growth rate.

Many reaction-diffusion equations have a travelling wave solution, i.e. a wave that moves through an environment at constant velocity while maintaining the shape of the propagation front (figure 1.4). In mathematical terms, if the solution of the system is written as $n(x, t)$, then the travelling wave solution can be written as $n(x, t) = Q(x \pm ct)$ where c is a constant representing the velocity of the spread. For equation 1.1, the predicted asymptotic rate of spread can be calculated as $2\sqrt{f'(0)D}$ (Bramson, 1983), where $f'(0)$ is the population growth rate of a species f at time 0 (i.e. the intrinsic growth rate). According to this prediction, the rate of population spread depends on simple life-history characteristics (Hastings et al., 2005). Moreover, it predicts that the radial spatial spread of the population is a linear function of time, agreeing with much of the classical empirical evidence described in (Skellam, 1951, Hastings et al., 2005). Whilst this result was widely accepted in spatial ecology models throughout the mid to late 20th century (Skellam, 1951, Andow et al., 1990, Andow et al., 1993, White et al., 2012, Clark et al., 2001), the previously discussed cases of accelerating spread (i.e. the radial spatial spread of the population as a non-linear function of time) has led to a distrust of the model predictions arising from equation 1.1 (Hastings et al., 2005).

The constant rate of spread prediction arises because of a number of implicit and explicit assumptions made during the construction of equation 1.1. First, the formulation of equation 1.1 assumes each individual moves and reproduces at the same time as one another, which may not be suitable for populations with distinct life cycles whom undergo dispersal before they reproduce during each time step e.g. migrating birds and insects (Yamamura, 2002, Levin et al., 2003). Secondly, equation 1.1 assumes the reproduction rate is homogeneous across the whole population, thereby not taking into account various extrinsic effects such as the environmental variance nor intrinsic effects such as individual

heterogeneity within the population (Clark et al., 2001, Richardson and Pyšek, 2008). Finally, it assumes a diffusive process with an underlying Gaussian dispersal kernel is a suitable representation of dispersal. Consequently, equation 1.1 does not take into account the possibility of long distance dispersal events nor the possible evolution of the dispersal kernel through time (Clark et al., 2001).

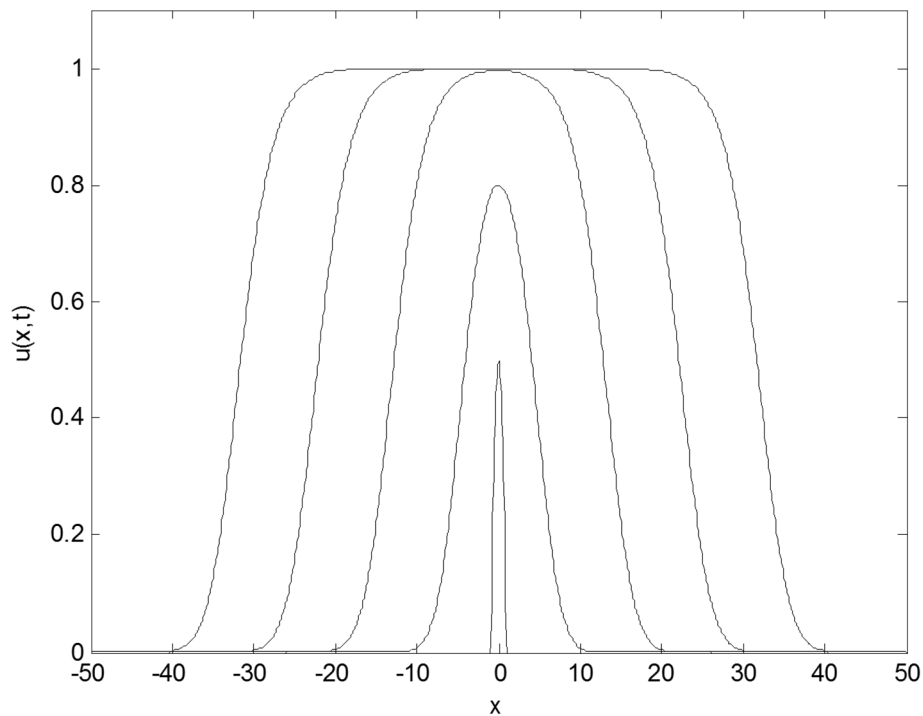


Figure 1.4: The predicted propagation of a substance through a one-dimensional environment according to equation 1.1. Note the shape of the spreading wave changes until it reaches an equilibrium point at which point the shape of spreading wave stays the same through time.

In response to the accelerating rates of spread observed in empirical studies, recent studies using reaction-diffusion models are appreciating the need to deviate from the assumptions made by the classical reaction-diffusion equations used by Skellam (1951), which lead to the prediction of the population radius increasing as a linear function of time. To date, deviations have included the incorporation of distinct dispersal phenotypes (Yamamura, 2002), stochasticity (Lewis and Pacala, 2000, Hastings et al., 2005), and the inclusion of long distance dispersal events (Roques et al., 2010, Hanert, 2012). However, many of these reaction-diffusion models have yet to be clearly linked to findings in empirical studies (Facon and David, 2006, Hastings et al., 2005) and can quickly become mathematically intractable (Higgins and Richardson, 1996).

Reaction-diffusion equations can be a useful tool to determine the mechanisms responsible for the shape of spatial spread. Indeed this is perhaps their most appealing feature to mathematicians who want to understand how patterns form in nature (Murray, 1993). An example briefly discussed later in this review is the irregular patterns of spread exhibited by microbial populations when propagated on agar plate surfaces (Woodward et al., 1995, Ben-Jacob and Levine, 2006, Golding et al., 1998). However, many of the reaction-diffusion equations focusing upon the shape of population spread do not take into account enough of the intrinsic and complex ecological characteristics behind the spread of the population, causing them to often be overly simplistic.

From this brief review, it is clear that model predictions based on the classic reaction-diffusion equation formulated by Fisher and Kolmogorov (such as the radial spread of a population being a linear function of time - equation 1.1) are also based upon overly simple assumptions. Accordingly, whilst the predictions resulting from these classic models have provided qualitatively useful results (Levin et al., 2003), models based on assumptions which deviate from those made in the construction of the classic model have since been proposed. Indeed, the incorporation of parameter stochasticity, variability in the population dynamics and long distance dispersal events into model assumptions are increasingly being considered. However, their study may be best achieved in methods other than a reaction-diffusion modeling approach (Hastings et al., 2005).

Integro-difference equations

In response to the predictions and assumptions made by the classical reaction-diffusion equations posed by Fisher and Kolmogorov (Fisher, 1937, Kolmogorov et al., 1937), an alternative approach based on discrete time integro-difference equations have been suggested (Kot 1996). For each time step, the integro-difference equation calculates the population density at a location, x , by summing all the individuals which move to location x from all possible locations, y . Similar to reaction-diffusion equations, the construction of integro-difference equations are formulated as two components. One component representing the growth rate of the species $N_t(y)$, where $N_t(y)$ is the population density at location y , time t , and a second component representing the movement of the species via a dispersal kernel, $k(x, y)$. The dispersal kernel describes the

probability of individuals dispersing from their source at time t , to a position x , at time $t+1$. We show a simple example representing the spread of a population through a one-dimensional environment in equation 1.2.

$$N_{t+1}(x) = \int_{-\infty}^{\infty} k(x, y) f(N_t(y)) dy \quad (1.2)$$

The shape of the dispersal kernel can take a number of forms depending on the dispersal of individuals in the population. This is because it is the fundamental determinant of the range and rate of spread predicted by the model (Levin et al., 2003). For instance, integro-difference equations with Gaussian dispersal kernels (as is assumed in classical reaction-diffusion equations) exhibit constant rates of spread (Clark, 1998, Neubert and Caswell, 2000, Clark et al., 2001). Contrastingly, integro-difference equations with ‘fat-tailed’ dispersal distributions (distributions which are exponentially unbounded) (figure 1.5) representing individuals which undergo long distance dispersal events, can exhibit accelerating rates of spread (Kot et al., 1996, Richardson and Pyšek, 2008, Hastings et al., 2005). The greater degree of freedom in the modelling of dispersal afforded by integro-difference equations has led to a number of successful predictions of the rate of spread (Veit and Lewis, 1996, Clark, 1998, Neubert and Caswell, 2000). Additionally, integro-difference equations, in contrast to the continuous time reaction-diffusion equations, enable the processes of movement and reproduction to occur in discrete time steps, a factor that is considered more representative of the processes behind the spread of some invasive species (Hastings et al., 2005).

While some researchers believe integro-difference equations to be more realistic than the overly simplistic predictions made by the classical reaction-diffusion equation formulated by Fisher and Kolmogorov, they are reliant upon dispersal kernels informed by empirical evidence at all possible dispersal distances. This can be problematic as it is more difficult to acquire data at longer dispersal distances than at shorter dispersal distances. As a result, the dispersal kernel can be poorly fitted at the tails of the distribution upon which the rate of spread is highly sensitive (Hastings et al., 2005). Moreover, the shape of these tails can result in the model assuming a proportion of individuals travelling infinite dispersal distances, thus resulting in unrealistic predictions (Phillips et al., 2008). Until we develop better methods of acquiring this data, we

are forced to create artificial bounds to stop this effect from occurring (Clark et al., 2001).

Recent advances in integro-difference equations have shown that spatial selection can cause the dispersal kernel of a population to evolve into a fat tailed distribution (Phillips et al., 2008). The dispersal kernel can evolve rapidly as the (initially rare) individuals that undergo long distance dispersal mate with each other along the expanding front to become the dominant phenotype, thereby shifting the mean of the dispersal kernel. Researchers suggest that this is a factor behind Reid's paradox, the seemingly impossible rate of spread exhibited by trees after the previous ice age compared to their current rate of spread. Integro-difference equations have been increasingly utilised to represent the spatial dynamics of population spread, but future work needs to investigate the effect of evolutionary factors upon the dispersal kernel.

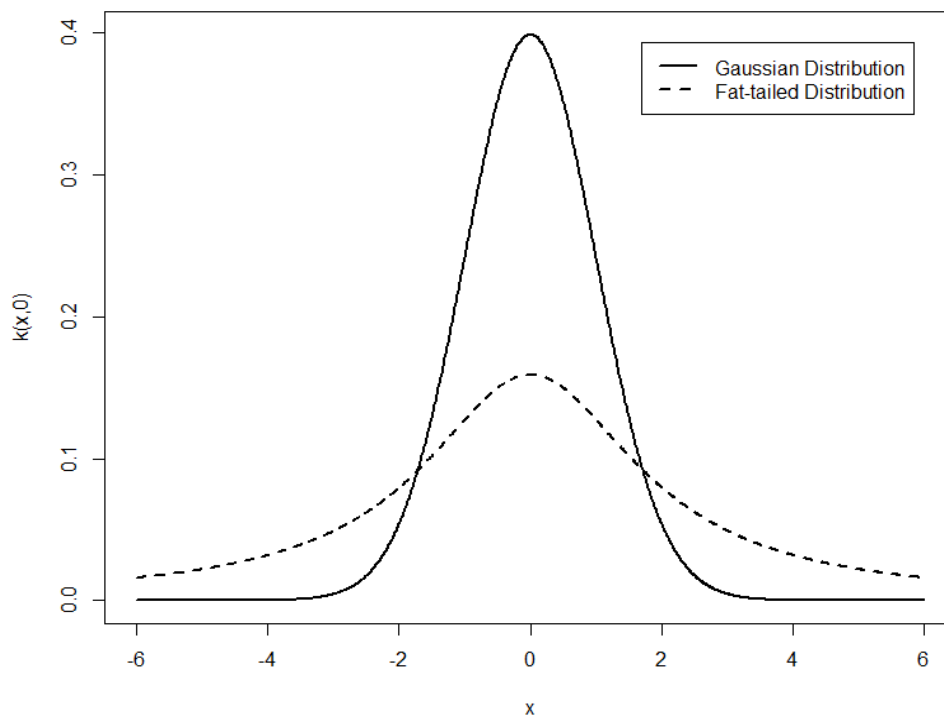


Figure 1.5: The classical reaction-diffusion model proposed by Fisher and Kolmogorov assumes movement of a species is via natural diffusive processes, which follow a Gaussian distribution. By manipulating the shape of this distribution, we can obtain “fat-tailed” distribution where long distance dispersal events are more likely to occur.

Individual-based models

The increasing accessibility to computers combined with massive increases in computational power has led to some modellers moving away from the

analytical approaches discussed so far, and instead utilising a class of computational models known as **Individual-Based Models** (IBMs – also known as agent-based models) (Grimm and Railsback, 2013). IBMs are a modelling approach incorporating aspects of game theory, emergence and evolutionary theory to represent systems in social sciences, economics and ecology. In contrast to analytical top-down approaches, which use averaged quantitative parameters of the individuals to represent the characteristics of the population as a whole, IBMs are a bottom-up approach, which explicitly simulate individual-scale interactions to ascertain the properties of the system at a global scale. The ability to account for the heterogeneity of traits at the individual-level has resulted in IBMs playing a key role in ecology due to the increasingly appreciated effect individual variation and adaptive behaviour has upon the global dynamics of the system (Grimm and Railsback, 2013).

The construction of an IBM requires the model to define each individual entity of the system in terms of their behaviours (procedural rules) and characteristic parameters. As the IBM is iterated, the localised interactions resulting from these behaviours cause changes in the characteristics of the individuals, which are then recorded through time (Grimm et al., 2006). Consequently, over the course of many iterations, changes in the characteristics at the individual-level lead to the emergence of system dynamics at a global level. IBMs are therefore considered a useful tool in developing our understanding of the determining factors behind the emergence of various ecological phenomena (such as seemingly organised collective behaviour) (DeAngelis and Mooij, 2005).

While IBMs are gaining popularity as an alternative to analytical approaches, they suffer from a number of drawbacks. Many of these drawbacks are because IBMs are a relatively young approach, with little-to-no framework as to how they should be developed and reported in the scientific literature. Differences between how IBM models are communicated can make them difficult to understand and therefore duplicate (Grimm et al., 2006). This drawback is steadily being diminished with the establishment of the ODD protocol, a protocol which aims to standardise the published descriptions of individual-based and agent-based models, thereby making model descriptions more understandable and reproducible (Grimm et al., 2006, Grimm et al., 2010). Other problems stem from the IBM approach itself, with IBMs suffering from high complexity and

limited generalisation. This has led some to believe that IBMs are only useful for answering fairly narrow questions of local behaviour, consequentially not offering a new perspective compared to analytical approaches (DeAngelis and Mooij, 2005). However, the IBMs ability to represent individual heterogeneity has been shown to give results that are more accurate than analytical approaches, suggesting that IBMs are indeed a useful modelling approach (Grimm et al., 2006). For example, modelling the invasive spread of *Heracleum mantegazzianum* using a transition matrix model approach predicted the area of population spread was decreasing (Hüls, 2005, Pergl et al., 2007). In contrast, an IBM approach based on the same empirical data illustrated that the inclusion of individual heterogeneity, the area of spread was increasing, agreeing with results from other empirical studies (Nehrbass and Winkler, 2007). This is not to say that IBMs are necessarily better than analytical approaches, rather that the ability of IBMs to represent individual heterogeneity make them a useful complementary method when used in conjunction with analytical approaches (Travis et al., 2011). Their increasing prevalence suggests IBMs will be (and already are) an integral part of ecology.

Metapopulation models

Metapopulation modelling is an analytical method for modelling the spatial distribution of a species across large landscapes (Facon and David, 2006, Schreiber and Lloyd-Smith, 2009). Metapopulation models are based on the idea of a 'population of populations' i.e. a population consisting of a number of unstable groups of spatially explicit (sub)populations which arise due to the patchy distributions of suitable habitats (Levins, 1969, Levins, 1970). These subpopulations, combined with other suitable unoccupied habitats (patches), form a large network in which subpopulations interact with each other via a limited level of dispersal (Hanski, 1998). Consequently, subpopulations in these patches undergo a dynamic equilibrium of extinctions and re-colonisations (Fronhofer et al., 2012).

For a population of subpopulations to meet the classical definition of a metapopulation, multiple conditions must be met (Hanski et al., 1995):

- (1) each patch in the population must be able to sustain a breeding population;

- (2) the subpopulations cannot be permanently self-sustaining (i.e. extinction must be possible in each subpopulation);
- (3) patches must be sufficiently close together such that they can be reached by colonisers from other patches;
- (4) there must exist an equilibrium between colonisation and extinction such that the population is not prone to mass extinction

However, populations in nature meeting these strict conditions are extremely rare, with the Glanville fritillary *Melitaea cinxia* (Hanski, 1994) providing the only undisputed example (Fronhofer et al., 2012). Consequently, many studies use variations of the base metapopulation modelling framework as they are believed to better represent the dynamics of the population (See Harrison (1991) for details on the most common variations).

The ability of metapopulation models to represent the effect of large scale spatial stochasticity of habitat environments on the dynamics of populations, makes them an effective modelling approach in the conservation of native species and an essential part of many management/recovery strategies (e.g. the western snowy plover, *Charadrius alexandrinus nivosus* (Nur et al., 1999)) (Schreiber and Lloyd-Smith, 2009, Facon and David, 2006, Hanski, 1998). For example, metapopulation models are frequently used to represent the increasing fragmentation of habitats as a result of human impact and climate change, a factor known to influence the rate of populations range expansion, including populations of invasive species (Hodgson et al., 2012, Hanski and Gilpin, 1991, Opdam and Wascher, 2004, Hanski, 1998). Metapopulation analysis has shown that as the area of habitat and connectivity increases, the speed of population spread increases, thereby helping to inform future conservation strategies (Wilson et al., 2010). Other factors often examined via metapopulation approaches include the effect of habitat corridors (i.e. increasing connectivity), investigating what the optimal timetable for reintroduction of an endangered species and revealing possible hidden benefits of patches with seemingly disadvantageous characteristics (Akçakaya et al., 2007).

While metapopulation models have traditionally been used for the conservation of native species, they are also being used to model the early stages of invasion (Facon and David, 2006, Lenda et al., 2010). By revealing which patches are

most likely to be invaded, metapopulation analysis may enable us to take action limiting the negative consequences of invasive spread ahead of time (Lenda et al., 2010). Actions which metapopulation analyses can specifically investigate include the artificial alterations of habitat networks, which can either reduce the connectivity of invasive species or increase connectivity for desirable species (Glen et al., 2013). A study by (Facon and David, 2006) illustrated the benefits of metapopulation analysis with respect to the dynamics behind the invasive spread of *Tarebia granifera*. Their study showed that the size of the metapopulation network (the number of subpopulations) and the distances between patches significantly affect the rate of invasion. Moreover, they showed that patch heterogeneity could be an underlying cause of accelerating rates of spread during the early phases of colonisation. By colonising a large central patch early in the invasion, the rate of spread could accelerate due to this central patch acting like an “invasion pool” or source from which propagule pressure results in increased immigration (Lenda et al., 2010, Lockwood et al., 2005, Schreiber and Lloyd-Smith, 2009). Future work is required on the application of metapopulation models to the invasive spread of the population.

While metapopulation approaches are frequently utilised in conservation to ascertain how population dynamics change throughout space, they have a number of weaknesses. First, the metapopulation approach does not model the spatial spread of individuals in detail, i.e. it simplifies the possible areas of spread into set patches of environment (Facon and David, 2006). Whether an environment constitutes a patch is a somewhat artificial decision by the modeller and this can affect the resultant dynamics of the system. Second, there are many types of metapopulation model and it is not known how realistic these models are as representations of the population (Akçakaya et al., 2007, Fronhofer et al., 2012). Accordingly, researchers need to establish which aspects of metapopulation models are viable and whether a metapopulation framework can accurately model the spread of invasive species.

Statistical models

Analytical models represent a system as a series of ideal functional relationships between the governing parameters. However, because they are simplified depictions of the real system of interest, predictions from these models are subject to a degree of error. Statistical models that infer the

characteristics and relationships from empirical data may be better suited for predictive models as they incorporate the same sources of uncertainty as found in nature. Indeed, one of the benefits of statistics is the derivation of confidence intervals, which show the possible error bounds of the predictions, a factor often missed in spread studies (Hastings et al., 2005).

Generalised linear models (GLMs) have been widely applied across ecology (Nelder, 1972). These flexible statistical tools allow researchers to use normal regression analysis on response variables to find trends within the data, thereby helping to inform our predictions. For the spread of a species, we can use these tools to measure the rate of invasion and perhaps, more importantly for conservation, the likelihood of a location being invaded by the spreading population. A good example of the application of a statistical model was carried out by Urban et al. (2008). Using the extensive prior knowledge provided by the cane toad case study in northeast Australia, certain climatic, physiological and ecological variables were chosen as a predictor of whether the toad will invade a patch or not. They found that the cane toad has evolved a greater tolerance to extreme conditions previously thought to be inhabitable. Consequently, conservation managers have had to revisit their previous strategies to account for new potential areas of spread, thus illustrating the power of statistical models.

Technological advances have aided the use of statistical techniques in the past 20-30 years. With hardware becoming more powerful and open source software like the statistical programming language R (R Development Core Team, 2014) increasing access to complex statistical techniques, researchers are now able to statistically infer answers from complex spatial data that were previously intractable (Liebhold and Gurevitch, 2002).

Statistical techniques that have been developed and applied in other fields of science could be useful in the study of spatial spread (Dungan et al., 2002). Geostatistics are one such branch of applied statistics originally developed to predict the distribution of ores below ground for applied mining operations (Magalhães et al., 2011). Geostatistics may to a useful method of quantifying the autocorrelation in spatial observations, allowing us to analyse cases where the assumed independence of observations in GLMs is invalid. The use of such

methods is currently limited due to the differences in terminology between fields, thereby highlighting the need for more interdisciplinary research.

How useful are these models and how can we improve them?

Through the combined use of these modelling approaches, it has been established that simple factors, such as diffusive movement and propagule pressure, are key drivers behind the spread of an invasive species (Lockwood et al., 2005, Levin, 2013). However, we have yet to establish all of the factors and their significance on the spread of a population in general, with most successful predictive models being species specific and subsequently not applicable across all populations (Gilpin, 1990, Williamson, 1996, Godfray and Rees, 2002, Richardson and Rejmanek, 2004).

A recurrent theme throughout the review has been the difficulty of accumulating high-resolution data, particularly at the longer ranges of dispersal (Hastings et al., 2005). The inaccuracy of data at these ranges can potentially alter the parameters of the models, thereby leading to erroneous predictions.

Experimental design is a fundamental part of ecological studies and influences the eventual quality of the data. In an ideal world, we would have infinite time, money, labour, equipment, etc. to conduct empirical field studies. However, due to various limitations, the techniques at our disposal require us to consider how we can capture a sufficient sample of the total population such that the hypothesis being investigated can be answered while obeying certain time-frames and budgets.

Empirical spatial studies investigating the rate of spread utilise a range of techniques to capture the spread of a population (depending upon the species being measured, examples include seed shadows and mark-recapture methods). The difficult nature of ecological systems involving macroorganisms can cause these techniques to produce data not entirely representative of a population's spread. For instance, if a survey does not cover a wide enough area at each time point, it may fail to capture those individuals who have undergone long distance dispersal events, resulting in us underestimating the spread of a species (Kokko and Lopez-Sepulcre, 2006). Other problems include the time taken to collect sufficient data from a spatial field study, with studies often taking months or years; a lack of control, with studies often at the behest

of the weather or other uncontrollable extrinsic/intrinsic factors; and a lack of repeatability. This is potentially a reason for the relatively limited number of empirical studies of species spread (White et al., 2012). Statistical methods can help negate some of these problems (such as GLMs with random effects), however this should be a last resort and not used as an alternative to a rigorous experimental design. While researchers should continue to research new surveying techniques, we believe another solution might be to use a microbial model system to study spatial ecology in a controlled laboratory environment.

The microbial model system

A fundamental part of biology is the study of microcosms in a controlled laboratory setting, which use model organisms to study biological phenomena. Researchers usually choose certain organisms to be model systems because they have a series of desirable traits (i.e. a short life cycle or they exist in easily replicable and sustainable habitats) and are amenable to experimental manipulation. The microbial model system is increasingly recognised in studies of ecology and evolution as a suitable model organism due to their ability to exhibit a wealth of information in a controlled environment relatively quickly (Jessup et al., 2004, Buckling et al., 2009). Excellent examples of studies utilising microorganisms include the phenotypic diversity and niche specialisation of *Pseudomonas fluorescens* colonies (Rainey and Travisano, 1998), the interplay between evolution and ecological dynamics in a microbial predator prey system (Yoshida et al., 2003) and the link between coexistence and spatial structuring in communities (Kerr et al., 2002).

The microbial system provides a number of advantages compared to field-based spatial ecology studies, the biggest of which is the experimental control it offers. We can observe spatial dynamics in microbiology by inoculating bacteria upon agar plate surfaces and placing them in controlled incubator environments. As agar plates are the only environment the microbial species interacts with, we can eliminate any unpredictable noise from uncontrollable external effects. Moreover, we can capture the entire global region of colonization easily and efficiently by taking pictures during their spread. Hence, the microbial model system enables us to investigate spatial ecology without two of the key problems commonly associated with spatial ecology studies,

namely unpredictable extrinsic effects and the difficulty of capturing long-range dynamics.

Another key advantage of the microbial model system is the ability to replicate studies. For example, replication enables us to repeat the same experiment multiple times but with key factors altered to investigate extrinsic and intrinsic effects on spatial spread. The ability to easily replicate studies also allows us to increase the power of our experimental design, reducing the need for statistical techniques to cover up potential problems with the experimental design.

Microbial organisms also grow at a rapid rate, colonizing their environment in very short timescales compared to the often time-consuming data collection techniques usually utilized in field-based spatial ecology studies. Finally, the genetic basis of microbial dispersal has been investigated extensively, as have the mechanisms microbes utilize to traverse across their environment, allowing us to investigate the genetic basis of spatial spread.

We believe that studying the spatial dynamics of microbial systems is not only useful for spatial ecology but may be useful in their own right. Understanding the spatial patterns exhibited during colonization of new environments could be important in the effort to control bacteria in hospitals, particularly with bacteria becoming increasingly resistant to standard antibiotic treatments (Spellberg et al., 2008). If we can outsmart the bacteria using methods not involving antibiotic treatments, then this could have significant positive ramifications for medicine (Ben-Jacob et al., 2000). Such information may also help against the spread of bacterial biofilms across artificial joints (Ehrlich et al., 2005), the colonisation of compromised organs (Oliver et al., 2000) or against the growth of cancerous tumours (which exhibit spread dynamics similar to bacterial biofilms) (Korolev et al., 2014). Moreover, microbial populations are prevalent in many ecosystems, playing a significant role in the regulation of ecosystem processes.

Consequently the study of microbial populations might also prove useful in protecting biodiversity in these ecosystems (Torsvik and Ovreas, 2002).

While there is a growing literature in ecology utilising the microbial model system, there has been some scepticism, claiming that microbial systems are too simple and not representative of the same ecological processes as in macroorganisms (Lawton, 1995, Carpenter, 1996). However, it is this simplicity

that makes the microbial model system advantageous compared to other model systems, as it enables us to test the fundamentals of ecological theories in an environment free from uncontrollable noise. As a new tool in spatial ecology, researchers should embrace the advantages microbial model systems offer and utilise them to answer fundamental questions in spatial ecology. Indeed, examples of how knowledge from the microbial model system has translated to macro-organism populations is increasingly prominent in the study of ecology. A review by Jessup et al. (2004) gives a good example of this in relation to explaining the processes governing species diversity with respect to spatial and temporal factors. Diversity is thought to be dependent upon the amount of energy available in the system (i.e. productivity) and several studies have demonstrated a hump-shaped relationship between diversity and productivity in both macroorganisms and some microorganisms (Kassen et al., 2000). However, the mechanisms underlying such trends are poorly understood. Using *Pseudomonas fluorescens* in both a heterogeneous and a homogenous vial environment showed that the hump-shaped relationship appeared in heterogeneous environment but not in the homogeneous environment (Kassen et al., 2000).. This thereby enabled the identification of key processes (i.e. those relating to heterogeneous environments) underlying diversity patterns in both micro and macro- organism populations, an experiment that would be almost impossible to do in field studies involving macro organisms where such patterns can occur on regional scales (Jessup et al., 2004).

To counter the arguments of detractors, there is a requirement to compare and contrast the processes behind the spatial spread of microorganisms and macroorganisms to ascertain where similarities exist. Indeed, the traditional thinking of microbes acting as only simplistic unicellular organisms has been largely debunked by the numerous studies dedicated to microbial evolution (Buckling et al., 2009, Griffin et al., 2004, West et al., 2007a). Historically, microbiologists have thought of microbial populations as groups with traits occurring due to species or community level benefits, with little to no influence from effects at the cellular level (West et al., 2007a). However, recent studies have shown interactions between cells within the bacterial population are highly influential upon the characteristics of the population at a group level. For instance, the ability of unicellular microbes to communicate and coordinate with

one another via quorum sensing mechanisms at the cellular level enables microbes to act as multicellular organisms. Mechanisms that enable the bacteria to form up and produce multicellular biofilms have beneficial effects for the persistence and virulence of the microbial population (West et al., 2007a). Such mechanisms are a form of social behaviour. The next section provides a brief overview of the evolution of social behaviour, which we expand upon throughout the thesis.

A brief overview of social behaviour within the microbial model system

Within a population, individuals interact with each other via an array of direct and indirect behaviours. These behaviours are social behaviours if an action by an individual directly solicits a response from another individual. In evolutionary terms, researchers define behaviour as social if it has a fitness consequence, either positive or negative, for both the acting individual and the recipient. According to Hamilton, there are four categories of social behaviour, dependent upon whether the social interaction is beneficial or costly to either the acting individual or the recipient (table 1.1) (West et al., 2006a, Hamilton, 1964). Among the most puzzling of these behaviours is altruism, where an individual sacrifices its own fitness for the benefit of another. Altruism seemingly contradicts the classical theory of natural selection proposed by Darwin which states an individual organism will act in ways to enhance its own individual fitness, thereby promoting the transmission of its genotype to future generations (Darwin, 1859). To explain this ostensibly contradictory behaviour, Hamilton mathematically formulated the well-known inclusive fitness theory (Hamilton, 1964). Inclusive fitness theory shows an individual can increase the evolutionary success of their genotype by helping closely related individuals to survive and reproduce i.e. helping their relatives by being altruistic (Hamilton, 1964). By helping closely related individuals, individuals achieve an indirect benefit to the fitness of other individuals who share a similar genotype, thereby making altruism a beneficial strategy. Inclusive fitness theory has been widely accepted and successfully verified in multiple studies (Dawkins, 1976).

Whether a phenotype arises depends upon its selection coefficient. In inclusive fitness theory, there are two parts to the selection coefficient, the direct (the

fitness of the focal individual with the exhibited phenotype) and the indirect (the fitness of individuals related to the focal individual with the exhibited phenotype) fitness components of the phenotype. Hamilton derived the following relationship to predict whether altruistic behaviour will spread throughout a population:

$$rb - c \quad (1.3)$$

where r represents the relatedness between individuals (specifically the probability above the population average that a gene is shared between individuals), b represents the indirect benefit to the recipient of the behaviour and c is the direct cost of the behaviour to the acting individual. This equation predicts selection with promote altruistic behaviour when this relationship exceeds one.

Table 1.1: The four types of social behaviour as defined by Hamilton.

	Beneficial for the Receiving Individual	Costly for the Receiving Individual
Beneficial for the Acting Individual	Mutual Benefit	Selfishness
Costly for the Acting Individual	Altruism	Spite

While inclusive fitness theory has been widely accepted, researchers who believe selection can take place across a number of levels (genes, cells, individuals and groups) simultaneously with each level having varying importance upon the result have formulated an alternative yet mathematically equivalent theory. This theory is known as multi-level selection theory (Sober and Wilson, 1998). While inclusive fitness theory breaks the selection coefficient into two parts as in equation 1.3, multi-level selection divides the selection coefficient into parts representing the within-group (the fitness of the phenotype against other individuals in the group i.e. individual-level competition) and between-group (the fitness of the phenotype against individuals in other groups i.e. group-level competition) fitness components (Queller, 1992). All studies, which have used both multi-level selection and inclusive fitness theory, to study the same empirical evidence have obtained the same result (Gardner et al., 2007, West et al., 2008, West et al., 2007b), albeit often with simplifications. This is because both inclusive fitness theory and multi-level selection are mathematically equivalent (Price, 1970, Marshall, 2011, Lehmann et al., 2007,

Wade, 1985). Indeed, one can consider the ratio of between-group fitness to within-group fitness fundamentally the same as the coefficient of relatedness used in inclusive fitness theory (Queller, 1992).

Whilst multi-level selection theory has been accepted as a credible tool, it is considered by some critics surplus to requirements compared to inclusive fitness theory (West et al., 2008). Critics state the construction of multi-level selection mathematical models as more complicated and less amenable to analysis, compared to models based on inclusive fitness theory. Combined with the difficulties of identifying what constitutes a group in natural populations, empiricists typically utilise inclusive fitness theory as it gives the same resultant outcome (West et al., 2007b). Furthermore, there is often confusion between users of inclusive fitness theory and multilevel selection theory due to the inconsistent usage of terminology (West et al., 2007b). However, proponents of multilevel selection suggest it is a better method for studying some aspects of selection theory, such as evolutionary transitions (Lion et al., 2011). Although the argument between inclusive fitness theory and multi-level selection theory is often heated, it is generally recognised that plurality in approaches should be embraced as it can help reinforce our understanding (Okasha, 2010). Until the two sides reach a consensus, investigating social behaviour from both an inclusive fitness and a multi-level selection perspective will reinforce our understanding of how social behaviour arises.

The social behaviour within a microbial population can affect the traits of the population significantly, including those traits related to spatial dynamics. Many of the cooperative social behaviours within a microbial population involve the production of costly molecules by individuals called public goods (West et al., 2007a). These public goods are shared amongst neighbouring individuals to achieve group-level benefits such as increased carrying capacity, antibiotic-resistance or persistence (de Vargas Roditi et al., 2013). Public goods therefore improve the group-level fitness component, while decreasing the individual-level fitness component (due to the cost of public good production) (West et al., 2007b). If a microbial colony grows in isolation of other colonies (i.e. no global competition/no between-group competition), individual-level selection intensifies, becoming the main driver of selection (Griffin et al., 2004). When

individual-level selection is favoured, cheaters can exploit the public goods produced by others in the population, without contributing to public good production themselves (West et al., 2002). The emergence of these cheaters can affect the spatial spread of the microbial colony, due to the emergence of spatial segregation between the co-operators and the cheaters, both of whom are fighting for the same space (Nadell et al., 2010). It is also known that the spatial structure of the population affects the social behaviour of the population (Tisue and Wilensky, 2004). However, our knowledge about the feedback between social behaviour and spatial spread is still limited. Studies utilising the microbial model system in spatial ecology need to be aware of the social behaviour within the biofilm and that these interactions within microbial biofilms are highly complex (López et al., 2010). To answer these questions, researchers require knowledge about the mechanisms used by microbes to traverse their environment.

Spatial dynamics in microbial systems

Bacteria use an array of dispersal mechanisms (also known as motility mechanisms) to spread across environments (Henrichs, 1972, Harshey, 2003, Kearns, 2010). Motility arises either due to the utilisation of motility machinery or because of natural physical forces. Bacteria have two types of motility machinery known as type IV pili and flagella. Type IV pili are hair-like appendages emanating from the main cell, which cause movement by first attaching themselves to either the local environment or to other cells and then retracting the pili, thereby dragging the cell through the environment. Flagella are tail-like appendages found upon the surface of the cell, which cause movement by rotating counter-clockwise to propel the cell forward, with occasional clockwise rotations to randomly change the direction. The most influential dispersal mechanisms in microbial colonisation are:

Swimming: individuals utilise their flagella to propel themselves forward through a liquid.

Swarming: a cooperative behaviour where individuals group up to form raft like structures, which propel themselves by the combined usage of their flagella.

Twitching: a process whereby individuals extend their type IV pili to pull themselves across environments.

Sliding: where population growth physically pushes individuals outwards to make room for new individuals.

Gliding: a mechanism that is still unknown but allows the bacteria to move under its own power without the use of flagella. Possible theories behind the gliding mechanism are the ejection of polysaccharides causing the propulsion of the cell (Wolgemuth and Oster, 2004) or by focal adhesion complexes (Mignot et al., 2007).

These motility mechanisms operate at different speeds, with those methods utilising flagella often faster than those utilising type IV pili. Furthermore, multiple mechanisms can be active at any one time during the colonisation of an environment (Harshey, 2003), although some combinations of motility operate exclusively from one another. For example, twitching motility is not observed during swimming motility as the velocity of swimming motility results in shear forces, which are thought to remove the type IV pili required for twitching motility from the surface of the cell (Taylor and Buckling, 2011, Touhami et al., 2006).

Motility is crucial as it enables the colony to overcome the limiting factors of bacterial growth. For instance, during the colonisation of agar plate environments, a nutrient gradient forms as nutrients diffuse towards the colony. If the velocity of motility is not great enough, then eventually resources become limiting and cells become starved, thereby affecting the ability of the cells to maintain further dispersal (de Vargas Roditi et al., 2013, Nadell et al., 2010). Additionally, motility mechanisms enable individuals in the colony to escape the build-up of toxic chemicals excreted by the colony during growth (Cooper et al., 1968).

The type(s) of motility exhibited by a microbial population depends upon the viscosity of the environment (as determined by the agar concentration) with swimming motility exhibited in liquid environments, swarming motility exhibited on semi-solid surface environments and twitching motility exhibited on hard surface environments. To ensure the correct motility is used, bacteria utilise sensing mechanisms to activate the required motility mechanisms (Okkotsu et al., 2013, O'May and Tufenkji, 2011). The activated mechanisms include quorum sensing mechanisms (to facilitate coordination between individuals), the

production of motility machinery and the production of surfactants to reduce surface tension (Be'er et al., 2009, Ochsner and Reiser, 1995).

Microbial populations can exhibit different patterns of spatial spread during their colonisation of agar plate surfaces. Patterns range from regular circular patterns (figure 1.6) to exotic, irregular patterns such as the fractal-like patterns seen in figure 1.9. Of particular note in this thesis are the dendritic patterns produced by *Pseudomonas* colonies (figure 1.6). Researchers believe these dendritic patterns of spread arise due to localised groups of individual bacteria having rates of motility greater than the global population growth. These dendrites seemingly stay separated from each other because of the production of chemicals, which repel and attract other dendrites (Caiazza et al., 2005, Tremblay et al., 2007). The patterns of exhibited microbial spread are typically species specific perhaps due to the different motility mechanisms used by different strains (Deng et al., 2014). A detailed discussion of the different patterns can be found in (Kearns, 2010).

As with the type of motility, the pattern of spread depends upon environmental conditions, with patterns typically deviating away from circular patterns of spread on semi-hard agar surfaces due to swarming motility. Another environmental factor thought to affect the spatial pattern of spread is the availability of food in the environment, with the classic studies of microbial spread on agar plate surfaces finding circular patterns of spread at high nutrient concentrations and fractal patterns at low nutrient concentrations for the bacterium *Bacillus subtilis* (Kawasaki et al., 1997, Matsushita and Fujikawa, 1990, Marrocco et al., 2010, Julkowska et al., 2005). Other studies have shown the same result for *Paenibacillus dendritiformis* (Ben-Jacob et al., 1994, Ben-Jacob et al., 1998, Ben-Jacob et al., 2000), *Salmonella anatum* and *Serratia marcescens* (Matsuyama and Matsushita, 1993). However, unlike agar concentration, it is not clear whether nutrient limitation is universally important for the pattern of spatial spread exhibited for all species of microbes. It has been found that the spatial pattern of spread exhibited by some strains of *Proteus mirabilis* (Rauprich et al., 1996, Esipov and Shapiro, 1998) are not affected by nutrient limitation. This suggests the effect of nutrient limitation is

highly specific to the species, although why this is the case is unknown and requires further evidence.

The spatial spread of bacteria on agar plate surfaces goes through similar phases as those seen in macroorganisms i.e. establishment, range expansion and saturation. When initially introduced to the environment, bacteria establish themselves within the area of inoculation and the radial spread of the colony does not increase, reminiscent of the lag phase seen in macroorganisms (Kearns and Losick, 2003). Similar to the dynamics seen in larger scale organisms, the time in this phase can be reduced by increasing the initial density of individuals or if the individual cells have been taken from a population which were already undergoing active dispersal (Kearns and Losick, 2003, Kearns, 2010). Once the population reaches a certain density, depending on the motility mechanism utilised by the colony, rapid colonisation of the surrounding area occurs thereby increasing both the area of spread and population density. Finally, the radial spread of the colony plateaus, possibly due to the limited space afforded by the agar plate, or by other mechanisms. The exhibition of all three phases of spread as seen in macroorganisms suggests that the spread of species has similar drivers irrespective of the type of organism. Consequently, there is a strong possibility of using the microbial model system to investigate the spread of populations in a relatively controlled laboratory setting.

Microbial systems are amenable to evolutionary questions, enabling us to investigate areas we would otherwise have difficulty testing in macroorganisms. For example, a study by Taylor and Buckling (2011) showed that microbial populations could evolve their dispersal machinery in order to best adapt to their local environment, but at a cost to other life history parameters. In macroorganisms similar examples can be seen, for instance cane toads have developed longer legs to disperse further in their environment, but this has come at a cost of being less resistant to lethal viruses and more prone to crippling arthritis (Phillips et al., 2006, Brown et al., 2007, Shilton et al., 2008). However, the study in the laboratory took place over a matter of days whilst the cane toad study took place across a number of years. Hence, researchers can use the microbial model system to study the evolution of dispersal.

The microbial model system may allow us to investigate areas of spatial ecology we currently cannot test via model systems with macroorganisms. One example is the shape of the spread, a factor we are often not able to analyse without using approximation methods such as convex hulls, due to the difficulty of capturing sufficient resolution data at macroorganism scales. It is still relatively unknown whether the shape of spread is an integral part to the persistence of the colony. Answering questions from a microbial level may help to improve our understanding of processes at all scales of organism. For example, figure 1.7 shows the spread of London's urban sprawl from the 18th century to the 20th century. While these are very different systems (with differences such as geographical topology and resource variation), a brief comparison of the microbial colonies seen in figure 1.6 and the urban sprawl in the year 1862 show that the patterns between microorganisms and macroorganisms can be very similar to each other, thereby suggesting a link between microbial and macrobial populations. Currently, the vast majority of studies investigating the shape of microbial colonies are theoretical modelling approaches. Most commonly, these involve reaction-diffusion models, similar to those already used in the modelling of larger organisms. We briefly discuss these modelling approaches in the next section.

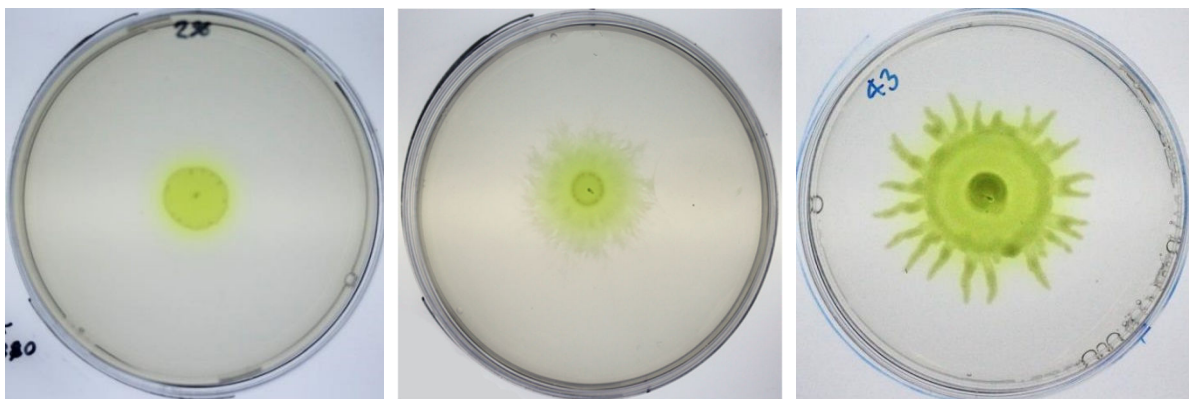


Figure 1.6: *Pseudomonas aeruginosa* grown on three different agar plates containing KB agar with 1% agar concentration on the left, 0.75% agar concentration in the middle and 0.5% agar concentration on the right.

Modelling microbial spread

The remarkable variety of patterns of organised spread exhibited during microbial growth on agar plate surfaces has attracted the attention of many modellers who wish to understand their underlying governing processes. A fundamental question in these studies is whether the variety of patterns among

strains is explainable by a set of governing rules or whether they arise because of intrinsic/extrinsic factors specific to each bacterial strain. To answer this, a common approach has been reaction-diffusion equations incorporating a number of biophysical factors. Typically, for reaction-diffusion equations to exhibit irregular patterns of spread (i.e. those deviating from homogeneous circular patterns of spatial spread), diffusion-driven instabilities are required to initiate deviations away from uniform radial spread. A review by (Marrocco et al., 2010) states that instabilities have typically been incorporated into reaction-diffusion equations describing microbial populations via the explicit modelling of either auto-chemotaxis or the gradient of nutrients in the environment.

Auto-chemotaxis occurs when cells in the population move towards or away from chemical stimuli produced by other cells in the population. Models incorporating auto-chemotaxis are based on the classic chemotaxis models popularised by (Keller and Segel, 1970) and incorporate short range directed (i.e. biased random walk) movement to create patterns of spread with localised cell aggregation at discrete spots throughout the colony. Equation 1.4 shows a simple system of reaction-diffusion equations incorporating auto-chemotaxis and the random motion of cells according to Fick's law:

$$\begin{aligned} \frac{\partial n(t, x)}{\partial t} - \Delta n(t, x) + \nabla \cdot (n\chi\nabla c) &= 0, \quad t > 0, x \in R^d \\ -\Delta c(t, x) &= n(t, x) \end{aligned} \tag{1.4}$$

Where at time t and position x , $n(t, x)$ is the density of cells, $c(t, x)$ is the concentration of chemo-attractant produced by the cells themselves and χ is a constant representing the sensitivity of the cells to the chemoattractant. By incorporating simple assumptions for cellular auto-chemotaxis behaviour, reaction-diffusion models such as equation 1.4 have typically been used to describe the concentric ring spot patterns of spread produced by *Escherichia coli* (Budrene and Berg, 1991, Tsimring et al., 1995) and *S. typhimurium* (Woodward et al., 1995), therefore providing evidence for chemo-attraction as an important factor behind the collective motion of these particular strains (figure 1.8). However, models based on auto-chemotaxis of chemo-attractants and chemo-repellents alone have been unable to convincingly describe the fractal-like patterns exhibited by some microbial colonies, such as *P. dendritiformis* (figure 1.9) or *B. subtilis* (Marrocco et al., 2010).

To model cases like the fractal-like patterns of *P. dendritiformis* colonies, researchers have used reaction-diffusion equations explicitly modelling the density of nutrients throughout the environment. In these models, microbial growth across the agar plate surface depends upon the concentration of nutrients and bacterial diffusion, with models usually assuming the cells in the population are either active or passive according to the local nutrient density. Active cells in the system are able to move, grow and perform cell-division, while passive cells are unable to exhibit these simple life cycle rules (Golding et al., 1998, Kessler and Levine, 1998, Marrocco et al., 2010, Mimura et al., 2000). Consequently, those cells at the tip of the colony increase their motility relative to those cells behind it, resulting in dendritic growth (Kawasaki et al., 1997). A simple example of such a model was proposed by (Mimura et al., 2000):

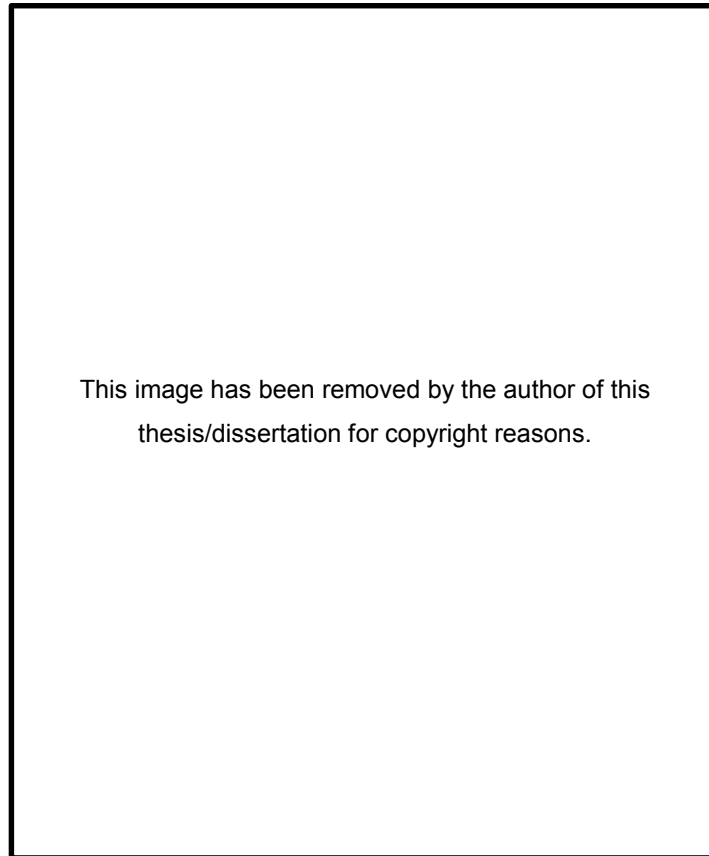


Figure 1.7: The urban sprawl of London from the late 18th century until the late 20th century. The spatial spread of human populations can remarkably mimic those exhibited by microbial populations (Sennet, 2009).

$$\left\{ \begin{array}{l} \frac{\partial a(t,x)}{\partial t} = \nabla(d(b)\nabla(a)) + av - c(a,n)a \\ \frac{\partial n(t,x)}{\partial t} = \Delta n - an \\ \frac{\partial p(t,x)}{\partial t} = c(a,n)a \end{array} \right. \quad t > 0, x \in R^2 \quad (1.5)$$

Where at time t , location x , $b(t, x)$ represents the population density, $a(t, x)$ represents the density of active cells, $p(t, x)$ represents the density of passive cells, $n(t, x)$ represents the density of nutrients (this parameter at $t=0$ is varied according to the nutrient concentration of the system being considered), $d(b)$ represents the ratio of diffusion rates between active and passive cells (this parameter is varied according to the agar concentration being considered and may be a linear or non-linear term), v is the conversion rate of nutrients into cellular growth and $c(a, n)$ represents the conversation rate from active cells to non-active cells depending on local nutrient density and active cell density. To represent this rate, (Mimura et al., 2000) used function 1.6 where k_a and k_n were positive constants. Note that any functions monotonically decreasing by a and n are suitable.

$$\frac{1}{\left(1 + \frac{a}{k_a}\right)\left(1 + \frac{n}{k_n}\right)} \quad (1.6)$$

Models similar to that of equation 1.5 can successfully recreate the spatial spread of *P. dendritiformis* across an array of values for the environmental parameters representing the nutrient and agar concentration (viscosity of the environment) (see figure 1.9 - (Golding et al., 1998)). Additional factors such as the incorporation of surfactant concentration (Golding et al., 1998, Kozlovsky et al., 1999) and the auto-chemotaxis discussed earlier (Leyva et al., 2013), into these type of models have led to similar dendritic patterns.

Reaction-diffusion equations incorporating factors such as auto-chemotaxis and nutrient gradients can successfully recreate spatial patterns of microbial spread similar to that seen in empirical studies. However, through these models and other approaches, researchers have discovered that a wide variety of factors can give rise to dendritic patterns of spread. With reaction-diffusion equations largely focused upon how biophysical factors give rise to the shape of spread, researchers must be careful that a strong empirical foundation informs the basis of the incorporation of certain factors in their models (Golding et al., 1998, Marrocco et al., 2010). In particular, many of these models make assumptions about how nutrient and agar concentration affects the pattern of spread and utilises these assumptions almost exclusively to underpin the underlying foundations of the pattern of spread (Leyva et al., 2013). Whether the

assumptions made by these models generalise across species is not clear and requires further investigation in order to answer whether there exists a set of governing principals behind the spatial pattern of spread during microbial growth (Marrocco et al., 2010).

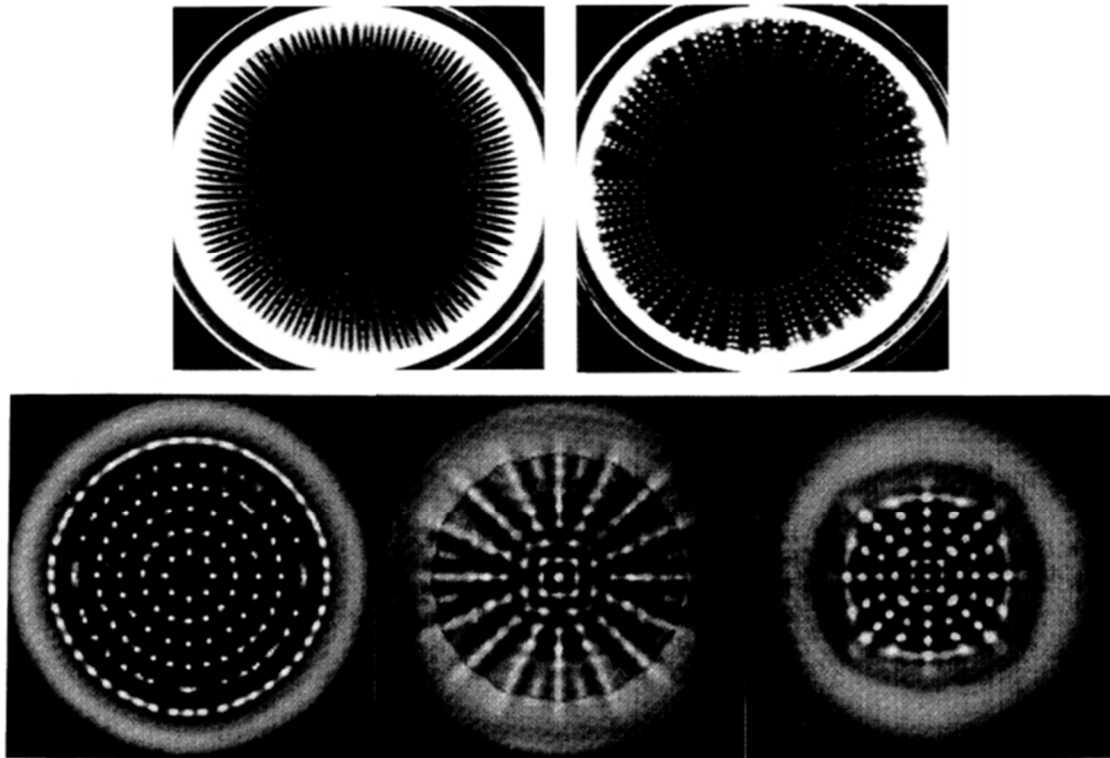


Figure 1.8: (Top) The growth of the bacterium *Escherichia coli* on a single carbon source medium results in aggregated spot patterns when under oxidative stress. It is theorised that the production of respiratory by-products during oxidative stress triggers auto-chemotaxis behaviour. (Bottom) A reaction-diffusion model incorporating auto-chemotaxis (similar to that seen in equation 1.4). By adjusting the chemotaxis strength of the model, we can recreate a variety of different symmetric spot patterns, closely resembling empirical observations. Pictures taken with permission from (Budrene and Berg, 1991, Tsimring et al., 1995).

A problem with some of the reaction-diffusion equations used to recreate microbial patterns is that they can become intractably complex. Therefore, it may be more suitable to use other modelling approaches. One example are computational mechanistic models which explicitly model the physical kinetic mechanisms bacteria use to traverse their environment (Du et al., 2011). As with other models based on reaction-diffusion equations, the focus of the majority of these alternative models are the biophysical basis for the shape of the spread. However, recent studies are increasingly asking questions about the evolutionary ecology of these patterns of spread (Korolev et al., 2014). For example, (Deng et al., 2014) uses kernel based models (similar to the integro-

difference models) to show that the contrasting ecological processes of colony expansion and colony repulsion across different scales can lead to dendritic patterns for a narrow range of parameters. This study illustrated that dendritic patterns may have arisen due to the fine-tuning of their ecological characteristics over evolutionary time. Moreover, with the increasing popularity of microbial evolutionary ecology, modellers are increasingly investigating how social interactions within biofilms can affect the spatial distribution of cells within the population. For example, (Xavier et al., 2009) used a mechanistic model to suggest competition for resources between cells along the surface of a biofilm must involve some level of cooperation for a biofilm structure matching that of empirical studies to emerge. Similarly, (Nadell et al., 2010) illustrated through the use of an individual-based model, that conflict within a mixed population consisting of co-operators and defectors combined with limited resources leads to spatial segregation between the two types of individuals as a result of the competition. This segregation seemingly results in spatial spread similar to that seen in some strains of *Pseudomonas aeruginosa*, although this study does not specifically look at the patterns of bacteria spread. Indeed, studies looking at the influence of evolutionary and social ecology upon the spatial spread of bacteria are extremely limited, an area we believe more research is required as it is increasingly recognised in macroorganisms that evolutionary and social factors are a key components driving the spatial ecology of populations (Bowler and Benton, 2005).

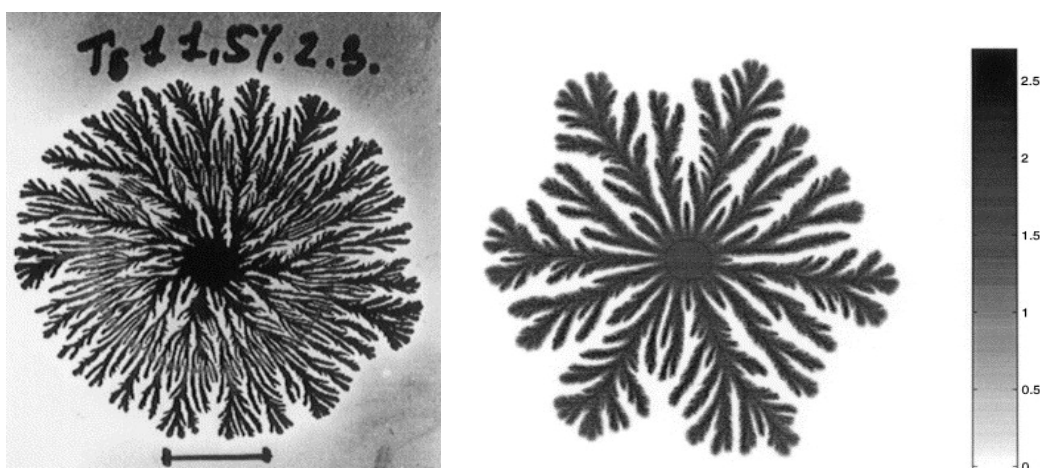


Figure 1.9: Left figure: *Paenibacillus dendritiformis* growth upon low nutrient, low agar concentration conditions. Right figure: the results from a 2D reaction-diffusion model based upon the Kitzunezaki set of equations (Kitzunezaki, 1997) with non-linear diffusion, nutrient chemotaxis and lubrication density included. Taken with permission from (Golding et al., 1998).

Conclusion

Although the spatial spread of a population is a fundamental aspect of ecology, its study has been a technically difficult task, with numerous obstacles still to overcome. A concerning aspect of recent studies of spatial spread is the observation that some invasive species can spread at an accelerating rate through time, disagreeing with our previous predictions. Conservation managers believe the accelerating spread of invasive species can lead to disastrous consequences for worldwide biodiversity. Our theoretical understanding suggests invasive populations exhibit an accelerating rate of spread because of a range of intrinsic (e.g. stratified diffusion and spatial sorting) and extrinsic (e.g. human activity) factors. However, empirical evidence for these factors has been limited due to the data collection difficulties encountered by empirical field studies. As a solution to the problems encountered by these field studies, we propose the microbial model system as an ideal model system for the accumulation of empirical evidence to underpin our theoretical understanding of spatial ecology. While some believe microbes to be a simple system, we believe it shares many of the same underlying ecological principles driving the spatial dynamics as macroorganisms. Consequently, we theorise that the microbial model system will allow us to pinpoint the important factors affecting how a population spreads.

Studies into the spatial ecology of microbes have historically been limited in number and have mainly focused on the recreation of spatial patterns of spread via biophysical mechanisms. The focus upon the exhibited spatial patterns (i.e. the shape of spread) is a unique aspect of microbial populations. This arises because researchers can easily observe the complete region of spread at a relatively high resolution in a controlled environment, in contrast to the often-approximated shapes of spread calculated for macroorganisms. We believe that the shape of spread holds a number of ecological and evolutionary implications for populations across multiple levels of selection, which researchers currently do not consider. Based on other studies of microbial ecology, we speculate that factors such as evolution or social behaviour are characteristics of the population affected by the shape of spread. Consequently, researchers should use the microbial model system to investigate these issues, not just the biophysical aspects considered to date. These are only a few things we believe

the microbial system offers spatial ecology and understanding these aspects further will help us to ascertain the underlying factors behind the spread of an invasive species. Indeed, the uniqueness of the microbial model system means there is a requirement to investigate the spatial spread of microbes and to understand how these dynamics relate to macro-organisms.

Thesis outline

In the following chapters of this thesis, we utilise the microbial model system both empirically and as inspiration, to ask questions relating to the spatial spread of populations across environments. We investigate the spatial spread of microbes using an array of interdisciplinary techniques including empirical laboratory studies, analytical numerical modelling and individual based modelling simulations.

We begin the study in Chapter 2 by empirically investigating the rate of spread exhibited by *Pseudomonas fluorescens* populations and asking whether these agree with the constant rate of spread result predicted by the classical studies of spatial ecology. By observing how intrinsic and extrinsic factors of the microbial model system affect the rate of spread, this chapter first aims to increase the number of empirical examples investigating the rate of spread. It also aims to establish the possible effect of intrinsic and extrinsic factors upon the rate of spread and it aims to provide empirical support for the use of the microbial model system in spatial ecology. In addition, we also investigate the shape of spatial spread and its possible effect on the rate of spread, the results of which form the foundation for the remainder of this thesis.

Based on the observed irregular patterns of spatial spread seen in the literature and the classical studies of microbial spread showing that environmental conditions affect the exhibition of these patterns (Matsushita and Fujikawa, 1990), Chapter 3 aims to establish the effect of environmental viscosity and food availability on the shape of microbial spread exhibited by *Pseudomonas aeruginosa* colonies. We particularly analyse whether this system follows the relationship between shape of spread and environmental conditions observed in other microbial systems. We then use a geometric model in Chapter 4 to investigate the selective pressures driving the spread of microbial populations and to ask how the shape of the colony affects the fitness of the colony at both

a micro and at a macro scale, via a multi-level selection approach. Specifically, we investigate how the exhibition of tendrils (long regions of growth emanating from a central point) by the colony during their spread across a two-dimensional agar plate environment affects the individual- and group-level fitness of the colony compared to colonies exhibiting a circular patterns of spread.

The next three chapters (Chapters 5 to 7) investigate the link between the shape of spread and individual-level competition along the population's leading edge. First, using microbial colonies as inspiration, we create a model framework in Chapter 5 to study how individual-level competition along the leading edge of the population changes as the colony spatially expands across the local environment through time. We then introduce a dispersal mechanism to this model in Chapter 6, to find out how dispersal affects the individual-level fitness and social behaviour between neighbouring individuals along the leading edge of a population. Chapter 7 then integrates these results into an individual based model framework with simple life history rules, to investigate whether the model framework in Chapters 5 and 6 can replicate the complex patterns of spread seen in Chapter 3. In Chapter 8, we finish by utilising artificial selection experiments to examine whether the shape of microbial spread is an evolvable trait of a microbial population. In Chapter 9, we conclude by discussing the implications of the preceding findings for our understanding of the microbial system and to spatial ecology as a whole.

In the empirical chapters of this thesis, we use two species of bacteria. These are *Pseudomonas fluorescens* strain SBW25 in Chapter 2 and *Pseudomonas aeruginosa* strain PAO1 in Chapters 3 and 8. *Pseudomonas* species are a gram-negative, rod-shaped motile bacterium with at least one polar flagella and type IV pili machinery (Rashid and Kornberg, 2000). Both *Ps. aeruginosa* and *Ps. fluorescens* are highly adaptive organisms, which survive in a number of different environments. In nature, *Pseudomonas* strains reside in a soil based environment on the tips of plant roots. They are also known to be extremely opportunistic and are a major cause of fatal infections in immunocompromised hosts (de Bentzmann and Plésiat, 2011). We utilise two different types of bacteria as the results of Chapter 2 suggest changing the species of bacteria to a strain, which exhibits more pronounced, irregular, shapes of spread during their growth across agar plate surfaces.

In summary, the overall aim of this thesis is to investigate the spatial spread of microbial populations on two-dimensional agar plate surfaces and use this as a basis to investigate fundamental evolutionary ecology questions about the spatial spread of populations, in particular those consisting of invasive species. Our first goal is to challenge the classical assumption of constant rates of population spread, by demonstrating violations of this assumption in very simple biological systems. We then aim to determine the ecological drivers of deviation from constant rate of spread, and the evolutionary mechanisms that might favour non-constant, and even exotic, patterns of spatial spread.

Chapter 2

The spatial dynamics of biological invasions: when and why do model systems defy model predictions?

Abstract

The spread of invasive species is one of the most important issues in conservation, requiring accurate predictive models to help inform us of the most effective control methods to combat their threat. Predictive models of invasive species have classically used reaction-diffusion equations to represent the spread of populations. A key prediction made by these classic equations is a linear relationship between the population radius and time i.e. that the rate of radial spread is constant. While this simple relationship initially proved to be a robust prediction, recent empirical studies exhibiting non-constant rates of radial spread have called into question the reliability of these predictions.

Consequently, there is a demand for more empirical evidence to ascertain the reliability of the constant rate of spread prediction and the validity of the assumptions made during the formulation of these classical models. However, to date there have been difficulties collecting sufficiently high-resolution empirical data to test these predictions. Due to its success in evolutionary ecology, we believe the microbial model system is an ideal solution.

In this chapter, we measure the rate of radial spatial spread of biofilms consisting of the *Pseudomonas fluorescens* SBW25 WS and SM morphologies on different viscosity agars and we classify the rates as either constant, accelerating or decelerating. While 59.6% of colonies exhibit a constant rate of spread, 40.4% of colonies do not, with 17.6% and 22.8% of biofilms exhibiting an accelerating and decelerating rate of spread respectively. These results first agree with much of the literature by highlighting the unreliability of the constant rate of spread prediction. Secondly, these results illustrate the important influence of intrinsic and extrinsic factors upon the rate of spread, with some combinations more likely to result in accelerating rates of spread than others. We also find a relationship between the shape of spread and the rate of spread, with irregular patterns of spread typically exhibiting an accelerating rate of spread, possibly revealing a factor behind accelerating rates of spread not previously reported in the literature. Finally, this experiment illustrates the usefulness of bacteria as a model system in spatial ecology.

Introduction

The spread of an invasive species can have a devastating effect upon biodiversity (Sanders et al., 2003, Urban et al., 2008), often causing irreversible environmental damage (Pimentel et al., 2000, Danell, 1996, Keller et al., 2007). For example, the introduction and subsequent spread of the cane toad (*Bufo marinus*) across north east Australia has led to a depletion of native species that die eating the toxic cane toads; a depletion of native fauna preyed on by cane toads; and a reduction in prey populations for native species, significantly affecting the biodiversity and thus health of the ecosystem (Urban et al., 2007). As a result, one of the key interdisciplinary research issues in ecology is to determine the factors behind the establishment and spread of invasive species such that researchers can improve their ability to predict the spread of invasive species and thus help control them (Gurevitch and Padilla, 2004, Hastings et al., 2005). However, biological invasions are highly complex phenomena, often occurring across large spatio-temporal scales. While investigations to date have been successful at establishing a number of key factors affecting the invasive spread of a species, our understanding of the rate and spatial spread of these species is still limited (Higgins and Richardson, 1996).

A variety of predictive modelling approaches have been used to investigate the spatial spread of invasive species (Hastings et al., 2005). Predictive models are used by conservation managers to decide how best to allocate resources in order to prevent further expansion of an invading species (Tingley et al., 2013, Urban et al., 2007). One predictive modelling approach commonly used in classical studies of species spread is reaction-diffusion models (Hastings et al., 2005, Fisher, 1937, Skellam, 1951). Reaction-diffusion models represent the spatial and demographic processes behind the spread of the population via a system of partial differential equations (Higgins and Richardson, 1996).

$$\frac{\partial n}{\partial t} = f(n) + D\nabla^2 n \quad (2.1)$$

The classical reaction-diffusion equation (based on the Fisher-Kolmogorov equation (Fisher, 1937, Kolmogorov et al., 1937)) used to model population spread is shown by equation 2.1, where $f(n)$, D and n represents the population growth rate, the rate of diffusion and the population density respectively. This model represents the spatial spread of a population as an

interaction between the two parts, a reaction part, $f(n)$ representing the population growth rate and a diffusion part $D\nabla^2 n$ representing the movement of the population through the domain. This simple equation predicts the asymptotic (constant) rate of radial spread to be equal to $2\sqrt{f'(0)D}$, where $f'(0)$ is the population growth rate of a species f at time 0 and D is the rate of diffusion (Richardson and Pyšek, 2008, Bramson, 1983). This result first predicts that the rate of radial spread depends upon simple life history characteristics. Secondly, it predicts a constant radial rate of population spread (i.e. the radial spatial spread of a population is a linear function of time) (Hastings et al., 2005, Skellam, 1951) (figure 2.1). Whilst the constant rate of spread prediction of this classical reaction-diffusion equation has seemingly proved to be a successful representation of the spread for a number of populations (Andow et al., 1990, Skellam, 1951, Lubina and Levin, 1988), recent studies have shown that the predictions of this classical model can significantly underestimate the rate of spread of many invasive populations, many of whom seem to exhibit increasing radial rates of spread i.e. not constant (Shigesada, 1997, Silva et al., 2002, Kot et al., 1996, Shigesada and Kawasaki, 2002, Hastings et al., 2005).

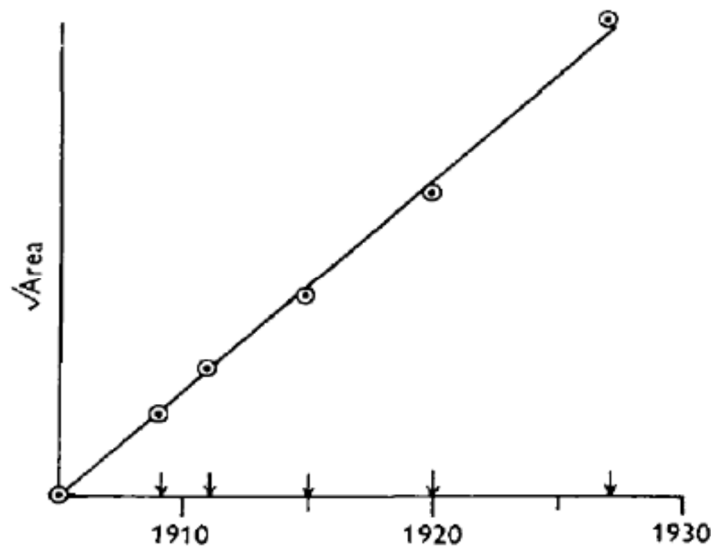


Figure 2.1: The radial range ($\sqrt{\text{area}}$) of muskrat spread increases at a constant rate through time during its invasion of central Europe after its introduction in 1905. Taken with permission from Skellam (1951).

The constant rate of radial spread prediction arises due to a number of assumptions made by these classical reaction-diffusion equations (Fisher, 1937, Kolmogorov et al., 1937, Higgins and Richardson, 1996, Skellam, 1951, Hastings, 1996). First, these reaction-diffusion equations assume the population

has no intrinsic variation amongst individuals i.e. they assume each individual moves and reproduces at the same rate through time and space. Secondly, these models assume the movement of individuals is not directed, with individuals able to move in any direction with equal probability i.e. by Brownian motion (Hastings et al., 2005). Finally, these assumptions do not represent possible environmental variation such as habitat heterogeneity (Hastings et al., 2005).

In empirical studies, researchers have begun to discover that some of the processes neglected in the formulation of the classical Fisher-Kolmogorov reaction-diffusion equations can result in accelerating or decelerating rates of spread (Urban et al., 2008, Hastings et al., 2005). For instance, studies into the spread of the invasive cane toad mentioned earlier, have shown how rapid adaptive evolution of dispersal mechanisms (namely longer legs arising via a spatial sorting process) results in an accelerating rate of spread (Phillips et al., 2006). Additionally, cane toads have accelerated their rate of spread by adapting their traits to the extremes of the heterogeneous habitat due to being released from the threat of native predators in these extremes (Urban et al., 2007). Other examples of intrinsic stochasticity affecting the dynamics of invasive spread include random long-range dispersal events (Suarez et al., 2001) and phenotypic plasticity (Hanfling and Kollmann, 2002). Ignoring the effect of these intrinsic and extrinsic factors can lead to errors in predictions of invasion rate, possibly resulting in cases where it becomes too late to take the action required to prevent the negative impacts associated with invasive species (Sharov et al., 2002, Tobin et al., 2004, Davey and O'Toole, 2000). In order to improve our ability to control the spread of invasive species, the assumptions made by classical models and their subsequent predictions must be empirically examined for a range of species to understand which factors impact the invasion dynamics, in what way these factors affect invasion dynamics and their significance (Wittenberg, 2001).

Empirically measuring the spatial spread of population can be a difficult and time consuming task in macro-organism populations, with data often low-resolution due to the methods used to capture data (Kokko and Lopez-Sepulcre, 2006). However, microbial aggregations on surfaces (called biofilms) provide a novel system from which we can readily observe various ecological

characteristics of spatial spread at high resolution without many of the difficulties commonly encountered by other empirical studies of invasive spread involving macro-organisms (Buckling et al., 2009). This is due to the array of benefits offered by microbial systems, in particular the overall control researchers have over the intrinsic and extrinsic aspects of the system (Buckling et al., 2009). Indeed, due to these benefits, studies have used the microbial model in a wide number of ways. For example, *Pseudomonas fluorescens*, a plant colonizing bacterium, is a commonly used microbial model system (Brading et al., 1995, Simoes et al., 2005, Ramsayer, 2012). Because of *Ps. fluorescens*' ability to diversify and generate a range of niche specialist genotypes in a spatially heterogeneous but controllable environment, the wild-type strain of *Ps. fluorescens* SBW25, has been used to effectively study the effect of adaptive radiation and evolution (Rainey and Travisano, 1998, Spiers, 2007). In static liquid microcosms, *Ps. fluorescens* strain SBW25 develops three niche specialists: a Wrinkly Spreader (WS) morphology at the top, a Smooth (SM) morphology in the middle and a Fuzzy spreader (FS) morphology at the bottom. Studies name these the WS, SM and FS morphologies after the distinguishable wrinkly, smooth or fuzzy pattern exhibited on agar plate surfaces by each colony respectively. The difference between the patterns produced by the WS morphology and the SM morphology is due to the production of extra cellulose machinery by the WS morphology during colonization of the air-liquid interface to increase oxygen intake (Spiers et al., 2003, Spiers and Rainey, 2005). While this cellulose machinery improves the fitness of the WS morphology in the static microcosm, it is maladaptive on agar plate surfaces, causing the WS morphology to exhibit a slower cellular growth rate compared to the SM morphology (Spiers, 2007). Consequently, when faced with an agar plate environment, the WS morphology reverts to a SM-like morphology with an increased cellular growth rate to improve its ecological success, providing a clear illustration of how the environment can affect the ecological and evolutionary characteristics of a population (Spiers, 2007). Moreover, this demonstrates how the microbial model system is a diverse and powerful tool for studying the links between ecology and evolution.

The constitution of the environment can affect the spatial dynamics of microbial growth across surfaces (Kearns, 2010, Matsuyama and Matsushita, 1993,

Golding et al., 1998). For example, in an agar plate environment, the agar concentration of the growth medium affects the viscosity of the agar plate surface, which in turn affects the type of motility used by bacteria within the colony (Murray and Kazmierczak, 2008, Mitchell and Wimpenny, 1997, Taylor and Buckling, 2011). The type of motility affects the pattern of spatial spread produced by bacterial colonies during colonisation of agar plate surfaces, with patterns of spatial spread ranging from circular patterns of spread on hard agar surfaces to irregular, non-circular patterns of spread on softer agar surfaces (Kearns, 2010). Some strains of *Ps. fluorescens* have been shown to exhibit irregular patterns (Sanchez-Contreras et al., 2002, Pechy-Tarr et al., 2005) making it potentially a useful system for studying irregular spatial invasion dynamics that we have not considered in macro-organism populations. While we believe that the microbial model system can help researchers understand more about the factors affecting the spatial dynamics of populations, the microbial model system has been relatively underutilised in spatial ecology. Consequently, we require more studies to demonstrate the usefulness of the microbial model system with regard to spatial ecology.

While the microbial model system could offer a new perspective in the study of spatial ecology, understanding the invasion dynamics of microbial species is potentially useful in its own right. For instance, the ever-increasing resistance of bacteria to antibiotics has alerted us to the need of developing a deeper understanding of how bacteria prosper across an array of environments (Ben-Jacob and Levine, 2006). The development of strategies to control microbial spatial spread could be extremely useful against the spread of bacterial biofilms across artificial joints (Ehrlich et al., 2005), the colonisation of compromised organs (Oliver et al., 2000) or against the growth of cancerous tumours (which exhibit spread dynamics similar to bacterial biofilms) (Korolev et al., 2014).

In this study, we propagate the WS and SM morphologies of *Ps. fluorescens* strain SBW25 on environments with different agar concentrations to investigate how intrinsic and extrinsic factors affect the spatial spread of invasive biofilms. We explore the relationship between the radial range of spread (measured as $\sqrt{\text{area}}$ consistent with (Skellam, 1951)) and time, to determine whether the constant radial rate of spread prediction (i.e. a linear relationship between radial

spread and time) made by the classical Fisher-Kolmogorov reaction-diffusion models, matches the spatial dynamics exhibited by these microbial populations. We hypothesize the constant radial rate of spread prediction to be incorrect in this system due to two possible factors:

1. Bacteria are able to adapt in ecological time to their environment, thereby introducing changes to the reproduction and movement rates of individuals within the population (Spiers, 2007).
2. Bacteria often grow in irregular shaped colonies, which the classic reaction-diffusion equations are unable to describe without introducing non-linear diffusion coefficients dependent upon the densities of the population and nutrients (Mimura et al., 2000).

With these hypotheses in mind, we measure the effect of the extrinsic factor, agar concentration (viscosity) and the intrinsic factor, morphology type, upon both the radial rate of spread and the geometry (circularity) of bacterial colonies to analyse how these factors affect the invasion dynamics of *Ps. fluorescens*. Moreover, we aim to demonstrate the usefulness of the microbial model system to spatial ecology.

Methods

Isolation of the WS and SM genotypes

We cultured a frozen glycerol stock population of *Ps. fluorescens* wild type strain SBW25 (kept at -80°C) overnight in twelve sterile tubes containing 5ml of King's B Medium (KB) (10g Glycerol, 20g Proteose Peptone No 3, 1.5g K₂HPO₄·3H₂O and 1.5g MgSO₄·7H₂O (w/v)) (King et al. 1954) at 28°C in an orbital shaker set at 250 rpm. To promote the rapid diversification of phenotypes, we passaged a 50µl sample of each of the twelve cultured populations into twelve separate 25ml sterile glass vials each containing 5 ml of KB medium. The 12 glass vial microcosms were statically incubated for seven days at 28°C with the lids loosely attached with porous tape to allow oxygen flow (consistent with (Rainey and Travisano, 1998)).

After seven days, we isolated one wrinkly spreader morphology (WS) and one smooth spreader morphology (SM) from each microcosm. To isolate a WS genotype, we took a 100µl sample of the biofilm found at the air-liquid interface of each static microcosm and diluted by a 1:10 ratio. We achieved this dilution

by adding the 100µl sample to a sterile 1.5ml eppendorf containing 900µl of KB medium. We repeated the dilution five times to achieve a dilution with a ratio 1:100000. 50µl of each diluted sample was plated and spread onto the surface of a 1.2% (w/v) KB agar plate (KB medium with 12g/l agar powder added).

We incubated these agar plates at 28°C for approximately twenty-four hours (such that individual colonies had sufficiently established themselves on the agar). For each of the twelve populations, we selected and isolated one established WS genotype colony from the agar plate. We then passaged each isolated colony into a sterile tube containing 5ml of KB and cultured overnight in an orbital shaker at 28°C on 250 rpm. At this point, each of the 12 cultures achieved an optical density around 1.6 OD (approximately 1.6×10^{10} bacteria per ml). The genotypes were archived at -80°C in a 20% (v/v) glycerol solution. We used the same process to isolate 12 SM genotypes, with the exception that we took the samples from the middle portion of the microcosm (rather than the top portion of the microcosm for the WS morphology (see figure 2.2)).

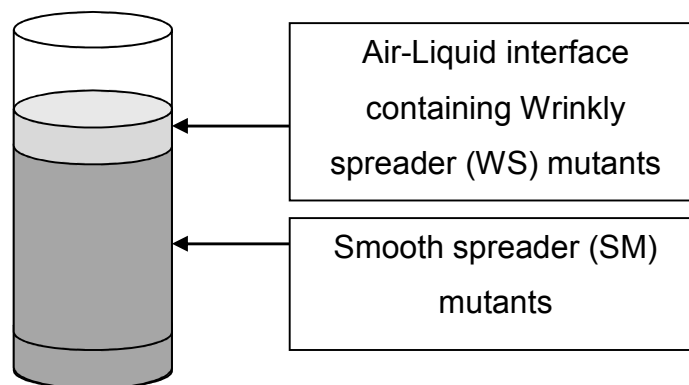


Figure 2.2: We took samples from certain areas of the static microcosm in order to isolate WS and SM mutants.

Experimental Design

We used three concentrations of King's Agar (King's Medium B with either 0.5%, 0.75% or 1% (w/v) of agar added) (King et al., 1954) to test the effect of surface solidity upon the invasion dynamics of *Ps. fluorescens* morphologies. We inoculated each of the twelve WS genotypes and twelve SM genotypes onto the centre of 30 agar plates, 10 replicate agar plates of each of the three agar concentrations (figure 2.3).

Agar plates were prepared the day before by first allowing them to dry for 15-20 minutes under an airflow hood and then leaving them overnight at room temperature. We allowed plates to dry for 10 minutes before inoculation and for a further 15 minutes after inoculation. After inoculation, we placed agar plates in an incubator set at 28°C. Starting from 6 hours after inoculation, we captured the invasion dynamics of each colony by taking photographs every 3 hours until 30 hours had elapsed. We took pictures using a Canon EOS 600D SLR digital camera on a background lit by a LP554 Hama light box in a dark room (See figure 2.4 – left image).

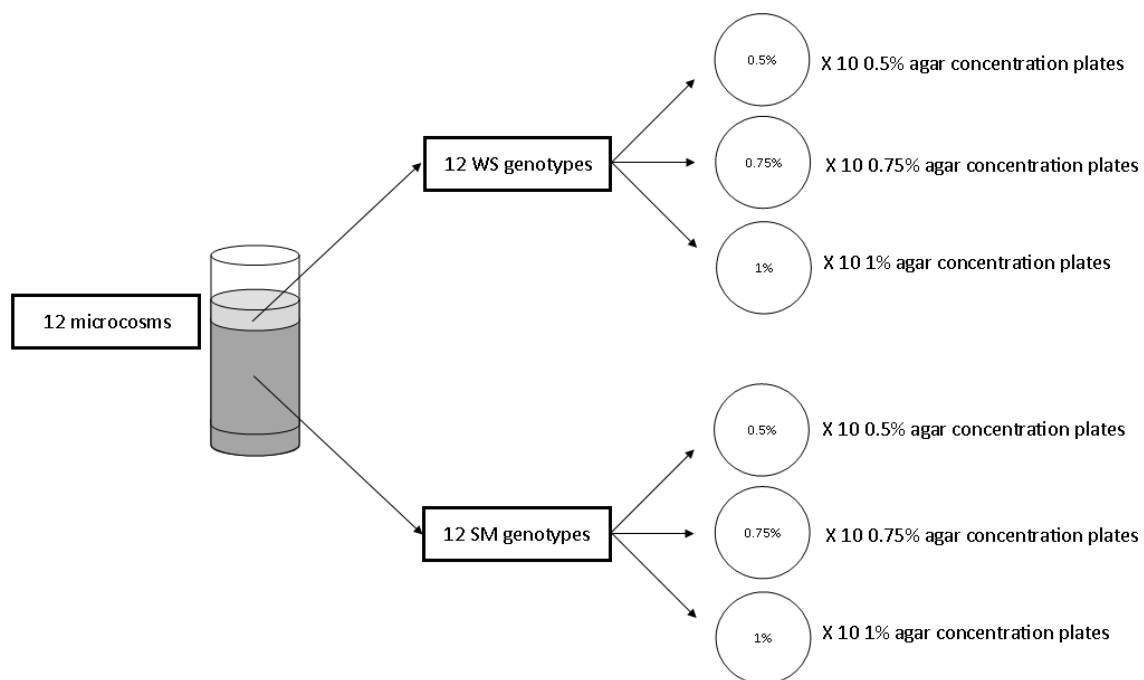


Figure 2.3: An overview of the experimental design. The 12 genotypes of the WS and SM morphologies of *Ps. fluorescens* were inoculated onto 10 replicate plates of each of the three agar concentrations. In total, there was 720 colonies.

Image Analysis Process

To derive the characteristics of the colony, we utilised an automated image analysis script. This script utilised six different thresholds to differentiate the bacterial colony from the agar plate background (We describe the thresholds in Appendix A) and then converting the pictures of bacterial spread into binary images (figure 2.4 - right). We judged the six resultant binary images from these thresholds by eye, with the most accurate one chosen to represent the colony at that point in time. If none of the six resultant images were suitable, then for as many pictures as possible, we obtained the binary image via a manual threshold using the threshold command in Adobe Photoshop CS6. Failure of the

automated image analysis script occurred either when the spatial spread of the biofilm was very faint against the agar backdrop or when the light-box background distorted the image (See discussion).

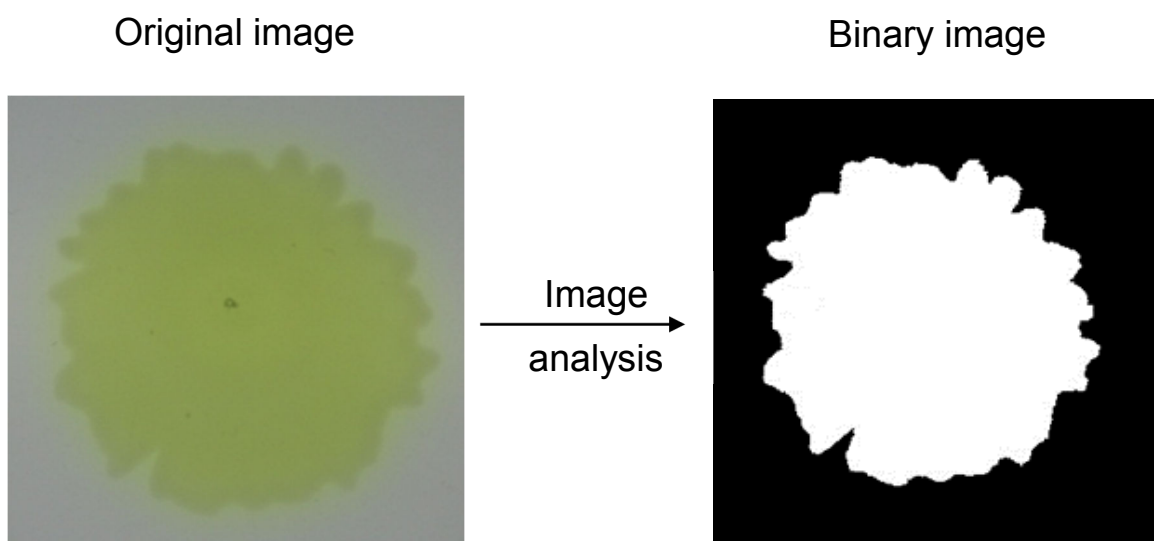


Figure 2.4: (Left) A *Ps. fluorescens* WS biofilm exhibiting a non-circular pattern of spread as it grows on 0.75% agar. Note that we took this photo 24 hours after inoculation. (Right) The resultant binary image produced when the left image is processed using the automated image analysis script.

In order to measure various physical properties of the colony, the binary images were processed in R version 2.13.0 (R Development Core Team, 2014) via the R image analysis package EBImage v3.8 (Sklyar et al., 2014). The measurable characteristics used in this study were:

- a) The area occupied by the colony (measured in pixels – there were 41.16 pixels per mm²)
- b) The perimeter of the colony (measured in pixels)
- c) The circularity of the colony. This was a normalised measurement using physical characteristics of the colony to quantify how irregular the shape of colony is. Circularity was calculated by the following:

$$\text{Circularity} = \frac{4\pi A}{p^2}$$

Where A equals the area occupied by the colony and p was the length of the colony's perimeter. A colony is a perfect circle when this circularity value is equal to 1 and not at all circular when this value was equal to 0.

Statistical Analyses

Statistical analyses were performed using R 3.0.3 (R Development Core Team, 2014). We note that due to some replicates being unusable (either through contamination, through us dropping the plates or by images being difficult to analyse), we only used those time-series of microbial spread with more than three time points in the analyses. Consequently, we discarded nine out of the 720 time series obtained during analysis. To see the rate of microbial spread, we created plots of the change of radial area against time by aggregating the radial area (\sqrt{area}) of all replications for each combination of genotype, agar concentration and morphology type. To make the plots representative of the microbial spread, if a colony had colonised the total plate, we substituted a value representing the area of the plate in its place. Note that we did not use these dummy values or these aggregated values in the statistical tests.

As part of our analyses, we examined whether different genotypes of a phenotype respond to the environmental variation in different ways i.e. whether there was an interaction between the effect of genotype and environment. This interaction is known as a genotype-environment (GxE) interaction (Leggett et al., 2013). To test whether there was a possible GxE interaction, we considered the average rate of spread of each genotype as a trait. For each genotype replicate, we used GLMs with Gaussian error structures to find the linear coefficients for the rate of spread through time. We plotted each genotype's aggregated average rate of spread coefficient against the agar concentration to create a reaction norm to visualise the effect of the morphology and environment upon the average rate of spread for all genotypes. Additionally, to visualise whether some genotypes had a GxE response, we normalised coefficients by dividing each rate coefficient by the average linear coefficient for each morphology and subtracting 1 to make 0 the mean rate of spread for each morphology type.

To determine whether a linear or a non-linear relationship between time and the radial range of spread (\sqrt{area}) best described the spread dynamics of *Ps. fluorescens* colonies, we tested whether a GLM with both linear and quadratic terms (the quadratic term accounted for any nonlinearity in the relationship between time and the range of spread) fitted the time series significantly better

than a GLM with just linear terms. We determined the significance of the quadratic term by standard model-simplification F-ratio tests. The quadratic and linear slope coefficients were extracted from these GLMs. Using p-values from the two GLMs and the quadratic and linear coefficients, we calculated the proportion of colonies that spread at constant (non-significant quadratic term), accelerating (significant, positive quadratic term) and decelerating rates (significant, negative quadratic term) of spread (table 2.1).

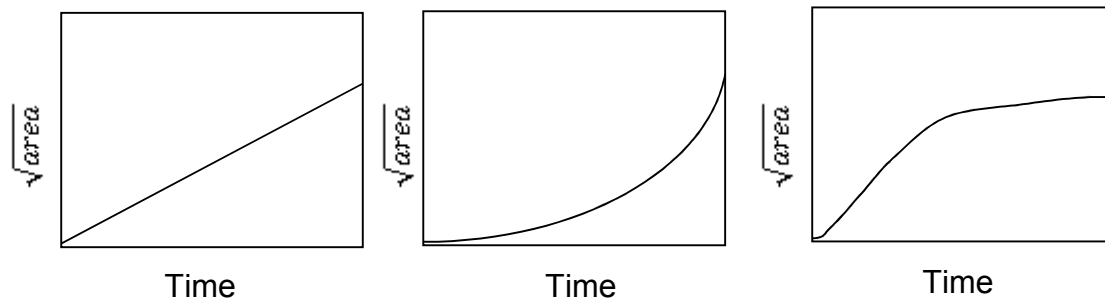


Figure 2.5: Illustrative figures representing the three categories used to measure the rate of spread of each colony. (Left) Colonies with a constant rate of spread. (Middle) Colonies with a significantly accelerating rate of spread. (Right) Colonies with a significantly decelerating rate of spread.

To analyse the effect of morphology and agar concentration upon the probability of a colony exhibiting accelerating dynamics, we used a GLM with quasi-binomial error structures and model simplification using F-tests. F-tests combined with quasi-binomial error structures were used due to the over dispersion of data when using chi-squared tests with binomial error structures. We also used a GLM with Gaussian error structures to detect the effect of agar concentration and morphology upon the difference in circularity between the start- and end-point of a measured time series. Finally, we used a GLM with Gaussian error structures to detect whether those colonies with the largest decreases in circularity are also those that accelerate through time. To see how circularity changed through time, we created plots by aggregating the circularity of all replicates for each combination of genotype, agar concentration and morphology type.

Results

The relationship between spread range and time

We found distinct variation in radial spread amongst colonies through time, with effects seen at the agar concentration, morphology and genotype levels (figure 2.6). Indeed, using the average rate of dispersal as a measurable trait, we found the majority of SM morphologies dispersed faster than WS morphologies across all agar concentrations (figure 2.7). Furthermore, we found dispersal speed decreased as the agar concentration increased, with the rate of spread advantage obtained by the SM morphology narrowing as agar concentration increased (figure 2.7). Continuing to use the average rate of dispersal as a trait, the GxE reaction norm showed a significant interaction between agar concentration, morphology type and genotype (GLM, $F_{22,639}=13.586$, $p<0.0001$, figure 2.8). Whilst the majority of SM genotypes dispersed faster than WS genotypes (the effect of morphology), there were two SM genotypes, which were consistently poor dispersers in all environments, thereby revealing the effect of genotype (figure 2.8). Focusing upon the interaction between the agar environment and the genotype revealed some cases of GxE interactions, with some genotypes showing a preference for dispersing in certain environments over others (as shown by the intersecting isoclines in figure 2.8).

We found the rate of spread of the bacterial colonies through time exhibited both constant and non-constant dynamics, with accelerating, decelerating and constant rates of spread all detected. In total, 59.63% of bacterial colonies exhibited a constant rate of spread while 17.58% and 22.78% of colonies exhibited accelerating and decelerating rates of spread respectively (table 2.1). We found that the probability of a colony exhibiting an accelerating rate of spread was significantly affected by an interaction between agar concentration and morphology (GLM: $F_{2,705} = 35.231$, $p<0.001$, figure 2.9). In general, there was a low (below ~15% chance) probability of colonies exhibiting an accelerating spread except for the WS morphology on 0.5% agar, which had a 65-70% chance of exhibiting an accelerating rate of spread.

Table 2.1: Top row: the overall proportion of the colonies exhibiting constant, significantly accelerating or significantly decelerating rates of spread. Bottom rows: the percentage of colonies, which exhibited constant, significantly accelerating or significantly decelerating rates of spread for each morphology and agar concentration.

	Proportion with a constant rate of dispersal			Proportion with a significantly accelerating rate of dispersal			Proportion with a significantly decelerating rate of dispersal		
Overall	59.63%			17.58%			22.78%		
Agar Conc.	0.5%	0.75%	1%	0.5%	0.75%	1%	0.5%	0.75%	1%
WS	32.77%	55%	55.83%	67.22%	6.67%	0.83%	0%	38.33%	43.33%
SM	85.71%	63.16%	65.55%	11.76%	3.51%	15.13%	2.52%	33.33%	19.32%

The relationship between circularity of the spread and time

In general, there was a decline in the circularity of colonies through time, suggesting patterns became more irregular as time increased (figure 2.10). We found a significant interaction between agar concentration and morphology for the change in circularity between the start and end points of each time series (GLM: $F_{2,705} = 79.443$, $p < 0.001$, figure 2.11). This interaction arose because of the significantly larger decrease in circularity for those WS morphologies spreading across 0.5% concentration agar compared to other combinations. We note that those colonies with the largest decreases in circularity (typically WS morphology in 0.5% agar) were also those which exhibited accelerating radial rates of spread (GLM: $F_{1,709} = 113.03$, $p < 0.001$), suggesting a relationship between accelerating rates of population spread and irregular shapes of spread.

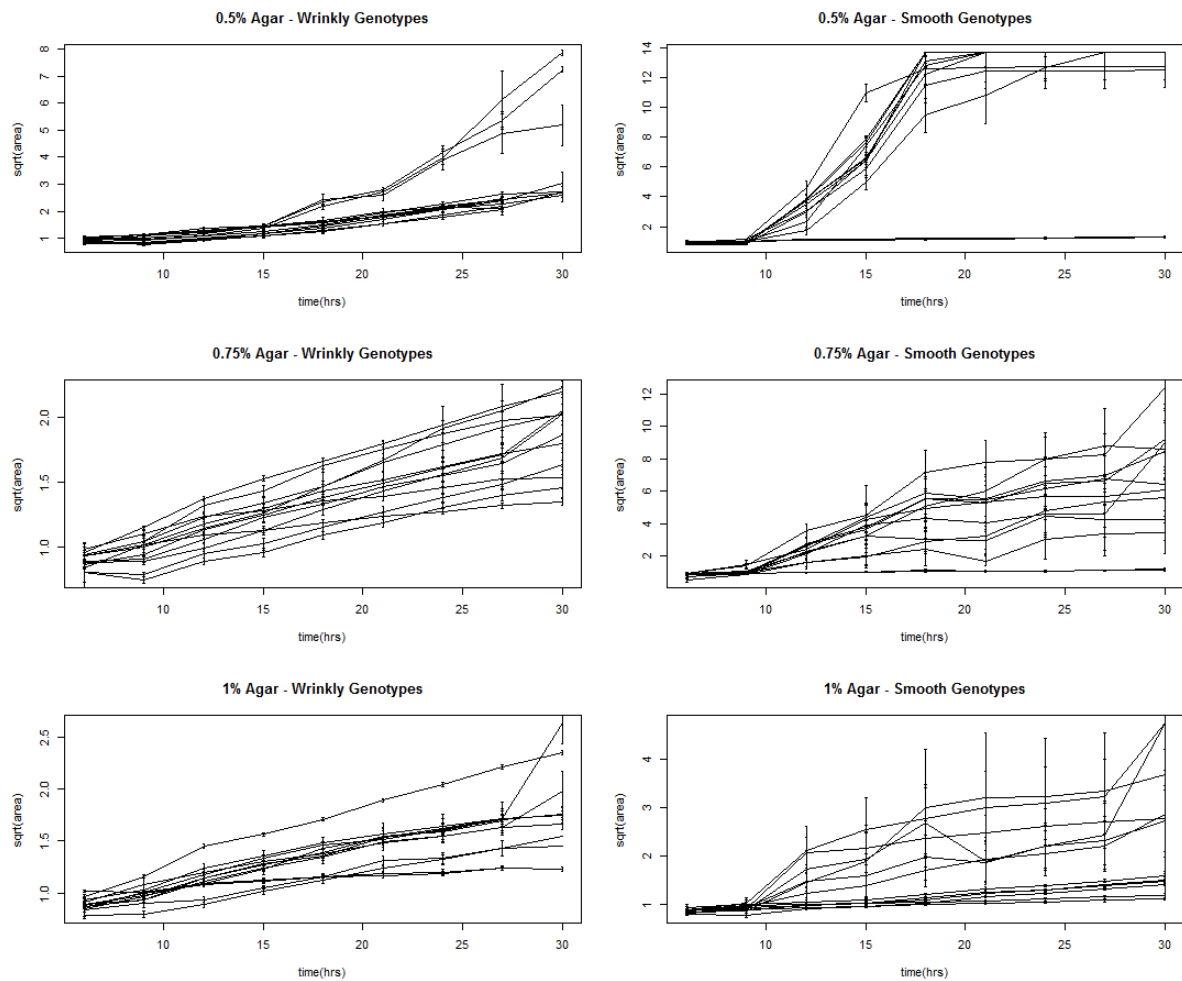


Figure 2.6: The change of radial area ($\sqrt{\text{area}}$) against time (hour) for each colony, categorised according to morphology and the agar concentration of the environment. We measured area in mm^2 . Each line is the aggregated spread for each genotype up to hour 30 (± 1 SE). For the purpose of this plot, where the colony reaches the edge of the plate, we substituted a value representing the area of the plate. Due to missing data points, the aggregation of area for each genotype can result in some lines showing a decrease in area through some time points.

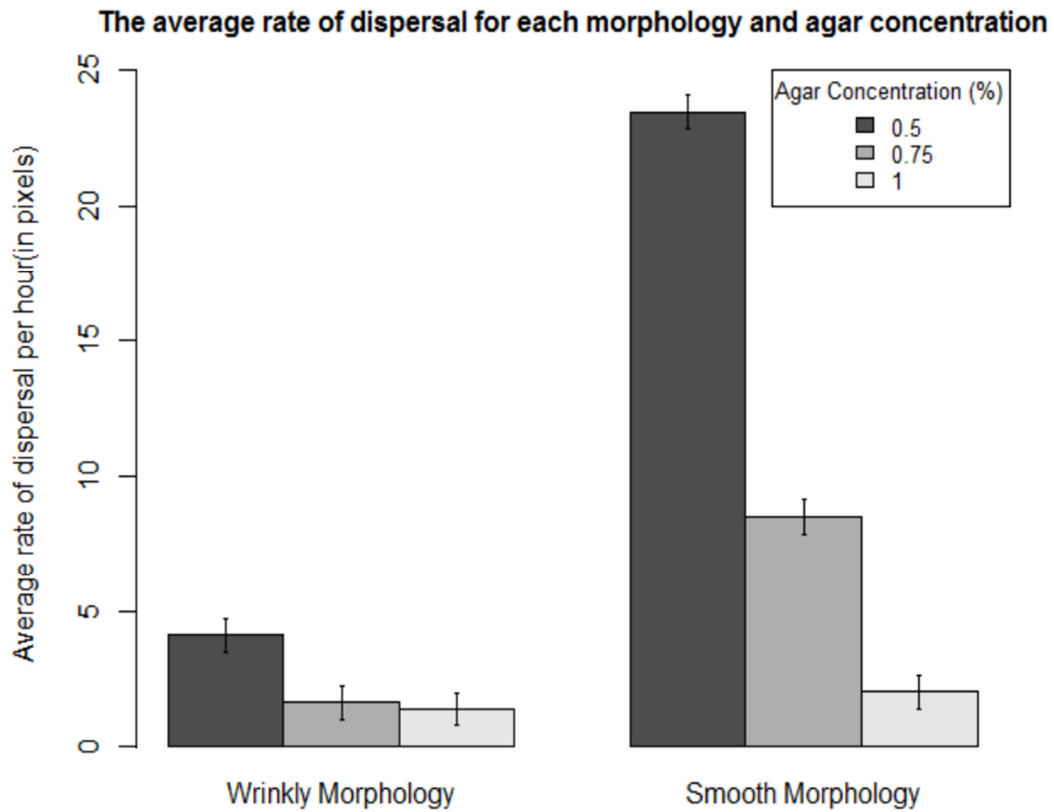
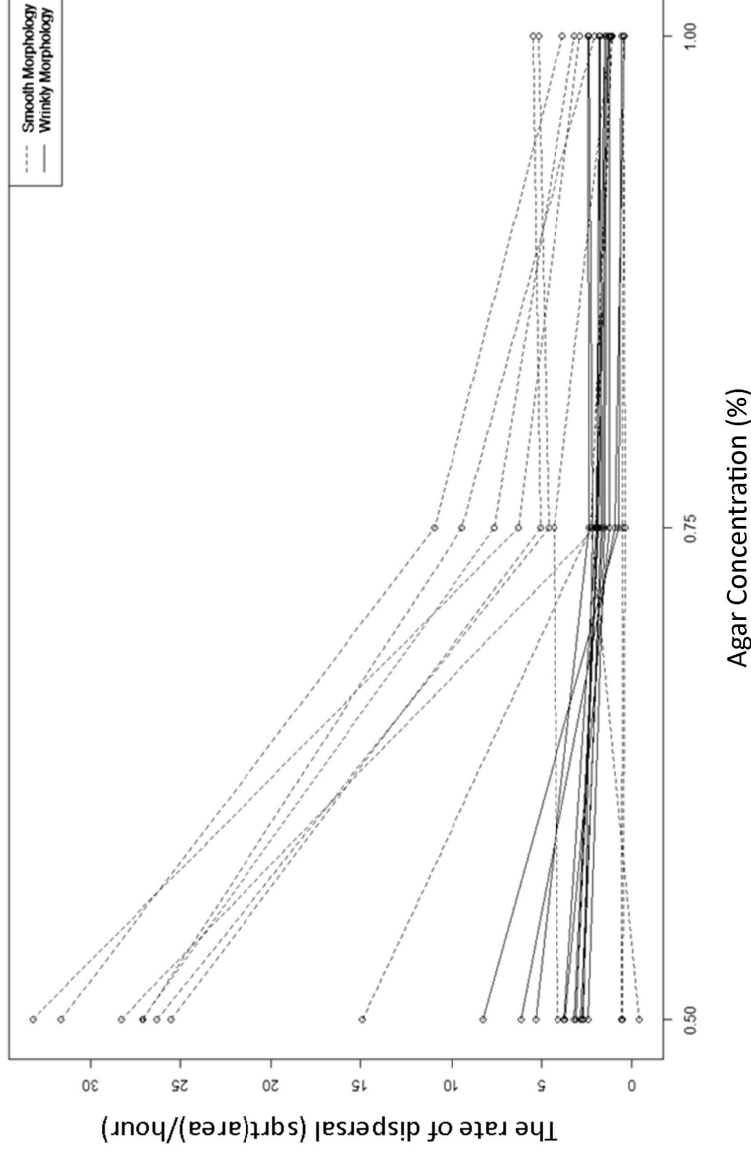
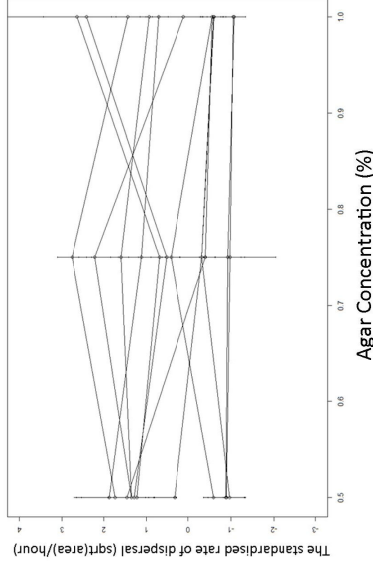


Figure 2.7: The average rate of dispersal for each combination of agar concentration and morphology (± 1 SE). As agar concentration increased, the rate of dispersal decreased. There was also a clear difference between morphologies as the SM (smooth) morphology disperses faster than the WS (wrinkly) morphology in 0.5-0.75% agar concentration environments. At 1% there is no significant different between the two morphologies.

GxE plot of bacteria dispersal on different types of Agar



A standardised GxE plot showing the effect of agar upon the rate of dispersal: Smooth Morphology



A standardised GxE plot showing the effect of agar upon the rate of dispersal: Wrinkly Morphology

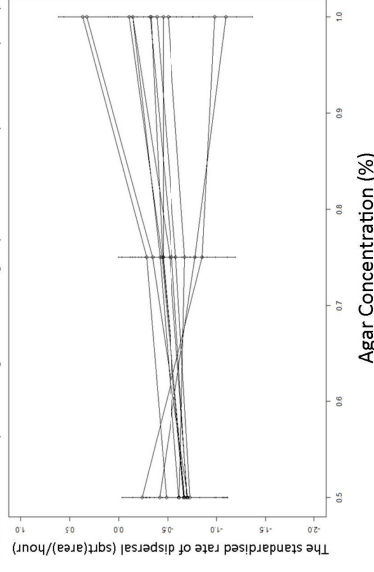


Figure 2.8: (Left) Reaction norm graph showing the extrinsic effect of agar concentration upon the average rate of dispersal for each of the 12 evolved wrinkly and smooth morphology genotypes. We notice the majority of SM morphologies have a faster rate of dispersal than the WS morphologies, with a significant reduction in average rate of spread as agar concentration increases. (Top right) The effect of agar concentration upon the rate of dispersal for each SM genotype via a standardised reaction norm graph (± 1 SE). Many genotypes exhibited a relatively consistent rate of spread across all environments, i.e. they were either relatively fast growing in all environments or slow slowing in all environments. However, some genotypes displayed a plastic response to their agar conditions suggesting a GxE interaction. (Bottom right) The effect of agar concentration upon the rate of dispersal for each WS genotype via a standardised reaction norm graph (± 1 SE). As in the WS morphology, genotypes generally exhibited a consistent rate of spread across all environments, however two genotypes in particular which exhibited relatively fast rates of spread in 0.5%, were relatively noticeably slower than their counterparts in higher agar concentrations.

The probability of a genotype having a significantly accelerating spread in each agar environment

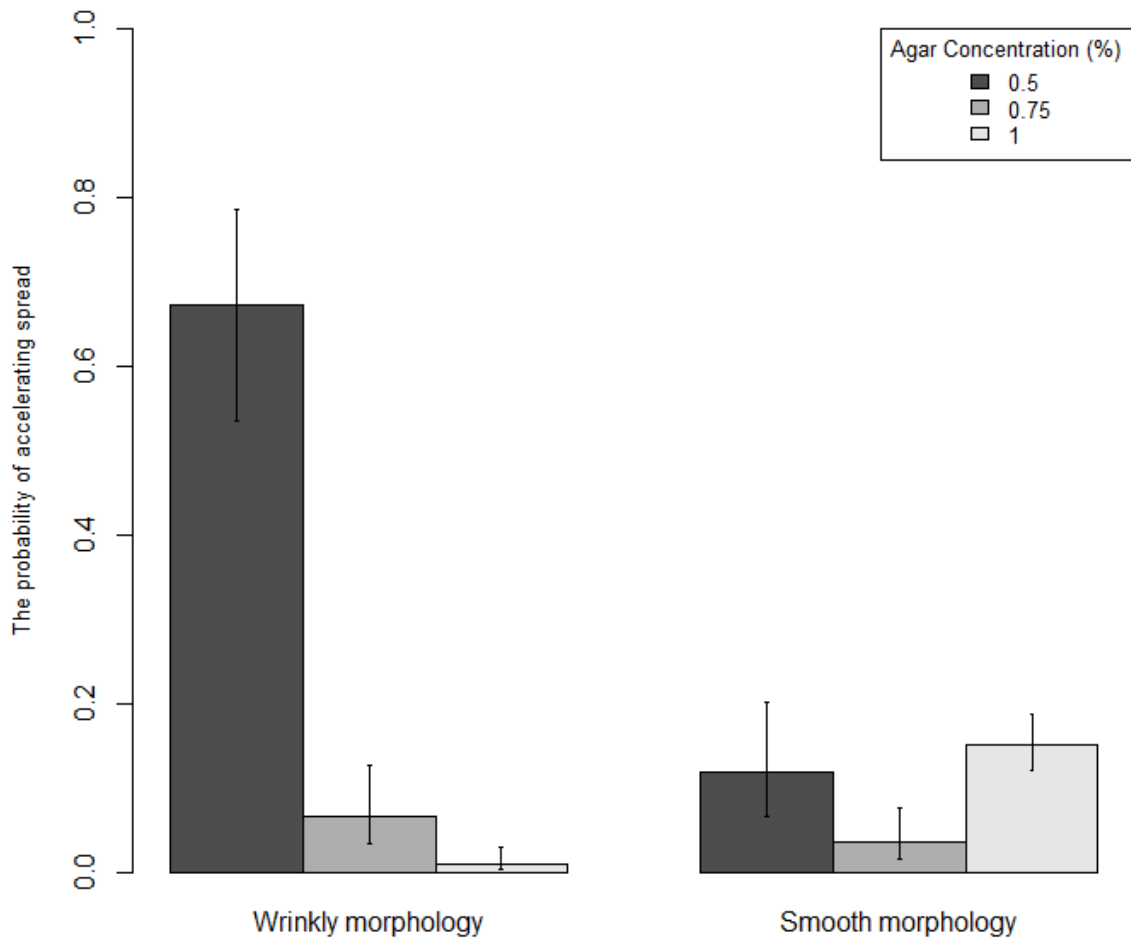


Figure 2.9: The probability of a significantly accelerating spread for the WS (wrinkly) and SM (smooth) morphologies in 0.5%, 0.75% and 1% agar concentrations (± 1 SE). There was a noticeably larger probability of a WS morphology exhibiting accelerating rate of spread in a 0.5% agar concentration compared to other agar concentration/morphology combinations.

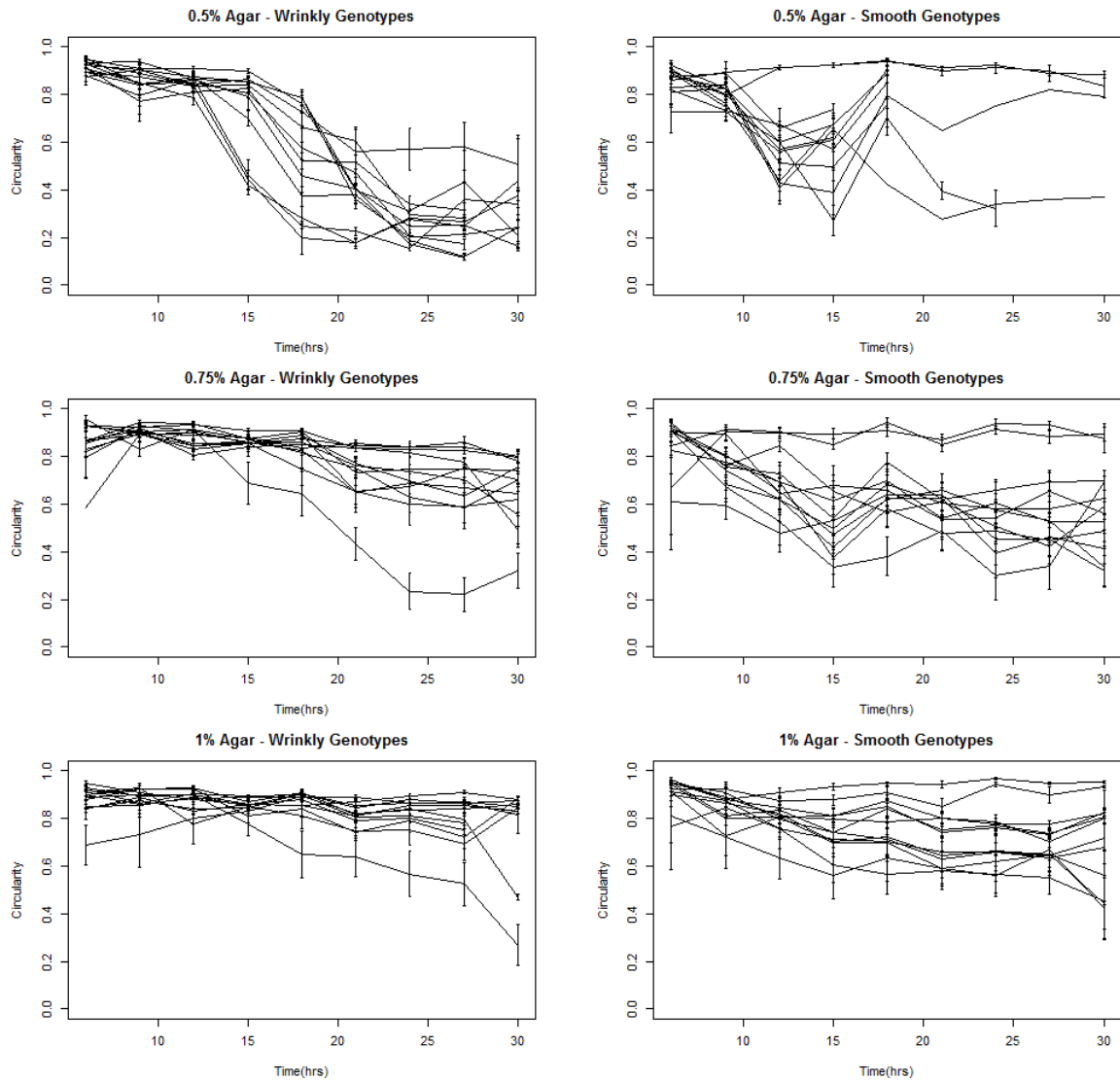


Figure 2.10: The aggregated circularity of each genotype through time (hr) for the 12 WS and 12 SM morphologies (graphs on the left and right respectively) upon the three different agar environments. From the relatively circular colonies at hour 6, we saw a general decline, with the greatest decline exhibited by the WS morphology in 0.5% agar concentration plates.

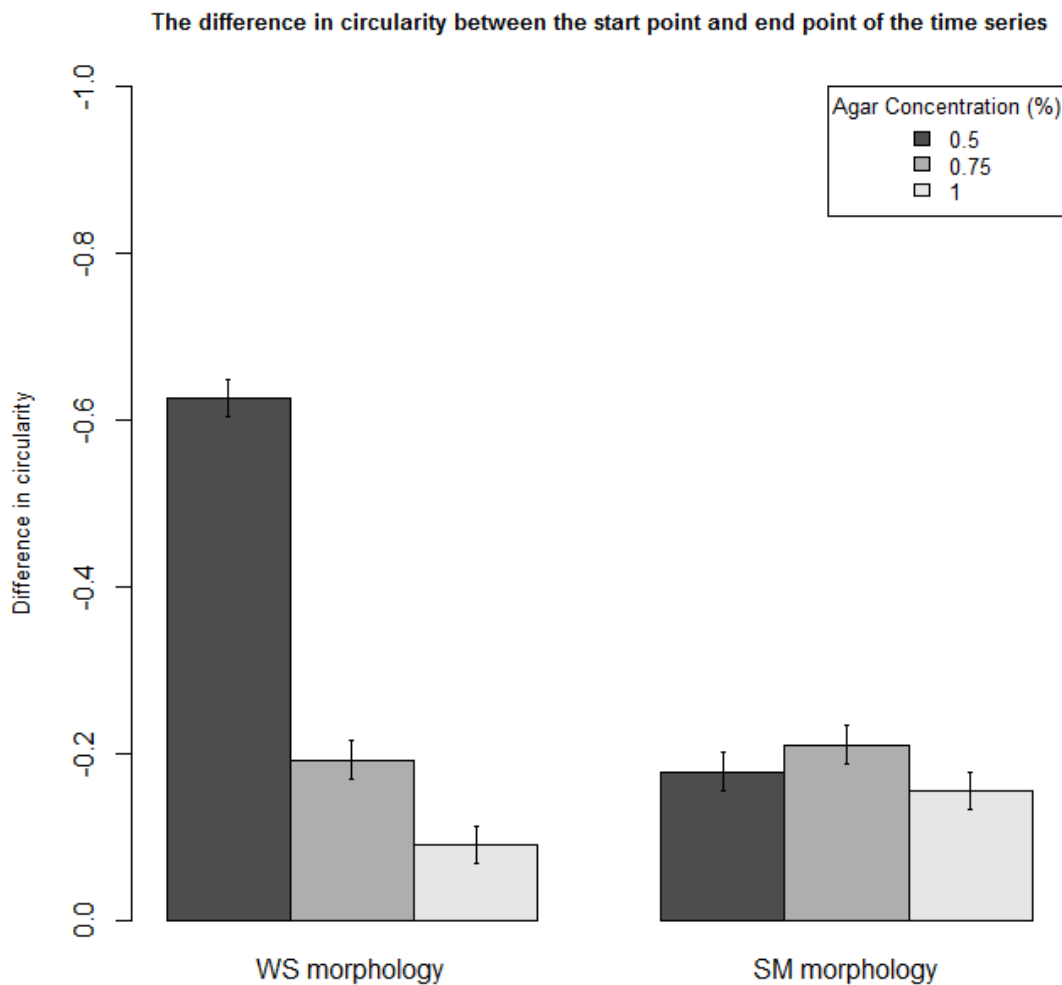


Figure 2.11: The change in circularity between the start point and end point of a time series. Noticeably, there was a larger change in circularity in WS morphologies grown in 0.5% agar than in other agar concentration/morphology combinations.

Discussion

Reaction-diffusion equations have been the classical modelling approach used in spatial ecology to predict the spatial dynamics of invasive spread (Hastings et al., 2005). These approaches have had mixed results, with erroneous predictions thought to arise because of the overly simplistic assumptions made by these classical reaction-diffusion equations in their formulation (Clark et al., 2001). A particular prediction of these classical models was that the radial range of population spread could be represented as a linear function of time i.e. a constant radial rate of spread (Hastings, 1996, Hastings et al., 2005). Whilst the evidence at the time these models were formulated suggested that such a prediction was reasonably reliable, recent evidence has suggested otherwise (Hastings et al., 2005). Subsequently, researchers believe we require more evidence from a range of populations to establish the factors affecting the rate of spread in order to improve our predictive models (Wittenberg, 2001). Whilst

spatial ecology has typically only used macroorganism populations, we believed that the microbial model system could provide researchers with a novel means to investigate the spatial spread of populations. Subsequently, the aims of this study was to investigate the spatial dynamics of microbial spatial spread across agar plates, in particular the reliability of the constant rate of spread prediction as predicted by these reaction-diffusion equations and to demonstrate the possible application of the microbial system to spatial ecology.

Our results showed that intrinsic genetic factors and extrinsic environmental factors influence the spread dynamics of *Ps. fluorescens* biofilms through time, thereby clarifying the combined influence of genotype/phenotype and environment upon *Ps. fluorescens* microbial spread. Specifically, we illustrated how some combinations of these factors can cause microbial spatial spread to exhibit both accelerating and decelerating rates of spread (i.e. the radial range of spread is a non-linear function of time), with colonies consisting of the WS morphology grown upon soft 0.5% agar environments the most likely to exhibit accelerating rates of spread. In addition, the results demonstrated a relationship between a colony exhibiting an accelerating rate of spread and the circularity of the colony, with those colonies exhibiting an accelerating rate of spread (notably those consisting of the WS morphology when grown on soft 0.5% agar) also exhibiting the largest decrease in circularity.

After classifying 711 colonies (720 in total minus the 9 for which there was not enough time points or were spoiled) we found that 59.6% of biofilms exhibited a constant rate of spread. More importantly, 40.4% of colonies exhibited a non-constant rate of spread, with 17.58% and 22.78% of biofilms exhibiting an accelerating and decelerating rate of spread respectively. This result demonstrates that while the constant rate of spread prediction arising from these classical reaction-diffusion models is suitable for many populations, the relatively high probability that the rate is not constant suggests that the predictions made by these classical reaction-diffusion equations are unreliable, agreeing with the discourse from empirical results based on other macroorganism model systems (Andow et al., 1993, Silva et al., 2002, Shigesada and Kawasaki, 2002, Hastings et al., 2005). The unreliability of these classical models could have significant consequences for the effectiveness of

invasive species management strategies, as the effectiveness of the control methods used to counter the spread of invasive species are at their best in the earlier stages of establishment (Mack et al., 2000). Subsequently, underestimating the spread of a species may result in invasive species establishing themselves to such an extent that conservation managers have little to no ability to effectively control their effect upon the ecosystem they have invaded. This could have a destabilising effect on the ecosystem, possibly leading to a decrease in biodiversity (important for a number of ecosystem services), a change to food webs (via destruction of native food sources) and an alteration to ecosystem conditions (such as changes to the soil chemistry) (Pimentel et al., 2000, Danell, 1996, Keller et al., 2007). These results highlight that users must confirm the assumptions behind the constant rate of spread prediction for the species in question before assuming that they are applicable as a suitable basis in their predictive models, as non-constant rates of spread are indeed a real phenomenon.

In our study, it was clear that both intrinsic and extrinsic factors affected the average rate of microbial spread, matching the findings of other spatial spread studies (Urban et al., 2008). For example, studies into the invasion of the cane toad across north-east Australia, have found evidence suggesting that both environmental heterogeneity and the intrinsic evolution of leg size lead to an increase to the rate of cane toad spread (Urban et al., 2008). For our results, we hypothesise the noticeable extrinsic effect of agar concentration upon the average rate of microbial spread is mainly due to the effect of substrate viscosity upon the motility mechanisms of the bacteria. On softer agar plate surfaces (i.e. relatively low agar concentrations < 0.8%), bacteria are able to use a cooperative motility mechanism known as swarming motility, where bacteria group up to form rafts, which then propel themselves forward across the surface. Swarming motility is known to be significantly faster at traversing surfaces than the twitching motility typically utilised by bacteria upon harder, high agar concentration surfaces (agar concentrations > 1%) (Kamatkar and Shrout, 2011, Harshey, 2003, Kearns, 2010). However, it is less clear why the SM morphology has a faster rate of spread than the WS morphology upon agar plate environments i.e. the effect of intrinsic factors in our experiment.

The WS morphology, in contrast to the static liquid microcosm it originally arises in, is maladapted to the solid surface microcosm presented by the agar plate environment. This is due to the increased cellulose expression of the WS morphology (compared to the SM morphology - this cellulose was required for the bacteria to float on the surface of the static liquid microcosm) diverting energy away from processes responsible for cellular growth (Spiers, 2007). As a consequence, in order to divert energy back towards cellular growth (thus raising its fitness), when presented with an agar plate environment, the WS morphology undergoes further adaption to become what is known as an SM-like morphology (Spiers, 2007). As the dispersal mechanisms responsible for relatively fast translocation across agar plate surfaces (such as swarming) are promoted by high cellular growth rates (Kearns, 2010), we theorise that during the time period between sensing the environment and adaptation to the environment, the colony undergoes a period of relatively low dispersal compared to the SM morphology. Additional evidence for this is the fact that within the static liquid microcosm, the SM morphology is relatively motile, using its flagella to swim through the liquid broth, whereas the WS morphology is relatively static within the produced biofilm, as the development of flagella machinery is typically selected against in biofilms as time increases (Bailey et al., 2013, Houry et al., 2010). This suggests that the SM morphology is more suited for spreading than the WS morphology in the initial stages, as the motility machinery required for dispersal can also take time to develop (Taylor and Buckling, 2011). We speculate the difference in spread rates between the initially slow rates of spread exhibited by the WS morphology on 0.5% concentration agar and the potentially faster rates of spread exhibited by the SM-like morphology also on 0.5% concentration agar, causes the accelerating (biphasic) rates of spread associated with these colonies. Such adaptation would be consistent with that found for the spread of the cane toad as it adapts its traits (leg size) to the extrinsic factors of the environment (Urban et al., 2008) and the adaptation of crickets in Britain via the development of larger wings (Simmons and Thomas, 2004).

We believe this WS morphology to SM-like morphology adaptation occurs in our experiment for a number of reasons. First, the stability of the WS morphology on agar plate environments depends on the initial density of the population on

the agar plate and the level of resources in the environment, with stability decreasing as initial population density increases and as the level of resources increases (Spiers, 2007). Due to the relatively high population density at the point of inoculation onto the agar plate (the bacteria grew overnight such that the optical density of the population was above 1.6 OD₆₀₀) and the high resources levels of the King's agar environment, we believe that colonies consisting of the WS morphology would have been under relatively high pressure to adapt. Secondly, we observe that a number of the WS morphologies transformed from colonies with the quite distinctive wrinkly patterns associated with the WS strain, to patterns similar to those exhibited by SM morphologies (figure 2.12). To ascertain whether this speculation is correct, further testing should look to sample and sequence the bacteria from within the original inoculation area and from the leading edge of the colony to ascertain the differences between them and whether these match those genetic adaptations stated in the literature (Spiers, 2007). Moreover, more research is required to ascertain the differences of spread between the WS, SM and SM-like strain, so that researchers can understand how these results might correspond to those of other populations.

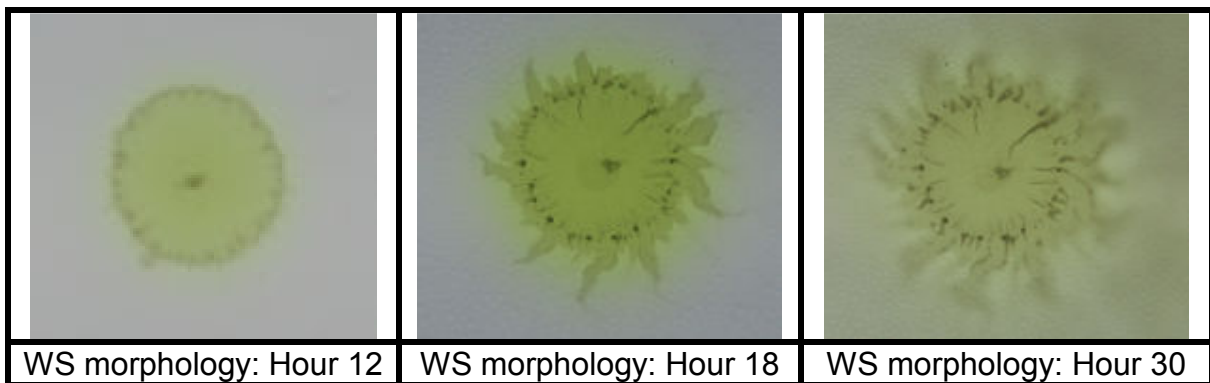


Figure 2:12: An WS morphology grown on 0.5% agar at hours 12 (left), 18 (middle) and 30 (right). The colony does not maintain the defined shape of the colony at hour 18 by hour 30, with the smooth green biofilm spreading out from the area previously colonised at hour 18, in a way similar to that exhibited by the SM morphology upon 0.5% agar plate environments. Note that at hour 30, the entire plate was colonised in this example.

The suspected change from a WS morphology to a SM-like morphology potentially highlights the effect of the cellular growth rate of the bacteria on the rate of spatial spread. The change in the growth rate of the SM-like morphology compared to the WS morphology is in contrast to the constant population growth rate (e.g. Malthusian growth equation $f(n) = rn$, where r is the constant

assumed to represent the population growth rate through time and n is population density and similar growth rate equation) assumed by these classic reaction-diffusion equations to model population spread (Skellam, 1951, Fisher, 1937). Consequently, the non-constant rates of spread seen in our study are possibly partly due to the different growth rates of the different morphologies. This explanation would be consistent with Sax et al. (2005), whom theoretically suggests that accelerating range shifts in macroorganism populations are not only driven by increasing dispersal rates, but increasing population growth rates too. This was recently empirically backed up by an empirical study involving cane toads which showed that those offspring from newer individuals along the frontier of the population spread (assumed to be evolved individuals) had a faster growth rate than those from within the population (assumed to be ancestral individuals) (Phillips, 2009). The fact that these classical reaction diffusion equations assume a constant growth and diffusion rate, in contrast to the increasing number of empirical cases where this is not true (such as these results and (Simmons and Thomas, 2004, Berthouly-Salazar et al., 2012, Phillips, 2009, Phillips et al., 2008, Sax et al., 2005)) suggests that modellers should consider whether the parameters of the population they are modelling agree with these assumptions. More research is required to ascertain the effect of the intrinsic and extrinsic factors upon population growth rates and their link to the rate of spread.

We found that some colonies exhibited a decelerating rate of spread during their colonisation of agar plate environments, matching results seen in some other model systems (Urban et al., 2008, Silva et al., 2002). There are a number of explanations for the exhibition of decelerating rates of spread. The first explanation stems from the observation that decelerating rates of spread only occur at higher agar concentrations, where colonies exhibit a low average rate of dispersal. Dispersal in biofilms is important for two reasons:

- a) to prevent localised resources at the periphery of the colony from being depleted (Nadell et al., 2010, de Vargas Roditi et al., 2013) which would otherwise halt the spatial spread of the population due to those individuals along the periphery being responsible for the majority of microbial growth and dispersal processes, both of which require adequate resource reserves (Cooper et al., 1968).

b) to escape harmful toxic waste products produced by the colony which can also prevent microbial growth (Hochberg and Folkman, 1972).

Therefore, we speculate that if dispersal is not fast enough, then a combination of these factors will hinder growth, leading to a decelerating rate of spread. A second possibility for why decelerating rates of spread occurred was the limited space within the petri dish environment. It was possible that the microbial population detected the artificial boundary of the petri dish and reduced their rate of their spread to compensate. Future experiments may wish to utilise bigger petri dishes than the 90mm ones used in this study to verify these findings but we believe this is not a major factor, as those colonies with decelerating rates of spread did not reach the edge of the agar plate.

Our results showed a non-linear (accelerating and decelerating) relationship between population radius and time for a significant proportion of colonies. However, because not all of the colonies reach the edge of the agar plate in the timeframe of our experiment, an issue possibly arising in the collection and analysis of our data is that colonies, which appear to have a constant radial rate of spread, could possibly exhibit a non-constant radial rate of spread over a longer timeframe and vice-versa. We speculate this, because bacteria can undergo lag phases during their spread across agar, where they do not exhibit their full radial rate of spread across environments (Déziel et al., 2001, Taylor and Buckling, 2011). For example, bacteria can undergo a lag phase for swarming motility, i.e. time to employ the swarming motility mechanisms (swarming motility for *Ps. fluorescens* typically occurs on agar plates below 0.8% agar concentration). The length of this swarming lag phase is affected by both the initial population density and the environment from which the bacteria is isolated from before inoculation onto the agar plate (Kearns, 2010). For twitching motility (twitching motility for *Ps. fluorescens* typically occurs on agar plates above 0.8% agar concentration), once the colony has initially established itself in the area of inoculation, there is no such lag phase, although the growth rate of bacteria is lower on higher concentration agar plates and thus it may take longer for these colonies to establish themselves compared to swarming colonies (Mitchell and Wimpenny, 1997, Semmler et al., 1999). This could be a different type of lag phase. Another factor possibly adding a lag phase to our results is the time for the WS morphology to adapt into the SM-like morphology,

which we believe has a higher dispersal rate due to an increased cellular growth rate. Consequently, it is debatable whether we capture a wide enough timespan such that all colonies leave these lag/establishment phases. While no other study in the literature has specifically studied the rate of spread of *Ps. fluorescens* SBW25 morphologies across agar plates and their lag phases, the following discusses how this issue might affect our results with regard to the microbiology literature.

fluorescens SBW25 morphologies across agar plates and their lag phases, the following discusses how this issue might affect our results with regard to the microbiology literature.

For bacteria in general, there has been no evidence that agar concentration affects the time a microbial population stays in the swarming lag phase (i.e. those colonies in 0.5% and 0.75% agar) before advancing into the rapid expansion phase (Ayati, 2006, Kearns and Losick, 2003). The radial rate of spread of colonies consisting of the SM morphology on the 0.5% concentration agar plates, suggests that the transition between the swarming lag phase and the rapid expansion phase occurs between hours 9-12, due to the sudden increase to the area occupied by many of these colonies. This rapid expansion eventually results in the majority of these colonies reaching the edge of the plate in the timeframe of our experiments. Generally, these had a constant radial rate of spread. It is worth noting that the two genotypes of SM morphology that seemingly do not exhibit this increase in 0.5% agar, were poor spreaders in all environments and thus it is possible another unknown factor is affecting these genotypes. Those colonies grown on 0.75% agar typically did not reach the edge of the agar plate, but they did also seemingly exhibit a rapid increase in the area covered at the same point (between hours 9 and 12) as those colonies on 0.5% agar, thereby suggesting that many of these colonies had also left the swarming lag phase. The fact they did not reach the edge of the plate was likely due to the slower velocity of cells as a result of the slightly increased agar concentration (Be'er et al., 2009). Because there is no evidence of agar concentration affecting these transition points in the literature and because those colonies which seemingly haven't transitioned, have had ample extra time to exhibit this transition, we believe that swarming motility lag would not largely affect our results for these colonies and thus we believe the proportion of SM morphology colonies exhibiting non-constant (accelerating) rates of spread on 0.5% or 0.75% agar would not be significantly affected.

As for twitching motility on 1% agar, there was an increase in the rate of spread between hours 9 and 12 for some of the SM morphology colonies, suggesting they had established themselves in the environment and had begun to actively use twitching motility, although none of these colonies reached the edge of the agar plate. These colonies typically exhibited constant or accelerating rates of spread. We note that it is common for colonies exhibiting twitching motility to not reach the edge of the agar plate in experiments as these colonies are typically more compact than those which swarm due to the slower velocity of twitching motility compared to swarming motility (Kearns, 2010, Taylor and Buckling, 2011, Mitchell and Wimpenny, 1997). However, a number of colonies in 1% agar did not exhibit an increase to their spread rate at all during the period we measured. Hence, it is possible that those colonies that have not yet developed an increase to their rate of spread could eventually exhibit this increase, possibly resulting in an increase in the proportion of accelerating colonies. We suggest this would not be the case because of the limiting factors of the environment slowing down growth when a colony does not spread quickly enough i.e. a build-up of toxic products (Hochberg and Folkman, 1972) and because of the difference in time between the point at which many colonies exhibit this increase (hour 12) and the end point of our time-series (hour 30), suggesting again, that these colonies have had ample time to exhibit this increase.

With regard to the WS morphology, it has not been established in the literature how the agar concentration of the environment affects the time taken for the WS morphology to adapt into the SM-like morphology (assuming this adaptation occurs) which we believe has a faster rate of spread due to the higher population growth rate of the SM-like morphology compared to the WS morphology (Spiers, 2007). There is some evidence that some (but not all) of the WS morphology colonies are exiting the swarming lag phase (and thus we believe had reverted to an SM-like morphology) on 0.5% agar within the timeframe of the experiment, due to the sudden increase to the area occupied between hours 15 and 18. This means that over the course of our experiments we may not have captured the point at which all of the WS morphology colonies completely exit the swarming lag phase nor the intrinsic adaptation phase. If so, then we predict this to result in an increase in the proportion of WS morphology

colonies in 0.5% agar exhibiting non-constant (in particular accelerating) rates of spread. This is due to the speculated spread speed differential between WS and SM-like morphologies and the accelerating rates of spread generally associated with those WS colonies that seemingly do exit the swarm lag phase on 0.5% agar within the timeframe of this experiment (Spiers, 2007). It is likely a similar result may occur for those grown on 0.75% agar, as swarming motility is also possible in these conditions and none of these colonies seems to have transitioned from a slower rate of spread to a faster rate of spread as we predict.

For twitching motility, we do not see any obvious increase in the rate of spread for those WS colonies grown in 1% agar. We note that many of these colonies were exhibiting decelerating rates of spread, possibly suggesting the factors of the environment are limiting growth (i.e. toxic products)(Hochberg and Folkman, 1972). Hence, over the course of a longer period, while these WS morphologies on 1% agar may later on begin to utilise the (potentially faster) twitching motility of the SM-like morphology and thus potentially develop an accelerating/constant rate of spread (instead of decelerating), we speculate more colonies in this combination may exhibit a decelerating rate of spread compared to others as it is difficult for these colonies to overcome the limiting factors of the environment associated with decelerating rates of spread described previously (Hochberg and Folkman, 1972). These possible shortcomings in our results reveal that an avenue for future research would be to investigate whether the likelihood of the WS morphology reverting into a SM-like morphology changes according to the agar concentration and how this adaptation changes the length of the lag phases. Additionally, a topic of future research might be to investigate whether there is a trade-off between dispersal and biofilm formation within the WS morphology as we find a dispersal advantage for the SM morphology compared to the WS morphology at 0.5% agar concentration compared to 1% agar concentration.

Together, the possible shortcomings we discuss here highlight the possible effect of lag phases, a common problem in the study of the spread of invasive species (Crooks, 2005, Crooks et al., 1999). Although lag phases typically occur in the initial phases of spatial spread, they can occur multiple times at any point

during the spread of a population, causing studies of spread rate to possibly miss the actual relationship between radial spread and time (Crooks, 2005, Crooks et al., 1999, Urban et al., 2008). Researchers do not fully understand what exactly the underlying causes for these lag phases are but explanations include the inherent features of population growth, environmental factors (i.e. agar concentration in this study) and evolutionary changes (i.e. changes in morphology in this study). Due to their uncertain nature, these lag phases can cause many problems in our predictive models (Suarez et al., 2001). Our results illustrate that the microbial model system might be a good system to study the factors responsible for lag phases if we can establish the existence of these lag phases for these morphologies and the links between micro- and macroorganisms. Particularly as the intrinsic and extrinsic factors responsible for the variability in the timescales these lag phases occur is relatively unexplored (Crooks, 2005, Crooks et al., 1999). However, for future studies investigating the rate of microbial spread, we recommend the size of the study to be limited such that an automated process could capture the spatial spread of microbial populations over a longer timeframe to avoid these issues. Despite these caveats, these results demonstrate that microbial populations (in particular *Ps. fluorescens* SBW25 morphologies) can exhibit non-constant rates of spread, thus contradicting the rate of spread predicted in the classical models of spatial spread and agreeing with the discourse in other empirical systems.

Looking at the characteristics of spread in more detail, we found a statistical relationship between the rate and the shape of spread, with those colonies exhibiting the largest decrease in circularity, also exhibiting accelerating rates of spread. This was particularly true for colonies consisting of bacteria with the WS morphology when grown on 0.5% concentration agar. We speculate two possible reasons for this. First, by spreading in an irregular shape, the colony has a larger perimeter than those colonies exhibiting a circular shape of spread. Even in the early stages of spreading in an irregular shape, this increases the availability of unoccupied space for those individuals at the edge of the colony to spread into. If the colony maintains the irregular shape of spread, we believe this would enable the colony to maximise both the speed and total area of spread by the colony. This explanation is consistent with the model shown by Lewis and Kareiva (1993). They used a numeric simulation, to show that

invasive populations with corrugated boundaries between invaded and non-invaded areas (i.e. a non-straight line boundary) are able to increase their range of spread faster than populations with planar (straight line) boundaries. They believed this occurred due to the increased surface area of the non-planar population edge allowing more individuals along the population edge to spread into non-colonised environment. Based on this, we believe irregular shapes of spread are more likely to increase the rate of spread compared to a circular shape of spread. With regard to classical microbiology studies which found the rate of microbial spread to be constant, we recognise that their studies focused upon the diameter of circular, relatively slow growing, *Escherichia coli* colonies, thereby not realising the possible effect of irregular shaped microbial spatial spread (Hochberg and Folkman, 1972, Cooper et al., 1968). Consequently, our study possibly provides evidence of the ecological effect of shape with regard to the rate of spread. Secondly, the WS phenotype, during its adaptation to the SM-like morphology, may not have developed these adaptations homogeneously throughout the population. This could give rise to perturbations to the spread of the population, as some regions may grow faster than others, thereby resulting in an irregular shape and the possible accelerating dynamics associated with irregular shaped spread. Ascertaining whether one of these explanations is the reason for our results needs further exploration.

Based on the relationship in our results between the rate of spread and the shape of spread, we theorise that the geometry of population spread can significantly affect the ecological characteristics of not only microbial populations, but also those populations consisting of macroorganisms. Unfortunately, the sampling techniques employed in macro-organism empirical studies, combined with a limited understanding of how the topology of the habitat affects the shape of spread, has to date prevented researchers from examining these geometric characteristics, thus resulting in researchers ignoring the shape of spread (Gilbert and Liebhold, 2010, Mack et al., 2000, Cumming, 2002). Consequently, our evidence is to our knowledge, the first possible empirical evidence for the relationship between accelerating rates of spread and the shape of spread. As we can easily capture the entire spatial dynamics of the microbial system, the microbial model system is well suited for further investigations into the ecological effect of the shape of spread. Yet, there

is a requirement to investigate the shape of spread in macroorganism populations to verify our speculation of the links between micro- and macro-organisms. This will require the development of new or alternative data collection methods for this purpose, an issue that is particularly important as it has been theoretically shown that the low resolution data collection techniques used to capture the spread of macro organism populations, frequently underestimate the true rate of spread, especially if the shape of spread is irregular (Cumming, 2002).

In our results, we found variation amongst the responses of genotypes of both morphologies to changes in the environment (as illustrated by the apparent GxE interactions). We speculate there are two possible explanations for this. The first explanation is that when sampling from the static microcosm, the area we sampled from in the regions containing the morphologies, may have been slightly different between the 12 samples. This could give rise to variation amongst the genotypes and hence the variation in genotypic responses to the environment may be an artefact resulting from this. However we note that we tried to keep the area selected as consistent as possible in the experiment, e.g. we sampled from the direct middle of each microcosm for the SM morphology and the direct middle of the air-liquid interface for the WS morphology. We also note that we eliminated the possibility of sampling a WS morphology as opposed to a SM morphology when isolating colonies on the agar plate. The second explanation is the possibility that the system is exhibiting phenotypic plasticity i.e. the ability of an organism to change its phenotype (dispersal ability) in response to changes in the environment (Leggett et al., 2013). This speculation is due to the reaction norms of the GxE plot (of the average rate of spread) intersecting with each other as the environment changes. Phenotypic plasticity is an important aspect of invasive spread which helps to maximise the average fitness of the colony in sub-optimal conditions and is thought to increase the likelihood of accelerating rates of invasive spread (Funk, 2008, Pichancourt and Van Klinken, 2012). However, to date there have been relatively few studies investigating the role of phenotypic plasticity upon the invasion dynamics of a species. This is due to the many practical problems encountered by researchers during data collection (Mack et al., 2000). While we do not investigate this in much detail, these results suggest that we require

more work to understand the variation in SM and WS morphologies in the static microcosm, particularly with regard to dispersal ability and to establish whether the *Ps. fluorescens* microbial model system might be utilised to investigate the effect of phenotypic plasticity upon the invasion dynamics of a species.

While there are a number of benefits associated with the microbial model system, it is not without its own challenges. In this study, we intended to utilise an automated image analysis algorithm to extract the data from the images. However, while we implemented a number of the recommendations similar to those suggested in (Pennekamp and Schtickzelle, 2013), it proved difficult to create an image analysis algorithm which could automate the process. Many of the problems stemmed from problems caused by the light box background distorting the information in the picture and/or the spread of the bacteria producing almost transparent biofilms. This meant that many of the time series pictures were threshold manually by eye to ensure the image detected by the image analysis was correct. This possibly had an effect on the results (i.e. stochasticity), although we did manually check each threshold by eye to make sure it was truly representative of the spread of each population. We recommend staining the colony in future investigations of bacterial spread following our protocol, in order to make the spread of the colony more distinct from the agar background. Such a method is demonstrated in (Spiers, 2007). Even with these problems, for the 711 time series considered in this study, each time series on average consists of 7.05 time points out of the 9 time points possible. This rose to an average of 7.75 time points when we substituted the area of the plate for the time points of those colonies, which had colonised the full area of the agar plate. This number of data points was consistent across all treatments used in this study (each category has an average number of time points above 7 when taking into account those colonies which colonised the whole agar plate), thereby reducing any likelihood of results bias between treatments.

In conclusion, using microorganisms as a model system to avoid many of the complications associated with data collection in spatial ecology, we examined the spatial spread of *Ps. fluorescens* strain SBW25 populations and found that the spread dynamics of microbial populations were more complex than

previously thought, with both extrinsic and intrinsic factors affecting the rate of spread. In particular, we found that combinations of these factors resulted in some *Ps. fluorescens* populations spreading at a non-constant radial rate of spread, contrasting with the constant radial rate of spread prediction by the classical reaction-diffusion models used in spatial ecology. Through novel usage of the *Ps. fluorescens* model system, these results agree with the recent discourse from other macroorganism model systems, which suggest that the assumptions made by these classic models should be used with caution and that other predictive models, based on more accurate assumptions (which can possibly lead to non-constant radial rates of spread) might be more suitable (Hastings et al., 2005). By identifying a not previously reported intrinsic effect of the WS and SM morphologies upon the relationship between the radial area of spread and time, we suggest that the assumptions relating to intrinsic/extrinsic factors, the constant rate of dispersal and the constant rate of reproduction should be particularly scrutinised in these models, agreeing with findings in other macro-organism studies (Simmons and Thomas, 2004, Berthouly-Salazar et al., 2012, Phillips, 2009, Phillips et al., 2008, Sax et al., 2005). This study has also illustrated the benefits of the microbial model system to spatial ecology and we believe the microbial model system should be utilised more in spatial ecology to ascertain the key factors behind population spatial spread, thus allowing researchers to improve the reliability of the predictive models used to model invasive spread. Finally, our results highlight the ecological effect of the shape of spread, with those populations exhibiting irregular shapes of spread also seemingly exhibiting accelerating rates of spread. Indeed, our study possibly provides some of the first empirical evidence for the link between the shape of spread and the rate of spread. Consequently, while the shape of spread has to date been often ignored, we speculate it can have a significant effect on a number of ecological factors of the population. Hence, we believe this requires further study to understand more about the ecological/evolutionary factors affected by the shape of spread and vice versa. This would help to advance our knowledge of the factors affecting the spatial dynamics of population spread.

Chapter 3:

How does food and viscosity affect the pattern of invasive microbial spread

Abstract

Microbial colonies can exhibit a range of patterns during their spread across agar plate environments. Classic studies utilising strains of *Bacillus subtilis* have shown that these patterns depend upon the food availability (peptone) and the viscosity (agar concentration) of the agar plate environment, with the irregular patterns exhibited by strains of *Bacillus subtilis*, occurring in agar plate environments with low food concentrations and low viscosity. In this chapter, we investigate how these environmental parameters of the system affect the spread of *Ps. aeruginosa* strain PAO1. Our results find that the effect of viscosity is consistent with that observed for *B. subtilis*, however irregular patterns of *Ps. aeruginosa* spread occur at high, not low, food concentrations. These results confirm the significant effect of environmental conditions upon the patterns of spread exhibited by microbial populations. Moreover, they also show that this effect is not consistent across bacteria strains and species.

Introduction

Bacteria can exhibit a range of spatial patterns of spread as they colonise agar plate surfaces (Kearns, 2010). Examples of spatial patterns of spread exhibited by microbial colonies include: “bull’s eye” patterns, where patterns look like a series of a concentric circular rings; vortex patterns, where patterns are reminiscent of nebulae in space, and tendrils (also known as dendritic) patterns, where long finger-like regions of microbial colonisation emanate from the colony centre (Kearns, 2010). The ecological and evolutionary relevance of these patterns of spread for the microbial colony is relatively unknown (Kearns, 2010). However, we suggest the shape of spread has potential importance due to the results of Chapter 2 illustrating a possible link between the shape (pattern) of microbial spread and the rate of spread, a key ecological attribute of a population that affects how quickly the population can colonise and sequester resources from the environment. Because of the potential for the driving ecological and evolutionary processes to be similar in both micro- and macro-organism systems (as seen in other studies (Buckling et al., 2009, Jessup et al., 2004)), we speculate that the shape of spread might one such process with important ecological and possibly evolutionary implications for micro-organism and macro-organism populations alike. Indeed, the finding that the shape of spread may be an influencing factor for the rate of spread could be important for macro-organism populations consisting of invasive species, due to the negative consequences associated with the increasing rates of invasive spread (Mack et al., 2000). Hence, we suggest that we need to understand more about the ecological and evolutionary relevance of these patterns of spread in microbial populations and the drivers responsible for these patterns of spread, as this may allow us to understand more about the spread of populations (including those consisting of invasive species) in general. Indeed, we believe the advantages of the microbial model system make them the ideal tool to study the shape of spread due to difficulties studying this aspect in macroorganism populations (Kokko and Lopez-Sepulcre, 2006, Cumming, 2002, Buckling et al., 2009, Jessup et al., 2004).

A determining factor of the pattern of microbial spread are the environmental attributes of the agar plate surface (Kearns, 2010). Traditionally, experiments investigating the spatial spread of bacteria have focused upon the fractal-like

growth of *Bacillus subtilis* (Fujikawa and Matsushita, 1989), *Paenibacillus dendritiformis* (Golding et al., 1998, Ben-Jacob et al., 1998) and more recently *Serratia marcescens* (Hiramatsu et al., 2005). A common result from these studies was that both agar (viscosity) concentration and peptone (nutrient) concentration significantly affected the spatial pattern of bacterial spread. These studies found that colonies grown in low peptone concentration conditions exhibited fractal branching patterns, with the density of these branches increasing as the agar concentration of the environment decreased (Fujikawa and Matsushita, 1989, Matsushita et al., 1999). Whilst, those colonies grown in high peptone conditions exhibited relatively circular patterns, with low agar concentrations resulting in a circular pattern of spread, intermediate agar conditions resulting in a “bull’s eye” pattern of spread and high agar concentrations resulting in relatively circular patterns of spread, albeit with a less circular edge than those exhibited in low agar concentrations.

In the microbial system, the agar concentration (viscosity) affects the type of motility the bacteria can utilise to traverse the environment. Irregular (i.e. non-circular) patterns of spread typically require swarming motility, a cooperative behaviour where individuals group up to form raft like structures, which are then propelled by the combined usage of their flagella (a tail-like appendage). Swarming motility requires the surface to be relatively moist such that the surface friction is not too great (Tremblay and Deziel, 2008). Subsequently, for *Pseudomonas aeruginosa* populations, the exhibition of swarming motility occurs in agar concentrations between ~0.3%-0.8% (Bees et al., 2002, Kearns, 2010). In these particular conditions, bacteria help facilitate swarming motility by producing surfactant public goods called rhamnolipids to reduce the friction of the cell (by increasing surface moisture) against the surface of the agar (Julkowska et al., 2004). Due to the production of these surfactants and the subsequent swarming motility, it is thought that irregular tendril/fractal-like patterns of spread are formed due to the localised movement exceeding the rate of bacterial growth (Kearns, 2010, Marrocco et al., 2010, Kozlovsky et al., 1999, Tremblay et al., 2007, Dechesne and Smets, 2012, Be'er et al., 2009). At agar concentrations lower than ~0.3%, the agar does not solidify and in these conditions, bacteria utilise swimming motility (where individuals utilise their flagella to propel themselves) to move through water channels within the agar

environment. At agar concentrations higher than ~0.8%, the moisture of the agar plate surface is insufficient for swarming motility and so in response, bacteria activate a twitching motility mechanism (movement arising because of the pili of the cell attaching themselves to the surface and 'dragging' the cell along). At the same time, bacteria deactivate the quorum sensing mechanisms required for cooperation, which in turn deactivates production of the surfactants required for swarming motility (Okkotsu et al., 2013, O'May and Tufenkji, 2011). This twitching motility operates at a much lower velocity than swarming motility, generally eliminating the possibility of tendril dynamics, as localised motility cannot significantly exceed the growth rate of the colony (Kearns, 2010). The exhibition of sliding motility (movement due to the growth and reproduction of cells pushing each other) can also occur at high agar concentrations.

The effect of peptone concentration (nutrient) on the other hand is unclear, with the classical studies of microbial spread, suggesting a link between how peptone concentration affects the pattern of spread and the limited diffusion of nutrients towards the colony in agar plate environments (Golding et al., 1998). Namely, in lower nutrient environments, resources upon the outskirts of a colony are more available to those bacteria in regions of the population more exposed to non-colonised area (e.g. the tip of a tendril), thereby conferring a reproduction and diffusive motility advantage to these bacteria compared to those bacteria in less exposed areas (e.g. at the base of the tendril) whom get access to little or possibly none of these resources. This results in an irregular pattern of spread, where those bacteria in the most exposed areas of the shape continue to disperse, while those bacteria in less exposed areas become passive, thereby ceasing to disperse (Golding et al., 1998, Marrocco et al., 2010, Ben-Jacob et al., 1998). In higher nutrient substrates, the resources are assumed to be able to diffuse further into the region of colony before the bacteria depletes them (Nadell et al., 2010). Consequently, as the bacteria in less exposed areas do not become passive, this negates the reproduction and motility advantage resulting from being at more exposed regions along the population outskirts and thus patterns are generally circular. Because of this speculated nutrient-limited mechanism, some researchers speculate the initiation of irregular patterns exhibited by these colonies on lower nutrient agar arises because of small perturbations in the peptone level of the agar when

peptone is limiting (Be'er et al., 2009, Ben-Jacob et al., 2000). In addition, we note that it has been shown that the velocity of individual bacteria, the rate of colony spread in *Paenibacillus dendritiformis* and the production of surfactants are affected by the concentration level of peptone as well as an interaction between agar concentration and peptone concentration (Be'er et al., 2009, Santos et al., 2002).

The fractal patterns of *B. subtilis* and the tendril patterns of *Ps. aeruginosa* strain PAO1 share many of the same geometric characteristics (such as an increased perimeter) and both require relatively low agar concentrations. However, in contrast to *B. subtilis* which requires relatively low peptone concentration conditions, tendril patterns of *Ps. aeruginosa* are known to arise in relatively high peptone concentration conditions (Tremblay and Deziel, 2008). To our knowledge, it is unknown what pattern of spread *Ps. aeruginosa* strain PAO1 exhibits in relatively low to medium peptone conditions. It is also not reported in the literature whether an interaction exists between agar concentration and peptone concentration upon the shape of spread for *Ps. aeruginosa* strain PAO1, as it does for *B. subtilis* (Fujikawa and Matsushita, 1989) and *S. marcescens* (Hiramatsu et al., 2005). Thus, we identify that there is still more to learn about how these extrinsic factors affect the spatial spread of microbial populations in order to understand the possible ecological purpose(s) of these organised patterns of spread and to understand more about how populations spread in general.

In this chapter, we focus on how changing two environmental parameters of the system (the agar concentration (viscosity) and peptone concentration (nutrient)) and the interaction between these two environmental parameters affects the spatial pattern of spread of the *Ps. aeruginosa* strain PAO1 upon agar plate surfaces. We switch from *Ps. fluorescens* strain SBW25 in Chapter 2 to *Ps. aeruginosa* strain PAO1, due to the more striking patterns of microbial spread produced by *Ps. aeruginosa* strain PAO1. Modifying these two parameters of the environment was used in the classic paper for the bacteria strain *B. subtilis* (Fujikawa and Matsushita, 1989) as well as *S. marcescens* (Hiramatsu et al., 2005). Based on studies in other microbial systems, we expect to see the pattern of microbial spread change according to changes in the parameters of the environment.

In this study, we used King's agar, an agar environment commonly used for the propagation and isolation of *Pseudomonas* strains (King et al., 1954, Johnsen and Nielsen, 1999). We use King's agar as it is relatively simple to make and it is high in the nutrients *Ps. aeruginosa* needs to thrive and consequently spread across agar plate surfaces. King's agar comprises of agar powder, proteose peptone no. 3 and nutritional pH buffers: magnesium sulphate and di-potassium phosphate. We note that we use the terminology *high* and *low* as descriptions of the environmental parameters relative to the concentration of agar powder/proteose peptone commonly used in the preparation of King's agar.

Methods

We cultured a frozen stock population (kept at -80°C) of *Ps. aeruginosa* strain PAO1 overnight in a sealed test tube containing 5ml of King's B medium (10g/l glycerol, 20g/l proteose peptone No 3, 1.5g/l K₂HPO₄·3H₂O and 1.5g/l MgSO₄·7H₂O) at 37°C. To test the effect of the agar environment, we made 10 replicate King's agar plates for each combination of the three agar concentrations and five peptone concentrations tested in this study. The three agar concentrations tested were 0.5% (5g/l agar powder - encouraging swarming conditions), 0.75% (7.5g/l agar powder) and 1% (10g/l agar powder - encouraging twitching conditions). The five peptone concentrations tested were at 25% intervals of the normal amount used in KB agar: 0% (0g/l proteose peptone), 25% (5g/l proteose peptone), 50% (10g/l proteose peptone), 75% (15g/l proteose peptone) and 100% (20g/l proteose peptone). These plates were prepared the day before by first allowing them to dry for 15-20 minutes under an airflow hood and then leaving them overnight at room temperature.

We inoculated 2.5µl of *Ps. aeruginosa* PAO1 culture onto the centre of each agar plate. We allowed plates to dry for 10 minutes before inoculation and for a further 15 minutes after inoculation (to remove surface water, which could lead to swimming motility). We then placed the inoculated agar plates into an incubator kept at 37°C. We took photographs of each plate using a Canon E600D Digital SLR camera every 6 hours for the 1st 30 hours and then at 48 and 72 hours. Images were then analysed using the java-based image analysis software, ImageJ (Rasband, 2014.). This was used instead of EBImage due to its widespread use in other microbial studies (Taylor and Buckling, 2010) and

due to some of the difficulties in using the R-based code interface of EBImage in Chapter 2. Plots were created in the statistical software package R v3.0.3 (R Development Core Team, 2014).

Results

In general, the rate of spread of *Ps. aeruginosa* strain PAO1 colonies increased as the peptone concentration increased and the agar concentration decreased, although there were some exceptions to this (figure 3.1). Moreover, we found the pattern of spread was significantly affected by the agar concentration and peptone concentration of the agar plate environment, with distinct tendrils formation (defined as an obvious finger-like area of growth extending from the otherwise circular main colony) clearly exhibited for some peptone/agar environment parameter combinations but not in others (figures 3.2 and 3.3).

A high proportion of colonies grown on agar surfaces consisting of 100% peptone concentration and 0.5%-0.75% agar concentration, best exhibited and maintained tendrils at hours 24, 30 and 48 (figure 3.4). We observed a high proportion of colonies grown on agar surfaces consisting of either 25% or 75% peptone concentration and 0.5% agar concentration exhibited tendrils after 24 hours. However, many of these colonies at these peptone concentrations (particularly those in 25% peptone concentration) did not maintain these tendrils as time progressed (figure 3.4). We also found that while colonies grown on 0.5% agar, 50% peptone conditions stayed relatively circular for the first 30 hours, a small proportion of colonies started exhibiting a small number of tendrils by hour 48 (figure 3.4). At other agar/peptone concentrations, the pattern of spread was generally circular, with little to no growth occurring at 0% peptone.

Focusing on those agar conditions that consistently promoted tendrils, we found that colonies grown on relatively high peptone concentration (100%), relatively low-to-medium agar concentration (0.5%-0.75%) surfaces exhibited many long tendrils, the number of which was generally maintained through time (figures 3.5 and 3.6). As the peptone concentration decreased (75%), in relatively low agar concentration conditions (0.5%), colonies generally only exhibited a few long tendrils, while in medium agar concentration conditions (0.75%), tendrils were not typically exhibited at all, thereby revealing an interaction between the

two environmental parameters (figures 3.5 and 3.6). Furthermore, those colonies grown on relatively low peptone (25%), relatively low agar (0.5%) concentration surfaces exhibited many smaller tendrils during hours 24 and 30, which were not maintained by hour 48 (figures 3.5 and 3.6).

There was noticeable spatial population heterogeneity throughout, with clusters of bacteria forming dark spots in otherwise pale biofilms indicative of regions of high population. We also note that those colonies in relatively low peptone environments (0-25%) typically grew in a greyish colour signifying the lack of siderophore production due to the peptone-limited environment.

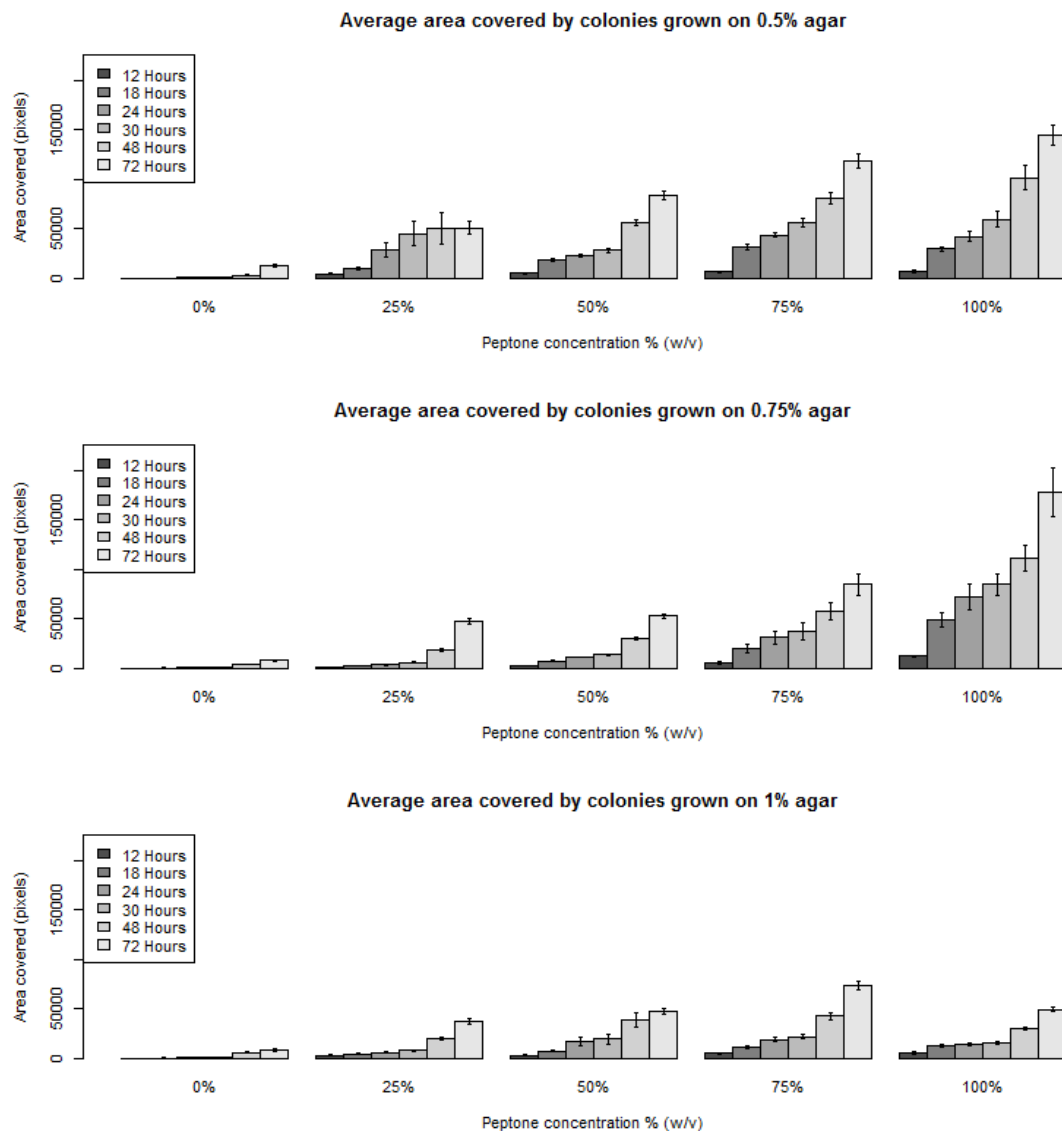


Figure 3.1: The average area of spread across all ten *Ps. aeruginosa* replicates for each of the environments tested. We measured area in pixels. Error bars represent ± 1 SE.


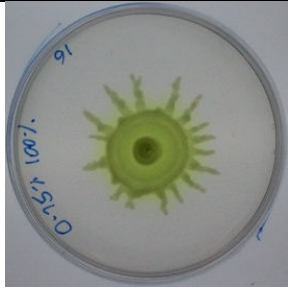
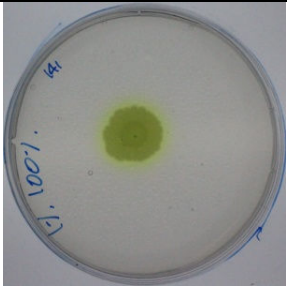
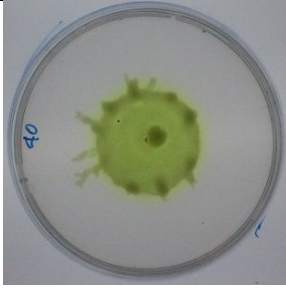
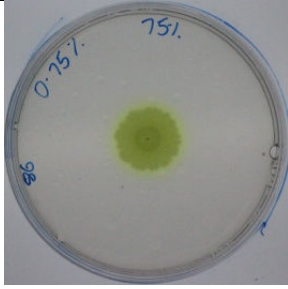
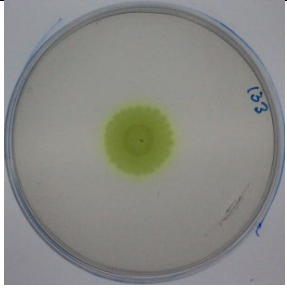
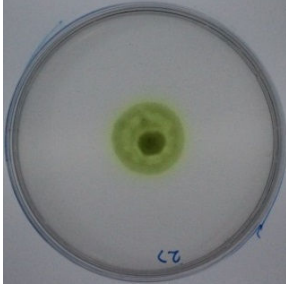
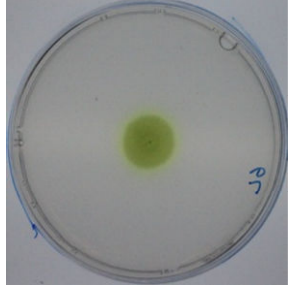
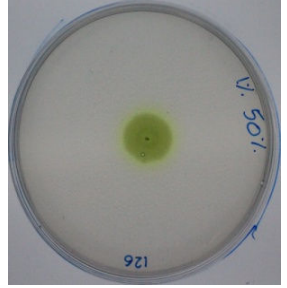
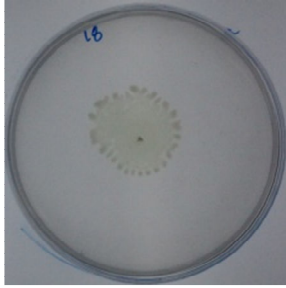
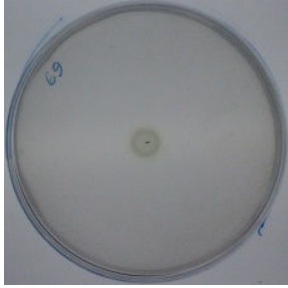
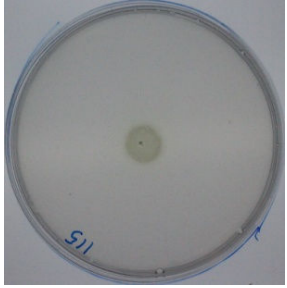
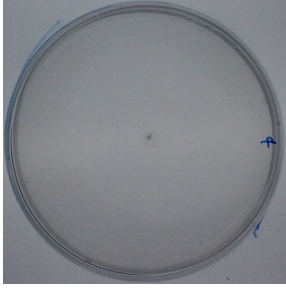
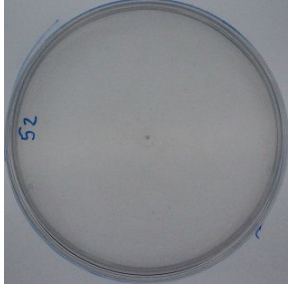
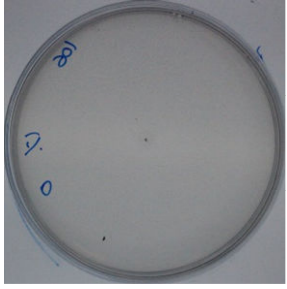
Hour 24		Agar Concentration		
		0.5%	0.75%	1%
Peptone Concentration	100%			
	75%			
	50%			
	25%			
	0%			

Figure 3.2: The spatial spread of *Ps. aeruginosa* strain PAO1 in each of the 15 different environments after 24 hours. Biofilms began to exhibit tendrils in environments encouraging swarming motility with abundant nutrients. We also noticed some smaller tendrils exhibited by the colony grown in low nutrient, soft agar plate surfaces. Note: The plates shown in this table are the ones with the most irregularity out of the 10 replicates.

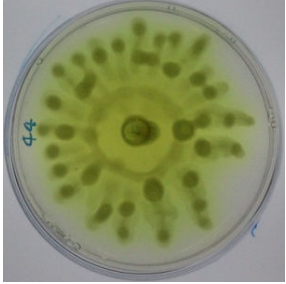
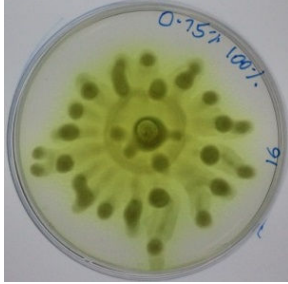
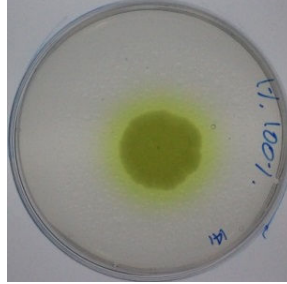

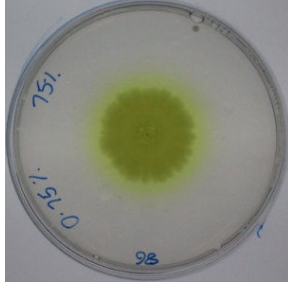
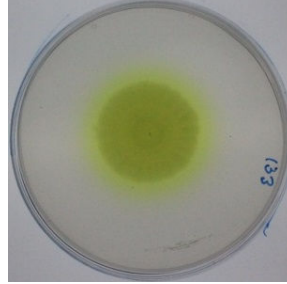

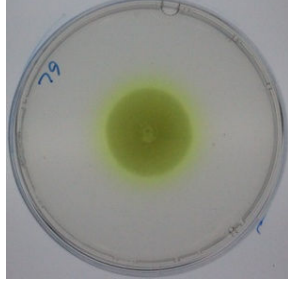
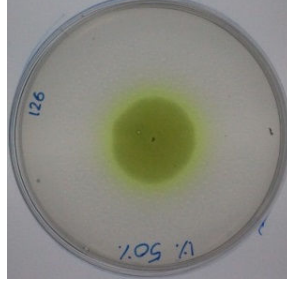

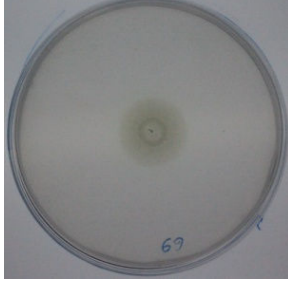
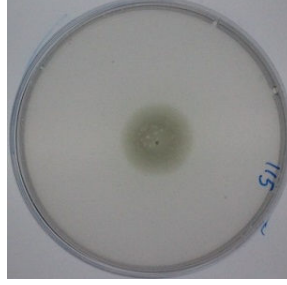
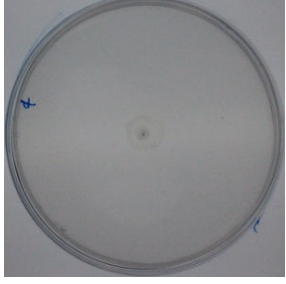
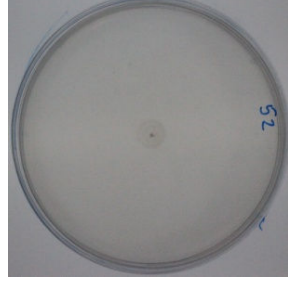

		Agar Concentration		
		0.5%	0.75%	1%
Peptone Concentration	100%			
	75%			
	50%			
	25%			
	0%			

Figure 3.3: The spatial spread of *Ps. aeruginosa* in each of the 15 different environments after 48 hours. Note: The plates shown in this table are the ones with the most irregularity out of the 10 replicates.

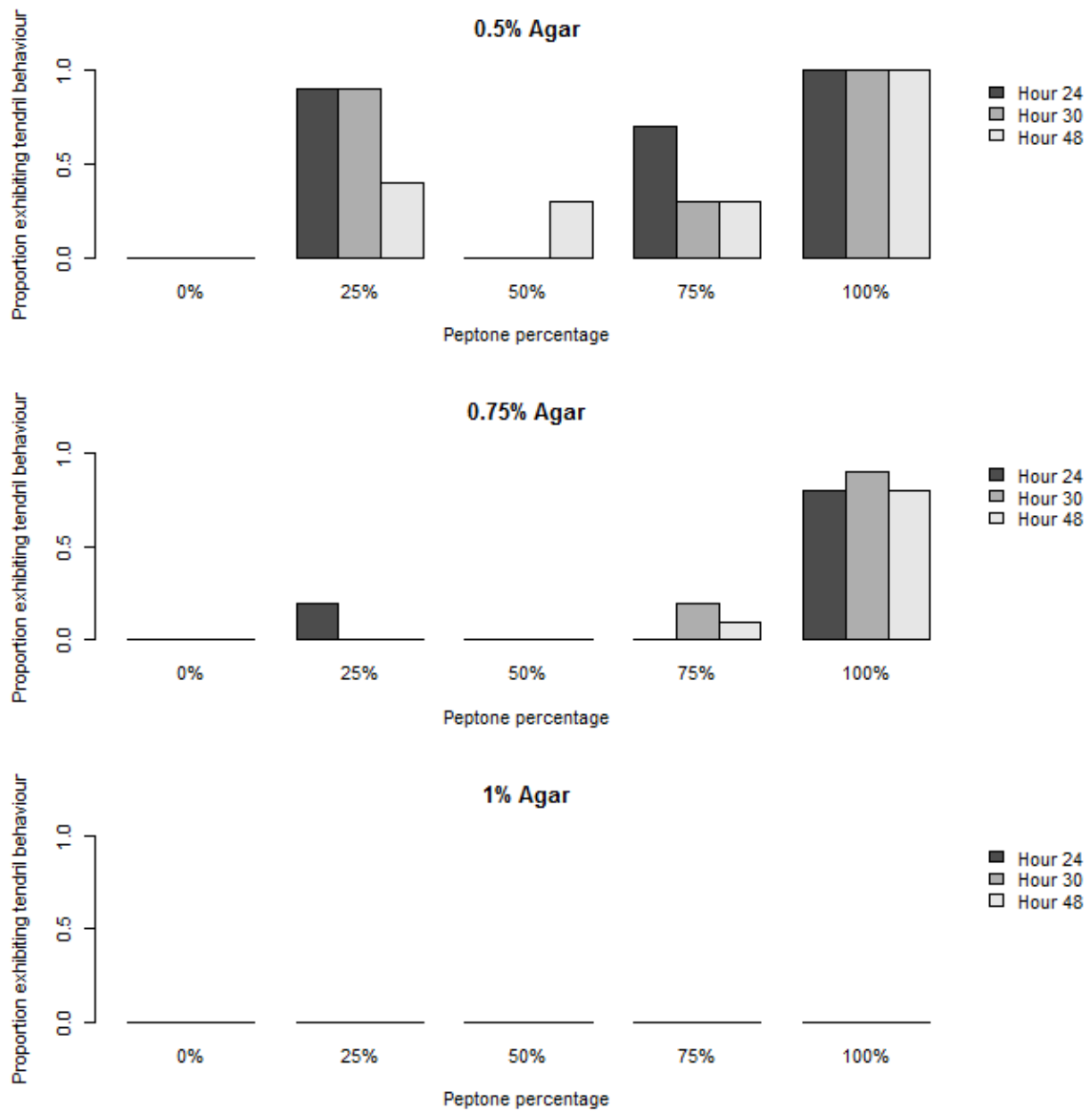


Figure 3.4: The proportion of the ten inoculated *Ps. aeruginosa* colonies exhibiting at least one tendril for each environment treatment at hours 24, 30 and 48.

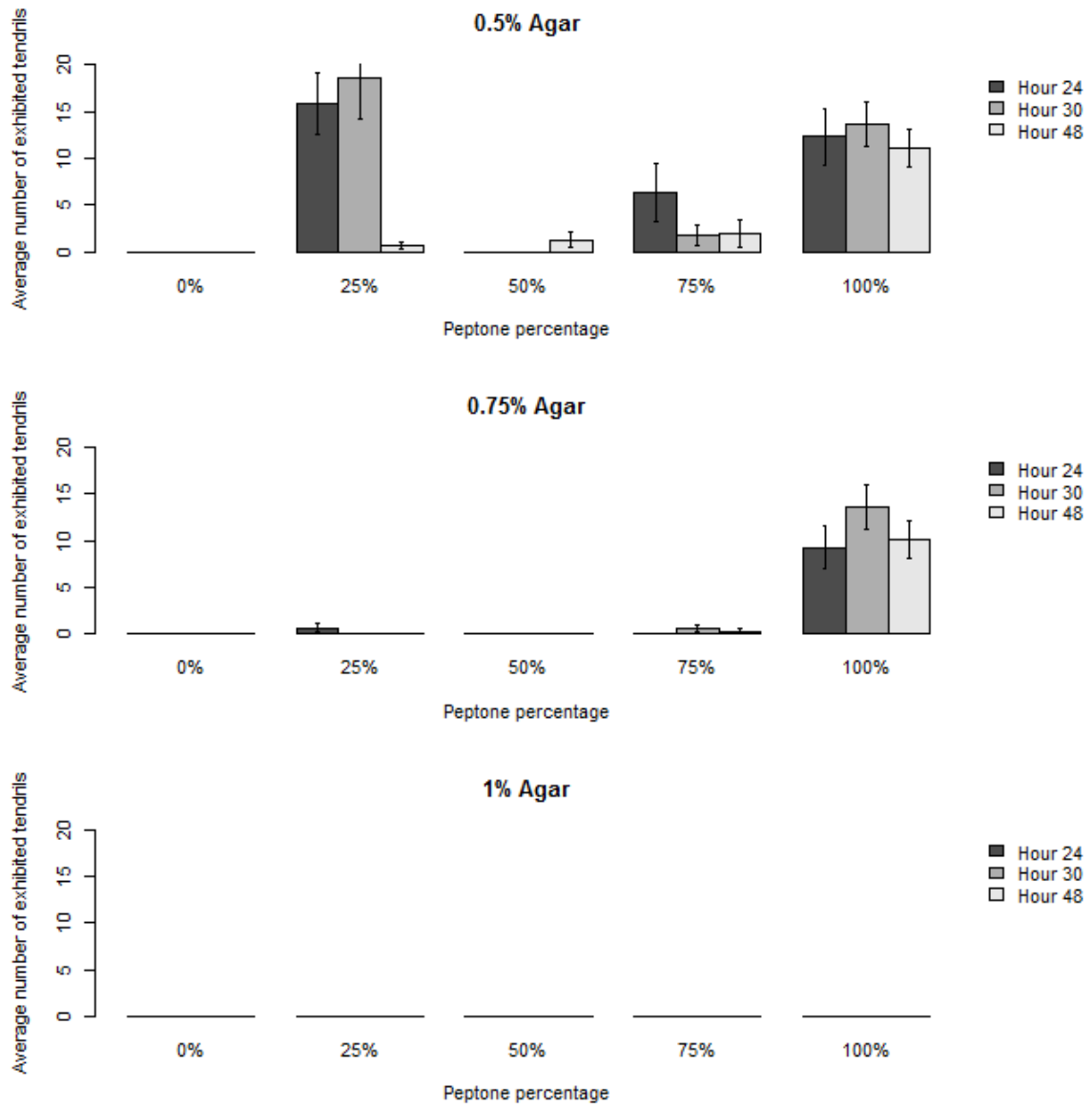


Figure 3.5: The average number of tendrils exhibited by the ten *Ps. aeruginosa* colonies grown in each environment treatment at hours 24, 30 and 48. Error bars represent ± 1 SE.

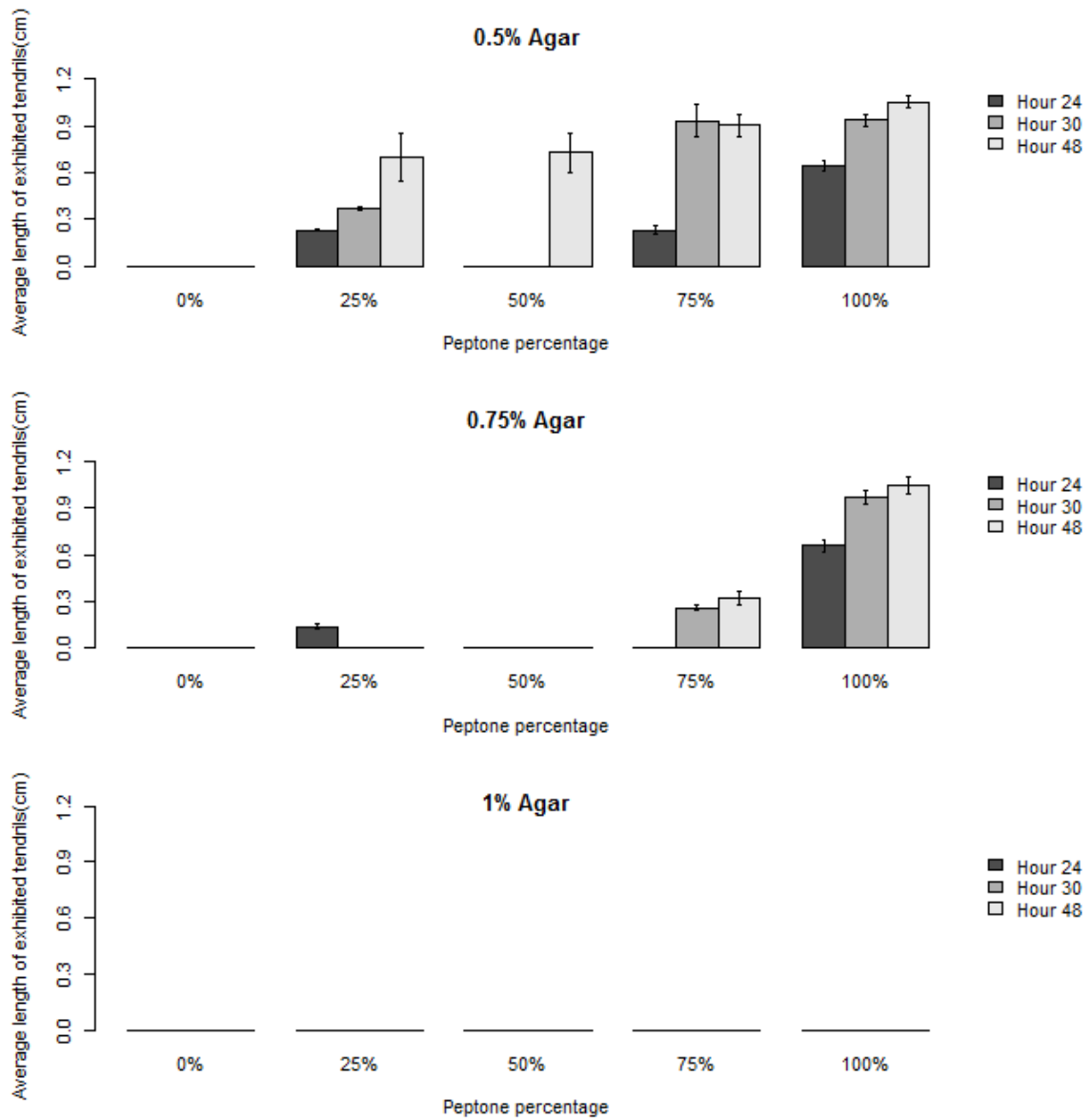


Figure 3.6: The average length of the tendrils exhibited by *Ps. aeruginosa* colonies grown in each environment treatment at hours 24, 30 and 48. Error bars represent ± 1 SE.

Discussion

We have found that agar plate surfaces consisting of a relatively low agar concentration (viscosity) and a relatively high peptone concentration (nutrient) best promote tendril formation by *Ps. aeruginosa* strain PAO1. In comparison to the studies of species of bacteria that exhibit maintained fractal-like branching patterns of spread (i.e. *B. subtilis* (Fujikawa and Matsushita, 1989)), our results agree that agar concentration must be sufficiently low for irregular patterns of spread to occur, with relatively circular patterns occurring in relatively high agar conditions. However, in our study, maintained non-circular patterns typically only occurred in environments with high peptone concentrations, contrasting with the results for other microbial species where the exhibition of maintained irregular patterns required the environment to have a relatively low peptone concentration (Fujikawa and Matsushita, 1989). Furthermore, our results suggest an interaction between agar concentration and peptone concentration for King's agar not previously reported for *Ps. aeruginosa* strain PAO1.

Agar plate surfaces with 100% peptone concentration combined with 0.5%-0.75% agar concentration best exhibited tendril formation. At these environment parameters, we observed numerous long tendrils, which the colony maintained throughout the first 48 hours. However, as peptone concentration decreased, these tendrils generally decreased in frequency, in size and in how long the colony maintained them. The surfactant mechanisms required to reduce the surface tension for tendril patterns to arise require certain carbon/nitrogen sources (Santos et al., 2002). By reducing the concentrations levels of peptone, we are restricting the availability of nitrogen, carbon, sulphur and other trace elements. Consequently, as peptone concentration decreases, we speculate that these colonies decrease their rhamnolipid (surfactant) production due to the lack of essential nutrients, thereby leading to an increase in surface tension and thus reducing the formation of tendrils (Yeung et al., 2009). We found the effect of reduced peptone concentration was greater as the agar concentration increased (i.e. an interaction). For example, in 0.75% agar concentration, tendril formation only occurred at 100% peptone concentration, while tendril formation occurred at lower peptone levels in 0.5% agar concentration. We speculate this interaction arises due to the increased water availability of the surface in 0.5% agar concentrations compared to 0.75% agar concentrations, as more moist

surfaces require less rhamnolipid production to reduce the surface tension of the agar sufficiently for the exhibition of swarming motility (Caiazza et al., 2005).

An exception to this effect of reduced peptone concentration occurred for colonies grown on agar plates containing 0.5% agar concentration and 25% peptone concentration. We found colonies grown in these conditions exhibited a large number of smaller tendrils at hour 24, which the colony did not maintain by hour 48. The cause of this result is unknown but we speculate two alternative explanations of why this result occurs:

1. It is postulated that the cooperative velocity benefits of swarming leads to localised areas of increased motility along the leading edge, causing some cells along the leading edge to advance further than others (Kearns, 2010). In lower peptone concentrations, the velocity of cells along the leading edge of the colony is reduced, possibly as a result of decreased surfactant production (Be'er et al., 2009, Santos et al., 2002). Consequently, while the agar concentration conditions promote swarming motility and therefore tendrils, we postulate that after the initial stages of tendril formation, the lack of resources in the environment renders cells unable to produce enough of the required surfactants and other mechanisms needed to maintain the localised velocity advantage for extensive tendril formation. Indeed, due to being more isolated, we suspect that cells at the tip of the tendril require a greater degree of individual effort to maintain the velocity required to exhibit tendril formation. This phenomenon enables the cells behind the transient tendril formation to “catch up”, resulting in the relatively circular patterns of spread seen after 48 hours.
2. Alternatively, the decreased rhamnolipid production resulting from the decreased peptone concentration may have prevented swarming motility altogether (Santos et al., 2002). Instead, the patterns of spread may be reliant upon other types of motility such as sliding and twitching motility. Indeed, sliding motility has been observed to produce patterns of spread exhibiting smaller tendrils (Murray and Kazmierczak, 2008). However, we notice that such a result does not hold in 0.75% agar. It is possible that in these conditions other types of motility play a larger role than sliding motility (Rashid and Kornberg, 2000).

This observation highlights that more work is required to decipher how the environmental parameters of the agar plate environment affects the mechanisms driving the spatial spread of the colony, possibly at a metabolic systems level.

In order to model irregular patterns of spread, many of the classical models have based their assumptions upon the limited diffusion of nutrients towards the colony in lower nutrient substrates, such that those at the tendril tip acquire a reproduction advantage over those behind the tendril tip (Marrocco et al., 2010). The results of this study have shown that these assumptions are not suitable for modelling the spread of *Ps. aeruginosa* strain PAO1, as the tendril patterns in these models require low-nutrient environments in contrast to the generally high-nutrient environments required for tendril patterns in *Ps. aeruginosa* strain PAO1. The distinct effect of peptone concentration upon the spread of *Ps. aeruginosa* strain PAO1 compared to other bacterial strains is perhaps due to the different mechanisms used to traverse an environment (such as quorum sensing and the development of biosurfactants acting as long-range signals) and the different degrees these mechanisms are being used compared to other microbial species (Deng et al., 2014). Consequently, these nutrient-limited models are not an appropriate basis for modelling *Ps. aeruginosa* strain PAO1 and we highlight that irregular shapes of spread are not always reliant on these nutrient-limited environment assumptions.

Clearly, more research is required to understand the effect of environmental parameters on the shape of spread. A greater understanding of how environmental parameters affect the shape of microbial spread could have many applications from both a microbiology and conservation perspective. First, it would help us establish the links between the spatial spread of micro- and macro-organism populations, thereby increasing the viability of the microbial model system as a system to study the spatial spread of populations in general (Buckling et al., 2009). Secondly, this knowledge is potentially useful to our understanding of how different patterns of spatial spread arise and the possible ecological purpose of these patterns of spatial spread (such as the possible link between the shape of spread and the rate of spread in Chapter 2). Finally, this knowledge could help to inform future models of microbial spread, possibly offering a number of medical benefits, such as helping researchers to

investigate different control strategies to prevent the spread of microbes across artificial joints (Ehrlich et al., 2005, Korolev et al., 2014).

In conclusion, the constitution of King's agar can affect the tendril development of *Ps. aeruginosa* strain PAO1. In contrast to the irregular patterns of spread seen in other bacterial strains (which require relatively low peptone, low agar concentration conditions), tendril development of *Ps. aeruginosa* strain PAO1 occurred best in relatively high peptone (food), relatively low agar (viscosity) concentrations. We also found an interaction between agar concentration and peptone concentration, which had previously been unreported in the literature for *Ps. aeruginosa* strain PAO1. Consequently, these results suggest that there are other factors responsible for the shape of spread, not just those factors associated with limited resources in difficult environments. More work is required to understand how environmental parameters affect the mechanisms responsible for irregular patterns of spread and why these environmental parameters affect microbial strains differently.

Chapter 4

How does the geometry of the microbial colony affect the multi-level selection of social behaviour?

Abstract

As microbial colonies spread across agar plate surfaces, they can exhibit a variety of spatial patterns. While the mechanistic processes behind these patterns are well known, our knowledge of the ecological and evolutionary implications these patterns have on both the individual cells in the colony and the colony as a whole is still limited. We make the observation that during their spread across agar plate surfaces, *Pseudomonas aeruginosa* colonies produce siderophore public goods, which diffuse into the area surrounding the growth of the colony. This enables the colony to sequester the surrounding iron-based resources required for growth. We utilise a multi-level selection framework, combined with a geometric model, to investigate how the geometry of the pattern of spread affects the individual- and group-level fitness of the population with respect to resource acquisition. The results suggest that individual-level fitness is maximised by spreading in a regular circular pattern while group-level fitness is maximised by spreading in an irregular pattern of spread i.e. non-circular. While it is clear many other factors have an effect upon the fitness of individuals inside the colony and the colony as a whole, our results show that the geometry of the colony can be a significant factor with evolutionary implications.

Introduction

The evolution of social behaviour in microbial biofilms is a prominent area in microbiology (Crespi, 2001, Kreft, 2004). Biofilms are structured communities of microbes where individuals interact with each other via physical and chemical stimuli. By structuring themselves in biofilms, bacteria are able to behave as multicellular organisms, coordinating their actions to improve their persistence in otherwise difficult environments (Watnick and Kolter, 2000). Traits of these biofilms have traditionally been explained in terms of their effect at a group-level, ignoring effects at the cellular level, due to biofilms being thought as clonal groups with shared interests (Monds and O'Toole, 2009). However, evolutionary biologists with backgrounds in other model systems have revealed how traits can arise via social behaviour between cells within the colony (West et al., 2007a, Foster et al., 2004, Nadell et al., 2009). The evolution of these social behaviours has typically been analysed utilising inclusive fitness theory (or more specifically kin selection). This theory quantifies the evolutionary success of a trait according to how it benefits the individual itself and neighbouring highly related individuals (West et al., 2006b, Hamilton, 1964, Queller, 1992). However, an alternative yet mathematically equivalent theory known as multi-level selection has gained some popularity as a framework for investigating the evolutionary success of a trait (Sober and Wilson, 1998, Lion et al., 2011, Wade, 1985, Wilson and Sober, 1994). In contrast to inclusive fitness theory which looks at selection at the gene level, multi-level selection quantifies the evolutionary success of a trait according to its effect across multiple selection levels (i.e. gene, cell, individual and group) simultaneously. Some researchers believe the multi-level selection framework can be a more intuitive method of exploring the evolutionary outcome of a trait (Lion et al., 2011, Okasha, 2010).

Many of the cooperative social behaviours within a microbial population involve the production of costly molecules by cells (West et al., 2007a). Researchers call these costly molecules public goods, as cells share these molecules ("goods") amongst neighbouring individuals to achieve group-level benefits such as an increase to carrying capacity and/or the persistence of the population. In this study, we focus on iron-chelating public goods called siderophores, which bind to naturally abundant insoluble iron (Fe^{3+}) molecules in the environment to

create a soluble complex (Neilands, 1982, West and Buckling, 2003). For the *Pseudomonas aeruginosa* strain PAO1, these siderophores (specifically pyoverdins – a type of siderophore specific to *Ps. aeruginosa* (West et al., 2007a)) produce the characteristic fluorescent green/yellow colour of the colony (figure 4.1) and are crucial for cellular growth and reproduction (Griffin et al., 2004). Due to natural diffusive processes, these siderophores spread out into the extracellular area surrounding the colony to produce a fuzzy green halo region, thereby allowing the colony to access iron outside of the perimeter of the biofilm (Wensing et al., 2010). A pioneering study by Griffin et al. (2004), found that factors both within- and between-group affect the production of siderophore public goods. Specifically, they found increased within-group competition reduced the likelihood of siderophore production, even when between-group conditions would otherwise promote siderophore production. This result illustrates how metabolically costly siderophore public good production can provide a group-level benefit by helping neighbouring highly related individuals (via kin selection), so long as local individual-level competition is sufficiently low enough. Consequently, different levels of the system can influence the evolutionary outcome of traits.

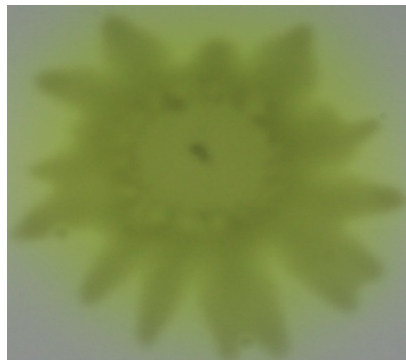


Figure 4.1: A *Ps. aeruginosa* strain PAO1 colony grown on 0.5% KB agar. We see the distinctive siderophore-induced green/yellow hue of the otherwise grey bacteria. The secreted siderophores diffuse into the area surrounding the colony, producing what we describe as a ‘siderophore halo’. The siderophore halo enables the colony access to iron resources outside of the boundaries of the colony.

Microbial biofilms spread across surface environments via the use of multiple motility mechanisms. Of these, swarming motility has received the most attention. Swarming is a cooperative behaviour in which individuals group up to form raft-like structures. These raft-like structures then propel themselves across semi-solid surfaces by the combined usage of their flagella (Kearns,

2010). Swarming motility requires the use of costly rhamnolipid surfactant public goods to moisten the surface and facilitate movement (Caiazza et al., 2005). By using swarming motility to disperse, the colony is able to expand the area it sequesters, thereby reducing competition among kin, reducing the exposure of individuals in the colony to toxic waste products produced by other individuals and potentially increasing access to resources (de Vargas Roditi et al., 2013, Nadell et al., 2010). During the process of swarming, colonies can form irregular, fractal-like patterns of spread across surface environments (Golding et al., 1998). These patterns have been the focus of interdisciplinary research with reaction-diffusion models comprising much of the classical work (Golding et al., 1998). A recent empirical example indirectly investigating the effect of irregular tendril patterns utilised strains of *Ps. aeruginosa* that were either cooperative via a swarming mechanism (and therefore produced irregular shaped colonies) or were defective and lacked a swarming mechanism (and therefore produced circular shaped colonies) (de Vargas Roditi et al., 2013). They revealed the carrying capacity of the colony over time was greater (i.e. a larger group-level benefit) for those colonies that swarmed compared to those colonies that did not swarm, even though growth rates in liquid media were the same for both strains. However, they also showed that swarming motility would only occur if the relatedness in the colony was high (i.e. the system did not have a significant degree of individual-level competition), agreeing with the findings of Griffin et al. (2004), thus showing that the processes responsible for the shape of spread have individual-level and group-level trade-offs. Recently there has been an increased interest into the ecological and evolutionary basis of irregular spread patterns (Deng et al., 2014), yet there is still much to understand. Consequently, we focus on the evolutionary implications of these spatial patterns of spread across multiple levels of selection to help understand why these patterns of spread might arise.

We have previously shown that extrinsic environmental factors affect the pattern of microbial spread and these patterns of spread may have important ecological consequences (Chapters 2 and 3). Because *Ps. aeruginosa* colonies exhibit a variety of different patterns of spread as they traverse across different agar plate environments, we consider the pattern of spread to be a trait of the colony. We predict that the shape of spread affects a colony's ability to extract

resources from their environment, thereby affecting fitness both at the individual-level and at the group-level. Consequently, from an evolutionary perspective, natural selection should favour the evolution of a spatial pattern, which maximises the fitness across all levels of selection according to the parameters of the system. We predict that a colony maximises its perimeter by spreading in an irregular pattern of spread (i.e. non-circular), thereby gaining access to a greater region of unexploited resources when compared to those colonies that exhibit a circular pattern of spread (Lewis and Kareiva, 1993). Furthermore, we predict that as the colony exhibits more tendrils (finger-like, elongated structures stemming from the central portion of the colony), the colony and its siderophore halo should extract more iron resources from the environment, thereby maximising fitness at the group-level. Indeed, we believe the colony should exhibit tendrils so long as the costs at the individual-level does not counteract the group-level benefit of tendril dynamics. Consequently, in nature where colonies are often competing against each other for resources, we expect those colonies with an irregular shape of spread to outcompete those colonies that exhibit circular shapes of spread. As an aside, with regard to the spread of populations in general, understanding the evolutionary basis behind the shape of spread would help to improve our ability to predict the spread of a population. Particularly as it has been increasingly recognised that evolutionary processes are significant factors behind the spread of an invasive species (Lion and Baalen, 2008, Phillips et al., 2010).

The effect of spatial environmental heterogeneity (e.g. variation in the topology of the environment or variation in the distribution of resources) is a key topic in ecology, as it can influence various ecological and evolutionary characteristics of a population and its members (Barraquand and Murrell, 2012, Day et al., 2003, Schreiber and Lloyd-Smith, 2009, Tilman, 1994). For example, environmental heterogeneity can result in the spatial structuring of a population (Lion and Baalen, 2008). This can affect the selective pressures faced by individuals in the population, thereby influencing the evolution/response of various traits and mechanisms responsible for ecological characteristics such as reproduction, resource sequestration and mortality (Lion and Baalen, 2008, Kendall and Fox, 1998, Stein et al., 2014). An empirical example of spatial environmental heterogeneity's effect upon traits of an individual/population is

the acquisition of nutrients from the soil by plants. In response to the distribution of resources in the environment, a plant can adjust their root morphology to achieve the optimal level of foraging (Casper and Jackson, 1997, Barber and Mackay, 1986). For instance, when the resources in an environment are distributed in clusters, the plant develops a different root branch morphology (i.e. make their roots shallower) than when the resources in an environment are distributed uniformly. Despite spatial environmental heterogeneity being increasingly included in ecological studies, the ecological and evolutionary links between the shape of population spread and the spatial heterogeneity of environmental properties has been relatively unexplored (Cumming, 2002). We believe this is because of the lack of appreciation for the possible influence of population shape upon various ecological and evolutionary characteristics. Based on the apparent reaction of colony shape to environmental parameters in Chapter 3, we speculate that the spatial heterogeneity of resources in the environment could affect the predictions made in the previous paragraph relating to the pattern of spread affecting a colony's ability to extract resources from their environment. Consequently, an avenue of this study is to investigate the effect of spatial heterogeneity in our system to see whether it does indeed influence the balance of selection across multiple levels with regard to population shape.

In this study, we use a simple geometric model to explore how the addition of a siderophore halo surrounding the shape of microbial spread affects the acquisition of iron from a variable environment (i.e. an environment with spatial heterogeneity) and to investigate the association between the shape of spread and the selective pressures of the system across multiple-levels. Specifically, we investigate how both the individual- and group-level fitness components (i.e. multi-level selection) respond to changes in the irregularity of the shape while keeping the actual area of the colony consistent, where we define irregularity as the number of tendrils exhibited by the colony. We calculate two geometric measurements of fitness to ascertain the individual and group levels of fitness (to clarify, this does not mean the geometric mean fitness, rather we intend this as a measurement of fitness based purely upon the geometric properties of the colony). First, we evaluate the area the siderophore halo covers as a proxy of group-level fitness i.e. the foraging region of the colony per unit/individual (we

do not need to account for area of colony, as it is consistent between colonies). Secondly, we consider the area the siderophore halo covers per perimeter unit to be a proxy of the individual-level fitness of individuals along the edge of the colony i.e. the resources each individual along the edge of the colony gains. We make this measurement because we assume these individuals along the population edge are also those most affected by the shape of spread itself and are the main individuals whom initiate the key processes (cellular growth and particularly outwards motility) responsible for the shape of spread (Nadell et al., 2010). With these measurements, we ascertain which shapes of spread benefit the colony both at an individual-level and at a group-level. We also check our results for when the perimeter of the colony is consistent between irregular shaped colonies and circular colonies, to check that the effect is from the shape and not due to differences in the perimeter.

Methods

Modelling the shape of the colony

In this study, we represented the shape of the colony with standard geometric equations. The shape of these colonies ranged from a regular circle to irregular ‘flower patterns’ or ‘polar rose patterns’ representing colonies exhibiting tendrils. We first defined colonies in the polar coordinate system, a two-dimensional coordinate system where each point on a plane was determined by a distance from a fixed point (r) and an angle from a fixed direction (θ). The outside edge of the colony was represented in the polar coordinate system by modifying the frequency of a sine curve (equation 4.1), where k represented the number of tendrils of the colony and θ ranged between 0 and 2π . We added the sine curve to an integer, α , to represent the radius of the central inner part of the colony.

$$r = \alpha + \sin(k\theta), \theta = 0, \dots, 2\pi \quad (4.1)$$

Using this, we investigated two different scenarios in this study. First, we matched the area of each irregular shape such that it was equal to the area of an equivalent circle. We used this to measure the effect of the population shape upon the individual and group levels of fitness. Second, we matched the perimeter of an irregular shape such that it was equal to the perimeter of an equivalent circle. We used this in order to make a fair comparison for our measurement of individual-level fitness (i.e. so that the individual-level fitness of the colony did not incur a double cost of both the increased number of individuals along the leading edge - due to the increased perimeter of a shape

with more tendrils - and the effect of the population shape itself). To ensure all shapes covered the same area in the first scenario, we adjusted the radius of the central part of the shape such that as the frequency of the sine curve increased, the radius of the inner circle α , decreased. To ensure all shapes had the same perimeter in the second scenario, we first drew the irregular shape with $\alpha = 3$. We then calculated the perimeter by summing the distance between each neighbouring point along the shapes outline (we did this for 250000 points to ensure accuracy). We then drew a circle with a matching perimeter according to the circle identity $P = 2\pi r$, where P represents the perimeter and r represents the radius of the circle.

For the shapes in both scenarios, we represented the siderophore halo as an outline surrounding the shape (figure 4.2). To create the siderophore halo, we transformed the shapes from polar coordinates into Cartesian coordinates. We then used Pythagoras' theorem to project points perpendicular to tangents along the leading edge of the shape such that they were at a set minimum distance away, h , from at least one point on the perimeter of the shape (figure 4.2). We adjusted the characteristics of the shapes according to the values in table 4.1. Although we investigated shapes with up to 300 tendrils, we note that the observed tendril patterns of *Ps. aeruginosa* on agar plates did not typically exhibit more than 30-40 tendrils (see Chapter 3 for evidence).

Table 4.1: The parameters used for shapes in both the matching area and matching perimeter scenario.

Parameter name and description	Values used in matching area scenario	Values used in matching perimeter scenario
α = Radius of a circle with zero tendrils	3	
k = number of tendrils	0 , (5,6,7,...,39,40), (45, 50, 55, ..., 295,300)	0 , (6,8,...,38,40)
h = perpendicular length of halo	0.2	

To measure the area and perimeter of each shape and its siderophore halo, we utilised the java-based standalone image analysis software ImageJ (Rasband, 2014.) on pictures of the shapes that were created in R to a specified 4000x4000 resolution. This was used instead of EImage because of its widespread use in other microbial studies (Taylor and Buckling, 2010) and because of some of the difficulties in using the R-based code interface of

EImage in Chapter 2. While this image analysis methodology can have a number of accuracy issues (e.g. it uses a lattice), we used this image analysis technique due to the lack of an appropriate analytical equation describing the siderophore halo surrounding the shape. The image analysis technique calculated the area by first transforming the picture into a 4000x4000 matrix representing the shape of the colony across a lattice grid whereby entities in this matrix equalled one if the picture of the shape occupied that part of the lattice and zero if it did not. From this, the image analysis technique calculated the area by summing those entities of the shape lattice equal to one. We then made these measurements proportional to the area covered by a circle of the same area or perimeter depending upon the scenario, eliminating effects resulting from the scale of the lattice used and allowing us to reference the between-group aspects of any results. We used this method to both measure the area covered by each shape and the area covered by each shape combined with its siderophore halo. We measured the perimeter of each shape and its siderophore halo in ImageJ by fitting a spline to the edge of each shape. We then measured the perimeter of this spline. We did this to limit problems arising from the pixilation of the perimeter. We note that the pictures for the matching area and the matching perimeter scenarios were on different scales from each other. We drew all pictures in the matching area scenario within axis limits equal to 4 and we drew all pictures in the matching perimeter scenario draws all pictures within axis limits equal to 40. The difference arose due to the size of the circles with a perimeter matching the perimeter of an irregular shape being much larger than the size of irregular shape (figure 4.5).

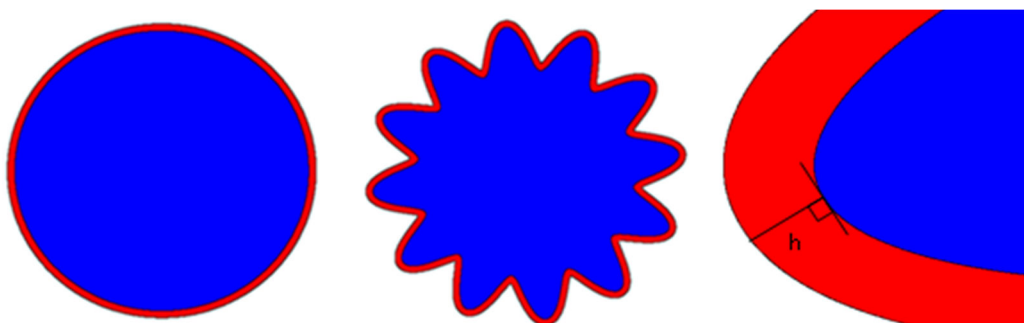


Figure 4.2: The blue region on the left and middle plots was the shape produced by equation 4.1 for $k = 0$ (left) and $k = 12$ (middle - representing a shape with 12 tendrils). Each shape had a siderophore halo projected around them, as shown by the red region. We projected these halos from the shape by using Pythagoras' theorem at each point of the shape (as shown on the right plot). This ensured that each point of the halo was exactly a set minimum range from a point on the edge of the shape.

Scattered distribution of resources Clustered distribution of resources

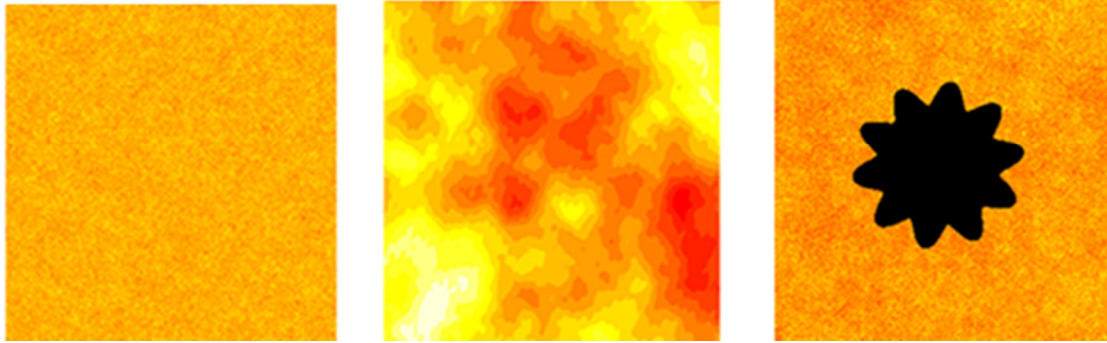


Figure 4.3: We based background environments upon the matern covariance function. Resources in these backgrounds ranged from scattered distributions of resources (Left) to clustered distributions of resources, with clusters of high and low resources (Middle). (Right) An illustration of the colony shape and the auto-correlated environment lattices placed on top of each other.

Modelling the background environment

Our study also investigated how different environment types affected the ability of the colony shape to sequester resources. Specifically, we utilised environments with different degrees of resource autocorrelation to detect the effect of spatial heterogeneity upon the shapes of the colony (figure 4.3). The environments were created such that the distribution of resources was either a scattered distribution of resources (a distribution of resources with relatively little spatial autocorrelation) (figure 4.3 – left) or a clustered distribution of resources (a distribution of resources with relatively large spatial autocorrelation) (figure 4.3 - middle).

We created the background lattices representing these backgrounds with the RandomFields R package (version 2.0.65 - <http://ms.math.uni-mannheim.de>). This package created a lattice representing Gaussian environments with an underlying stochastic process. To test the effect of different spatial distributions of resources, we used the Matern autocorrelation function (equation 4.2) due to its common usage in geo-statistics to recreate auto-correlated environments. Examples of auto-correlated environments produced by this function include mountain ranges and ocean temperature gradients (Gneiting et al., 2010, Minasny and McBratney, 2007, Liu et al., 2010).

$$C_{\text{matern}}(d) = \frac{2\sigma^2 \left(\frac{d}{2\alpha}\right)^\nu K_\nu\left(\frac{d}{\alpha}\right)}{\Gamma(\nu)} \quad (4.2)$$

In this Matern cross-covariance, $K_\nu(\cdot)$ represents the modified Bessel function of the second kind of order ν , $\Gamma(\cdot)$ represents the gamma function, d represents the Euclidean distance between two sites, σ^2 was the non-spatial Gaussian variance of the function, α represents the rate of decay between points and ν represents the smoothness of the environment. In our study, we adjusted the random field environments dependent upon the Matern cross-covariance function by three key factors: (1) the Gaussian mean of the resource distribution, (2) the non-spatial Gaussian variance around the mean and (3) the scale of spatially auto-correlated variance (controlled by the smoothness parameter, ν). By varying the smoothness parameter of the Matern function, we controlled how clustered the resources were in the environment. A small smoothness parameter ($\nu = 1$ – Table 4.1) represented a scattered distribution of resources (left plot of figure 4.3) and a large smoothness parameter ($\nu = 1000$ – Table 4.1) represented a clustered distribution of resources (middle plot of figure 4.3). The parameters used for both types of environment are in table 4.2.

To investigate how the shape of the colony and its surrounding halo affected the colony’s ability to acquire resources, we created background environments upon a 4000x4000-lattice grid, which was the same size as the pictures of the colony. To calculate the resources acquired by the shape of the colony, we placed the 4000x4000 lattice of each shape on top of the 4000x4000 lattice representing the background environments. We repeated the environment models 25 times in order to see a clear signal from these runs and account for the stochasticity in these matern based random field environments.

Measurements were conducted in R v3.0.3 (R Development Core Team, 2014).

Sensitivity analysis

We checked the sensitivity of our results to the initial parameters of the system in Appendix B. We found the qualitative results to be consistent.

Table 4.2: The parameters used in the auto-correlated environments

Parameter	Values
Global mean value of resources	5
Global resource variation	0.1 and 1
Smoothness parameter of the autocorrelation	1 (Scattered Environment) 1000 (Clustered Environment)

Results

We have divided the results into three parts, one reporting the raw geometric measurements of fitness for each shape, one reporting an approximation of the theoretical optimum number of tendrils and one reporting the geometric measurements of fitness for each shape in the auto-correlated environments. We subdivided the raw geometric measurements of fitness into a further two parts, one for shapes with equal area and one for shapes with equal perimeter. For the matching area case, we measured two characteristics. First, the area sequestered by the siderophore halo only (this represented the foraging region of the colony – measuring the total area of the shape and halo was not required as area of the shape was consistent for all shapes). Second, the area of the siderophore halo divided by the perimeter of the shape (this represented the resources gained by the assumed active individuals along the leading edge). In the case of shapes with matching perimeter, we calculated the area of the siderophore halo only (the other measurements were not required as perimeter was matching in this case and figure 4.5 illustrates the obvious size differential between a circle and an irregular shape with matching perimeter as the number of tendrils increases). We used this matching perimeter measurement to check how the shape of spread exclusively affected the individual-level fitness property of the colony without the possible influence of the increased perimeter (increased number of individuals competing for resources) in the matching area scenario.

Measurements

Shapes of matching area

The area covered by the siderophore halo increased as the number of tendrils increased up until a peak (~4.4 times the area of a siderophore halo surrounding a circular colony) at which point the area covered by the siderophore halo began to decline (figure 4.4 – top left). We believe this was due to the perimeter of the shape combined with its halo initially increasing towards a peak before also decreasing over time. The decrease in perimeter arose due to the decreasing amount of space in-between tendrils as the number of tendrils increased. Subsequently, this caused the siderophore halo from one tendril to overlap with the siderophore halo of the opposite tendril, thereby creating a double accounting effect, where the area in-between two tendrils was

sequestered by double the amount of siderophores needed for optimal extraction. Consequently, the shape of the colony combined with its siderophore halo became more circular past a critical point. This result shows that the colony achieved maximum group-level fitness (i.e. the point at which the colony as a whole sequestered the maximum possible resources from the environment) when it exhibited an intermediate number of tendrils.

Conversely, we found that as the number of tendrils increased, the area acquired by active individuals along the edge of the colony (i.e. the area of the siderophore halo divided by the perimeter) proportionally decreased towards zero when compared to a circular colony of the same area (figure 4.4 – top right). This was due to the perimeter of the shape increasing faster than the increased area gained by the halo as the number of tendrils increased. The result showed that a circular shaped colony achieved a higher individual-level of fitness (based on our individual-level of fitness measurement) compared to irregular shaped colonies, as individuals along the colony frontier acquired proportionally more of the food when the perimeter of the colony was smaller.

Shapes of matching perimeter

As the irregularity of the colony shape increased (i.e. as the number of tendrils increased) so did the perimeter of the colony. Consequently, the radius of a circular colony with a matching perimeter increased (based on the equation for the perimeter of a circle of radius r , $2\pi r$). The result was a circular colony with a vastly greater area compared to a colony exhibiting tendrils with a matching perimeter (figure 4.5). The resultant size difference meant the area of a siderophore halo surrounding a colony exhibiting tendrils was less than the area covered by a siderophore halo surrounding a circular colony with the same perimeter. Therefore, increasing the number of tendrils caused the proportional area covered by the halo, compared to a circular colony, to tend towards zero (figure 4.4 bottom). This matched the result obtained in the matching area scenario, that the individual-level of fitness (i.e. the resources gained by active individuals along the leading edge) was maximised when the colony was circular. This matching perimeter scenario showed that the individual-level fitness of the colony was not purely due to the increased number of individuals along the leading edge i.e. there was not a double cost of both increased competition arising from the increased perimeter and the effect of the shape.

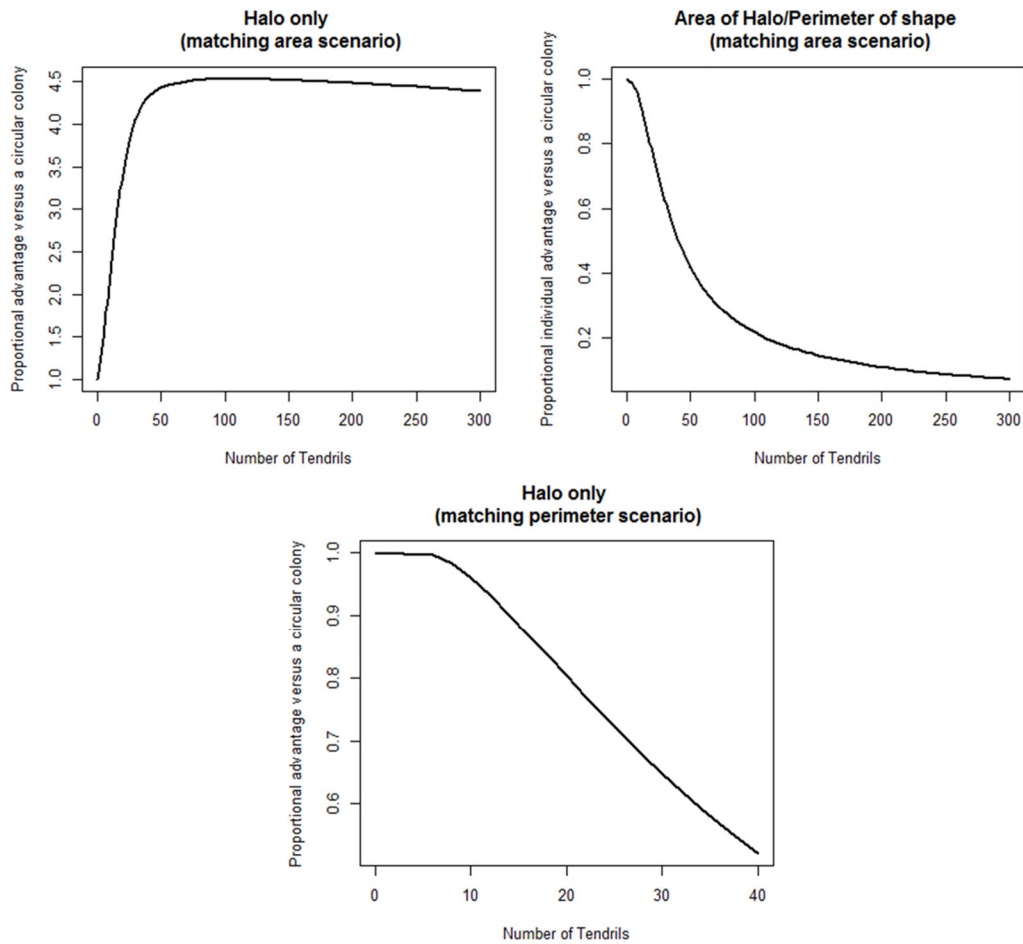


Figure 4.4: (Top left) The area covered by the siderophore halo surrounding an irregular colony compared to area covered by the siderophore halo of a circular colony with matching area. (Top right) The area covered by a siderophore halo of an irregular colony divided by the perimeter of the colony, proportional to the same measurement of a circle with matching area. (Bottom) The area covered by the siderophore halo surrounding an irregular colony compared to area covered by the siderophore halo of a circular colony with matching perimeter.

Analytically approximating the optimum number of tendrils

We approximated the optimum number of tendrils (i.e. the peak number of tendrils at which group-fitness was maximised) by using the assumption that double accounting with no increased benefit approximately began to occur when the distance between the tips of the two neighbouring tendrils, L , was less than the sum of the siderophore halo lengths, h , being projected from the edge of the colony into the space between the two tendrils (figure 4.6). Thus, the optimum number of tendrils was approximately when:

$$L \approx 2h \quad (4.3)$$

From this assumption, we could approximate the optimum number of tendrils, k , because of the trigonometric equation (4.1) used to represent the colony.

Therefore we could find the distance between tendril tips, L , according to their position on a circle of circumference, $2\pi(1 + \alpha)$. Note α was the radius of the inner circle and 1 was the length of the tendril, which combined, was the radius of the circle upon which the tips of tendrils are situated. Hence, for a number of tendrils k , we approximate the distance between tendril tips as:

$$L \approx \frac{2\pi}{k}(1 + \alpha) \quad (4.4)$$

Plugging (4.4) into (4.3) and rearranging, the optimum number of tendrils approximately occurred in our model when:

$$k \approx \frac{\pi}{h}(1 + \alpha)$$

Using the parameters in table 4.1 ($h = 0.2$, $\alpha = 3$), we calculated the approximate optimum number of tendrils as $k \approx 63$. Consequently, if the colony developed a number of tendrils below this point, the colony was not extracting the maximum amount of resources from the environment in-between tendrils, whilst if the colony developed a number of tendrils above this point, the effect of double accounting made the development of these extra tendrils counterproductive. This approximation corresponded well with the results shown in figure 4.4.





	Colony exhibiting 20 tendrils	Equivalent circular colony
Without Halo		
With Halo		

Figure 4.5: The difference in size between a colony, which exhibits tendrils, and a circular colony with matching perimeter. The top row was the shape without its siderophore halo and the bottom row was the colony shape combined with its siderophore halo. This example was for irregular shapes with 20 tendrils.

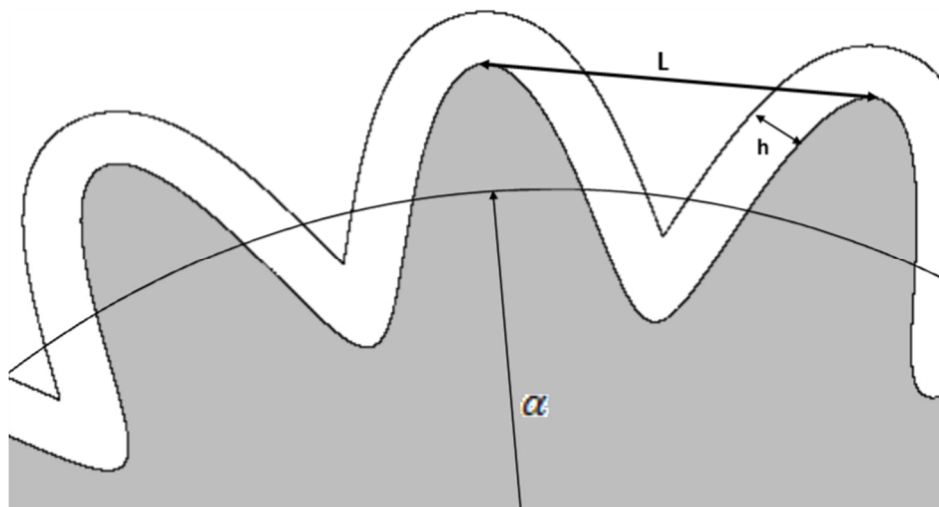


Figure 4.6: The setup used to calculate the approximate optimum number of tendrils, where L is the distance between the tips of two tendrils, α is the radius of a circle with zero tendrils and h is the perpendicular length of halo.

Spatially auto-correlated environments

We found that the fitness measurements in variable, spatially auto-correlated environments broadly followed those results seen in the previous section. Group-level fitness (the area sequestered by the siderophore halo only in the matching area scenario) increased as the colony developed more tendrils up until an intermediate number after which group-fitness steadily declined (figure 4.7). Whereas individual-level fitness was maximised when the shape of spread was circular, as this was when the amount of resources acquired per active individual along the leading edge of the population (the perimeter) was at its highest (for both the matching area and matching perimeter scenarios).

Analysis of the error envelopes in figure 4.7 showed that these results varied according to the parameters of the matern auto-correlation function (equation 4.2) used to generate the auto-correlated environment. Changes in the matern auto-correlation that led to increased variation were:

1. An increased value for the non-spatial Gaussian variation of the mean, σ , i.e. how variable the resources could be regardless of the spatial autocorrelation (comparing the blue and red error envelopes in plots on each row of figure 4.6).
2. Changing the distribution of resources in the environment from a scattered distribution to a clustered distribution (i.e. an increased value for the smoothness parameter ν in equation 4.2).

Because of the increased variation, the optimal number of tendrils changed slightly according to the parameters of the environment (figure 4.7).

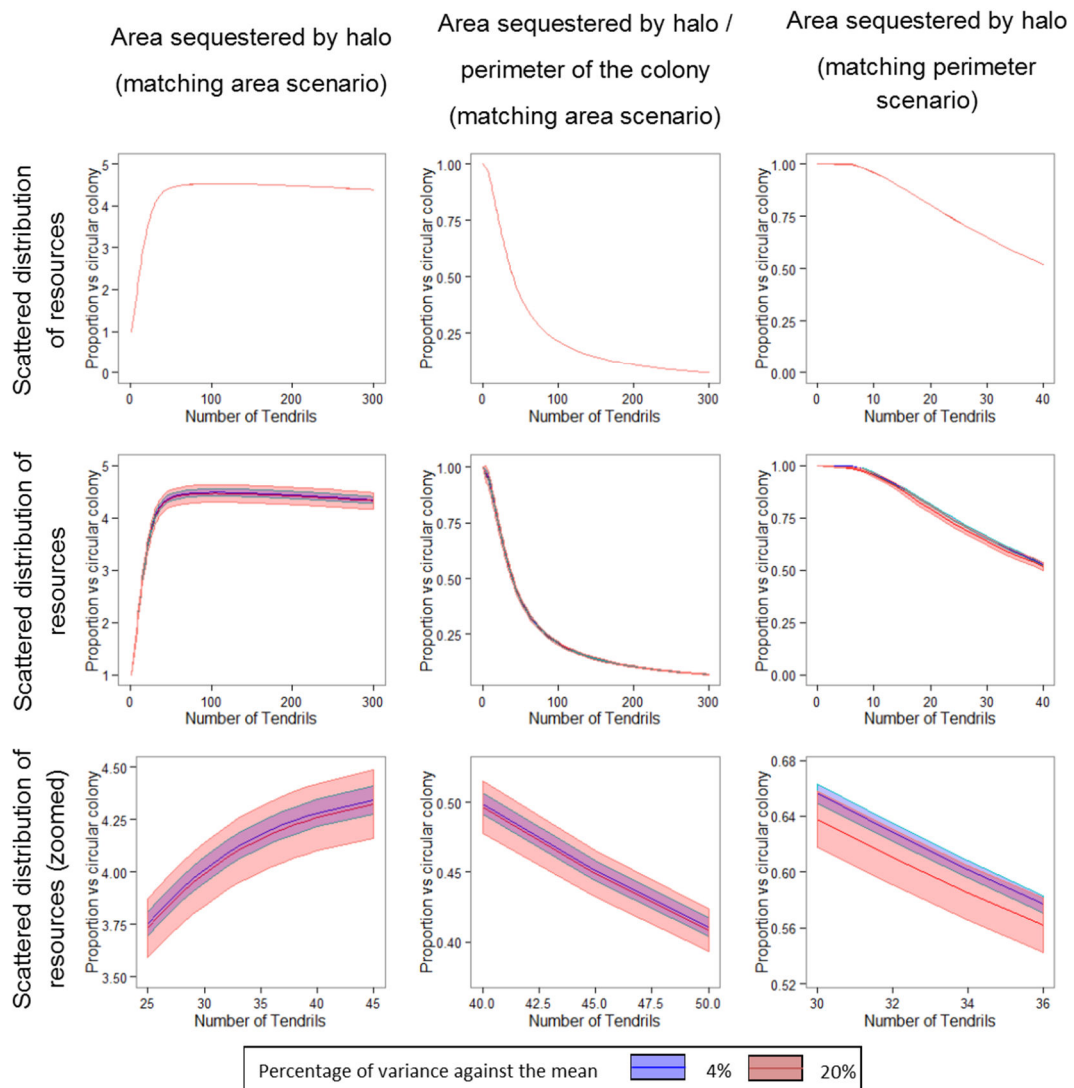


Figure 4.7: In general, environmental heterogeneity did not affect the qualitative results of our model. (Left) The area covered by only a colony's siderophore halo in the matching area scenario. (Middle) The measurement of the area occupied by the shapes siderophore halo divided by the perimeter of the shape in the matching area scenario. (Right) The area covered by only a colony's siderophore halo in the matching perimeter scenario. Those plots on the top row were for a scattered distribution of resources whilst those plots on the middle row were for a clustered distribution of resources. All values were proportional to a circular colony of the same area. Each plot contains two lines, a blue line representing an environment seeded with non-spatial variation equal to 4% of the mean and a red line representing an environment which variation equal to 20% of the mean. Each line has an error envelope of corresponding colour representing ± 1 SE of the mean value. Bottom plots are the same as the middle plots but at a zoomed in scale.

Discussion

In this study, we investigated how the geometric properties of bacterial spread across agar surface environments could affect the fitness of the colony, both at the individual- and group-level, consistent with multi-level selection theory. Noting the observation of a 'siderophore halo' surrounding the microbial colony, we found that the individual-level fitness of members along the leading edge of the colony was maximised when the spread of the colony was circular, whilst the group-level fitness of the whole colony was maximised when the spread of the colony was generally irregular (i.e. tendrill dynamics). Furthermore, we found that the group-level fitness of the colony was maximised for an optimum number of tendrils, as an increase to the number of tendrils past this point was counterproductive due to a double accounting effect. Therefore, our results show that the pattern of spread has evolutionary implications, with the shape of spread dependent on whether the system favours individual-level or group-level selection. While we consider purely the geometric characteristics of the colony in this study, the balance between whether individual-level or group-level selection is favoured in the system depends upon many intrinsic and extrinsic factors.

The first factor we consider is the energy cost of the swarming motility mechanism responsible for the irregular patterns of spread. In order to develop tendrils, individuals must incur a public good cost via the secretion of rhamnolipids to decrease the surface tension, thereby enabling swarming motility (Kearns, 2010, Kearns and Losick, 2003). Swarming behaviour offers a number of group-level benefits, such as an increase to carrying capacity and an increase to antibiotic resistance (de Vargas Roditi et al., 2013, Kim et al., 2003). Cooperation between individuals, via the sharing of production costs of these public goods, reduces the selection against swarming behaviour at the individual-level thus enabling the exhibition of tendrill-like patterns (de Vargas Roditi et al., 2013). Therefore, a determinant of whether or not a colony can produce tendrill dynamics depends upon the level of cooperation between individuals. If the group-level benefit from swarming motility outweighs the individual-level cost of rhamnolipid production then the colony should select for tendrill dynamics.

Similar factors are the costs and benefits associated with siderophore production (Griffin et al., 2004). We have shown that an irregular shape of spread, up to an optimum point, improved the utilisation of a siderophore halo compared to a circular colony (as the area covered by the halo of an irregular pattern was greater than the halo covered by a circular colony with the same area). We believe this would reduce the average metabolic cost of siderophore production across the population, possibly offering both a group-level benefit and an individual-level benefit (as individuals can spend more of their internal energy budget upon other mechanisms). Whilst such a mechanism can achieve a group-level benefit in low-resource environments, the probable costs and difficulties that individuals would experience in such an environment may encourage evolution to select for traits more advantageous at the individual-level over those at the group-level (Griffin et al., 2004). As resources in the environment increase, selection at the individual-level would decrease and therefore the system should then begin to promote traits improving fitness at the group-level.

We base the model used in this study on the assumption that the colony is homogeneous and does not contain any spatio-temporal variation in a colony's ability to acquire resources. However, introducing heterogeneity into the parameters of the system may affect the results (Lion and Baalen, 2008). For example, in comparison to those individuals within the colony, the individuals on the periphery of the colony could have higher fitness, either because they are able to sequester untouched resources outside the confines of the colony and/or because the competition for resources along the periphery of the colony is lower due to a lower population density (Webb et al., 2003). This factor could affect the balance of selection across multiple levels. Another example of heterogeneity in the system are the observable differences in the green/yellow hue of figure 4.1, where the siderophore halo is more visible in-between tendrils than at the tips of the tendril. The heterogeneity of siderophores can lead to various feedbacks affecting the balance between individual- and group-level fitness. For instance, in regions of the population where siderophores are abundant (i.e. the double accounting region in-between tendrils), individuals may reduce their individual contribution to the production of siderophores compared to those individuals at the tips of the tendrils (Kümmerli and Brown,

2010). By alleviating themselves from the cost of siderophore production, individuals within this region could then invest in other mechanisms such as dispersal, thereby increasing their rate of spread. Consequently we theorise such a feedback would promote a shift back towards a circular shape of spread in order to increase the average level of fitness for individuals along the leading edge of the colony. To study if such a feedback exists, researchers could use an empirical study, which artificially infuses the environment with siderophores.

Although results were qualitatively consistent in all of the heterogeneous environments we studied, we found that environmental heterogeneity in the form of patchiness could slightly affect the fitness of the colony across all levels of fitness. For instance, environmental variation in the amount and position of resources slightly affected the number of tendrils that the colony should develop in order to achieve optimum fitness. The limited effect of resource heterogeneity in our study is somewhat surprising as resource heterogeneity has a significant effect in similar biological situations where shape affects the ability to sequester resources (i.e. the adaptation of plant root morphologies discussed in the introduction (Casper and Jackson, 1997, Barber and Mackay, 1986)). However, we note that on reflection, the relatively limited effect of the environment in our study was probably due to the mean value of the resources staying consistent throughout each environment we modelled and the resolution of these environments reducing any impact of changes to these resource values. We speculate that variability in our results may change as the lengths of the tendrils change, the size of the colony changes and/or the parameters of the environment change. Consequently, we believe there is scope for future work to study other types of environment (i.e. those with a non-consistent mean) and different shapes of population spread.

Indeed, in our model we assumed that patterns of microbial spread were symmetric and lacked the ability to sense environmental heterogeneity. In reality, bacterial populations are able to sense chemical stimuli (such as resource availability via chemotaxis mechanisms) and move towards or away from these signals as appropriate (Keller and Segel, 1970). We theorise directed movement towards patches of high quality resources via chemotaxis will increase the amount of resources acquired by a colony with an irregular pattern of spread, such that the group-level and average individual-level

geometric measurements of fitness components both increase, similar to that seen in plant root morphologies (Casper and Jackson, 1997, Barber and Mackay, 1986). As such, we expect the addition of resource sensing and movement towards patches of high-quality or quantity resources to tip the fitness balance in favour of an irregular pattern of spread.

The distribution of resources is not the only potential environmental factor affecting the optimum shape of spread in a system. In the scenario where more than one population (group) is competing for resources in the global environment, the strength of competition can result in selection favouring those traits that benefit the persistence of the group, over traits that benefit individual fitness and vice versa in the absence of global competition (Griffin et al., 2004). For instance, van Ditmarsch et al. (2013) passaged isolated *Ps. aeruginosa* bacterial colonies across agar plate environments which favoured swarming motility for ten days. Whilst at day one, the initial wild type strain of *Ps. aeruginosa* exhibited distinct tendrill dynamics (therefore favouring group-level fitness), by day ten, the distinctness of these tendrills became less clear, reverting back towards a more circular pattern (favouring individual-level fitness). This was due to a large proportion of individuals within the population developing a hyper-swarming mechanism, conferring a motility advantage to these individuals in the population, regardless of the shape of the population, but at a trade-off against biofilm formation, a critical group-level trait for the persistence of colony (López et al., 2010). It is believed this behaviour developed due to the environment lacking the inter-group competition commonplace in the soil-based habitats where *Ps. aeruginosa* usually resides (van Ditmarsch et al., 2013). Their study shows that in the absence of group-level competition, maintaining the structural shape of the colony (i.e. such as an irregular shape of spread) is possibly not a significant factor upon fitness, with individuals possibly rushing to sequester as much area and resources as possible. Whether we can evolve the tendrill dynamics back again in this system via the presence of group-level competition is unknown. However, their study highlights the importance of external competition and its potential influence on the shape of spread.

Another environmental factor that we speculate can affect the balance of multi-level selection is the presence of predators in the environment. For example,

bacteriophages are viruses that infect and replicate themselves within bacterial cells (Barraquand and Murrell, 2012, Levin et al., 1977). By growing in a tendril shape, the swarm might increase the likelihood of encountering such predators (because those individuals at the tip of tendril are possibly more likely to reach new environments), thereby increasing exposure of the whole colony to a phage epidemic (Barraquand and Murrell, 2012, Levin et al., 1977). In this scenario, the group-level fitness coefficient might decrease and change the multi-level selection balance such that individual-level fitness is favoured instead.

We believe the model presented in this study should incorporate a number of improvements in future studies to ascertain the full effect of population shape on fitness across multiple levels. The three main improvements in our opinion are:

1. The inclusion of spatio-temporal variation of siderophore or population densities throughout the colony (Beyenal et al., 1998, Kamatkar et al., 2011).
2. The investigation of asymmetrical patterns of spread as opposed to the strictly symmetric patterns of spread we consider in this study (Doebeli, 1995).
3. The utilisation of a different method of analysis, as the image analysis methodology can introduce a number of inaccuracies to the measurements. These arise due to the transformation of the colony shape from an image into a lattice with discrete entries.

These improvements would help to verify these results and further establish the geometric effect of the population shape upon the fitness of the colony at both an individual- and group-level.

We speculate that individual based models (IBMs) which move away from analytical equations, may be more useful for investigating the group-level effects of the shape of spread and also for investigating the effect of cooperation on both the shape of the colony and selection at multiple levels (Xavier and Foster, 2007, Venturi et al., 2010). For instance, individual based models have shown that colonies of mixed populations consisting of two different strains (one which exploits the population and one which cooperates) might develop tendrils to segregate the population such that each tendril consisted exclusively of one of the two strains (Xavier and Foster, 2007). This illustrates how social interactions might influence the shape of spread, as if

cheaters arise within the population (those individuals who don't contribute siderophores), then it may be in the interest of the individuals producing siderophores to invest in dispersal strategies (such as tendrils) to segregate themselves from those who cheat (Venturi et al., 2010). With regard to siderophore production, we might also find that those individuals who cheat against the production of siderophores, particularly in low-iron environments, might invest in increased dispersal to reach patches consisting of high quality resources. Each scenario would influence the individual-level and the group-level fitness components of the system. Incorporating more than one type of bacteria to investigate these scenarios is a future direction of research.

The results of this study support and build upon the limited findings in the literature about the ecological/evolutionary purpose of these patterns of spread to microbial populations. First, studies in the literature have concluded that cooperative swarming motility (the motility mechanisms required for irregular patterns of spread in bacteria) is favoured by group-level selection but disfavoured by individual-level selection (de Vargas Roditi et al., 2013, Xavier et al., 2009). Their results suggest this because while swarming motility enables the colony to occupy a greater area through time (thereby offering an increase to the carrying capacity of the colony and a group-level benefit), these actively swarming bacteria lose in individual-level competition against those individuals not swarming (i.e. cheaters) within the colony. We note however that this study does not specifically study the shape of the colony itself, nor the siderophore halo. Hence, while our results agree with their findings, it is for different reasons due to our focus on the shape of spread. Indeed, while there is clearly a link between carrying capacity and the level of resources extracted from the environment, the inclusion of the siderophore halo surrounding the colony in our study reveals that a colony spreading in an irregular pattern of spread can sequester more food from the environment, thereby resulting in a group-level benefit even when the area of colony holds constant. Thus, the group-level benefits of irregular shaped spread are not limited to the potential for a population growth advantage resulting from increased spatial expansion over time relative to non-swarming, regular shaped spread (de Vargas Roditi et al., 2013), but also the influence that the shape of the colony has on resources across space in the environment, particularly if the colony is in competition with

other colonies. Our results also agree that individual-level fitness should not favour swarming and the associated irregular shapes of spread. Although, we suggest this is because individuals along the leading edge should not want to increase the number of individuals they are competing against (i.e. the perimeter) for those unused resources outside of the colony, not just the competition with other relatively unrelated individuals within the colony considered in (de Vargas Roditi et al., 2013). We believe this is an important consideration, due to the possible resource and reproduction advantages of being along the edge of the population (Kim et al., 2014).

Studies in the literature have also suggested that the parameters of the dispersal mechanisms behind these spatial patterns have evolved through long-term fine-tuning, as the parameters dictating these dispersal mechanisms must be in a relatively limited domain in order to exhibit tendrils (van Ditmarsch et al., 2013, Deng et al., 2014, de Vargas Roditi et al., 2013). Due to the existence of an optimum number of tendrils, we presume the number of tendrils and the distribution of these tendrils in space are attributes that should be under the same evolutionary fine-tuning.

Overall, the literature has typically focused on the multi-level selective pressures inside the colony between cheaters (non-swarming) and co-operators (swarming) and how these pressures within the colony translate to ecological benefits, such as spatial expansion, without explicit regard for the geometry of the population shape i.e. whether the number of tendrils changes or whether these tendrils are optimally distributed in space (de Vargas Roditi et al., 2013, Xavier et al., 2009). By considering the shape of spread by itself as a trait of the population, we have shown that it can offer benefits across multiple levels of selection and that an optimum number of tendrils mathematically exists for the colony to achieve the maximum group-level of fitness. Thus, we raise the importance of the geometric shape of spread itself as a trait with ecological and evolutionary relevance, not just an artefact of other processes and factors.

Showing that the shape of spread has evolutionary implications for the population may have potential importance in spatial ecology, with evolutionary processes (e.g. spatial sorting) known to be significant factor behind accelerating rates of spread for some invasive populations (Travis and Dytham,

2002, Urban et al., 2008). Indeed, by assuming macro-organism populations exhibit similar shapes of spread to microorganism populations, we theorise the shape of spread could affect these evolutionary processes. For instance, the shape of spread may cause the process of spatial sorting to intensify, as to spread in an irregular shape, we believe some individuals in the population (those at the tendril tips) would be required to disperse relatively long distances (i.e. have a better dispersal ability) compared to other individuals. By being at the tips of these tendril patterns, individuals are in a region with less choice of individuals to mate with for reproduction (if the population is not asexual), though those individuals available to mate with are similarly likely to have an enhanced dispersal ability in order to have reached that point in space at that particular time (Shine et al., 2011b). Thus, this is likely to result in further spatial selection for dispersal ability, which would increase the possibility of an accelerating rate of spread (Resasco et al., 2014). From a conservation management perspective, the results of this chapter show that management strategies which manipulate the shape of spread (either indirectly or directly through strategies such as environmental corridors (Akçakaya et al., 2007)) have an effect upon the evolutionary outcome of the population. Such a factor could explain why environmental corridors have sometimes helped invasive species to increase their rate of spread (Resasco et al., 2014). Consequently, researchers must give careful consideration to ensure conservation management strategies that change the shape of spread do not promote negative outcomes. Indeed, it may be beneficial in conservation management to consider how to manipulate the shape of spread for the intended purpose of the management strategy (e.g. via the closure of waterways (Tingley et al., 2013)).

In summary, we have shown that the geometry of microbial population spread influences both the individual- and the group-level fitness components of the population, with a direct trade-off between the two. Specifically, tendril development (up to a certain number of tendrils) can enable a colony and its siderophore halo to acquire more of the surrounding resources compared to a colony, which does not exhibit tendrils, thereby achieving a group-level benefit. In contrast, we found tendril development has a negative effect upon the individual-level fitness of members of the colony as the active individuals along the frontier of the colony acquire fewer resources and consequently a lower

mean fitness. While many other factors affect the balance of fitness according to multi-level selection, our results show that the geometry of the colony has evolutionary implications. Thus, if a link does exist between microbial and macrobial organisms, these results suggest that researchers need to pay a greater focus to the shape of population shape than they currently do, especially if conservation strategies are implemented which change the resultant shape of spread.

Chapter 5:

Games with frontiers – Part 1: Competition intensifies as invasion waves expand

Abstract

In a population, competition between individuals is a key driver of adaptation, affecting both ecological and evolutionary processes. Individuals along the frontier of the population face a unique situation, because of competition both from within the population and from other populations, and because they are thought to be the key individuals responsible for processes driving the spread of the population (particularly microbial populations). In this study, we focused on individual-level competition along the frontier of a population, in particular, how the curvature geometric property of the population affects the level of competition. Using microbial colonies on agar plate surfaces as inspiration, we make the observation that as a population expands, the curvature of the population's leading edge decreases. Through geometric numerical modelling, our results show that this decrease in curvature leads to increased competition between individuals along the leading edge. While this factor is applicable to all populations, we speculate that the increased competition is a factor behind the observed lag phase before the exhibition of tendrils for microbial populations.

Introduction

The spatial structuring of individuals within a population can significantly affect the ecological and evolutionary dynamics of the population as a whole (Lion and Baalen, 2008). For example, the propagation of *Pseudomonas fluorescens* strain SBW25 in an unshaken tube containing KB medium, results in the adaptive radiation of distinct morphologies according to the formation of a vertical oxygen gradient in the tube (Rainey and Travisano, 1998). While extrinsic effects (such as resource distribution, physical landscape variation and alternating habitats) can promote the structuring of populations, it is also apparent that the global structuring (both spatial and social) of populations can be an emergent property arising from local intrinsic interactions between individuals (Nadell et al., 2010). Bacterial biofilms are the classic example of a spatially self-structured population, enabling the unicellular microbial organisms to behave as a multicellular collective to promote their persistence (Shapiro, 1998).

The spatial structuring of a population is believed to influence the feedback loop between ecology and evolution (Lion and Baalen, 2008). For instance, on the one hand, the structuring of the population in relation to the local environment is likely to impose selective evolutionary pressures upon individuals to evolve beneficiary traits. While, on the other hand, the ecology of the environment changes according to the traits of these individuals (Lion and Baalen, 2008). This feedback can be a driver of invasive spatial spread, as spatial structuring due to diminishing resources in the environment, can lead to an increase in competition, which subsequently results in the development of mechanisms which can improve the invasive ability of individuals in a population (Wang et al., 2012, Day et al., 2003, Fransen et al., 2001). Consequently, understanding the effect of spatial structure is crucial to our understanding of invasive spatial spread, particularly in light of evidence suggesting that spatial structuring can influence the likelihood of a population becoming extinct (Lion and Baalen, 2008).

The thesis so far has focused on the spatial spread of microbial populations, in particular how the microbial model system might enable researchers to learn more about the evolutionary and ecological basis of population spread in general. It is apparent from our findings so far that the spatial shape of spread is

an important trait of the colony, with ecological and evolutionary implications for the colony at both the level of the individual and at the level of the group. However, our understanding of the factors affected by and affecting the shape of spread is relatively limited (Kearns, 2010, Deng et al., 2014, Misevic et al., 2015). Chapter 4 showed that the shape of spread has an impact upon the individual-level of fitness within a population (at least for those individuals along the leading edge), which in theory should affect the interactions and possible competition between these individuals (de Vargas Roditi et al., 2013). Motivated by evidence showing that individual-level behaviour (interactions) within these microbial populations can cause global traits to emerge (for example, the interactions between cooperative cells and non-cooperative cells in a mixed population can result in segregation between the two types of cell (Nadell et al., 2010)), combined with the evidence in Chapter 4, the next few chapters focus on how the shape of the population affects these individual-level interactions, the possible subsequent competition and how this might itself feedback on the global shape of spread.

The classical mathematical approach to modelling the spatial spread of an invasive population are reaction-diffusion equations (Skellam, 1951), which can recreate the morphological shape and velocity of population spread with a system of partial differential equations. Reaction-diffusion equations can exhibit a number of exotic spatial patterns of spread, however to recreate these patterns, the system must typically be driven unstable via an intrinsic mechanism of the population. In two or more dimensions, a factor that can drive a reaction-diffusion system unstable is the local radius of curvature along the population's leading edge. This is a process known as curvature-driven instability (Volpert and Petrovskii, 2009, Horváth et al., 1993).

Studies explicitly investigating the effect of the local radius of curvature upon the spatial spread of a population have to date been limited, with many studies typically avoiding the effect of curvature by studying spatial dynamics in one dimension (Volpert and Petrovskii, 2009). An early study explicitly recognising the possible effect of curvature upon population spread showed that populations which start off as non-circular and spread according to the Fisher-Kolmogorov model, eventually became circular again after a period of time (Lewis and Kareiva, 1993). This occurred because localised areas along the edge of the

population with higher curvature (e.g. fingers that advance ahead of the average front) have fewer individuals along the perimeter at that particular point spreading outwards, thereby resulting in a slower diffusion velocity into the non-occupied area than those areas with a lower curvature. Accordingly, as populations expand and leading edge curvature reduces (based on the reciprocal relationship between the population radius and the leading edge curvature) populations during initial phases can increase their rate of spread until the curvature of the population reaches a critical asymptotic curvature such that the population reaches its asymptotic velocity (Allstadt et al., 2007).

The same curvature mechanism can theoretically influence the likelihood of a mutation at the wave front surfing throughout the population (i.e. the frontier of the population carries a mutation until it becomes high in density). This is a phenomenon where mutations arising along the leading edge of a population with large positive curvature more likely to persist (due to there being more room to reproduce into i.e. decreased intraspecific competition) than those mutations arising in a region of negative local curvature (Miller, 2010). Other studies have considered how the curvature of the invasive population edge affects the competition for space between individuals of an invasive species and a native species (Allstadt et al., 2007). Specifically, these studies considered that for any point along the leading edge of a population, the probability of either the invasive species or the native species occupying that point depends on the proportion of native individuals versus invasive individuals within a surrounding defined radius and the life-history characteristics of these species such as mortality and reproduction rates. The curvature also affects the time an individual spends travelling along the border between two habitats. When there are well-defined borders between two habitats, individuals are likely to travel along the border for a period before randomly choosing to travel into one of the two habitats (Casellas et al., 2008, Creed Jr and Miller, 1990, Ovaskainen and Cornell, 2003)). Empirical evidence using the Mediterranean seed-harvesting ant *M. sanctus* showed the time spent along the border increased as the curvature of the border decreased (Casellas et al., 2008). Together, these studies suggest that simple geometric characteristics of the spread of a population can influence the invasive dynamics and success of the population.

Microbial populations, during the early stages of inoculation on an agar plate surface, initially undergo a lag phase during which the shape of spread is relatively circular (Kearns and Losick, 2003). As the microbial population establishes itself, the colony begins to enter the range expansion phase and spreads rapidly across the local environment (Kearns and Losick, 2003). In the case of *Ps. aeruginosa* strain PAO1, this spread is also initially relatively circular. However, if the extrinsic conditions of the agar plate environment are conducive (i.e. relatively high peptone concentration and low agar concentration – Chapter 3), at a point between 21 and 24 hours, a *Ps. aeruginosa* strain PAO1 colony begins to exhibit tendrils, which are long regions of microbial growth emanating from the central portion of the colony. We make an observation that as the colony goes through the lag phase towards the range expansion phase, the curvature of the shape of microbial spread decreases due to the radial direction of the spread expansion. We believe this fundamental geometric phenomenon can affect the dynamics between individuals along the leading edge.

The aim of this study is to understand more about how the shape of spread during population expansion affects the interactions and subsequent behaviour between individuals along the leading edge of a population. We base the inspiration for this study on the spatial patterns of spread exhibited by *Ps. aeruginosa* colonies during their colonisation of agar plate surfaces (Chapter 3). We focus upon those individuals along the population frontier because we believe they have specific importance for the shape of population spread, particularly as the key processes (cellular growth and especially outwards motility) responsible for the shape of population spread in microbial populations is thought to be largely driven by these individuals (Nadell et al., 2010, Du et al., 2011, Kearns, 2010, Motoike, 2007). As a result of the decreasing curvature of the population's leading edge as the population expands, we postulate that competition between individuals along the population frontier increases during population expansion. This is because of the increased exposure of individuals to their neighbours along the leading edge. Therefore, to test this, we utilise a geometric model to calculate the effect of the leading edge curvature upon the resources acquired by an individual along the leading edge of the population with competing neighbours i.e. to see the effect of curvature upon individual-

level competition. Although the inspiration for this study are bacterial biofilms, we believe that the proceeding theory is applicable to many populations.

Methods

This study focused on the competition between three asexual individuals situated on the leading edge of the population. Of the three individuals, we defined the central individual as the focal individual and the other two individuals as neighbouring individuals. We represented the leading edge of the population as a circle of radius R and we placed the three individuals along the leading edge such that they were equally spaced around the circumference.

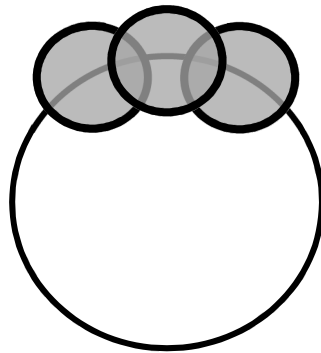


Figure 5.1: An illustration of three neighbouring individuals situated on the leading edge of the population such that they intersect.

To study the effect of leading edge curvature, we considered that each individual was able to sequester resources from the surrounding environment (we consider this similar to a siderophore halo from Chapter 4). We assumed the area available for an individual to sequester could be represented by a circle of radius r (also known as its circle or region of influence), with $R \gg r$. We placed each individual such that their circle of influence partially overlapped with the circles of influence of neighbouring individuals, in order to represent the individual-level competition for resources along the leading edge (figure 5.1). We note that we could only analytically calculate the area of overlap between either two or three circles. Therefore, to ensure calculations were tractable, we limited the amount two circles of influence could overlap such that one individual's circle of influence could not overlap with the circle of influence of an individual the other side of the neighbouring individual i.e. the distance between individuals along the circumference, h , must obey the following $r < h < 2r$.

We specifically defined the resources available to an individual as the area their circle of influence occupies outside of the region of the main population. We did

this because we assumed the individuals within the colony had already exploited the resources from within the region occupied by the main population. Indeed in microbial populations, it is thought that the majority of cellular growth and outwards motility (the key processes responsible for the spread of a microbial population (Kearns, 2010)) occurs along the leading edge of the population due to the general dependence of these processes on the availability of substrates (resources), which are mainly found outside the confines of the population (Nadell et al., 2010, Motoike, 2007). Additionally, due to the severely nutrient limited conditions in the central region of the colony (i.e. not on the leading edge), cells in this region are known to become dormant/non-motile (Xue et al., 2011), and in some cases can initiate cellular death mechanisms via autolysis to help improve the fitness of surrounding highly-related kin (Webb et al., 2003). Therefore, for the purposes of this model, we only modelled competition for resources outside the confines of the population between individuals along the leading edge.

We also determined an individual's fitness as a proportional relationship with the amount of resources it could sequester from available surrounding area. We made this assumption because of the lack of empirical data examining this relationship for populations consisting of *Ps. aeruginosa* (the systems used as the inspiration for this study) and to keep the calculations of this study mathematically tractable. This assumption has been made in other studies modelling competition for resources (Seger, 1985) and has an empirical basis across a number of populations (e.g. the bacterium, *Escherichia coli* (Dykhuizen and Dean, 1990), the brook trout, *Salvelinus fontinalis* (Hutchings, 1991) and the kittiwake, *Rissa tridactyla* (Thomas, 1983)). However, we note that a different relationship between resources and fitness might be possible, particularly as some other populations have exhibited a convex relationship between resources and fitness, due to the diminishing fitness returns associated with increasing resources levels (Whitlock et al., 2007). Because of this mixed evidence, we maintained a proportional relationship to keep the results straightforward and concise.

In addition to these assumptions, if any part of an individual's region of influence outside of the main population overlaps with a neighbouring individual's region

of influence, then the benefits gained from that region of overlap was assumed to be evenly split between the two individuals (equation 5.1), thereby representing scramble competition. For simplicity, our results defined the area sequestered as a proportion of the total possible area by an individual's circle of influence.

$$\begin{aligned} \omega_{benefits} &= (\text{area unshared forward of the population perimeter}) \\ &+ \frac{1}{2}(\text{area shared with neighbours forward of population perimeter}) \end{aligned} \quad (5.1)$$

In order to calculate the area of the lens-shaped overlap between two circles of different radii r_i, r_j , (i.e. between two individuals or between the individual and the main colony) in our system we used equation 5.2:

$$\begin{aligned} Area_{intersection \text{ between two circles}} &= r_i^2 \cos^{-1} \left(\frac{d^2 + r_i^2 - r_j^2}{2dr_i} \right) + r_j^2 \cos^{-1} \left(\frac{d^2 + r_j^2 - r_i^2}{2dr_j} \right) \\ &- \frac{1}{2} \sqrt{(-d + r_i + r_j)(d - r_i + r_j)(d + r_i - r_j)(d + r_i + r_j)} \end{aligned} \quad (5.2)$$

Where d was the distance between the centres of the two circles. Note that for an intersection to exist the following inequality must have held $0 \leq d \leq r_i + r_j$. See Appendix C for the proof of this equation (Weisstein, 2010). In order to calculate the area of the circular triangle overlap between three circles of different radii (i.e. between two individuals and the main colony) in our system, we used equation 5.3:

$$\begin{aligned} Area_{intersection \text{ between three circles}} &= \frac{1}{4} \sqrt{(c_1 + c_2 + c_3)(c_2 + c_3 - c_1)(c_1 + c_3 - c_2)(c_1 + c_2 - c_3)} \\ &+ \sum_{k=1}^3 \left(r_k^2 \arcsin \frac{c_k}{2r_k} - \frac{c_k}{4} \sqrt{4r_k^2 - c_k^2} \right) \end{aligned} \quad (5.3)$$

Where r_k were the three radii of the circles and c_k were the three chord lengths between the intersections of each of the three circles. We calculated the chord lengths by Pythagoras' theorem:

$$c_i = \sqrt{(x_{ij} - x_{ik})^2 + (y_{ij} - y_{ik})^2} \quad i, j, k \in 1, 2, 3, 4$$

Where x_{ij} , y_{ij} were the coordinates of the intersections between circles i and j and similarly x_{ik} , y_{ik} were the coordinates of the intersections between circles i and k . See Appendix D for the proof of this equation (Fewell, 2006).

Table 5.1: The parameters and values used in this chapter

Parameter Name	Parameter Description	Parameter values used
Main Population Radius = R	The radius of the main population.	0.025-1
Individual circle radius = r	The radius of influence of each individual	0.01
Distance between individuals = h	The distance between individuals along the leading edge.	1.25* Individual circle radius

To investigate the effect of the curvature upon competition between individuals situated along the leading edge, we adjusted the radius of the main population according to the values in table 5.1. This affected the local curvature of the population's frontier according to equation 5.4 (figure 5.2).

$$\text{Curvature of the leading edge} = \frac{1}{\text{Radius of main population}} \quad (5.4)$$

All calculations were run in R v3.0.3 (R Development Core Team, 2014).

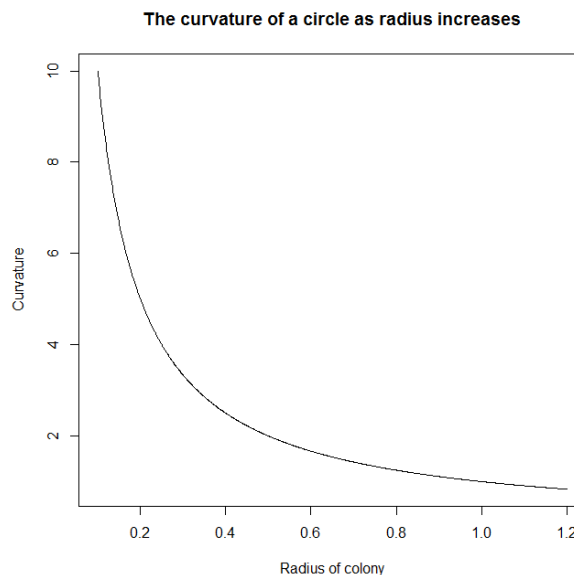


Figure 5.2: As the radius of the population increased, the curvature of the leading edge of the population tended towards zero.

Results

Consistent with our prediction, we found that the curvature of the population affected the resources available to an individual situated on the frontier of the population (figure 5.3). Specifically, the amount of resources available to an individual along the population frontier decreased towards an asymptote as $R \rightarrow \infty$. We found this occurred for all components of fitness (i.e. the overlap with the main population and the overlap with neighbouring individuals)(figure 5.3). This result illustrated that competition between individuals along the leading edge of the population intensified as the main population expanded radially outward, purely as a consequence of the geometry of spread.

Varying the radius of each individual's circle of influence along the leading edge showed that the magnitude of increased competition was greater as the radius of the circle of influence increased (figure 5.4). However the asymptotic proportion of resources obtained as the radius of the main population tended towards infinity stayed the same regardless of the size of the circle of influence. Conversely, varying the distance between individuals along the leading edge of the colony did not change the magnitude of increased competition but it did change the asymptote towards which the fitness of individuals tends as the radius of the main population increased, thereby reflecting the change in overlap between individuals (figure 5.4). Our derivation of an approximation of this asymptote (corollary 5.1) showed the calculation of the asymptote was dependent upon the distance between individuals along the circumference (figure 5.4) consistent with our findings.

Corollary 5.1: By considering the case when the radius of the main population goes towards infinity, we approximated the asymptote that an individual's fitness tends towards as the following:

$$\begin{aligned} \lim_{R \rightarrow \infty} (\omega) \approx & \pi r^2 - \frac{1}{2} \pi r^2 \\ & - \left(\frac{1}{4} \sqrt{(r^4(2+h)(2-h)^3)} + 2r^2 \sin^{-1} \left(\frac{\sqrt{(2-h)}}{2} \right) \right. \\ & \left. - \frac{1}{2} \sqrt{r^2(2-h)} \sqrt{(2+h)r^2} \right) \end{aligned}$$

See Appendix E for a proof of corollary 5.1.

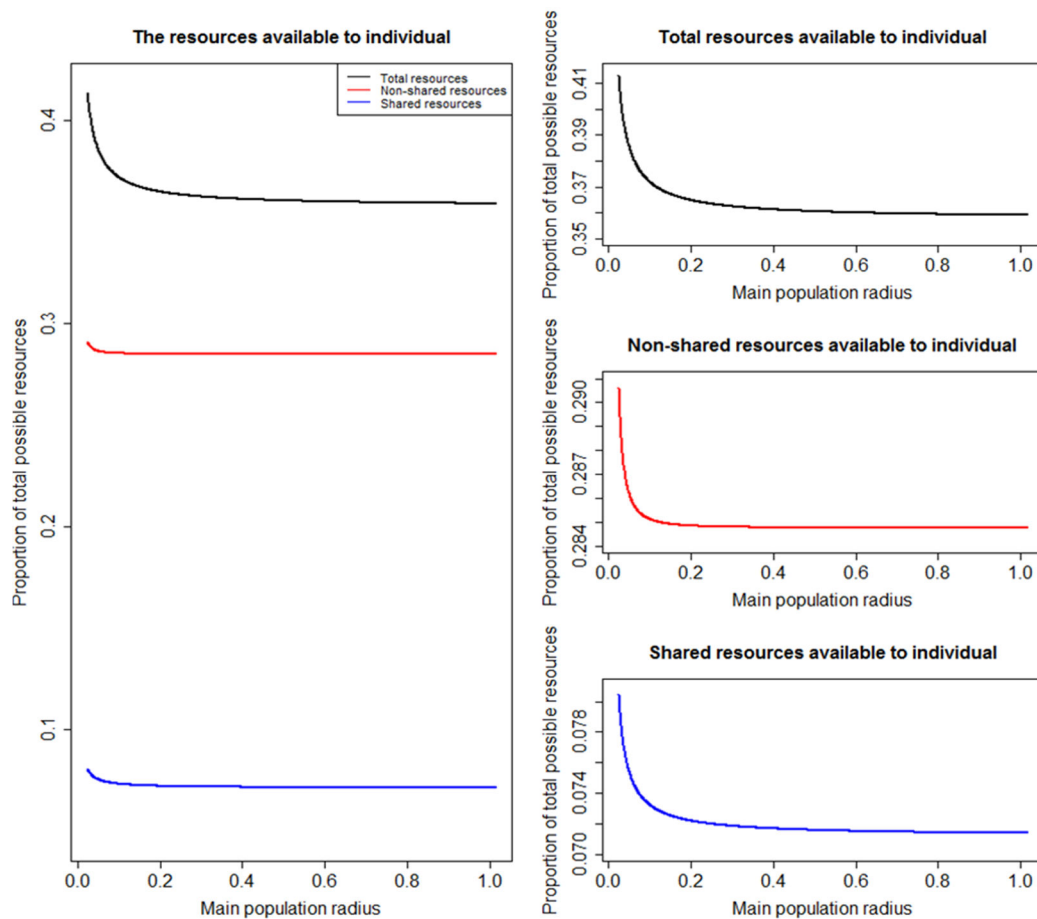


Figure 5.3: The effect of the radius (curvature) of the main population on the fitness of a focal individual neighbored by two other individuals, all situated along the edge of the population. Note that the curvature decreased from left to right. The blue and red lines represent the resources sequestered from the region outside the main population which were and were not shared with a neighbouring individual respectively.

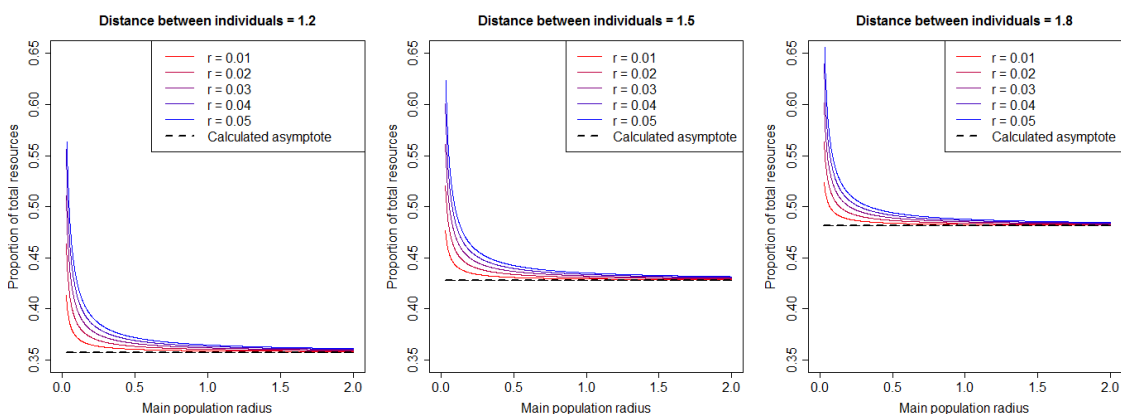


Figure 5.4: The effect of colony radius on the fitness of a non-dispersing individual neighbored by other non-dispersing individuals on the leading edge of the population. From left to right, the distance between individuals increases along the circumference of the circle. The dashed line is our calculated asymptote for the total resources acquired by an individual. Note that axes are the same for each plot.

Discussion

The results of the thesis so far have demonstrated the shape of spread as an important attribute of a population, with different shapes of population spread having different ecological and evolutionary implications. However, the shape of spread is an often-ignored trait in spatial ecology and thus our knowledge of the factors both affecting and affected by the shape of spread is relatively limited. Using the observations of Chapters 2-4 as inspiration, this study shows that the curvature of the population frontier, a fundamental geometric property of a population, can affect individual-level competition between individuals situated along the frontier of a population. Specifically, as an initially circular population expands across an environment, the curvature of the population's leading edge decreases. Thus, along the leading edge, this increases the exposure of an individual's feeding neighbourhood to the feeding neighbourhoods of their neighbours i.e. individual-level competition between neighbouring individuals increases for the non-sequestered resources outside of the confines of the population.

Increased competition can drive adaptation, resulting in the development of new mechanisms either to outcompete or to alleviate competition with other nearby individuals. Microbial populations (as with many other populations), undergo a lag phase during their spread across an environment while they adjust to their new environment (Kearns and Losick, 2003). During this lag phase, the radius of the initially circular population spread increases and thus, by the results of this study, competition along the population frontier increases. Researchers believe tendrils form because of a localised increase in the rate of dispersal (Kearns, 2010, Marrocco et al., 2010). Because dispersal helps to alleviate competition (Ronce, 2007), we theorise that if the environment conditions allow (see Chapter 3), the increased competition along the frontier could be a factor in the apparent lag phase before the initiation of tendrils during the spread of *Ps. aeruginosa* populations across agar plate surfaces. This consequently affects ecological (Chapter 2) and evolutionary (Chapter 4) characteristics of the population. Subsequently, we believe that more work should look to consider the curvature of the leading edge in future models of population spread, rather than evading it as many currently do in the construction of their models (Volpert and Petrovskii, 2009).

Chapter 6

Games with frontiers – Part 2: Dispersal games along an invasion front

Abstract

Competition is one of the main drivers of adaptation. An adaptation commonly arising due to intensified competition between individuals is the development of dispersal mechanisms. While dispersal can provide a benefit by alleviating competition, it can also prove costly, both to the individual itself and to other nearby, interacting individuals. Consequently, the interactions resulting from dispersal are an example of social behaviour, forming the basis of an evolutionary game. Using a geometric framework incorporating the curvature of a population's frontier, this study examines an evolutionary game between individuals situated along the leading edge of a circular population and identifies the various dispersal strategies possible and their fitness consequences. Due to curvature-driven competition, we speculate that this game can result in the emergence of exotic patterns of spatial spread, reminiscent of those seen in microbial populations.

Introduction

A fundamental determinant of the ecological dynamics of a population is its spatial structure, a factor that can affect the social behaviour between the individuals within the population (Débarre et al., 2014, Lion and Baalen, 2008). In conservation biology, understanding the effect of population spatial structure is important due to its influence upon the likelihood of population extinction (Lion and Baalen, 2008). Investigations into the impact of population spatial structure on social behaviour typically utilise an evolutionary game theory approach, allowing researchers to analytically derive and quantify the outcome of the interactions between individuals employing various life history strategies (Nowak and May, 1993). For example, a well-known scenario in evolutionary game theory is the prisoner's dilemma, a theoretical situation whereby two individuals are able to interact with each other to acquire a benefit (e.g. a beneficial resource) for their own reproductive success. The rules of the scenario enable each individual to sequester the beneficial resource being competed for, either by selfishly taking the resource for itself or by choosing to share the resource with the other individual (Rapoport, 1965). The prisoner's dilemma scenario assumes that while cooperation offers a benefit to both individuals, an individual actually achieves a higher benefit by defecting and taking advantage of the other individual's cooperative behaviour. But this scenario comes with the caveat that if both individuals act selfishly, the resulting outcome for both individuals is typically worse than if both individuals had cooperated (Doebeli and Hauert, 2005). This creates a social dilemma, because while natural selection favours selfishness at the individual-level, the average payoff for the population is lower when everyone is selfish than if everybody had cooperated. Consequently, studying how to resolve the prisoner's dilemma (and similar game theory scenarios) is a central tool for understanding how cooperative behaviour might arise against the possible advantages of selfish behaviours (Hauert et al., 2006). A number of studies investigating the effect of population spatial structure on social behaviour, in the context of evolutionary game theory, have shown the spatial structure of a population to be as influential on the eventual outcome as the strategies employed in these evolutionary games (Killingback and Doebeli, 1996). This highlights the

importance of geometric spatial structure upon the persistence and ecological dynamics of a population.

The dispersal strategy employed by individuals in the population is a life-history characteristic often studied in studies of spatial evolutionary game theory, as it is a crucial component in the ecological success of a population (Roff, 1992, Prosser et al., 2007). A fundamental topic in ecology and evolution is to understand whether a developed dispersal strategy is evolutionarily stable. The answer depends on the fitness benefits and fitness costs of the dispersal strategy relative to other possible dispersal strategies (May and Hamilton, 1977, Johnson and Gaines, 1990, Ronce, 2007). Possible fitness benefits of dispersal can include a decrease to within-group competition, a decrease to inbreeding within the population and an increase to the access to resources for members of the population (Ronce, 2007). Possible fitness costs include the metabolic cost of the dispersal mechanisms and a possible increase to the likelihood of encountering non-beneficial environments or predators, possibly resulting in an increase to mortality and/or a decrease to fecundity (El Mouden and Gardner, 2008, Lion and Baalen, 2008, Bonte et al., 2012, Travis et al., 2012). Viable dispersal strategies also depend upon intrinsic factors, such as the risk of not finding a mate (Miller and Inouye, 2013, Caswell et al., 2003, Neubert and Caswell, 2000) and the possible loss of diversity within a population (Kerr et al., 2002).

To study the development of dispersal, evolutionary game theory studies model the effect of competition between individuals and how this might give rise to the evolution of dispersal strategies (Gandon and Michalakis, 1999, Innocent et al., 2010). For example, the classic model by May and Hamilton (1977) theoretically showed how the competition between related non-dispersing individuals, could give rise to costly dispersal in order to reduce this competition via indirect fitness benefits i.e. the system they modelled was in favour of group-level fitness as opposed to individual-level fitness (West et al., 2007a). This model has spawned a number of realistic extensions, asking questions about the population dynamics, sex ratios and age structure as well as the spatial structure (See (Innocent et al., 2010) for a non-exhaustive list). While many of these game theory studies recognise the effect of spatial factors upon the evolution of dispersal (Killingback and Doebeli, 1996), the effect of the actual

shape of the population is rarely, if at all, considered, with those evolutionary game theory models examining spatial effects, typically discretising space as a lattice (Misevic et al., 2015). Consequently, we believe these models are missing fine-level geometric characteristics of the population that could affect the resultant outcome of these evolutionary game theory models. For example, we have previously shown that the curvature of the population's leading edge affects competition between those individuals situated along the leading edge (Chapter 5), which is a fine-level geometric factor missed in these other studies. Indeed, we speculate that this curvature-driven competition itself could give rise to evolutionary competition games between these individuals along the leading edge. This is because those individuals on the leading edge of the population are in a unique spatial environment compared to other individuals in the population as they are able to sequester resources from parts of the environment that have no conspecifics (Phillips et al., 2008). However, for these unexploited resources they are also in competition with other neighbouring individuals along this leading edge and thus as competition increases due to changes to the leading edge curvature during the expansion of the population (Chapter 5), it is probable that dispersal may evolve in order to alleviate this increase to competition (Starrfelt and Kokko, 2010). Consequently, we believe there is a requirement to understand how these fine-level geometric factors of the population shape (particularly curvature) affect the social behaviour and competition between individuals along the population leading edge, with regard to the evolution of dispersal, in an evolutionary game theory situation.

Bacteria can spread in a variety of patterns across agar plate environments, with *Pseudomonas aeruginosa* populations exhibiting tendril dynamics that are long regions of growth emanating from a central point of the population (Chapter 3). For bacterial populations to exhibit irregular, non-circular patterns of spread, bacteria must typically invest into dispersal machinery at an initial fitness cost to themselves (Kearns, 2010, Rashid and Kornberg, 2000). This investment into dispersal is an underlying ecological determinant driving the pattern of spread (Kearns and Losick, 2003, Matsushita and Fujikawa, 1990, Kearns, 2010). In this thesis, we have demonstrated that in microbial populations, the shape of spatial population spread can possibly affect ecological traits of the population (e.g. the rate of spread - Chapter 2) and has

evolutionary implications for the selective pressures influencing the population across multiple levels of selection (Chapter 4)(de Vargas Roditi et al., 2013). While spatial ecology has yet to establish the links between micro- and macroorganism populations, we hypothesise that patterns of spread (and the underlying dispersal strategies) at a microbial level may scale up to be similar to those patterns of spatial spread of larger multicellular organisms. This is due to recent evidence showing that many of the key ecological and evolutionary processes driving dynamics in macroorganism populations are the same as in microorganism populations (Buckling et al., 2009). Consequently, it is possible that the ecological and evolutionary implications of the shape of spread so far observed for these micro-organism populations are also true for macro-organism populations, with potentially important implications for conservation with regard to invasive species (Perkins et al., 2013). While the shape of spread is a potentially important trait of populations in general, we have relatively little knowledge about the factors (both at a local-level and at a global-level) affecting the shape of population spread and the factors affected by the shape of population spread (Deng et al., 2014, Kearns, 2010). Consequently, we believe that more research is required to understand the total effect that the shape of population spread can have on the ecological and evolutionary properties of a population as well as more research about how and why these different shapes of spread arise. By using microbes as inspiration, we believe that studying the factors causing bacteria at the individual-level to invest and develop the dispersal mechanisms responsible for these patterns of spread will help us understand the basis of population shape for populations in general.

We have previously established that as a population expands, the change in the curvature of the leading edge causes competition between individuals situated along this leading edge to intensify (Chapter 5). We assume that this increase to competition could lead to the development of dispersal mechanisms in order to alleviate competition (consistent with general theory (Starrfelt and Kokko, 2010)), thereby possibly initiating tendrill spatial dynamics. Therefore, in this chapter, we investigate how the inclusion of dispersal into the geometric system that we outline in Chapter 5 affects the social interactions between individuals along the leading edge. We focus on those individuals along the leading edge because it is thought that the key processes (cellular growth and particularly

outwards motility) responsible for the spatial spread of microbial populations – the basis of this study - occurs along the leading edge due to access to non-sequestered resources (Nadell et al., 2010, Motoike, 2007, Kearns, 2010) and because of the uniqueness of their situation compared to other individuals in the population (i.e. they are surrounded by space with no conspecifics (Phillips, 2009)). By including the curvature geometric characteristic of the population in our model, we discover that the introduction of dispersal can lead to an evolutionary game between neighbouring individuals along the leading edge. We analyse the various dispersal strategies employable by these individuals, how the curvature of the leading edge affects the exhibition of these strategies and the subsequent social behaviour between these individuals. Due to the obvious link between the population shape and dispersal, we speculate that such an evolutionary game is a significant factor behind the resultant spatial patterns of spread for both microbial populations and possibly for populations in general.

Methods

The model described in this chapter was set-up as detailed in Chapter 5, with the exception that we classified individuals along the leading edge of the population as either actively dispersing or non-actively dispersing. We assumed non-actively dispersing individuals moved radially outwards at the same rate as the main population whereas actively dispersing individuals moved radially outwards at a rate faster than the main population. To account for the increased dispersal, we imposed a dispersal cost upon the fitness of an actively dispersing individual. For simplicity, we defined the cost as a linear relationship, where we multiplied the extra distance moved by a disperser compared to a non-disperser situated along the leading edge by a scalar coefficient representing the dispersal cost (equation 6.1):

$$\omega_{cost} = (\text{extra distance moved}) \times (\text{dispersal cost coefficient}) \quad (6.1)$$

Consequently, the net fitness change of an individual was:

$$\omega = \omega_{benefits} - \omega_{cost} \quad (6.2)$$

where $\omega_{benefits}$ was equation 5.1 in Chapter 5.

As in the previous chapter, we used this formulation to consider the case of three neighbouring individuals along the leading edge of the population. Since

individuals were characterised as either actively dispersing or non-actively dispersing, there were six different cases, depending on whether the focal individual and neighbouring individuals along the leading edge were actively or non-actively dispersing (figure 6.1). In the results, we initially assumed in cases with more than one actively dispersing individual, that all actively dispersing individuals dispersed the same distance as each other. We followed these results by studying the social interaction between two actively dispersing individuals along the leading edge, both of whom could disperse different distances from one another. We ran the simulations in R v3.0.3 (R Development Core Team, 2014) according to the parameters of table 6.1.

Table 6.1: The parameters and values used as part of this study

Parameter Name	Parameter Description	Parameter values used
Main Population Radius (R)	The radius of the main population, R .	0.025-0.5
Individual circle radius (r)	The radius of influence, r , for each individual	0.01
Extra Movement	The extra movement by a disperser	0.0001-0.1
Distance between individuals (h)	The distance between individuals (This is set such that individuals overlap with each other)	1.2-1.8* Individual circle radius
Movement cost	The cost parameter of extra movement	0-100

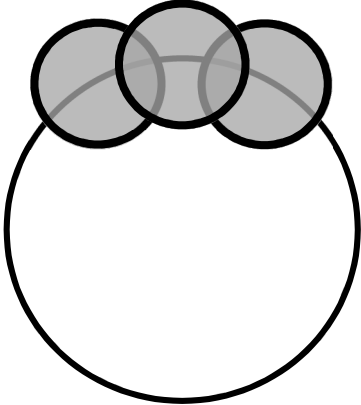
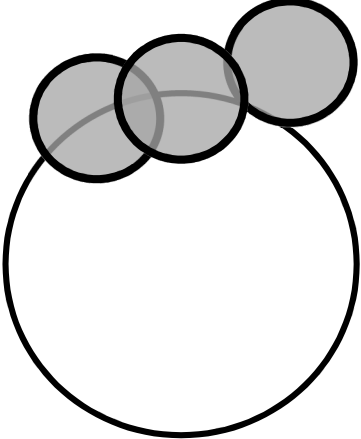
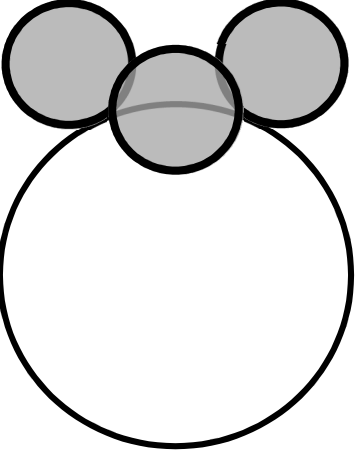
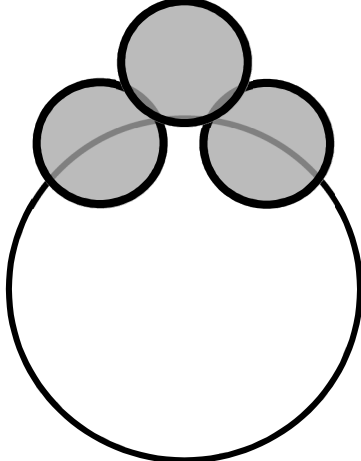
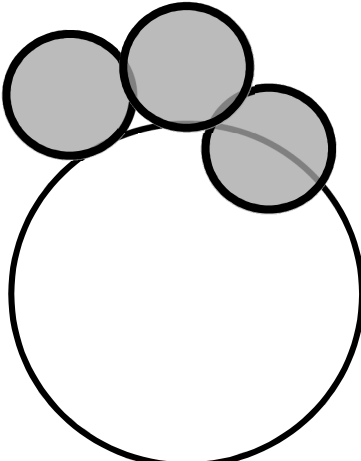
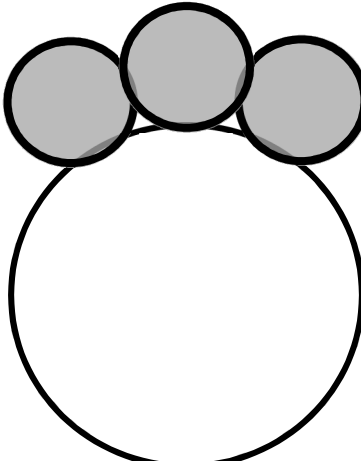
		
<p style="text-align: center;">Case 1</p> <p>Individual = Non-actively dispersing Neighbours = Both non-actively dispersing</p>	<p style="text-align: center;">Case 2</p> <p>Individual = Non-actively dispersing Neighbours = One non-actively and one actively dispersing individual</p>	<p style="text-align: center;">Case 3</p> <p>Individual = Non-actively dispersing Neighbours = Both actively dispersing</p>
		
<p style="text-align: center;">Case 4</p> <p>Individual = Actively dispersing Neighbours = Both non-actively dispersing</p>	<p style="text-align: center;">Case 5</p> <p>Individual = Actively dispersing Neighbours = One non-actively and one actively dispersing individual</p>	<p style="text-align: center;">Case 6</p> <p>Individual = Actively dispersing Neighbours = Both actively dispersing</p>

Figure 6.1: The six cases possible for three neighbouring individuals situated on the leading edge of the population. Cases 1, 2, 3 were the cases possible when the focal individual is non-actively dispersing and cases 4, 5, 6 were the cases possible when the focal individual is actively dispersing. The neighbouring individuals in each of these cases were either non-actively dispersing or actively dispersing, thereby representing all six possible combinations for the two states of dispersal considered in this chapter.

Results

We have split the results of this study into three parts. (1) The case where individuals could actively disperse without a cost of dispersal, (2) the case where individuals could actively disperse but with a cost of dispersal (with all actively dispersing individuals dispersing the same distance as each other) (3) the case where two actively dispersing individuals could disperse different distances also with a cost of dispersal.

No cost of dispersal

When there were no costs associated with dispersal, independent of the radius of the main population, actively dispersing individuals could escape competition with both the main population and neighbouring individuals (whether they be non-actively or actively dispersing), thus improving their own fitness at no cost (figure 6.2). Consequently, individual-level natural selection favoured an active dispersing strategy for the focal individual in this scenario (figure 6.3 – cases 4, 5 and 6). However, by actively dispersing, the focal individual affected the fitness of neighbouring non-actively dispersing individuals (figure 6.3 – cases 2 and 3). Whether the resultant effect was positive or negative ultimately depended on the distance dispersed by the neighbouring actively dispersing individuals.

When a focal actively dispersing individual moved a relatively small distance, the overlap between the focal individual and a neighbouring non-actively dispersing individual, outside of the confines of the main population, actually increased, resulting in a decreased fitness for the neighbouring non-actively dispersing individuals (figure 6.3 – cases 2 and 3). This arose because as the actively dispersing individual disperses outwards perpendicular to the leading edge, the area of its circle of influence which overlaps with the already sequestered area occupied by the main population decreased and instead began to occupy more of the non-sequestered area outside of the main population. As a result of this, at small distances of dispersal, the area of influence of the actively dispersing individual which previously overlapped with the neighbouring non-dispersing individual in the region of the main population (dark grey region of figure 6.2), now instead overlapped with the neighbouring individual in the region outside of the main population from which the food was

assumed to be sequestered (light grey region of figure 6.2), thus the neighbouring non-actively dispersing individual suffered a decreased fitness, as the reduced overlap in the region of the main population offered no short term benefit to the non-dispersing neighbouring individual.

As the distance moved by an actively dispersing focal individual increased, at a critical point, the converse became true and neighbouring non-dispersing individual obtained a short-term benefit rather than a fitness penalty. The distance at which this critical point was reached depended upon the curvature of the main population and the initial distance between the two individuals along the leading edge (figure 6.5 – left and table 6.2). Consequently, from an evolutionary game perspective, if the distance of dispersal was small enough such that competition for resources outside of the region occupied by the main population increased between the actively dispersing individual and a neighbouring non-actively dispersing individual, then the non-actively dispersing individual could be prompted to become an active disperser. Alternatively, if the distance of dispersal was large enough such that individual-level competition decreased, then there was a reduced immediate need for a neighbouring non-actively dispersing individual to become an actively dispersing individual, as it gained a fitness benefit at no risk to itself (at least in the short term).

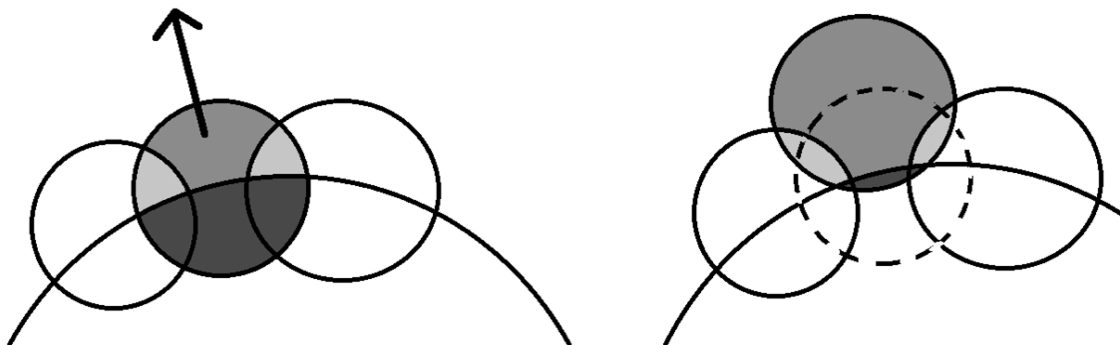


Figure 6.2: As an individual disperses, its overlap with the main population decreased (dark grey) and it gained access to more non-sequestered resources outside of the confines of the main population (grey). However, the amount of overlap outside the confines of the main population with neighbouring non-dispersing individuals could either increase or decrease (light grey), depending upon the distance dispersed.

Table 6.2: The movement, m , required by an actively dispersing individual to eliminate overlap with neighbouring individuals in the various scenarios detailed. Note R was the radius of the main population, r was the radius of influence for an individual, h was the distance between individuals and M was the distance moved by a neighbouring actively dispersing individual moving a different distance to the focal actively dispersing individual. See Appendix F for proofs.

Scenario	$m =$
Overlap between dispersing individual and main population	r
Overlap between dispersing individual and non-dispersing neighbour	$R \cos\left(\frac{hr}{R}\right) - R + \sqrt{R^2 \cos\left(\frac{hr}{R}\right) - R^2 + 4r^2}$
Overlap between 2 dispersing individuals moving same distance as each other	$\frac{R \cos\left(\frac{hr}{R}\right) - R + \sqrt{2r^2 - 2r^2 \cos\left(\frac{hr}{R}\right)}}{1 - \cos\left(\frac{hr}{R}\right)}$
Overlap between 2 dispersing individuals moving different distances	$R \cos\left(\frac{hr}{R}\right) + M \cos\left(\frac{hr}{R}\right) - R + \sqrt{(R + M)^2 \cos\left(\frac{hr}{R}\right)^2 - (R + M)^2 - M^2 +}$

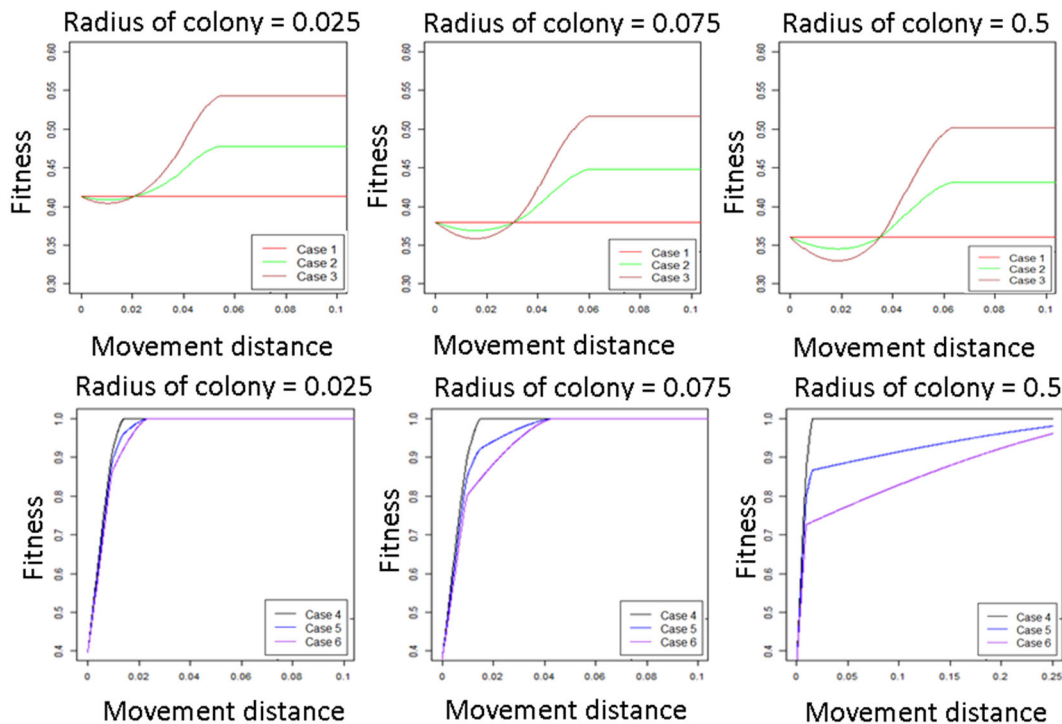


Figure 6.3: How the distance dispersed by those individuals actively dispersing in each of the six cases described in figure 6.1, affected the fitness of the focal individual when the cost of dispersal was set to zero. From left column to right column, the effect of decreasing curvature (implying increasing colony radius, and intensified competition on the frontier). The top row were the cases where the focal individual was not actively dispersing and the bottom row were the cases where the focal individual was actively dispersing.

When dispersal was costly

When a cost was associated with dispersal, the potential negative effects of dispersal could outweigh the benefits for a dispersing focal individual, possibly resulting in the situation where it was not beneficial for an individual to become an active disperser (figure 6.4). The balance of benefits and costs of a particular dispersal strategy depended on four factors. (1) **The magnitude of the cost coefficient of dispersal:** As the cost coefficient of dispersal increased, the net benefit of dispersal decreased, until such a point that there was no benefit to dispersal. (2) **The distance of dispersal:** The explicit link between the total cost of dispersal and the distance of dispersal meant the further an individual dispersed, the greater the overall cost of dispersal, until such a point that there was no benefit to dispersal. (3) **The curvature of the main population:** As the curvature of the main population decreased, the distance of dispersal required for maximum fitness increased, due to the increased competition along the leading edge pre-dispersal (figure 6.4). (4) **The dispersal strategy employed by neighbouring individuals:** If neighbouring individuals also actively dispersed, then the distance required to obtain the maximum possible benefit (irrespective of the cost of dispersal) increased (figure 6.4). Subsequently, there existed an optimum distance an individual should disperse in order to achieve the greatest fitness at the least possible cost, i.e. when the gradient of the benefit matched the gradient of the cost (equation 6.3).

$$\frac{d\omega_{benefits}}{d(movement)} = \frac{d\omega_{cost}}{d(movement)} \quad (6.3)$$

As finding the optimum distance of dispersal was analytically intractable, we used a numerical simulation to find the optimum distance of dispersal (figure 6.5). When looking at how changes to the cost of dispersal and the radius of the main population affected the minimum distance a focal actively dispersing individual with non-actively dispersing neighbours has to move in order to obtain optimum total fitness, we found three observable phases. The first phase occurred when the cost of dispersal was sufficiently low, such that the actively dispersing individual could disperse far enough to decrease competition for uncolonised space with both the main population and neighbouring individuals, whilst still obtaining its optimum possible fitness (i.e. none of the focal individual overlaps with the population behind). The second phase occurred when the cost

of dispersal was such that the actively dispersing individual obtained its optimum fitness by dispersing far enough to ensure a decreased overlap (but not completely eliminated) with the main population but not far enough to decrease competition between itself and neighbouring individuals for the uncolonised space (in fact competition increased between neighbouring individuals). This arose due to the way we structured our system, as reducing competition with the main population was more advantageous than decreasing competition with neighbouring individuals (individuals gained the full amount of resources by reducing overlap with the colony, but only gain half the resources by reducing overlap with neighbouring individuals). The third phase was when the cost of dispersal was overwhelmingly high such that dispersal was not viable.

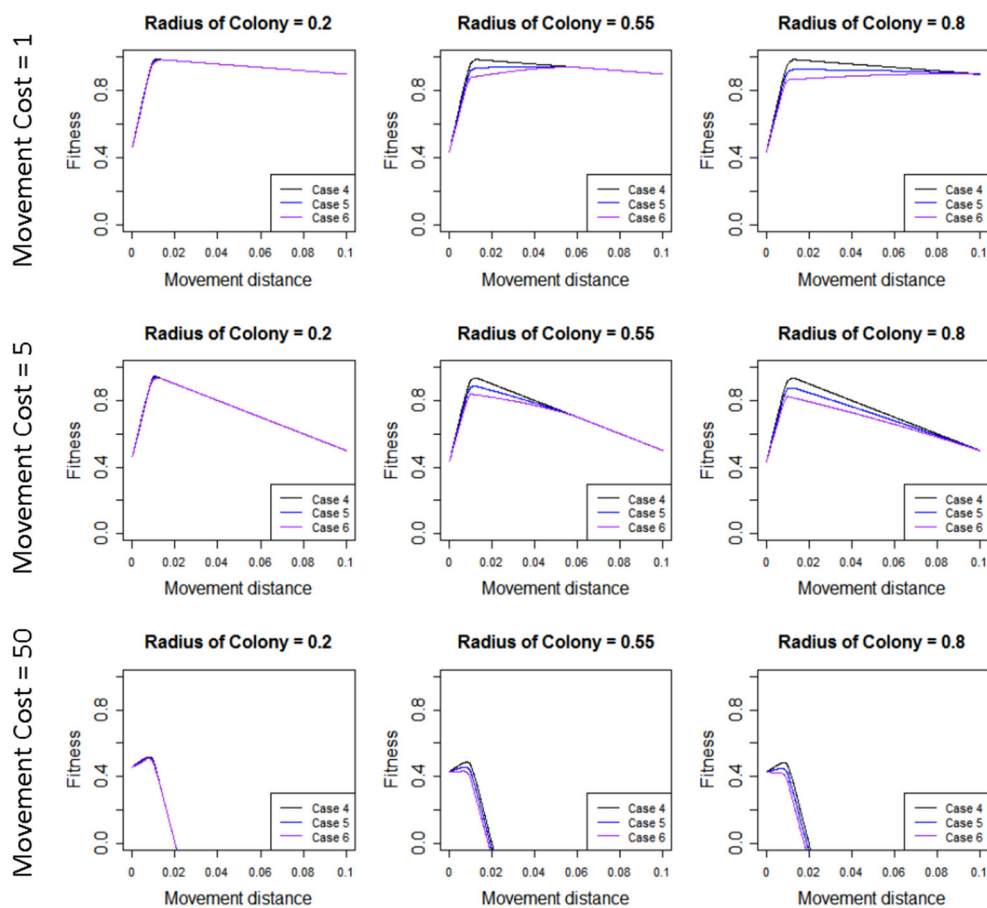


Figure 6.4: The fitness of the dispersing focal individual according to the distance dispersed when there existed a cost of dispersal. The effect for each of the three cases where the focal individual was actively dispersing. Curvature decreased from the left plot to the right plot. The cost coefficient increased from the top plot to the bottom plot. Note parameters used in these plots were individual radius = 0.025 and distance between individuals = 1.5.

The leading edge curvature (radius) of the main population and the initial distance between individuals along the leading edge also affected the distance an actively dispersing focal individual must move in order to reduce the overlap outside of the confines of the main population with a neighbouring non-actively dispersing individual (figure 6.5). We found that the curvature of the population had a marginal effect. Specifically, as the frontier curvature decreased, the distance an individual must traverse to obtain optimal fitness increased slightly (due to increased initial overlap outside of the confines of the main population). This caused the third phase to occur at a slightly lower cost of dispersal. Similarly, as the initial distance between individuals along the population frontier increased, the less an active disperser had to move in order to achieve its optimum fitness (figure 6.5).

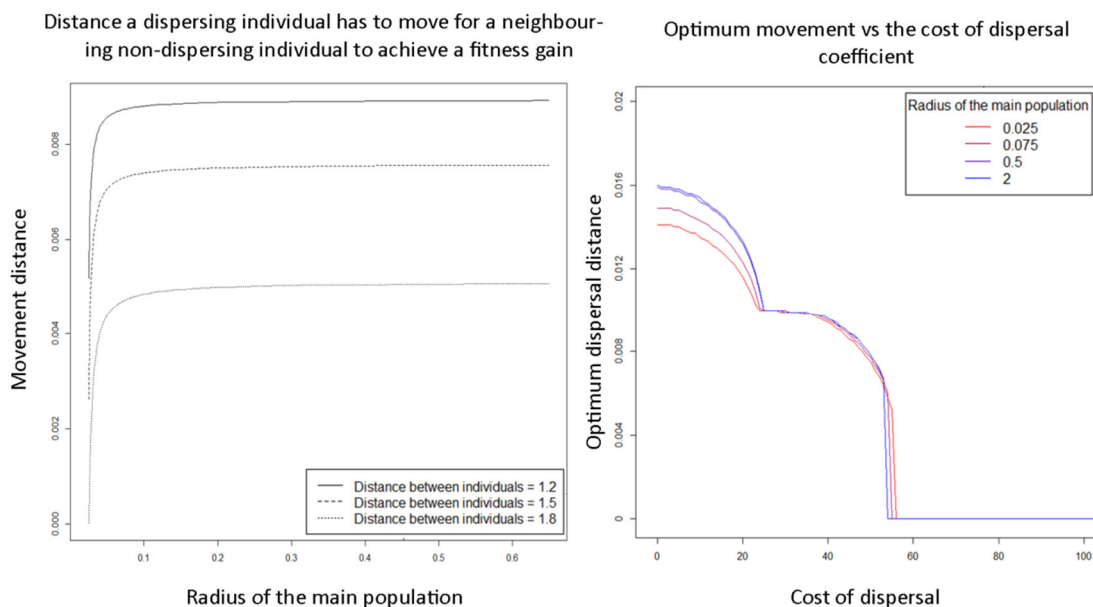


Figure 6.5: (Left plot) The effect of the main population radius upon the distance an actively dispersing individual has to move before a non-dispersing neighbour gains an advantage. The three lines represent how the initial distance between individuals along the leading edge of the main population also affects this distance. (Right plot) The distance an individual must move in order to achieve optimum movement based on the cost of dispersal. As the cost of dispersal increased, the dispersal distance required an individual to acquire optimum fitness, decreased. The three distinct phases were due to the reduced benefit of reducing overlap outside of the confines of the main population with neighbours compared to the main population. We used four different values for the main population's radius to show how the initial radius of the main population affects the distance required for optimum fitness.

The process of dispersal affected both the fitness of the focal individual and the fitness of neighbouring individuals. Consequently, the system showed that the process of dispersal resulted in social behaviour between individuals along the leading edge, with all four categories of social behaviour observed (altruism, mutual benefit, spite and selfishness). The key factors determining the qualitative type of social behaviour were the cost coefficient associated with dispersal and the distance of dispersal within one time step (figure 6.6), with the curvature of the population's leading edge and the initial distance between individuals also influencing the type of social behaviour.

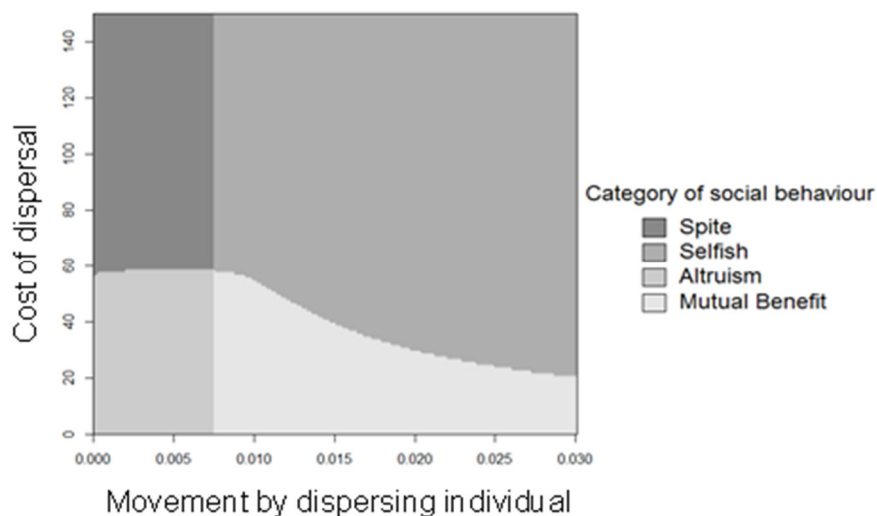


Figure 6.6: The exhibited social behaviour between an actively dispersing individual and a neighbouring non-actively dispersing individual according to changes in the distance of dispersal and cost of dispersal. Note this plot was for a main population with radius, $R = 1$.

At small dispersal distances, competition for resources outside of the region occupied by the main population between two individuals employing an active dispersal strategy and a non-active dispersal strategy, increased relative to the scenario when both individuals did not actively disperse. Subsequently, dispersal strategies which only move small distances were classed as selfish when the dispersal cost coefficient was sufficiently low (due to the dispersing individual acquiring a fitness gain for itself but a cost to its neighbours) and spiteful if the dispersal cost coefficient was prohibitively high (due to both individuals incurring a cost to their fitness)(figure 6.6). Alternatively, dispersal strategies that disperse large distances could lead to a decrease in this competition. This resulted in a mutual benefit for both individuals when the dispersal cost coefficient was sufficiently low enough and an altruistic effect at

higher dispersal cost coefficients (due to the actively dispersing individual incurring a cost for itself whilst giving the neighbouring individual a fitness advantage - figure 6.6). This dichotomy suggested that by dispersing a small distance, an individual was acting purely for its own interests, whilst by dispersing longer distances the individual was cooperating more with other individuals, possibly at a cost to itself. This scenario gave rise to a game between individuals, a game in which each individual could employ a dispersal strategy to improve its own chance of success.

The interplay between two actively dispersing individuals

Up to this point, results have considered all actively dispersing individuals to be dispersing the same distance (i.e. figure 6.4). In this section, we considered the scenario when two neighbouring actively dispersing individuals moved different distances to one another. To analyse the results in this section we considered two aspects, the fitness of each individual along the leading edge (as in previous sections) and the combined fitness of two neighbouring individuals along the leading edge. We investigated the combined fitnesses of two neighbouring individuals interacting with each other along the leading edge to ascertain which strategies achieved the highest overall possible fitness for all individuals along the leading edge. We defined this as a possible proxy measurement of group-level fitness, i.e. where we define the group in this situation as all of the individuals situated along the leading edge. Whilst the sum of the two (or more) individual's fitness was not a typical measurement in evolutionary game studies, we did this because we based our results around a multi-level selection framework described the introduction rather than an inclusive fitness framework that measures fitness according to relatedness between individuals.

When there was no cost associated with dispersal, two individuals both employing active dispersing strategies, benefited from the decreased competition with the main population as well as the decreased competition with each other. The optimum combined fitness arose when competition between the individuals and the main population reduced to zero, consistent with previous results (figures 6.7 and 6.8). Whilst the optimum combined fitness was obtainable when both individuals dispersed the same distance (as in previous

results), our results suggested it was possibly more optimal when both individuals move different distances from one another (figures 6.7 and 6.8); this depended on the curvature of the leading edge of the main population. Specifically, as $R \rightarrow \infty$, if both individuals moved the same distance as each other, the dispersal distance required to achieve the maximum fitness increased due to the trajectories of both individuals during dispersal causing their circles of influence to coincide with each other for a longer distance. This is because competition between individuals along the initially circular leading edge increases as $R \rightarrow \infty$ - see Chapter 5. By moving slightly different distances from each other as $R \rightarrow \infty$, competition between the two individuals could be eliminated at a smaller combined dispersal distance (i.e. the distance moved by both individual 1 and individual 2 added together) than when both individuals both moved the same distance.

When a cost was associated with dispersal, there were three different fitness outcomes. Either both individuals increased their fitness, both individuals suffered a decrease/no change to their fitness, or one individual increased their fitness whilst the other suffered a decrease/no change to their fitness (figure 6.7 and 6.8). Typically, both individuals gained a fitness benefit when dispersal resulted in a decrease in the overlap outside of the confines of the main population between the two individuals, so long as neither individual incurred an intolerable dispersal cost by initiating the process of dispersal. This became increasingly less likely as the cost of dispersal increased. Both individuals suffered a fitness decrease if both individuals dispersed a distance such that the cost of dispersal was prohibitive or overlap outside the population increased. As the cost of dispersal increased, this became increasingly likely. There were two scenarios where one individual gained a benefit whilst the other suffered a penalty. This case first occurred when one individual dispersed far enough such that the cost of dispersal was intolerable and the overlap outside of the confines of the main population between the two individuals reduced. Alternatively, this case occurred when one individual dispersed a small distance and the other a negligible distance such that the overlap outside of the confines of the main population between the two individuals increased, without enough benefit from the decreased overlap with the main population. The likelihood of this case occurring initially increased as the cost of dispersal increased, but at a critical

point, the likelihood decreased at higher costs of dispersal, with the likelihood of both individuals suffering a penalty increasing instead. The curvature of the frontier edge affected the likelihood of each of these cases. As the curvature of the population frontier decreased, the shape of the parameter space in which both individuals obtain a benefit became skewed (figure 6.8). This was due to the increased initial overlap along the leading edge and the resulting trajectories of each individual's circle of influence coinciding with each other for longer during dispersal. The effect of this was significant. For example, at large frontier curvatures, when both individuals disperse the same intermediate distance as each other, this resulted in both individuals obtaining a benefit. However, at small curvatures, this resulted in a fitness loss for both individuals.

Consequently, as with previous results, which of the fitness outcomes arose depended on the cost and distance of dispersal, as well as the curvature and distance moved by the other individual.

Focusing on the total combined fitness of two neighbouring individuals, we found the peak total combined fitness occurred in the parameter space where both individuals obtained a fitness benefit (figures 6.7 and 6.8). Consequently, similar to the case with no cost of dispersal, the key result we found was that when the colony was small (figure 6.7), there was little advantage to differences in dispersal between individuals, because the peak combined fitness was obtained when individuals both move the same distance, which gave both individuals a fitness benefit. Nevertheless, as the colony expanded and competition along the frontier intensified, peak combined fitness occurred when neighbouring individuals employed strategies, which moved different dispersal distances from each other whilst still achieving a benefit for both individuals. This suggested that the key finding in the interplay between two dispersing individuals was that as the main population expanded, the most optimal strategy was to be in an alternating pattern of dispersers and non-dispersers. This strategy became more optimal as the cost of dispersal increased, such that dispersal was still beneficial. Such a mechanism could encourage the development of irregular patterns such as the tendril patterns of spread exhibited by microbial populations during their spread across agar plate environments.

Radius = 0.025

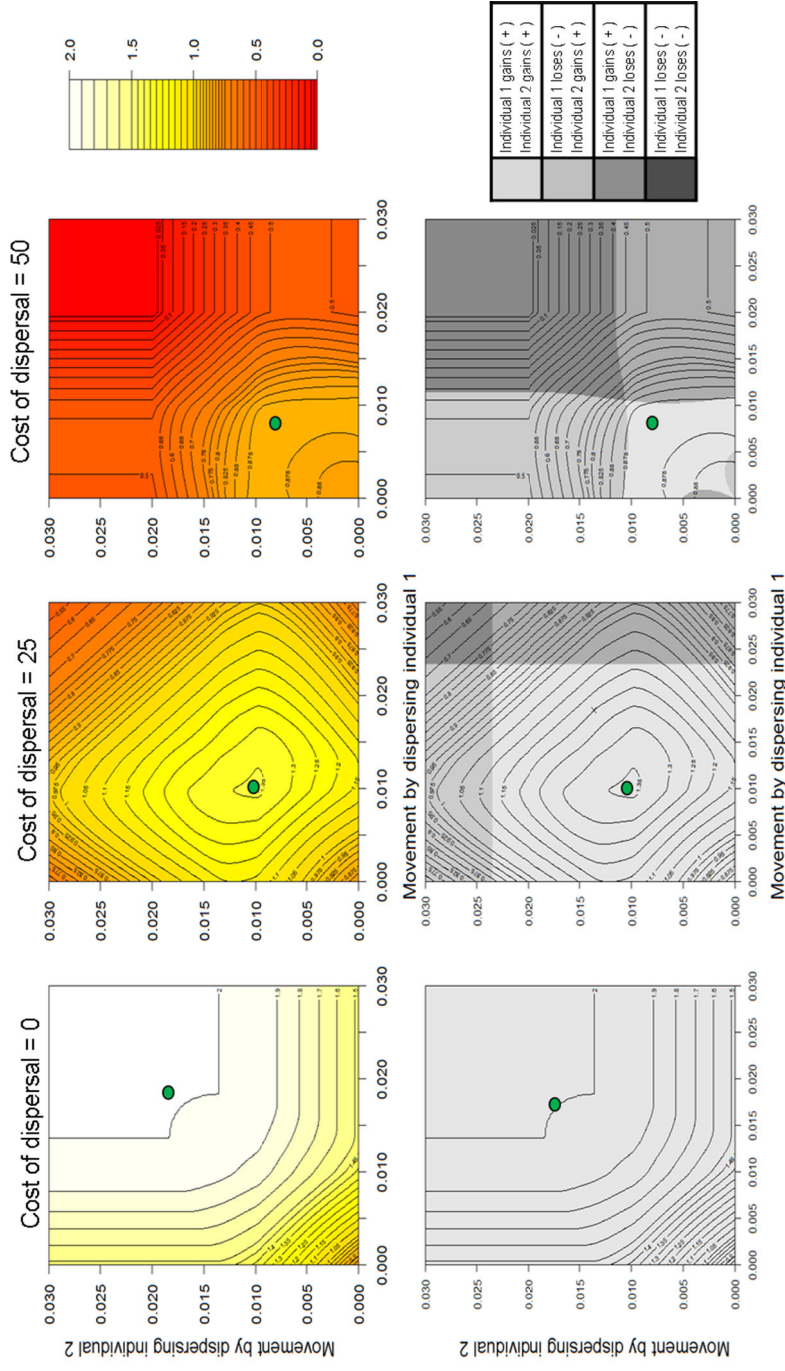


Figure 6.7: The resultant interaction between two neighbouring dispersing individuals who can move distinct dispersal distances. (Top row) The combined total fitness of the two neighbouring dispersing individuals, where 2 represents the maximum fitness obtainable. There was a clear effect arising because of changes to the dispersal cost. Note that green dots mark the point where the individuals obtain their highest total fitness. (Bottom row) For the two parameters representing movement of individual 1 and individual 2, this was the parameter space in which an individual gains or loses fitness because of the dispersal strategy. Overlaid on this parameter space are the contours representing the total fitness acquired by the two individuals.

Radius = 0.5

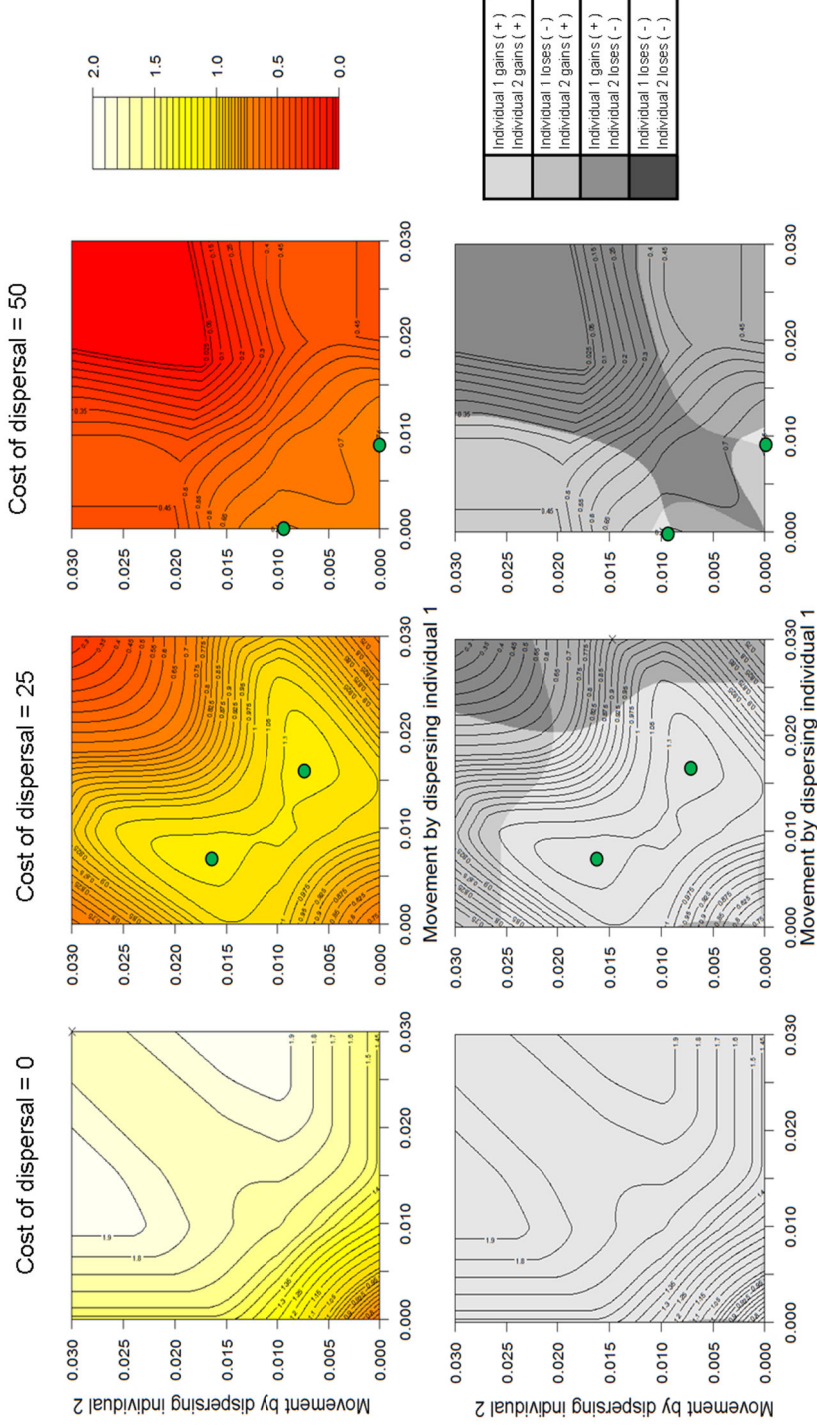


Figure 6.8: The resultant interaction between two neighbouring dispersing individuals who can move distinct dispersal distances. (Top row) The combined total fitness of the two neighbouring dispersing individuals, where 2 represents the maximum fitness obtainable. There was a clear effect arising because of changes to the dispersal cost. Note that green dots mark the point where the individuals obtain their highest total fitness. (Bottom row) For the two parameters representing movement of individual 1 and individual 2, this was the parameter space in which an individual gains or loses fitness because of the dispersal strategy. Overlaid on this parameter space are the contours representing the total fitness acquired by the two individuals. This was for a smaller curvature than figure 5.7.

Discussion

The results thus far in this thesis show that the shape of spread has important ecological and evolutionary implications for the population. However, in the spatial ecology literature, the shape of spread has been an often-ignored trait (Cumming, 2002). Therefore, our knowledge to date of the factors linked to the shape of spread is relatively limited (Misevic et al., 2015), leading us to believe more research is required to understand the factors both affecting the shape of population spread and those factors affected by the shape of the population. The curvature of the leading edge, a fundamental geometric property of a population, can affect individual-level competition between the individuals situated along this leading edge (Chapter 5). A number of mechanisms can alleviate competition, one of which is the process of dispersal (Ronce, 2007). By initiating dispersal, an individual can affect both its own fitness and the fitness of neighbouring individuals with which it interacts. Dispersal will also have an effect on the shape of the population. The results of this study show that the increased competition and the assumed associated dispersal arising from changes related to the population leading edge curvature, during the spatial expansion of a population, leads to an evolutionary game along the population's frontier with the exhibition of social behaviour between actively dispersing and non-actively dispersing individuals. We find the type of social behaviour depends on not only the cost of dispersal and the distance dispersed by actively dispersing individuals, but also the curvature of the leading edge of the population.

From our study of this evolutionary game, as the main population expands, each individual along the leading edge faces the dilemma of whether to stay put and accept the increase to individual-level competition or to disperse and take the chance that life outside of the confines of the main population is more beneficial. In this dilemma, we theorise that there are three different dispersal strategies within this game for a focal individual to consider.

Strategy 1 - 'Cooperate' – choose to not disperse and stay on the edge of the main population thereby cooperating with neighbours and the main population.

The advantage of this strategy is that the individual does not have to invest in dispersal. However, whether the outcome of this strategy will ultimately be beneficial, depends on the strategies employed by surrounding individuals. If

neighbouring individuals are not dispersing, then this strategy will only be a suitable option if the resources available in the environment are sufficiently high enough such that the increase to competition does not cause the individual to experience mortality. If neighbouring individuals are actively dispersing, then this strategy will only be beneficial (at least in the short term) if the actively dispersing individual(s) moves far enough such that competition for available resources reduces i.e. the neighbouring individuals employ the 'go for it' strategy as opposed to the 'be selfish' strategy (see strategies 2 and 3). However, while this strategy might have short-term benefits, there may be negative ramifications in the long-term i.e. becoming trapped behind the leading edge.

Strategy 2 - 'Be selfish' – choose to disperse but only a small distance such that the overlap with the main population decreases, but the overlap with neighbouring non-dispersing individuals, outside of the population, increases.

If the cost of dispersal is not intolerable, then a small investment into dispersal enables the individual to increase its own fitness selfishly at the expense of neighbouring non-actively dispersing individuals. Such a strategy, while initially beneficial to the focal individual, can have a long-term impact on neighbouring individuals, possibly forcing them to develop strategies leading to a fitness decrease for the focal individual in the long term (e.g. the development of dispersal mechanisms or mechanisms to improve competitive ability). If an individual uses this strategy even though dispersal costs are prohibitively high, then we consider this strategy spiteful. Additionally, if neighbours employ the same 'be selfish' strategy then this can become a version of forced cooperation, as both individuals would potentially still overlap with each other, albeit less than if they all remain on the leading edge of the population.

Strategy 3 - 'Go for it' – Disperse a long enough distance such that the overlap with neighbouring individuals, outside of the population, decreases.

This strategy is similar to the 'be selfish' strategy, except an individual makes a relatively large investment into dispersal such that it increases its access to non-sequestered resources outside the confines of the population while at the same time, competition with neighbouring non-actively dispersing individuals decreases, thereby providing a mutual benefit for all individuals involved. This

strategy is mutually beneficial so long as the cost of dispersal is not prohibitive; else, it is an example of altruistic behaviour.

Ultimately, the best choice of strategy in this game depends on the point at which optimum fitness occurs and the strategies employed by neighbouring individuals, with the likelihood of the 'be selfish' or 'go for it' strategies increasing as the radius of the main population increases (i.e. as the radius of curvature decreases), due to increased competition (Chapter 5).

The dispersal strategies of individuals along the population's leading edge have an effect upon the shape of population spread (Kearns, 2010), which is linked to selective pressures across multiple levels of selection (Chapter 4)(de Vargas Roditi et al., 2013, van Ditmarsch et al., 2013). Thus, to understand the likelihood of an individual adopting a particular dispersal strategy, one must consider the selective pressures faced by the population both at an individual level and at a group level (Griffin et al., 2004, West et al., 2006b, May and Hamilton, 1977). In this evolutionary game, we consider this as the fitness of the individuals themselves (individual-level fitness) and the combined fitness of all individuals along the leading edge (i.e. group-level fitness that we measure via proxy as the combined fitness of two individuals along the leading edge).

Our results suggest that when the population is small, natural selection favours uniformity in dispersal strategies for individuals along the leading edge. However, as the population expands, these strategies become less desirable due to increased competition (Chapter 5), therefore resulting in evolutionary games. The ultimate result of these evolutionary games will then depend on the balance of selective pressures in the system across multiple levels of selection (Griffin et al., 2004). The results of this study leads us to believe selection at the group-level would favour the scenario when individuals along the leading edge alternate their strategies between actively/non-actively dispersing phenotypes (i.e. the co-operative and go for it strategies), because as the colony expands, the system obtains the maximum combined (group-level) fitness at these points. This is also the scenario where we believe the system is most likely to develop irregular, structured patterns of spread such as those patterns we see in Chapter 3 (as irregular shapes of spread maximise group-level fitness – Chapter 4), due to the tendril patterns of microbial populations requiring a

localised increase in the rate of dispersal (Kearns, 2010, Marrocco et al., 2010). While these strategies obtaining maximum group-level benefit are generally beneficial to all individuals at the individual-level (because of these strategies promoting mutual benefit social behaviour), natural selection at the individual-level will favour the scenario when individuals along the leading edge maximise their own fitness. We believe this occurs when an individual utilises a 'selfish' or 'go for it' strategy, so long as they disperse a distance such that it is tolerable. We speculate this might ultimately favour circular shapes of spread due to natural selection influencing neighbouring individuals to gain the same possible maximum advantage themselves in a system biased towards individual-level fitness (van Ditmarsch et al., 2013), unless another mechanism as a result of neighbouring individuals dispersing enables them to ultimately prosper at the individual-level. Clearly, there is more to explore in these evolutionary games and future research needs to investigate whether these strategies could indeed result in irregular shapes of population spread.

A number of evolutionary game theory studies model the effect of competition upon the evolution of dispersal strategies (Gandon and Michalakis, 1999, Innocent et al., 2010, May and Hamilton, 1977). Our results correspond to the main results of these classic models; competition between non-dispersing individuals can promote costly dispersal in order to alleviate competition and obtain a group-level benefit. Our study shows that in the spatial domain, this is especially true for those individuals along the leading edge, as they can move into space outside of the population with no conspecifics, thereby reducing competition for the individuals left behind. By considering only those individuals along the leading edge (due to their assumed importance for important ecological processes affecting the shape of spread in microbial populations (Nadell et al., 2010)), our results highlight that the curvature of the leading edge affects the dispersal strategy (thereby affecting the type of social behaviour) employed by those individuals situated along the leading edge. Specifically, the type of social behaviour for these individuals is not just dependent on the intrinsic dispersal cost and relatedness (Gandon, 1999), but also the effect arising from fine-level geometric factors (associated with the population shape) of the population too. To our knowledge, these fine-level geometric factors resulting from the shape of the population are largely ignored in these other

evolutionary game theory models modelling the effect of competition upon the evolution of dispersal, which either choose to discretise space into a square/hexagon lattice or do not model spatial factors at all (Doebeli and Hauert, 2005, May and Hamilton, 1977, Misevic et al., 2015). Therefore, we suggest that these studies are missing the importance of the shape of spread in the evolution of dispersal (especially for those individuals along the leading edge) and the type of social behaviour. Indeed, a recent computational evolutionary game theory study recognising the lack of consideration for the shape of spread, studied its effect upon the evolution of cooperation (involving the secretion of public goods) between individuals of a theoretical population (Misevic et al., 2015). It concluded that the shape characteristic in isolation, could affect the likelihood of whether individuals cooperate, with cooperation more apparent in less geometrically isolated parts of the population i.e. points in spaces where there are more surrounding individuals than at other points. Their recognition that a greater consideration of population shape is required for the study of the evolution of cooperation, lends support to our findings. Due to the ecological and evolutionary effect of the shape of the colony (Chapter 2 and 4) together with the significance of leading edge curvature upon the social behaviour and the dispersal strategies for those individuals along the leading edge, our results illustrate that future studies should look to consider models with a finer-level geometric basis (particularly taking into account leading edge curvature) due to its influence on both the qualitative and quantitative results.

Limited empirical evidence using a microbial population suggests that as a population spreads, cooperation should arise along the leading edge, due to cooperation increasing productivity and therefore the velocity of the leading edge (Van Dyken et al., 2013). In relation to our study, this could be analogous to the situation where individuals become actively dispersing but disperse such a distance that they still overlap with neighbouring active dispersers. We note that this empirical evidence utilises yeast populations of *Saccharomyces cerevisiae*, a non-motile microorganism that spreads across environment via natural diffusion because of reproduction and not the directed dispersal mechanisms we specifically considered in this study. We consider diffusive spread as an intrinsic characteristic of the main population (i.e. the main population spreads out over time, even without active-dispersal methods) and

therefore we believe our definition of a 'cooperative' strategy still stands. Moreover, as seen in Chapter 3, different microbial organisms can spread in a number of different patterns, not just the circular patterns produced by these *S. cerevisiae* colonies (Kearns, 2010). Consequently, we suggest that their evidence for cooperation arising along the leading edge is possibly dependent upon the types of dispersal available to the species (i.e. it is species specific), particularly if these dispersal methods enable the population to expand in a variety of patterns of spread, with different individual-level and group-level effects. However, their observation suggests some possible augmentations to this study, which may be the focus of future work. For instance, studying how reproduction (or population viscosity) behind the leading edge affects the dispersal of individuals along the leading edge and studying how relatedness might affect the dispersal strategies of individuals playing this game are two possible questions which could be tackled with such a model formulated here.

An additional future augmentation to our study could be to investigate more than the two dispersal states we limit ourselves to in this study. In reality, organisms disperse according to a continuous distribution (a dispersal kernel) (Kot et al., 1996). Future research may wish to study which dispersal kernels offer a competitive advantage in such a geometric framework we have posed here and how these kernels can represent the three strategies discussed here. Furthermore, this study focused upon the initial trigger for dispersal from a competition perspective. Over longer time scales, the rate of dispersal is likely to change either by mutations in its machinery (e.g. longer legs in *Bufo marinus* (Urban et al., 2008)) or by the ecological factors discussed in (Shigesada and Kawasaki, 1997, Shigesada, 1997). Further research could investigate how evolution results in changes in these dispersal kernels and/or how strategies evolve through time.

The results of Chapter 5 illustrated how individual-level competition along the frontier of an expanding population intensifies because of the geometric properties of the population. An increase to competition can drive adaptation, promoting the development of mechanisms to alleviate competition, of which dispersal is one such mechanism (May and Hamilton, 1977). The results of this chapter show that by initiating the process of dispersal, an evolutionary game arises along the leading edge between those individuals initiating dispersal and

their neighbours. Depending on the intrinsic cost of dispersal, the distance of dispersal, the leading edge curvature and the dispersal strategy used by the dispersing individuals, we show this game can result in all four types of social behaviour, namely spite, altruism, mutual benefit and selfishness. A key finding from our analysis of this game is that small populations, which initially favour circular shapes of spread, undergo evolutionary games as competition intensifies along the leading edge during population expansion, which depending upon the local and global selective factors of the system, may lead to irregular shapes of spread. To the best of our knowledge, the study of such a game along the leading edge of a population in a curvature-driven geometric format as we present in this study is not in the spatial ecology literature. Consequently, these results also highlight the effect of the leading-edge geometry upon competition, the resultant evolution of dispersal mechanisms along the leading edge and thus the shape of spread. Further analysis of this game is required, in particular analysis including factors related to multi-level selection, as this may help us to establish the mechanisms responsible for the patterns of spatial spread exhibited by microbial populations and populations in general.

Chapter 7

Games With frontiers - Part 3: An Individual Based Modelling Approach

Abstract

As an initially circular population expands across an environment, the curvature of the population's leading edge decreases, thereby increasing individual-level competition between those individuals along the leading edge. Competition can drive adaptation, which can result in the development of mechanisms to alleviate the negative effects associated with competition. A possible adaptation is the development of dispersal mechanisms, which allow individuals in a population to escape competition and/or gain access to new sources of food in order to improve fitness. Indeed, dispersal adaptations are a driver of the spatial pattern of population spread. Individual based models (IBMs) are increasingly popular due to their ability to recreate complex global dynamics via the modelling of localised interactions between individuals and simple life history rules. We synthesise a previously studied geometric framework into an IBM, in order to ascertain whether the effect of curvature upon individual level competition along the population frontier can result in patterns of spread similar to those exhibited by strains of *Pseudomonas aeruginosa* during their colonisation of agar plate environments. The results show that the pattern of spread depends upon the cost of dispersal, with circular patterns of spread occurring at low and high costs of dispersal and tendrils like patterns arising at intermediate costs of dispersal. We also highlight how these tendrils arise via a slipstream mechanism resulting from a stable polymorphism of dispersal phenotypes. These results illustrate that curvature driven competition between individuals along the leading edge of a population, can alone, be a factor that gives rise to patterns of spread observable in microbial populations and potentially populations in general.

Introduction

The spread of invasive species is a key ecological concern because of their potential threat to worldwide biodiversity, ecosystem functioning and habitat degradation (Shigesada, 1997, Soulé and Orians, 2001). Indeed, researchers believe the spread of invasive species threatens as much as 60% of all endangered species listed in the US Endangered Species Act (Arim et al., 2006, Soulé and Orians, 2001, Pimentel et al., 2000). Unfortunately, while knowledge of how the dynamics behind invasions arise is critical in our efforts to predict and control the spatial spread of invasive species, our current understanding is inadequate and research investigating the spread of invasive species is often lacking in generality (Arim et al., 2006, Andow et al., 1990). We believe an important trait of an invasive population is its spatial shape as it spreads across and colonises an environment, a trait often ignored due to the problems associated with data collection for macro-organisms (Cumming, 2002). The preceding results in this thesis have shown that the shape of spread has a number of ecological (Chapter 2) and evolutionary (Chapter 4) implications. In particular, the results of Chapters 4-6 show that the shape of spread can influence the fitness of the population at both the individual- and at the group-level due to its effect upon the acquisition of resources and its effect upon the development of adaptive mechanisms such as dispersal. Yet, our knowledge of the factors affecting and affected by the shape of spread is still relatively limited and thus more research is required.

Microbial populations enable researchers to study the processes driving various ecological and evolutionary phenomena in a unique and highly advantageous system (Buckling et al., 2009). Some microbial populations can exhibit a variety of patterns of spatial spread when inoculated on agar plate surfaces in a controlled laboratory environment (Golding et al., 1998, Matsushita and Fujikawa, 1990). Because of the increasingly recognised ecological and evolutionary links shared between micro- and macro-organisms (such as the competition ecological processes structuring communities (Jessup et al., 2004)) and because the spatial spread of micro-organisms is easily capturable (in comparison to macro-organisms), we believe the microbial model system is a good system to study the spatial spread of populations in general, both empirically and as a tool for inspiration. In this study, the patterns of spread we

focus on are tendril patterns of spread on agar plates (long finger-like regions of microbial colonisation emanating from the centre of the colony (Kearns, 2010)), often associated with *Pseudomonas aeruginosa* populations. Tendrils are thought to arise in microbial populations due to a localised increase in the rate of dispersal resulting from swarming motility (Kearns, 2010, Marrocco et al., 2010). While this swarming motility has a number of benefits (such as increased carrying capacity for the colony (de Vargas Roditi et al., 2013)), this swarming motility also comes at a metabolic cost and hence swarming motility is only viable in favourable conditions (Caiazza et al., 2005, Kearns, 2010, Rashid and Kornberg, 2000). This investment into dispersal is an underlying ecological determinant driving the pattern of spread of microbial populations in general (Kearns and Losick, 2003, Matsushita and Fujikawa, 1990, Kearns, 2010).

Traditionally, ecologists have utilised reaction-diffusion equations to represent the spatial dynamics of populations. However many of the classical reaction-diffusion equation models make a number of overly simplistic assumptions which can cause these models to be unreliable for use as a predictive model of invasive spread (as demonstrated in Chapter 2 (Urban et al., 2008, Andow et al., 1990, Veit and Lewis, 1996, Kot et al., 1996)). In response to this, researchers have suggested a number of different modelling approaches, amongst which are Individual Based Models (IBMs). IBMs are a relatively new class of computational model which have been increasingly used to study phenomena in ecology (Grimm and Railsback, 2013). In contrast to analytical reaction-diffusion equation models, IBMs represent each individual in the system, characterises them with a set of heterogeneous traits and processes each individual through a set of procedures. This enables the IBM to represent the effect of individual heterogeneity on interactions between individuals within a population, thereby showing how individual-level interactions can give rise to global scale dynamics. Because of the increased recognition of the importance of heterogeneity in spatial ecology, IBMs are believed to be one of the most natural modelling methods of describing biological systems (Bonabeau, 2002). Indeed, a greater understanding of how heterogeneity in processes such as individual competition and food acquisition affects the spatial composition of an invasive population during its spread would help to improve our ability to predict

the spread of invasive populations and consequently help us to create strategies to control them (Urban et al., 2008).

In microbiology, modellers have used a number of generic and bacteria specific IBM frameworks to study the spatial spread of bacteria. These frameworks have modelled the spread of bacteria both vertically from the surface (vertical interface) of microbial biofilms and horizontally across agar plate surfaces (Xavier et al., 2005, Nadell et al., 2010, Pitt-Francis et al., 2009, Tisue and Wilensky, 2004, Gorochoowski et al., 2012, Kim et al., 2014, Kreft et al., 2001). The IBM frameworks described in the literature have used a number of approaches to represent the spatial spread of microbial populations. The most common approach is to represent each individual bacterial cell of the colony as a sphere in order to model the entire microbial colony (i.e. they simulate every individual in the population). To represent the interactions between individual cells in the population as well as the interactions between these cells and their shared environments, modellers subject the individual cells to a number of processes such as dispersal, bacterial metabolism/cellular growth and cell division, to show how processes at these detailed levels scale up to a macro or population level. For example, (Kim et al., 2014) used an IBM framework model to demonstrate how competition between individuals for oxygen within a dense microbial biofilm, can generate strong natural selection for individuals to reach the edge of the population (in this case, the top surface of the biofilm). This natural selection arose because of the resource and competitive advantages received by individuals at the frontier of the population compared to individuals within the population (Kim et al., 2014). Another example of an IBM framework modelling an entire microbial colony demonstrated how spatial segregation of two genetically identical yet separate cell lineages into separate groups from an initially well mixed population could emerge under low-to-medium resource concentration environmental conditions, regardless of whether an active clone mate gathering mechanism exists (Nadell et al., 2010). This occurred because many of the cell lineages in the initially well mixed population were cut off from the advancing front where the resources assumed important for survival and reproduction were available and thus stopped growing and reproducing, leaving only those few lineages along the leading edge to reproduce into neighbouring space, resulting in the distinct segregation of lineages. These results illustrate

how spatial, physical and biological parameters of the system can affect the spatial structure of a population, thereby leading to changes in the social behaviour within the population (Nadell et al., 2010). While the IBM approach has to date been a successful modelling approach for the spread of bacteria, many of these models have focused upon the mechanistic biochemical processes driving bacterial growth, thus resulting in them having a limited generality across populations (Du et al., 2011, Deng et al., 2014). Moreover, these models generally have not specifically study tendrill dynamics as we aim to here. We suggest that an ecological, less mechanistic approach could enable us to discover how these patterns might arise for populations in general, not just the organism in question. The IBM approach is a diverse approach (Grimm et al., 2010), and thus we believe it can be adapted for this purpose.

Using microbial populations as inspiration, we have previously shown that competition between individuals along the leading edge of an asexual circular population increases as the population expands across a two-dimensional environment, due to the effect of the population shape (Chapter 5). Competition can drive the adaptation of mechanisms to alleviate the negative consequences of competition (May and Hamilton, 1977, Kubisch et al., 2013). Based on the literature, we believe one such mechanism is dispersal (Innocent et al., 2010). This is a key mechanism for the persistence of a general population, as it not only reduces individual-level competition (or more specifically kin competition) but it also affects a range of different ecological and evolutionary mechanisms (such as the shape of spread), offering benefits such as the discovery of new resources and the avoidance of inbreeding (Ronce, 2007, May and Hamilton, 1977, Taylor and Buckling, 2010). For microbial populations, dispersal (such as swarming motility) also enables individuals in the population to escape toxic products produced by other members of the colony (de Vargas Roditi et al., 2013). While dispersal has many benefits, dispersal also comes with associated costs (such as the metabolic costs associated with swarming motility in microbial populations (Rashid and Kornberg, 2000)). Therefore for dispersal to evolve, the benefits of dispersal must outweigh the costs associated with dispersal (Kubisch et al., 2013).

By developing dispersal mechanisms, individuals along the leading edge undergo evolutionary competition games with other individuals along the population frontier, with the curvature of the population, the dispersal strategy of neighbours, the distance of dispersal, and its associated cost affecting the type of social behaviour between individuals along the leading edge (Chapter 6). The results of this evolutionary game in Chapter 6 suggest that while selection promotes uniform dispersal strategies along the frontier of the population during the initial stages of population spread, as the population expands and curvature decreases, depending on the evolutionary parameters of the system, selection may promote non-uniformity in dispersal strategies along the frontier. We hypothesise that this individual-level competition could give rise to tendrill patterns of microbial spread across surface environments, similar to those patterns exhibited by *Ps. aeruginosa* (Chapter 3). To investigate whether this is the case, we utilise an IBM model in this chapter to extend the theory described in Chapters 5 and 6 to a landscape scale. Our model specifically considers the impact of curvature-driven individual-level competition along the leading edge and other simple life-cycle rules upon dispersal phenotype, with the aim to investigate how this might drive the shape of spread of a population through time. Based on the framework used in Chapters 5 and 6, we believe the key factors along the leading edge of the system are the cost of dispersal, the curvature of the population and the probability of mutating a dispersal phenotype. We format this study in accordance with the ODD protocol (Grimm and Railsback, 2013), a protocol designed to standardise the reporting of IBMs such that other researchers can recreate them.

In contrast to other computational studies utilising IBM frameworks (or similar) to study the morphology of microbial spread, we only represent those individuals along the leading edge. We do this in order to understand how behaviour between these individuals along the leading edge might affect the resultant pattern of spread exhibited by populations, irrespective of the processes behind the leading edge (consistent with Chapters 5 and 6). While the assumption that only those individuals along the leading edge affect the spread of a microbial population is a simplification, we believe this is reasonable, primarily as a large proportion of cellular growth and particularly outwards motility (key determinants for the shape of spread in microbial

populations) is thought to occur via processes initiated by these individuals (Nadell et al., 2010, Du et al., 2011, Kearns, 2010, Motoike, 2007). We provide a full discussion of this assumption in the discussion section.

Methods

Model description

Purpose of the model

The purpose of this IBM simulation was to investigate how dispersal mechanisms resulting from curvature-driven competition along the leading edge of the population, affect the spatial pattern of population growth across a generic environment. Our investigation focused on the cost of dispersal and the probability of mutation between an actively and a non-actively dispersing phenotype. This was because results from Chapters 5 and 6 suggested that these factors significantly impact the fitness of individuals situated along the population frontier, consequently affecting the choice of whether an individual along the leading edge will disperse or not. The inspiration for these simulations was asexual *Ps. aeruginosa* bacterial populations, however the results could be generalised for many types of populations.

State variables and scales

We considered the environment to be a flat homogeneous two-dimensional surface with no boundaries. We assumed resources in the environment were homogeneous, did not diffuse and were sufficient to promote the persistence of the population. Each individual in the simulation was characterised by their location in two-dimensional Cartesian space (x and y coordinates), the radius of their circle of influence, their dispersal phenotype (a binary choice between not actively dispersing and actively dispersing) and their internal energy budget (which we viewed as analogous to their fitness). All spatial and time characteristics were dimensionless. The values used in this simulation are contained in table 7.1.

As explained in the introduction, we only considered those individuals situated on the leading edge of population in our model. We allowed the radius of influence of each individual along the leading edge to overlap slightly with neighbouring individuals according to a set tolerance parameter (table 7.1). We kept this parameter greater than twice the radius of a circle of influence in order to avoid, as far as possible, overlaps with individuals other than direct

neighbours (figure 7.1 – We defined a neighbour as those individuals directly next to the focal individual in the ordered list of individuals, not necessarily the closest individual in Cartesian space). This was due to the analytical difficulty of calculating the overlap between two or more circles. During the running of this simulation, some individuals became stuck via collision and remained behind the leading edge of the population. We still subjected these trapped individuals to the same rules as other individuals across iterations, but we did not use their characteristics during analysis i.e. counts of individuals at each time point did not account for trapped individuals.

Table 7.1 - Overview of the parameters and default values of the parameters utilised.

Parameter	Values tested
Initial set up parameter values	
Starting radius of the main population(R)	0.01
The radius of each individual's circle of influence(r)	0.0025
Amount of allowed overlap between neighbouring individuals (c)	$\frac{r}{1.2}$
Starting number of individuals on the leading edge of the main population(n)	$floor\left(\frac{\pi R}{c}\right)$
Number of iterations	1000
Starting fitness	Resources in starting area
Movement parameters	
Movement of a non-active disperser	0.0001
Movement of an active disperser	0.0002
Dispersal cost parameter	0,250,500,...,5750,6000
If not otherwise specified, the values listed here are used.	Dimensionless parameters are either numbers or probabilities.

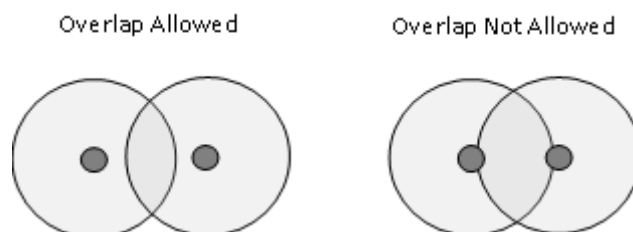


Figure 7.1: Circles of influence for each individual are allowed to overlap with each other up to a certain tolerance level, such that only one individual can be in any one circle of influence. In the figure, the dark grey circle represents the region occupied by an individual while the light grey circle represents the individual's circle of influence.

Process overview and scheduling

Our simulation proceeded in discrete time steps, with each step assumed the time taken for an individual to move one-step at the rate their dispersal phenotype dictates. During each discrete time step, individuals went through a number of phases broadly described as foraging, movement, survival and reproduction (figure 7.2), in this order.

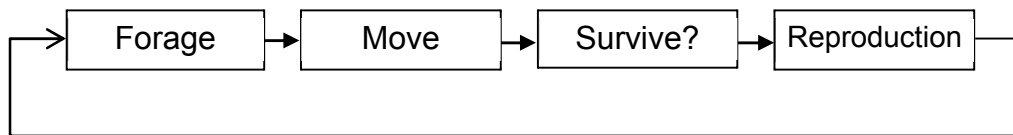


Figure 7.2: The set of life history processes each individual in the model goes through for each iterative time step.

The foraging phase: In this phase, individuals foraged the area according to their circle of influence, gaining energy according to equation 7.1.

The movement phase: In this phase, individuals moved into space not already occupied by another individual's circle of influence such that a collision did not occur (figure 7.1). The direction of movement was in a direction perpendicular to the edge formed by a line connecting the centres of the two individuals neighbouring the focal individual according to the ordered list of individuals (figure 7.3).

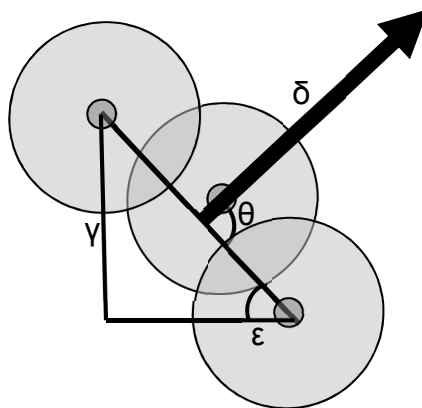


Figure 7.3: The direction of movement by the focal individual was perpendicular to the line joining the centres of the two neighbouring individuals. Here the inclination of the line is ϵ , the change in y coordinates is γ , the direction of movement is θ and δ represents the distance moved.

The survival phase: If actions in the other phases caused the individual to deplete its energy to below zero, we deemed the individual dead and we removed it from the system.

The reproduction phase: If there was space available along the edge of the population (i.e. the distance between two individuals was large enough such that a new individual can fit within the defined collision tolerance), then the neighbouring individuals competed with each other to reproduce into the space. The winner of the competition was the neighbouring individual with the highest energy. If there was no difference in energy budgets between the two neighbouring individuals, we decided the winner by a non-biased coin flip. The winning individual expended half of its energy reserves to the offspring and gave the new individual its phenotype, similar to that of binary fission in bacteria. If a chance of mutation existed then offspring could change their dispersal state between actively dispersing and non-actively dispersing from that of its parent.

We conducted each foraging, movement and death phase separately for all individuals before enabling the system to progress to next phase i.e. all individuals in the system forage at the same time before all individuals move at the same time, etc. This helped to reduce the run time of the model. If multiple cases of reproduction were required in a time-step, we filled the spaces in a random order until we had filled all of the available spaces in that time-step. If multiple individuals could fit into one space, then we filled the whole gap. We did this by placing multiple new individuals in the gap as close to their parent until we filled the entire gap. It was rare that such an occurrence happened, with the only observed cases arising in test cases where the system was instead seeded with either a few dispersing individuals with no mutation rate or with movement rules in place such that a big enough space could arise in each time step. We do not show these results in this study. We attempted an alternative to this reproduction process whereby each neighbouring individual could only produce one offspring to fill the gap, thereby leaving the remaining space as an unoccupied gap along the leading edge. However, the resultant gaps led to critical errors during the running of the code, as it was possible for individuals along another edge of the population (e.g. a tendril) to move into the resulting gap and spread into area, which had already been colonised. We could not find a solution to this.

We have chosen this sequence of life history events to ensure an individual who was foraging in a particular spot must have had a large enough energy reserve to reach that spot in the first place. In the absence of explicit modelling of the resources in the environment, this sequence of events ensured as far as possible that individuals in a previous time step had not previously sequestered the area being foraged. This sequence of events also ensured individuals have a positive energy reserve during the reproduction phase.

Design Concepts

There were seven different design concepts that the ODD protocol suggested we consider during the conceptualisation of this IBM model.

Emergence: We imposed life cycle rules upon each individual in our simulation, leading to changes in their internal energy budget. Depending upon the cost of dispersal and the size of the energy budget, the system favoured a dispersal phenotype, thereby resulting in the emergence of different spatial patterns.

Adaptation: Those individuals with a dispersal trait that resulted in an asymptotically decreasing fitness eventually died off, causing individuals upon the leading edge in the system to adapt and exhibit the dispersal phenotype best suited to achieve the greatest level of fitness. The best phenotype established itself along the leading edge because it was the best competitor during reproduction, thereby increasing the likelihood of individuals along the leading edge exhibiting that phenotype. Evolution of dispersal distance did not explicitly occur in the system i.e. dispersal distance was not defined as a continuous variable. We also allowed individuals to mutate during reproduction, consequently resulting in a form of natural selection to occur.

Fitness: Whilst researchers traditionally define the fitness of a dispersal allele by its rate of spread throughout a population, we based the emergent trait of an individual's fitness upon its core energy reserves. We defined fitness in this way because the core energy reserves commanded an individual's ability to compete with neighbours for the ability to reproduce, consequently enabling the propagation of its own phenotype.

Sensing: There was collision sensing to avoid overlap with other non-neighbouring individuals. This was to avoid overlaps between more than three individuals due to the intractable mathematical calculations involved.

Interaction: Interactions between individuals could occur during the movement and foraging phases. During the foraging phase, food was dependent upon the overlap with the main population and neighbouring individuals. During the movement phase, individuals were not able to move into area already occupied except for a small tolerance distance between neighbouring individuals.

Stochasticity: There was a random mutation chance during reproduction resulting in stochasticity in the inheritance of a dispersal phenotype by an individual's offspring. Stochasticity could also arise between two neighbouring individuals with the same energy reserve during the process of reproduction (where a nonbiased coin flip decides the winner).

Observation: The key characteristics of the system monitored were the spatial pattern of spread, the energy levels of each individual according to their dispersal phenotype and the proportion of the population exhibiting a particular dispersal phenotype.

Initialization

Individuals and their circles of influence of radius r , were placed equidistantly around the circumference of a circle (representing the main population) with radius R (based on the parameters of table 7.1, the edge of the population began with 15 individuals). Each individual was allowed to overlap a certain distance (c) with neighbouring individuals only. Each individual began with a certain amount of energy and started as a non-disperser. We set this initial energy to be the amount of resources an individual was able to acquire immediately from the surrounding area. The parameter values used for the simulation are contained in table 7.1 unless otherwise specified. All simulations were created and run in the MATLAB numerical computing environment (The MathWorks, 2014).

Input

Once we initialised the model, no further input was required.

Table 7.2: Describing the advantages and disadvantages of both dispersal phenotypes within the system

	Advantages	Disadvantages
Non-active disperser	<ul style="list-style-type: none"> In most cases, this phenotype enabled survival in conditions with little risk of competition against members of other populations 	<ul style="list-style-type: none"> The individual could find itself falling behind the leading edge as actively dispersing individuals occupy the space ahead.
Active disperser	<ul style="list-style-type: none"> The individual potentially gained more resources by moving into non-sequestered area. This combined with decreased competition with the main population resulted in a higher likelihood of reproduction if the cost of dispersal was low enough. 	<ul style="list-style-type: none"> The individual could possibly overextend itself. This may cause a decline in its internal energy reserves thereby reducing likelihood of survival.

Sub models

Resource acquisition

The calculation of an individual's energy reserves was dependent on its circle of influence and how much this circle of influence overlapped with both the main population and the circles of influence of its direct neighbours (equation 7.1).

$$\text{Resources acquired} = \frac{(\text{Area} - (\text{Overlap w/ neighbours} + \text{Overlap w/popn}))}{\text{Area}} \quad (7.1)$$

We used the same methodology as used in Chapters 5 and 6 for the calculation of equation 7.1. However, we used some slight simplifications to make calculations easier. In Chapters 5 and 6, we utilised the equation for the overlap of three distinct circles to calculate the overlap with the main population and neighbouring individuals. This assumed that a curved line represented the population edge. Here, we used a 'hinge' to represent the edge of the main population. This was the shape created by making two lines between the centre points of the two neighbouring individuals and the centre of the focal individual (figure 7.4 - left). We required this simplification in order to define the main population behind an individual after it had dispersed away from the edge of the main population – for instance the bottom picture on the left side of figure 7.4. The 'hinge' calculation introduced some slight errors to our calculation but the broad principal of the effect of curvature upon the energy gained by an individual was still maintained (figure 7.4 – right).

Movement Phase

Individuals moved according to whether they were an actively or a non-actively dispersing individual. A non-actively dispersing individual moved a set distance, m and an actively dispersing individual moved a set distance, M such that $M > m$. The trajectory of movement was perpendicular to the line formed by connecting the centres of the two neighbouring individuals. We decided the direction of movement from this line by whether the inclination of the line, ε , connecting the two individuals was positive or negative and whether the change in the y-coordinates between these two individuals, γ , was positive or negative.

We calculate the inclination of the line connecting the two individuals as $\varepsilon =$

$\arctan\left(\frac{y_2 - y_1}{x_2 - x_1}\right)$ and we calculate the change in y coordinates as $\gamma = y_2 - y_1$ (see

figure 7.3). We calculated the direction of movement, θ , as the inclination of the line going directly perpendicular from this line connecting the two neighbouring

individuals i.e. $\theta = \arctan\left(-\frac{1}{\frac{y_2 - y_1}{x_2 - x_1}}\right)$. Here, δ represents the distance moved.

For an individual with line angle, $\varepsilon > 0$ and $\gamma > 0$ or $\varepsilon < 0$ and $\gamma > 0$:

$$X_{iter+1} = X_{iter} - (\delta \cos(\theta))$$

$$Y_{iter+1} = Y_{iter} - (\delta \sin(\theta))$$

Similarly, for an individual with line angle, $\varepsilon > 0$ and $\gamma < 0$ or $\varepsilon < 0$ and $\gamma < 0$:

$$X_{iter+1} = X_{iter} + (\delta \cos(\theta))$$

$$Y_{iter+1} = Y_{iter} + (\delta \sin(\theta))$$

Note that a special case occurs for $\varepsilon = 0$, where for $\gamma > 0$

$$Y_{iter+1} = Y_{iter} + \delta$$

And for $\gamma < 0$

$$Y_{iter+1} = Y_{iter} - \delta$$

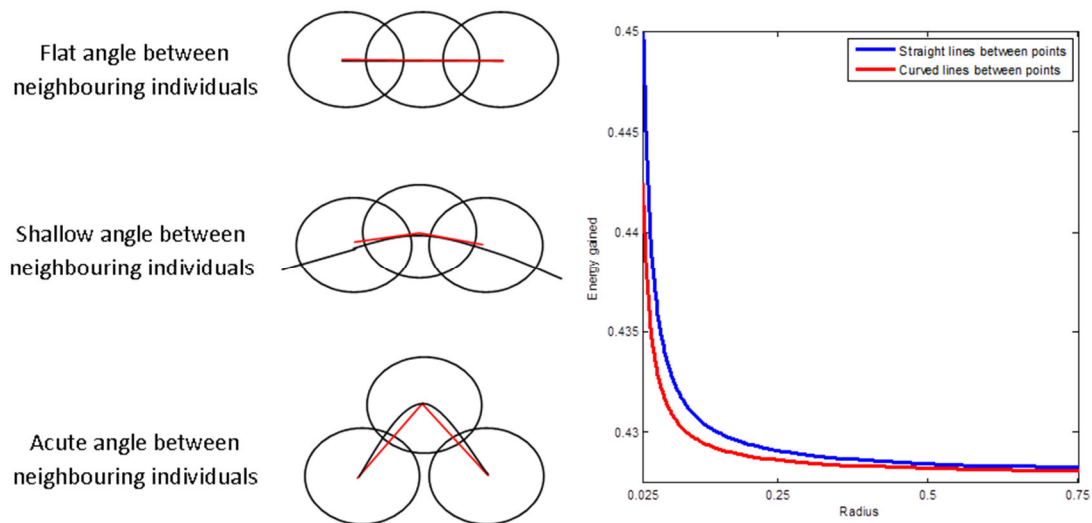


Figure 7.4: (Left) The simplified ‘hinge’ calculation - the black line represents the actual shape of the population frontier and the red line represents the shape of the population frontier made by our hinge simplification. (Right) The blue and red line is the energy gained by an individual as curvature decreases via the hinge method and normal method (as used in Chapters 5 and 6) respectively.

To prevent individuals along the population frontier moving into area previously occupied/previously exploited, each individual underwent an ad-hoc collision detection algorithm. The mathematical formulation of this collision detection algorithm is contained in Appendix G. In this collision detection algorithm, there were three cases depending on whether the individuals in question were neighbours (according to an ordered list) and if they were already colliding before the movement phase:

1. If the colliding individuals were neighbours then we allowed them to overlap slightly according to a collision tolerance. If during movement individuals overlapped such that the amount of overlap exceeded the tolerance then the collision detection algorithm stopped the individuals at the point at which collision takes place.
2. If colliding individuals were not neighbours but were already overlapping (individuals that are adjacent to the tip of a tendril for instance) then we allowed them to move as long as the overlap at their new position was less than at their previous position. If this was not the case then the individual stayed where it was.
3. If colliding individuals were not neighbours and were not already overlapping then they both stopped at the point of collision.

This collision algorithm could cause individuals to become stuck behind the leading edge. Removal of these individuals (either by the introduction of a respiratory cost phase or by simpler method of removal) resulted in errors occurring. These errors were because of the model dictating whether an individual was neighbouring according to their position in a list (vector) rather than by their Euclidean distance from one another. We adopted this approach to reduce the running time of the model, to reduce the complexity of the model (added complexity arises when more than 2 circles overlap with each other) and because of difficulties with arranging individuals via Euclidean distance. Therefore, individuals which became trapped were left in the model but as already stated, were not included as part of the analysis.

During movement, we considered that each individual must expend energy. As in Chapter 6, we defined the cost of dispersal by a linear relationship (equation 7.2).

$$\text{Movement penalty} = (\text{Movement} \times \text{Penalty coefficient}) \quad (7.2)$$

This cost represented the energy required to produce the machinery required to move and the energy required to move at that rate. In lieu of a specific respiration cost, the movement cost accounts for these aspects too.

Survival Phase

In this phase, an individual died if its energy reserves, E , reached or was below zero after the movement phase. This resulted in a gap appearing along the leading edge of the population.

Reproduction Phase:

Reproduction occurred when the space between two neighbouring individuals became sufficiently large enough such that a new individual could fit along the leading edge. The characteristics of the new individual depended upon which neighbour had the highest energy reserve, with the winning neighbouring individual giving half of its energy reserve to the new individual along with its phenotype. There was also a probability that the individual would change from one dispersal phenotype to the other in the proposed model.

Null Model

We also created a null model without the defined dispersal phenotypes and reproduction rules that we implemented in our main proposed model. This was

to make a fair comparison of the shapes exhibited by our proposed model to those shapes made by a model without the defined reproduction and movement rules stated in the proposed model. The null model was setup in the same way as the main proposed model (i.e. we only looked at those individuals along the leading edge and it underwent the same order of processes) but with the following modified stochastic rules in the movement and dispersal phases.

Movement phase

We assumed movement in the null model was a time-independent process with all individuals assumed to have the same dispersal phenotype and no chance of mutation to a different dispersal phenotype, i.e. individuals did not retain knowledge of the distance they moved previously and the distance of future movement was independent of the movement at previous time steps. In the null model, we assumed the average distance of dispersal was the same as a non-actively dispersing individual in the proposed model (table 7.1). However rather than all individuals moving the same distance for each iteration, we added stochasticity to each individual's distance of dispersal, in order to make the spread of the population in the null model possibly more indicative of an actual population. Subsequently, rather than follow the rules in our proposed model, where an individual's dispersal in a time-step was one of two set distances dependent upon its dispersal phenotype, we allowed each individual to disperse a distance via a truncated Gaussian distribution with a mean equal to that of the non-actively dispersing phenotype (0.0001) and a standard deviation equal to 0.00005. This was such that the distance of dispersal for each individual ranges between zero (we assumed this was the individual's minimum distance of dispersal) and the speed of the faster phenotype (0.0002 – which we assumed was the individual's maximum distance of dispersal) 95% of the time without truncation. If it went outside this range, it truncated to the maximum or minimum value, where appropriate.

Movement distance =

$$\text{Truncated Gaussian} \left(\begin{array}{l} \mu = 0.0001, \quad \sigma = 0.00005, \\ \text{range} = [0, 0.0002] \end{array} \right) \quad (7.3)$$

We downloaded the code for this truncated Gaussian distribution from the MATLAB depository via the link:

<http://www.mathworks.com/matlabcentral/fileexchange/23832-truncated->

gaussian. Note that movement in the null model was still subject to the same collision rules (Appendix G) as the normal model.

Reproduction phase

In the proposed model, we modelled reproduction by specifying a simple competition between neighbouring individuals when an empty site arose along the leading edge, with the winner being the individual with the highest energy reserve. Moreover, we also assumed that reproduction must always take place as soon as an empty space arises along the leading edge. In the null model, we represented reproduction as a stochastic process. First, when a space opened up along the leading edge, there was a set chance that a neighbouring individual would not fill the space that iteration. In these results, we set this to be 50%. If a neighbouring individual was to fill the space that iteration, then we randomly chose between the two neighbouring individuals irrespective of its energy reserve i.e. there was a 50% chance of either neighbouring individual winning the competition, so long as both individuals were capable of reproducing. We calculated these probabilities from uniform distributions ranging between zero and one.

Deriving the fitness benefit

To derive the relative performance of a phenotype in the system after 1000 iterations, we calculated the food accessible by individuals with that phenotype along the leading edge of a population in the next iteration. For all individuals with a particular dispersal phenotype along the leading edge, we summed the gained resources values to measure of how successful a dispersal phenotype was relative to the other phenotype (equation 7.4).

$$\sum \text{Resource benefits acquired by individuals with a dispersal phenotype } t=1000 \quad (7.4)$$

Classifying the pattern

In the results section, we classified the patterns produced according to tables 7.3 and 7.4. We provided the algorithm used to classify these patterns in Appendix I.

Note

The results section shows the combined results of 25 runs of both the stochastic null model and proposed model for each cost of dispersal to acquire the mean signal from simulations.

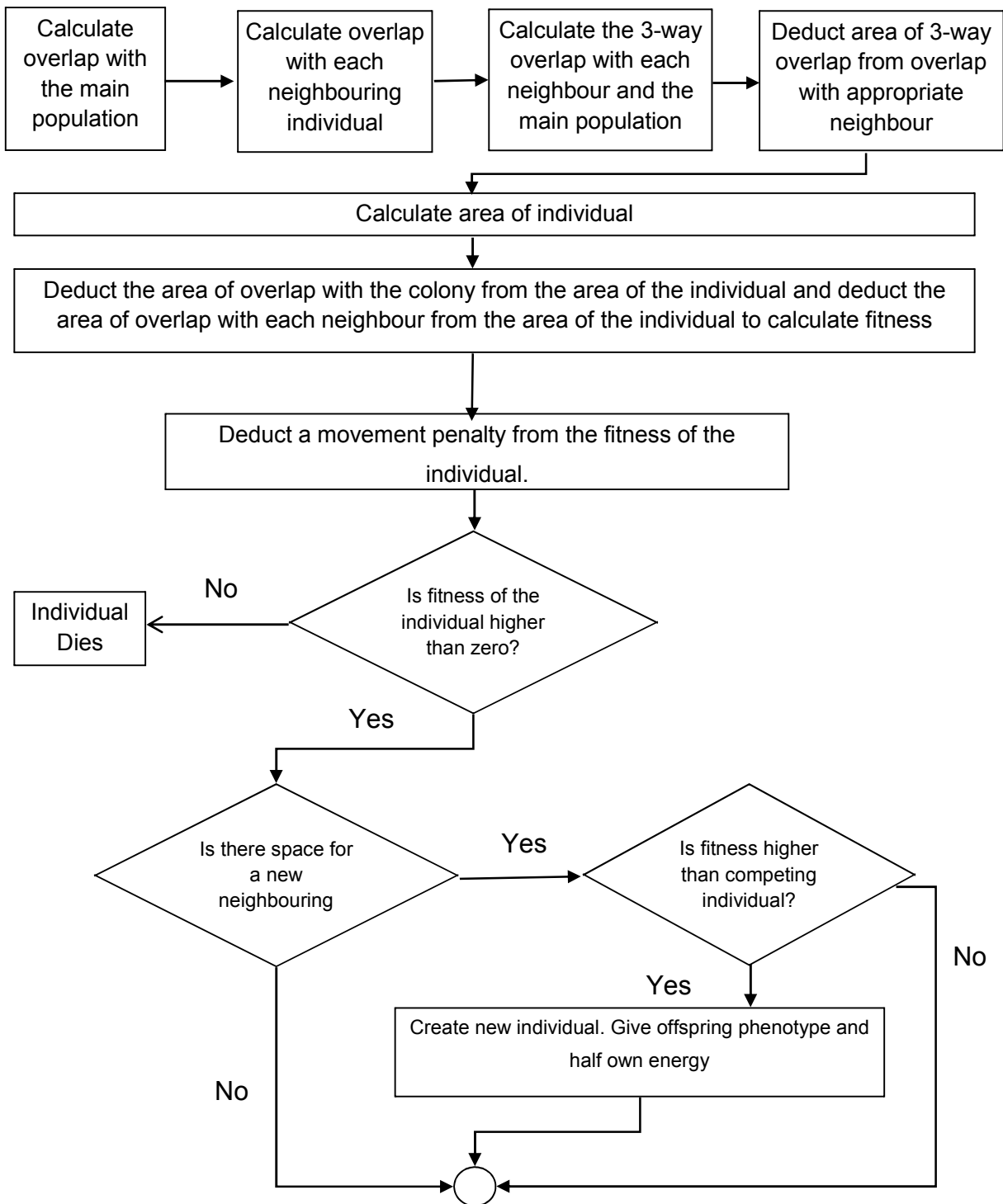


Figure 7.5: A flowchart of the calculations involved for each individual's energy budget during each time step.

Results

We have presented the results of the null model and the proposed model as two separate sections. In each of these models, the key variable manipulated was the cost of dispersal, as it was the main negative factor affecting the dynamics of dispersal evolution faced by the individuals in each simulation. We classified the emergent patterns from these models by two parts. The first part categorised the proportion of individuals situated upon the leading edge with a particular dispersal phenotype i.e. whether active dispersers or non-active dispersers occupied the leading edge (table 7.3) and by the exhibited pattern in space. The second part categorised the number of “wrinkles” that occur due to the collision of individuals (table 7.4). See appendix I for the definition of these classifications in more detail.

Null model

The results of the null model after 1000 iterations showed that the model repeatedly exhibited wrinkled, relatively circular patterns for all costs of dispersal (with the leading edge of these patterns exclusively consisting of one dispersal phenotype as $p(\textit{mutation chance}) = 0$ in the system - figure 7.6). We found that the number of individuals through time was consistent between runs of the model, irrespective of the cost of dispersal, so long as the cost of dispersal was not prohibitive i.e. individuals do not all die out (figure 7.6 – we found that costs of dispersal equal to 5250 and above were prohibitive). We did observe a decrease in the energy reserves of individuals in the system at $t = 1000$ as the costs of dispersal increased (figure 7.6) but we found that our measurement of fitness (the energy acquired by individuals in the next time step, $t = 1001$) was consistent across dispersal costs for non-prohibitive costs of dispersal. Consequently, the cost of dispersal was the reason behind the observed differences in average energy reserves of individuals across simulations. We also see average energy reserves of individuals along the leading edge levelling off. We believe this was because of the stochasticity of the movement and reproduction rules, causing variability in the times reproduction takes place and variability in the dispersal costs (without these rules, fitness goes to infinity), thereby preventing individuals along the leading edge from increasing their fitness towards infinity. We note that the probability of an individual filling a space in a particular iteration had a minor effect upon

these results (results not shown), with the shapes of spread and other measurements broadly in line with those seen in figure 7.6.

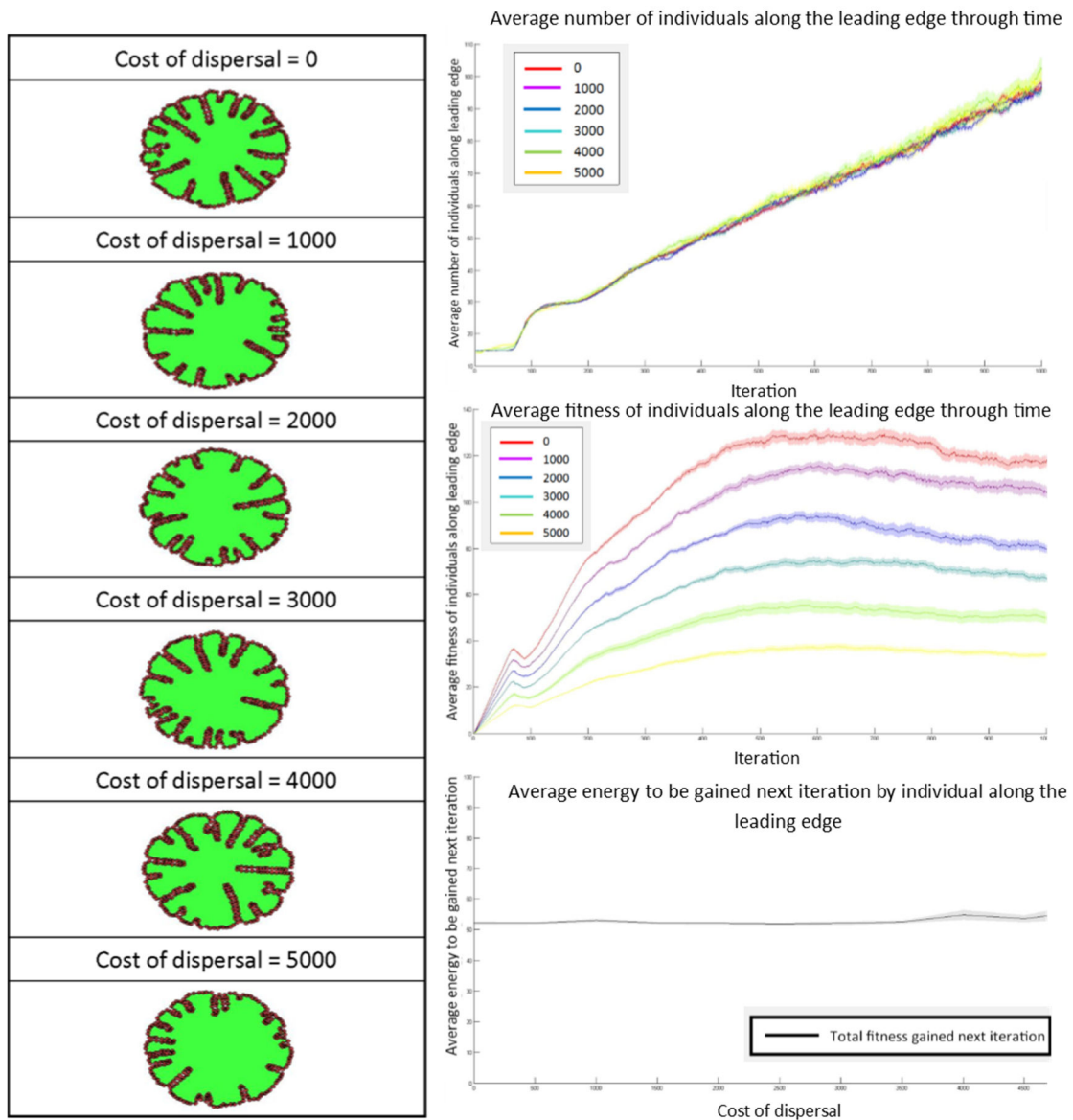
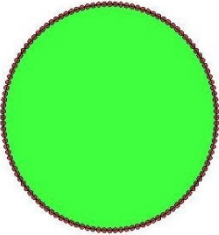
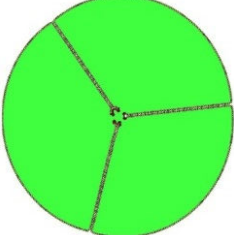
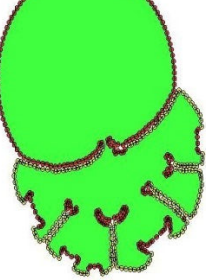
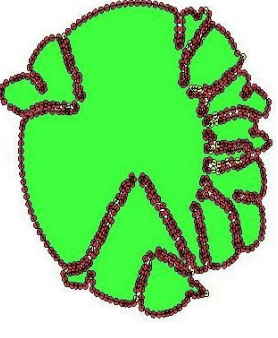
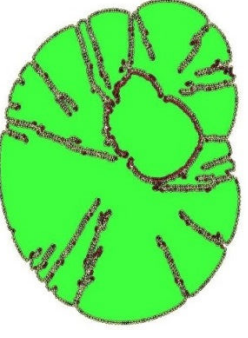
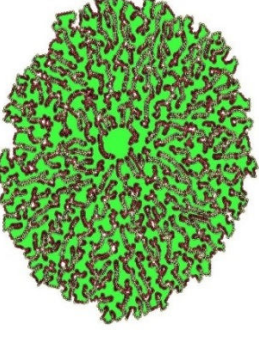



Figure 7.6: (Left) The shapes produced by the null models for different costs of dispersal. (Top right) The average number of individuals along the leading edge in colonies modelled by the null model for different costs of dispersal. (Middle right) The average fitness of individuals along the leading edge in colonies modelled by the null model for different costs of dispersal. (Bottom right) The average energy to be gained by individuals along the leading edge at $t=1001$.

Table 7.3: The first part of the pattern categorisation describing the spatial pattern of spread for those scenarios involving mutation. See Appendix I for more information on how these classifications are calculated.

Code	Classification	Pictures	Description
Cn	Circle		A circular pattern with a leading edge consisting solely of non-actively dispersing individuals. This pattern arises when the cost of dispersal is such that the actively dispersing phenotype is prohibitive.
Fc	Flowery Circle		A circular pattern with a leading edge consisting of only actively dispersing individuals emerges with 'wrinkles' arising from individuals getting trapped. This pattern extends further than the Cn classification due to the higher rate of dispersal. This pattern arises when some individuals choose to disperse and the cost of dispersal is sufficiently low.
FwG	Flowery circle with intermittent gaps		Similar to the Fc pattern but mutations of actively dispersing individuals to non-actively dispersing individuals leads to intermittent gaps of non-actively dispersing individuals along the leading edge of the main population.

Min	Mostly non-dispersing		<p>The leading edge of the population mainly consists of non-actively dispersing individuals with occasional mutations of dispersing individuals. These were usually unsuccessful.</p>
Md	Mostly dispersing		<p>The leading edge of the population mainly consists of actively dispersing individuals with occasional mutations. In this pattern, non-actively dispersing individuals behind the leading edge become stuck.</p>
I	Irregular/no clear majority		<p>The leading edge of the population contains both actively and non-actively dispersing individuals such that there is no clear majority. Consequently, many individuals become stuck resulting in lots of wrinkles.</p>
vST	Very small tendrils		<p>The leading edge contains mostly non-actively dispersing individuals but dispersers sometimes arise via mutations.</p>

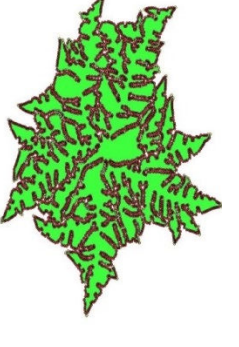

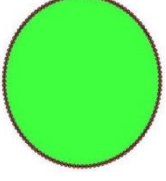
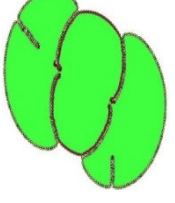
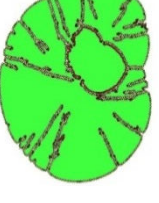
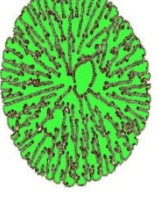
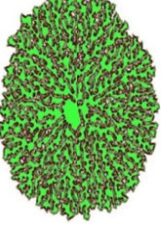
ST	Small tendrils		The edge contains mostly non-actively dispersing individuals but dispersers sometimes arise by mutation. These tendrils are slightly longer than those seen in vST .
LT	Large tendrils		The edge contains mostly non-actively dispersing individuals but dispersers sometimes arise by mutation. These tendrils are slightly longer than those seen in ST .
D	Death	N/A	Individuals die before the full 1000 iterations due to the cost of dispersal

Table 7.4: The second part of the pattern categorisation describing the spatial pattern of spread for those scenarios involving mutation. To take into account the trapped individuals we categorised them according to the resultant number of wrinkles. See Appendix I for more information.

Code	-	SW	W	vW	vvW
Classification	No wrinkles	Slightly wrinkled (1-5)	Wrinkled (5-25)	V. Wrinkled (25-50)	V. v. wrinkled (50+)
					

Proposed model

By varying the cost of dispersal parameter, we found active dispersers were favoured at low dispersal costs and non-active dispersers were favoured at high dispersal costs. In these cases, the patterns of spread exhibited by the model were generally circular, with wrinkles similar to those seen in the null model, although the phenotype along the leading edge was not homogeneous due to stochastic mutation events. At intermediate dispersal costs, we found that tendrill-like dynamics emerge, similar to those exhibited in Chapter 3. To discuss these results in more detail, we broke the results down into three categories of dispersal cost: low (dispersal cost parameter = 0-2000), medium (dispersal cost parameter = 2250-3000) and high (dispersal cost parameter = 3250-5000). At costs of dispersal higher than this, all individuals along the leading edge in this system died, consistent with the null model.

Low costs of dispersal

Once enough iterations had taken place, such that reproduction events could occur (i.e. once gaps open up along the leading edge), the actively dispersing phenotype became established along the leading edge, with the proportion of actively dispersing individuals along the leading edge greatly outnumbering non-actively dispersing individuals (figure 7.7). As non-actively dispersing individuals could only arise along the outer edge because of stochastic mutations during reproduction, an increase to the mutation rate increased the asymptotic proportion of non-actively dispersing individuals along the leading edge. Consequently, depending on the chance of mutation, the patterns arising were either classified as circular (figure 7.8 - 0% mutation rate), “flower like” with some wrinkles (figure 7.8 - 1% mutation rate), or very wrinkled and mostly dispersers (figure 7.8 - 10+% mutation rate). Note that wrinkles arose when neighbouring actively dispersing individuals envelop a non-actively dispersing phenotype. We found that the total energy (ignoring the direct cost of dispersal and internal reserves) acquired by individuals around the edge of the population at iteration 1001 was higher at lower costs of dispersal than at high costs of dispersal (figure 7.9). This was due to the increased range expansion of the colony at low costs of dispersal enabling the actively dispersing phenotype to remain stable along the leading edge, which thereby resulted in more space for reproduction events. This therefore increased the total number of individuals along the leading edge and the area sequestered.

Medium costs of dispersal

As the cost of dispersal increased past a critical point (between a cost of dispersal parameter equal to 1750 and 2000), the proportion of actively dispersing individuals along the leading edge decreased compared to that seen in low costs of dispersal. This was due to actively dispersing individuals having a lower likelihood of winning reproduction events against neighbouring non-actively dispersing individuals (figure 7.7). Consequently, the pattern of spread was highly irregular at this critical point for the cost of dispersal, with the leading edge consisting of both dispersal phenotypes in almost equal measures. This resulted in patterns with many wrinkles. Due to a reduction in their number, the total energy acquired at iteration 1000 by the actively dispersing phenotype decreased compared to that seen at low costs of dispersal (figure 7.9). At the same time, the total energy acquired by the non-actively dispersing phenotype increased compared to when the cost of dispersal was low, as the number of these individuals increased. In total, this initially resulted in a small dip in the total energy acquired by the individuals situated on leading edge of the population. This was presumably due to the lower likelihood of reproduction events occurring and therefore a reduced number of individuals along the leading edge (and space sequestered) because of a slower overall wave front speed.

As costs in this intermediate range increased, the patterns produced began to exhibit what we classified as tendril like dynamics (figure 7.10). Tendrils were the result of actively dispersing individuals dispersing outwards, in such a way that they formed an acute angle with the fully occupied leading edge directly behind. This gave the actively dispersing individual enough unoccupied resources to survive the otherwise high costs of dispersal, but the costs were sufficiently high that in competitive reproduction events, it lost most times against the non-actively dispersing individuals behind. On the rare occasion, the dispersing individual won a reproduction competition event and no mutation occurs, the actively dispersing offspring often failed to survive. Therefore, this mechanism enabled the surrounding non-actively dispersing individuals to increase their population along the leading edge via a 'slipstream' mechanism (figure 7.7). We note that this was not possible in our null model because of the lack of the competition rules during reproduction, time-independent dispersal

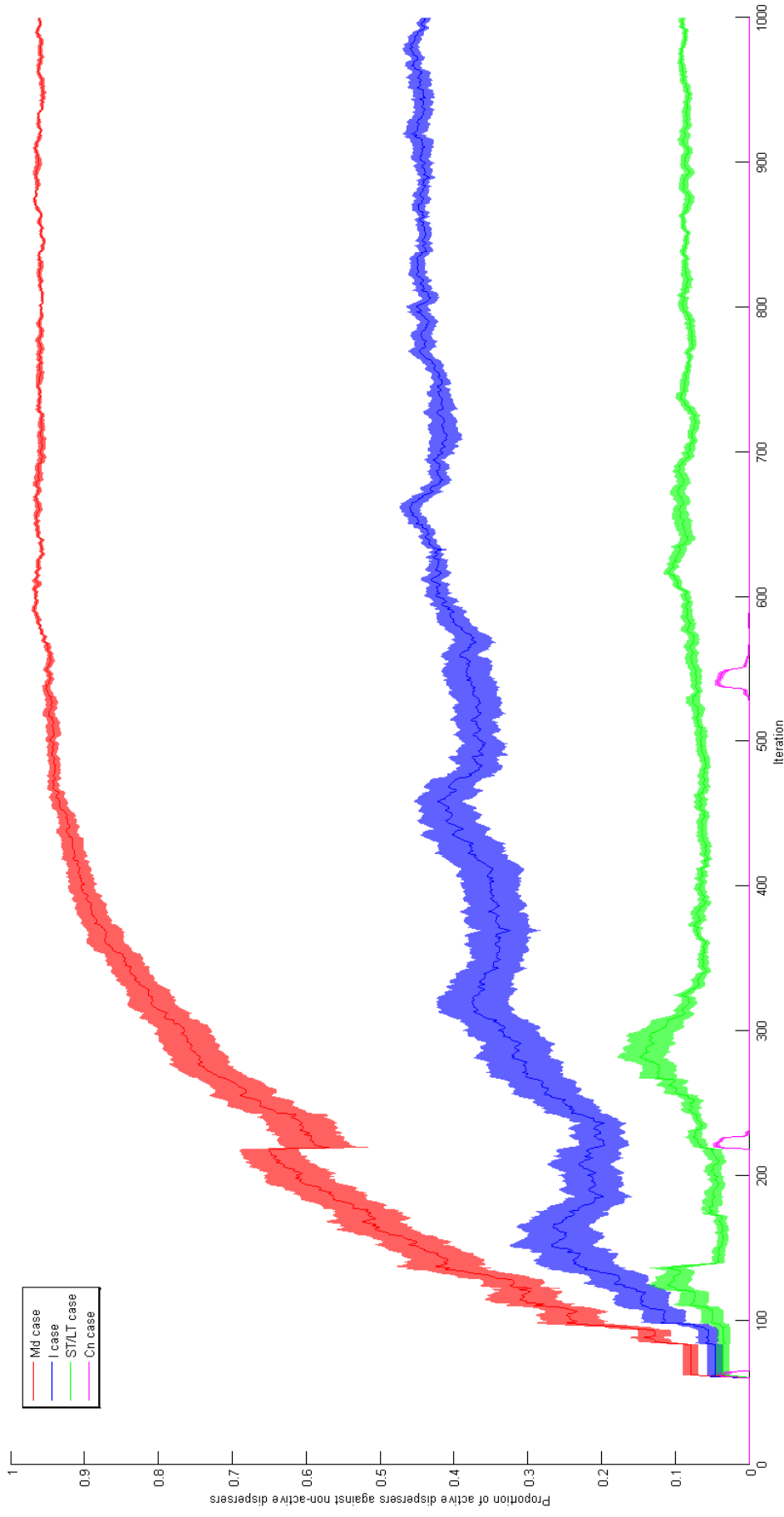


Figure 7.7: The proportion of actively dispersing individuals versus non-actively dispersing individuals for the **Mostly Dispersing, Irregular, Small/Large Tendrils, Circle** consisting of non-disperser cases in table 7.3 for $p(\text{mutate})=0.1$. Error envelopes show ± 1 SE for 25 runs of the model.

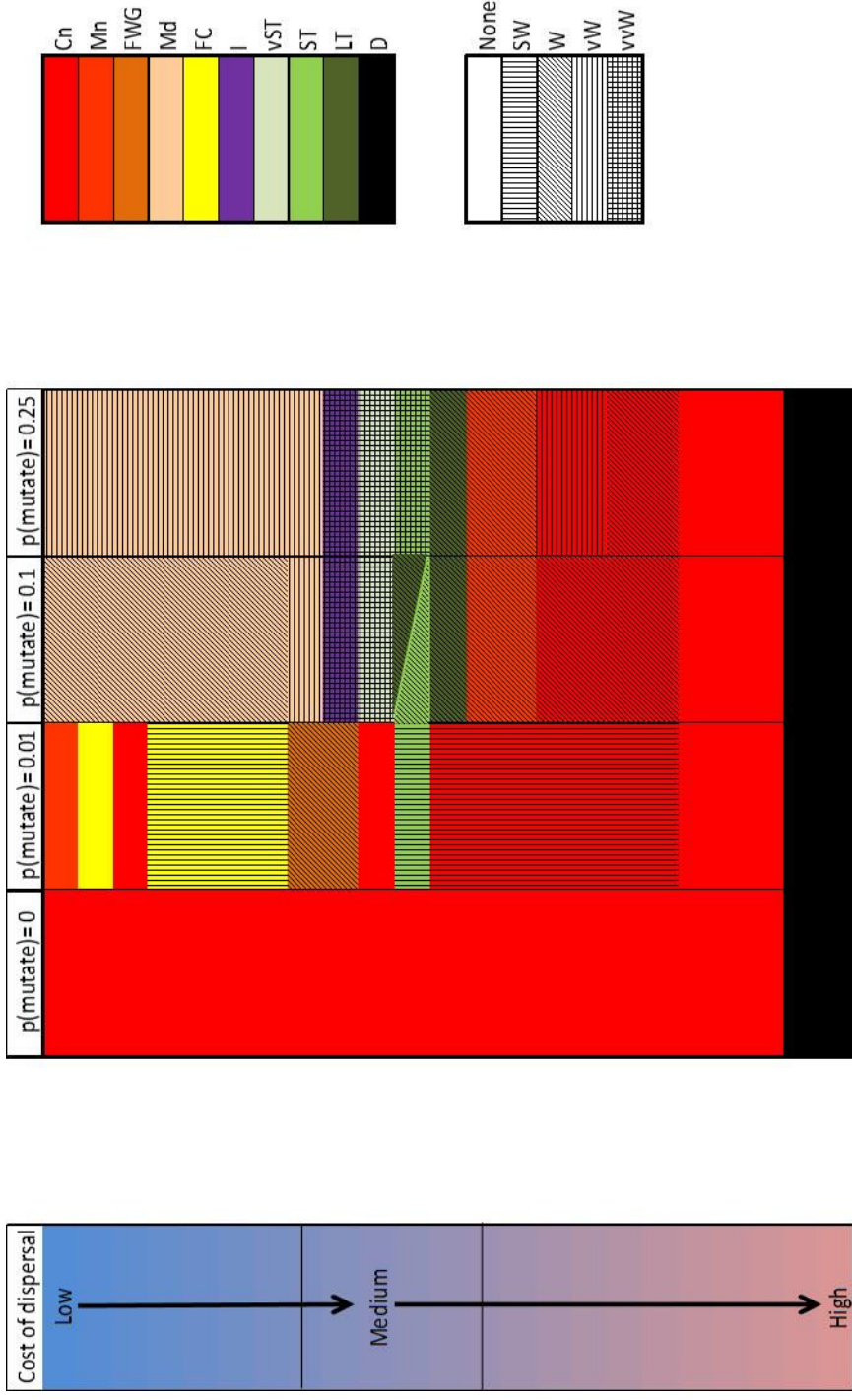


Figure 7.8: A colour code chart with the category of pattern (according to tables 7.3 and 7.4) produced most often after 1000 iterations for the proposed model for 25 runs of the simulation. We separated the results according to the cost of dispersal of the system and the probability of mutation used in the system. We note that this model tested for four mutation rates (0%, 1%, 10% and 25%).

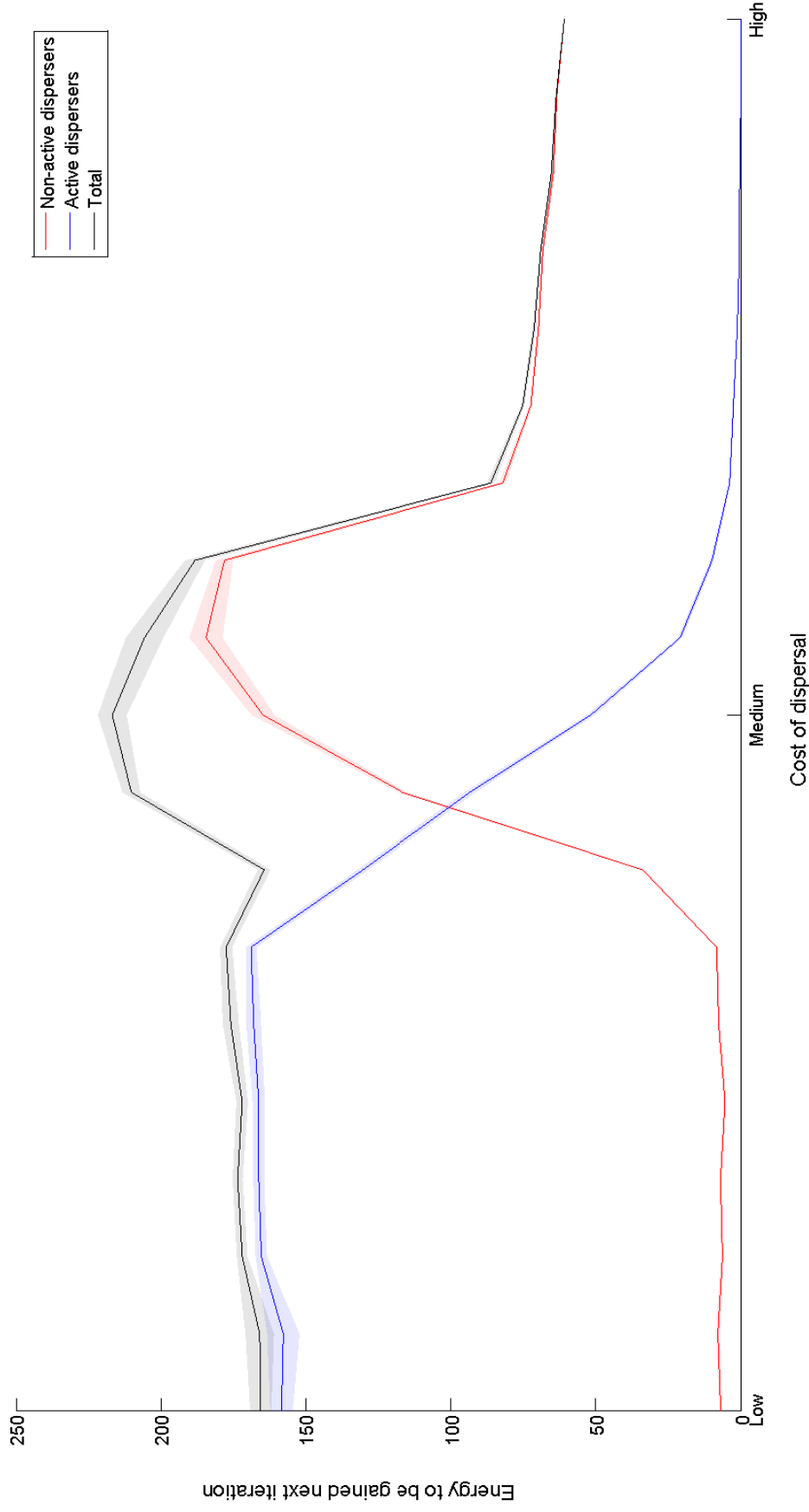


Figure 7.9: The derived fitness measurement (equation 7.3) for actively and non-actively dispersing individuals at different costs of dispersal for $p(\text{mutate})=0.1$ and the total food acquired by individuals along the leading edge of the population at 1000 iterations. Error envelopes show ± 1 SE at each of the costs of dispersal looked at across 25 runs of the model.

(i.e. dispersal in one iteration was independent of the previous iteration) and the lack of differential dispersal phenotypes. We found that the total amount of energy acquired by the population in the next iteration peaked at this cost of dispersal, showing that tendrils result in the greatest group-level fitness (where the group was defined as all of the individual's along the leading edge - as in Chapter 6)(figure 7.9). The total amount of energy acquired by individuals along the leading edge comprised mainly of the energy gained by non-actively dispersing individuals but with some contribution from a relatively low number of actively dispersing individuals as well.

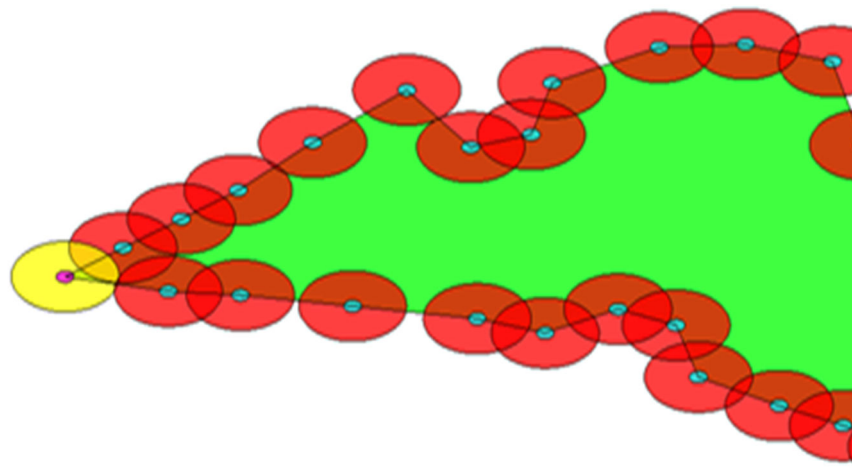


Figure 7.10: A close up view of the tip of a tendril, where the actively dispersing individual is represented by the yellow circle (with the zone of collision represented by the purple circle) and the non-actively dispersing individuals are represented by the red circles (with the zone of collision represented by the blue circle). We see that the tendril consists of one lone actively dispersing individual who was able to acquire enough energy to survive but not enough to consistently outcompete neighbouring non-dispersers in competitive reproduction events.

As the cost of dispersal increased in this intermediate range, up to a critical point, we found the length of the tendrils increased. We believed this occurred because of the lower likelihood of a dispersing individual being able to win a reproduction event (therefore the actively dispersing individual was less likely to give up half of its reserves) and the lower likelihood of its offspring surviving in the case a reproduction event did occur. From the images in table 7.3, we found wrinkles form where an actively dispersing individual's offspring had died. Occasionally, we observed smaller tendrils emerging from the side of a larger tendril. We believed this was because of the stochastic mutation chance within the system, as by mutating from a reproductive non-actively dispersing

individual with high-energy reserves; an individual could overcome the initial hurdles of early tendril development.

High costs of dispersal

At high costs of dispersal, the actively dispersing phenotype failed to take hold along the leading edge and died almost immediately from the point of mutation. Typically the resultant gap was then occupied by a non-disperser, causing the leading edge to consist almost entirely of individuals who were non-active dispersers (figure 7.9). The slower speed of the wave front, compared to those seen at lower costs of dispersal, caused the perimeter of the population to decrease, therefore resulting in a lower total population. As such, the total food acquired was lower than at other costs of dispersal (figure 7.9).

For all costs of dispersal, the rate of mutation affected the type of pattern produced and the number of wrinkles observed (figure 7.8). For example, the longer tendrils and irregular pattern classifications could only occur if the mutation rate was high enough. A low mutation rate typically resulted in either circular patterns similar to those in the null model or possibly in “flowery” patterns with occasional intermittent gaps (table 7.3). The lack of an irregular pattern occurring at low mutation rates was likely to be due to the limited number of reproduction events occurring within 1000 iterations when the population begins all as non-dispersers. Consequently, in these scenarios, the IBM possibly did not give enough opportunities for patterns to occur.

Our results have shown that the curvature-driven individual-level selection theory posed in Chapters 5 and 6, as modelled by our IBM in the form of differential survival, reproduction and phenotypic switching between dispersal phenotypes, could give rise to spatial dynamics similar to those seen in microbial colonies (Chapter 3). We found that the patterns exhibited were dependent upon the cost of dispersal, with circles or “flowery” circles occurring at low and high costs of dispersal respectively and tendril or irregular patterns of spread occurring at intermediate costs of dispersal.

Discussion

Individual-level competition can have a significant effect on the evolution of dispersal, which in turn can affect the evolutionary and ecological outcomes of the population (Taylor and Buckling, 2010, Kubisch et al., 2013, Ronce, 2007). We believe the shape of population spread is an aspect of spatial ecology, which based on the evidence thus far in the thesis, affects the characteristics responsible for the persistence of a population. However, researchers know relatively little about how the shape of population spread influences the ecological and evolutionary factors of the population, nor how these factors themselves might affect the shape of spread (Misevic et al., 2015). We have shown, via the use of an IBM model, that individual-level competition between individuals along the leading edge with differing dispersal phenotypes, in the form of the analytical formulation described in Chapters 5 and 6, could give rise to shapes of patterns of spread similar to those of *Ps. aeruginosa* colonies (figure 7.11). We believe these patterns are due to the individual-level differential survival and selection processes rather than the collision and movement rules employed as without the individual-level selection rules employed in this proposed model, the shape of spread would be similar to those shown in the null model, i.e. tendrils dynamics would not be exhibited in our proposed model.

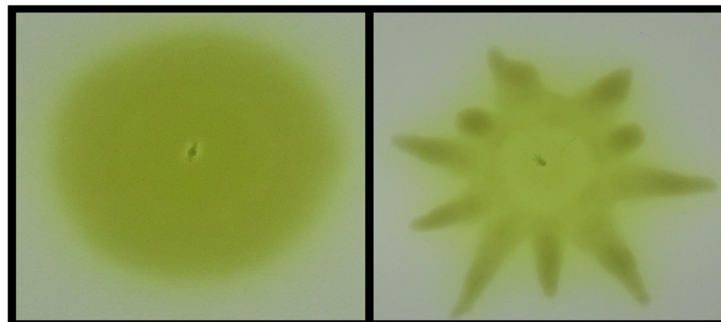


Figure 7.11: Pictures of *Ps. aeruginosa* strain PAO1 colonies spreading across an agar plate surface. The picture on the left is an empirical example of a colony exhibiting a circular pattern of spread and the picture of the right is an empirical example of a colony exhibiting tendrils similar to those produced by the IBM in this chapter.

The results showed that circular patterns of spread occurred when the cost of dispersal was either low or high and tendrils patterns of spread occurred when the cost of dispersal was intermediate. Comparing these results to the spatial pattern observations shown in Chapter 3, we believe that high dispersal costs are representative of the hard agar environment conditions upon which *Ps.*

fluorescens colonies exhibit small growing circular patterns of spread. This is due to the high levels of costly rhamnolipid surfactant production required to decrease surface tension in these environments such that in theory relatively fast methods of dispersal (active dispersal) would be possible (Rashid and Kornberg, 2000, Caiazza et al., 2005). In reality, because of these costs, these fast methods of dispersal do not occur in these environments and hence colonies stay in relatively compact circles. We also notice that the ‘flowery’ patterns of spread with wrinkles exhibited by the model, look similar to *Ps. fluorescens* strain SBW25 wrinkly spreader morphologies when they are isolated from the air-surface interface of a static culture to a hard agar surface environment (Rainey and Travisano, 1998). In this case, we speculate hard agar conditions are representative of the high costs imposed by the increased production of cellulose required to produce a wrinkly spreader biofilm upon an agar surface compared to its smooth morphology relative (Spiers, 2007). While there is an example environment in Chapter 3 representative of relatively high costs of dispersal, there is not an example in Chapter 3 of a surface environment for relatively low costs of dispersal. However, we believe that a similar environment is a liquid culture environment (or very soft liquid-like agar conditions). This is because in these liquid environments, individuals often have a high rate of dispersal due to the swimming motility mechanism utilised in these environments and the lack of surface tension in the environment i.e. dispersal does not require costly rhamnolipid surfactant production (Taylor and Buckling, 2011, Kearns, 2010). Consequently, we believe liquid environments are reflective of low costs of dispersal. At intermediate costs of dispersal, the proposed model exhibits tendril-like patterns, similar to those exhibited by colonies grown in semi-soft agar conditions (Chapter 3). The tendril dynamics of microbial populations arise in these semi-soft agar environments due to the swarming motility utilised by microbes to traverse their environment (Kearns, 2010). This cooperative swarming motility requires moderate levels of rhamnolipid production for the relatively quick dispersal rate associated with swarming – we believe this is reflective of the moderate costs of dispersal relative to the other types of environment, particularly as the rhamnolipid production costs are generally shared between individuals through cooperation (Rashid and Kornberg, 2000, Caiazza et al., 2005).

Our model demonstrates that tendrils develop due to a polymorphism of dispersal phenotypes along the leading edge (i.e. one individual at the tip of tendril with an actively dispersing phenotype and neighbouring individuals behind with a non-actively dispersing phenotype). We note that with regard to Chapter 6, this is similar to one individual utilising a “go for it” strategy while neighbours utilise what we described in Chapter 6 as a “cooperate” strategy. As such, we believe that the stable polymorphism of dispersal phenotypes verifies a prediction in Chapter 6, that alternating dispersal strategies along the leading edge could initiate tendril patterns that accordingly maximises fitness along the leading edge (as the exhibition of tendrils maximises the total food available to the edge of the population in the IBM). A stable polymorphism of dispersal phenotypes along the leading edge of a microbial population can arise in microbial populations due to the speed differential between those individuals swarming and those not swarming (Kearns, 2010). Moreover, cells can improve their ability to swarm by evolving a stable hyperswarming phenotype that increases the number of flagella developed by the cell, thereby conferring a swarming advantage to the cell independent of the cellular growth rate, compared to those individuals swarming without this phenotype or not swarming at all (van Ditmarsch et al., 2013, Hamze et al., 2011). Such a diversification of dispersal mechanisms can often be seen in macroorganism populations (Elliott and Cornell, 2012, Yamamura, 2002). For example, flowering plants can scatter large seeds across short distances and small seeds across long distances (Cain et al., 2000). Another example is the gypsy moth (*Lymantria dispar*) in North America where some females are able to fly and others are not (Robinet and Liebhold, 2009). We hypothesise microbial populations are able to represent many of the same characteristics as macroorganisms, as both have many life history characteristics/ecological factors in common (Jessup et al., 2004). Consequently, we suggest that a generic population, which develops a stable polymorphism of dispersal phenotypes along its leading edge (such as flowering plants and/or gypsy moths), has the potential to spread in an irregular pattern similar to those patterns exhibited by microbial populations.

The observation that the individuals at the tip of the tendril are motile whilst the individuals in the tendril behind are (relatively) non-motile is consistent with experimental evidence (Marrocco et al., 2010, Cerreti et al., 2011, Hamze et al.,

2011). However, classic models have assumed such a mechanism occurs due to the limited nutrients in the environment and the positional advantage of being at the tip in these environments (i.e. these individuals get first access to the resources in the environment compared to those individuals behind which may not get access to any resources – see Chapter 3). Due to the reliance of growth and movement processes on nutrients in these models, these models assume tendrils develop due those individuals at the tip to being ‘active’ and thus able to diffuse and reproduce while those behind the tip are thought of as ‘passive’ or ‘resource starved’ and therefore not able to reproduce or move (Golding et al., 1998, Kessler and Levine, 1998, Marrocco et al., 2010, Mimura et al., 2000, Cerreti et al., 2011). While this explanation is convincing for a number of strains, our results in Chapter 3 illustrate that this assumption is not universally applicable for all bacteria. This is because irregular patterns (tendrils) developed best in high nutrient (i.e. not resource limited) conditions for *Ps. aeruginosa* strain PAO1, thereby contradicting the general nutrient limitation assumptions made in these classic models.

Our model differs in a number of ways in order to move away from the nutrient limited approach in these classic models. First, instead of a reaction-diffusion nutrient-driven approach, we proposed an evolutionary curvature-driven competition-based IBM approach, whereby individuals along the leading edge evolve different dispersal phenotypes to compete against each other for resources in a resource-rich environment (i.e. nutrients are abundant for growth in any area not occupied by the main colony behind the leading edge). This allowed us to observe whether individual-level social interactions along the leading edge could give rise to adaptations resulting in irregular patterns of spread (i.e. consistent with the IBM approach (Grimm and Railsback, 2013)), as well as allowing us to keep track of the evolutionary fitness consequences of these adaptations. Within this competition, we considered the intrinsic cost of dispersal (i.e. the metabolic costs behind the dispersal mechanisms required to spread upon the agar plate environment (Rashid and Kornberg, 2000)) and the area available to sequester from outside of the confines of the main population as the determinants of phenotype evolution in the model (consistent with Chapter 6). This removed the reliance of the model on the environmental resource limitation assumption in other models (Golding et al., 1998). Through

this competition, we modelled two dispersal phenotypes, similar to an “active” and a “passive” cell in other models (Marrocco et al., 2010). However these dispersal phenotypes were also regardless of environmental nutrient limitations and they are formed on an evolutionary basis to outcompete others according to the rules of the system i.e. individuals keep their phenotypes until they die and offspring inherit these phenotypes. We also assumed that all individuals along the leading edge could reproduce and move, so long as there was available space.

Through this approach and its assumptions, we found that tendrils develop via a slipstream mechanism. This slipstream mechanism has similarities with a theory in the literature about the possible basis of the mechanisms responsible for tendril patterns of spread (Cerreti et al., 2011, Marrocco et al., 2010). This theory suggests that the development of tendrils is a process involving the division of labour (i.e. co-operation) between those motile individuals at the tendril tip, termed ‘swarmers’, that spearhead the shape of spread, and those non-motile individuals behind, termed ‘supporters’, that support the efforts of those spearheading the tendril by producing the public goods (surfactants) required to help those at the tip continue the swarming process and by reproducing into the region explored by those at the tendril tip (Julkowska et al., 2005, Cerreti et al., 2011, Marrocco et al., 2010)). This theory is based on empirical evidence in some *Bacillus subtilis* strains showing that those individuals at the tips of tendrils are genetically different (via the costly development of a hyper-flagella mechanism enabling them to disperse at a higher velocity (Hamze et al., 2011)) to those individuals within the tendril (which are non-motile but can reproduce for many generations, even when nutrients are limiting (Marrocco et al., 2010, Xue et al., 2011)). We note this theory does not rely on the nutrient-limited assumptions made in the classical models of microbial spread (Marrocco et al., 2010). While there has been an illustrative reaction-diffusion based modelling demonstration of this theory giving rise to irregular patterns of spread, the evolutionary, ecological and socio-biological basis responsible for initiating this possible cooperation has not been identified (Cerreti et al., 2011). The slipstream mechanism in our model (and the preceding theory in Chapters 5 and 6) makes a number of insights with regard to this theory.

First, based on the empirical evidence illustrating that those cells developing the hyper-flagella mechanism to become 'swarmers', develop this mechanism along the frontier region while the colony is circular (Hamze et al., 2011), we suggest this mechanism develops via evolutionary dispersal games (Chapter 6) in response to the increasing individual-level competition arising due to geometric factors of the population (i.e. the curvature – see Chapter 5)(Innocent et al., 2010). Thus, we suggest researchers investigating this theory should look towards this evolutionary dispersal game in order to understand more about the initial starting basis of these tendrils.

Secondly, these tendrils developed in our model when the cost of dispersal was such that the individuals at the tendril tip incurred a lower energy reserve compared to those behind the tip in the slipstream mechanism. Our model illustrates this by the fact that the actively dispersing individuals generally lose in the individual-level competition for reproducing into an empty space along the population edge at these costs of dispersal. With regard to the theory, because tendrils were formed in our model even without the slipstreaming individuals contributing to the development of the tendril in our model (i.e. by the production of public goods), we interpret our results to be evidence against the specific requirement of a cooperative division of labour mechanism for tendril formation. Non-dispersing individuals arise behind the tip of the tendril because of individual-level selection, not because of group-level selection. However, because those at the tip have a lower energy reserve, we recognise that at the individual-level, selection might select against the development of these hyper-flagella mechanisms responsible for the tendril unless either the group-level benefits are great enough (Chapter 4) and/or the individual-level costs are reduced sufficiently enough (via cooperation between those swarming at the tip) (Griffin et al., 2004, de Vargas Roditi et al., 2013, West et al., 2007b, Kearns, 2010, Rashid and Kornberg, 2000). If the selective conditions are such that they might indeed select against the exhibition of tendrils, then in this case, individuals behind might help to support the efforts of those actively dispersing at the tip via the production of public goods, in order to ensure they obtain the individual-level benefits associated with the slipstream mechanism. This would be as long as the costs of helping did not completely counter the benefits of the tendril dynamics (West et al., 2007b). Combined, we believe future work should

investigate the fitness dynamics of this slipstream mechanism in more detail, in particular the strategies responsible for its evolutionary basis, and that future work should continue to explore the theory poised in the literature (Cerreti et al., 2011), especially as it moves away from the nutrient-limited assumptions classically made in the modelling of irregular shapes of spread (Marrocco et al., 2010).

There are some possible caveats to these results. First, while our results show that the free riding non-actively dispersing individuals experience higher fitness benefits, we theorise the dispersing individuals at the tip may achieve some longer-term benefits (Travis et al., 2009, Kubisch et al., 2013). For instance, by being in the 'valley' between two tendrils, individuals are likely to experience less space to reproduce into (i.e. more likely to become trapped behind the leading edge) and in bacterial populations, possibly an increase of bacterial toxic waste products which can accumulate around the edge of the colony, compared to the individuals at the tendril tip (Hochberg and Folkman, 1972). This might affect the balance of selection discussed in the previous paragraph. Secondly, if we had considered the environment to consist of lower concentrations of resources, then due to the decreased energy available in the environment, this could affect the spatial dynamics of the colony as modelled by our IBM. For instance, a lower concentration of resources may theoretically decrease the likelihood of cooperation amongst individuals (i.e. those at the tip swarming (Nadell et al., 2010)), thereby increasing the resultant individual-level competition and selecting against those mechanisms responsible for irregular patterns of spread. Limited resources may also affect the speed of dispersal and the area covered (thereby lowering the carrying capacity of the colony (Roditi et al., 2013)) and with regard to our model, limited resources might manifest itself in a reduction in the transition points of the costs of dispersal and potentially narrow the range at which tendrils occur.

In an attempt to limit the complexity of the IBM model, there are a number of simplifications in the model, which future work could improve. First, the model shares the same problems as the analytical treatment seen in Chapters 5 and 6 i.e. there is only a binary choice between actively dispersing and non-actively dispersing phenotype. In reality due to the different dispersal mechanisms available and the heterogeneity in the dispersal ability of these mechanisms,

individuals in nature often move at a rate dictated by a continuous distribution (such as that in the null model) rather than a discrete set of movements (Kot et al., 1996). A natural extension is to allow individuals to move via an evolving dispersal kernel to see how this affects the shape of spread and whether there is an optimum dispersal distance. Secondly, reaction-diffusion equations in two dimensions have shown that the curvature of the population can affect the rate of spread. Specifically it has been shown that diffusion is slower at higher curvatures than at lower curvatures (Lewis and Kareiva, 1993). Whilst the basis of their model was diffusive movement processes rather than the directed movement in our model, this could still affect the rate at which individuals move e.g. for those individuals at the tips of the tendril. Finally, we also assume a linear cost of dispersal relationship with dispersal distance, whereas a non-linear relationship may be more suitable, as dispersal is likely to get progressively harder as the distance traversed in one-step increases (i.e. dispersal kernels - see (Chapman et al., 2007, Nathan, 2006, Kot et al., 1996)). However, research would need to measure the relationship between dispersal distance and dispersal cost to incorporate this factor into our model.

A further possible caveat of our model is the assumption during reproduction that neighbouring individuals must populate gaps along the leading edge. In reality, individuals behind the leading edge might also populate into space along the leading edge or those individuals along the leading edge might instead reproduce into the non-sequestered area outside the confines of the main population. We made this simplification in order to focus our investigation into understanding how evolutionary competition (for space along the leading edge) and ecological dynamics between individuals along the leading edge affects the resultant patterns of population spread, in line with the formulation posed in Chapters 5 and 6. This was to see whether the theory posed in Chapters 5 and 6 could result in irregular patterns of spread. This is in contrast to other IBM models which typically represent every individual in the system to model the spread of (microbial) populations (Nadell et al., 2010, Du et al., 2011, Xavier et al., 2009, Xavier and Foster, 2007, Xavier et al., 2005, Goroehowski et al., 2012). We believe this simplification assumption is a suitable basis for our model, particularly as it is believed that a large proportion of cellular growth and particularly outwards motility (the key life-history processes believed

responsible for the spatial spread of microbial populations) within a microbial population occurs via those active cells along the leading edge (Kearns, 2010, Nadell et al., 2010, Du et al., 2011, Hamze et al., 2011). However, we acknowledge that there could be a possible contribution to these processes by those individuals behind the leading edge. Indeed, some evidence suggests that those individuals behind can contribute to spatial shape of the biofilm via mechanical pressures resulting from cell growth and division (Xavier et al., 2009). The strength of this pressure is thought to depend upon the depth of the region behind the leading edge contributing to these pressures and the population density (i.e. the number of individuals) within this region (or similar factors such as the density of extracellular polymers which can also push cells) (Xavier and Foster, 2007, Nadell et al., 2010, Motoike, 2007). Evidence also suggests that irregular (but not necessarily tendril) patterns of spatial structure are more likely as the penetration of resources into the population decreases, due to less individuals behind the leading edge having access to the resources required for growth and causing spread to occupy the empty valley regions between tendrils (Nadell et al., 2010). Consequently, because we assume that no resources are available to any individuals behind the leading edge and thus are unable to reproduce in order to exert these mechanical pressures (i.e. there is no resource penetration), our model is possibly an extreme case, with the highest likelihood of developing irregular patterns of spread. While we note that these other studies do not consider the effect of swarming motility, future research could look to create an IBM modelling all individuals in the system (or use reproduction rules such that individuals can reproduce outside the colony) with the leading edge theory described in Chapters 5-7 to ascertain the contribution to spatial dynamics of population densities behind the wave front.

Another potential area of improvement in this IBM relates to the homogeneous distribution and homogeneous sequestration of resources throughout the environment. To introduce heterogeneity to these factors, one suggestion is to introduce a resource map, recording the parts of the environment, which the colony has or has not sequestered. This would help to ensure individuals are only able to exploit previously unexploited areas and would add variation to the amount of resources acquired at each time step. Similarly, we could improve competition within the system, as due to mathematical limitations, we have

constrained the competition for resources to be between neighbouring individuals in an ordered list and the main population. Potential improvements to competition in this model might be to: (1) Find an error-free way such that the neighbouring individuals are based upon Euclidean distance rather than their position in an ordered list, or (2) In the absence of a mathematical formulation which can calculate the overlap between more than 3 circles, utilise an image analysis method to calculate the overlap between more than one individual (for instance, each individual could be represented by a coloured semi-transparent disk such that overlaps between individuals are detectable due to their higher pixel intensities). However, we note that this has its own problems, as it is potentially inaccurate and computationally demanding. The lack of a mathematical formulation to calculate the overlap between more than three circles also limits the change of population density along the leading edge of the population. While we have adopted a methodology, which allows individuals to exist along the leading edge if it can fit such that a maximum of two circles of influence overlap at any one point. In reality, the density along the leading edge is likely to increase to capacity as individuals race towards the food for their own success, possibly resulting in multiple individuals competing for the same food. Future research could investigate these potential improvements.

The results of our IBM show that uncomplicated life cycle rules combined with the simple individual-level selection and the curvature-driven leading edge competition theory presented in Chapters 5 and 6 can give rise to a variety of spatial dynamics, closely resembling those seen in microbial populations. We found that the cost of dispersal was a key factor behind the pattern produced with tendril dynamics notably occurring at intermediate costs of dispersal because of a polymorphism of dispersal phenotypes along the leading edge. Moreover, we found that a slip streaming effect occurs during the exhibition of tendrils because of curvature-driven, individual-level competition and without the diffusion of nutrients towards the colony as previously assumed in many other models. Together these results highlight how the evolutionary games in Chapter 6 can indeed result in patterns of spread similar to those seen in natural biofilm populations.

Chapter 8

Getting into shape: can we select for the shape of spatial spread?

Abstract

Pseudomonas aeruginosa strain PAO1 can exhibit a variety of spatial patterns during its colonisation of agar plate environments. These patterns of spread range between relatively circular patterns to the exhibition of striking tendrill patterns. While research has explored the mechanistic processes behind these patterns, the ecological and evolutionary implications of these patterns are still relatively unknown. Previous research in Chapter 4 has shown that that these patterns can have an impact on the fitness of the colony at both the individual- and group-levels, therefore leading us to theorise that the shape of spread is a trait of the colony that can evolve in order to maximise fitness. To test this theory, there is a need to determine empirically the outcome of competition between different shapes of spread; this requires colonies that reliably exhibit these shapes of spread. To do this, we aimed to exploit the link between genotype and the shape of spread. In this study, we establish a number of selection lines, set up to artificially select either for or against the exhibition of tendrills, to evaluate how the shape of the colony responds to multiple generations of artificial selection. After two extensive attempts, our results conclude that the shape of the colony could not reliably be selected for, thereby suggesting that the shape of the colony is perhaps not a heritable trait of the colony.

Introduction

How members of a population exploit the surrounding environment is a key component of the population's long-term ecological success (Johnson and Stinchcombe, 2007). To exploit the resources in the local environment, individuals can develop a number of foraging strategies. Optimal foraging theory suggests natural selection favours foraging strategies, which maximise nutrient uptake per unit of effort (Pyke, 1984). Subsequently, there are many factors affecting which foraging strategy is most optimal. For example, in environments with patchy resource distributions, members of bee or wasp populations are under pressure to improve their access to patches of high quality resources. This is done by developing longer and faster dispersal mechanisms, such that they optimise their foraging strategy according to the parameters of the environment (Franzén and Nilsson, 2010, Wajnberg et al., 2012). Another example is the acquisition of nutrients from the soil by plants (Casper and Jackson, 1997, Barber and Mackay, 1986). In order to adapt to the below-ground spatial heterogeneity of resources, competing plants can adjust their root density, root surface area, rooting depth and morphological/physiological plasticity (Casper and Jackson, 1997). Optimisation of these foraging characteristics enables the plant to increase its productivity (i.e. the yield of fruit) and its own survival (Lynch, 1995), thus illustrating how individuals can increase their ecological success by optimising their ability to exploit the spatial domain. Developing the optimal foraging strategy is important when it comes to competition as by developing a foraging strategy more optimal than that developed by its competitors, an individual can improve its fitness relative to other competitors (Nonaka and Holme, 2007). Due to the assumed significance of its effect upon the traits and success of an organism, researchers have focused on the evolution of an optimal foraging theory in their attempts to predict and explain the behaviour of organisms with regard to their acquisition of resources.

Bacteria during their colonisation of agar plate surfaces form structured, multicellular biofilms, enabling cells to act collectively as a multicellular organism (Kreft, 2004). The advantages of living as multicellular biofilms are numerous, with individuals in the biofilm exhibiting increased persistence in resource starved environments and increased resistance to antibiotics/host

defences (López et al., 2010, Davey and O'Toole, 2000). Microbial biofilms exhibit a number of spatial patterns of spread during their colonisation of agar plate surfaces depending on intrinsic and extrinsic factors (as shown in Chapters 3 and (Kearns, 2010)). The ecological benefits of these patterns of spread is still relatively unexplored (Kearns, 2010). However, our previous work in Chapter 4 has suggested that a colony is able to sequester more of the resources from the environment (and therefore, by proxy, achieve a higher group-level fitness) by exhibiting an irregular, tendril-forming, patterns of spread as opposed to a circular pattern of spread. We theorised this was because an irregular shape of spread has a larger perimeter compared to a circular shape of spread, thereby exposing the whole colony to more of the environment. Consequently, these results suggest that developing an irregular shape of spread is a more optimal foraging strategy than a regular, circular shape of spread and thus selection at the group-level should promote irregular shapes of spread to improve fitness in the environment.

Microbial populations are amenable to selection experiments with their short generation times and large populations empowering us to observe rapid evolution in a controlled experimental setting (Buckling et al., 2009, Jessup et al., 2004). Combined with the ability to archive evolved strains and compare them to their ancestral counterparts, the microbial model system allows researchers to observe the traits, which underpin ecological phenomena in real time (Buckling et al., 2009, Jessup et al., 2004). Indeed, to date, the microbial model system has been extensively used to investigate the evolution of social behaviour (West et al., 2006b), predator-prey dynamics (Yoshida et al., 2003) and dispersal mechanism trade-offs (Taylor and Buckling, 2011). Assuming that the morphological shape of microbial spread is a trait of the colony (due to the exhibition of a wide number of spatial patterns in different environments), we hypothesise that the shape of microbial spread is an evolvable trait that we can select for across generations such that it affects the ecological characteristics of the population (similar to experiments which have artificially selected for certain plant root architectures (de Dorlodot et al., 2007)).

Based on the suggestion that the shape of spread affects the foraging ability of the colony and that there exists an optimum shape of spread which natural selection should select for in order to increase fitness, using *Pseudomonas*

aeruginosa strain PAO1 as our model system, we empirically investigate whether we can artificially select for the shape of microbial spread. We conduct an artificial selection experiment such that under negative selection, the number of tendrils reduces (i.e. the shape of spread becomes more circular), and under positive selection, the number of tendrils increases (i.e. the shape of spread becomes more irregular). We do this with the intention of conducting competition experiments between irregular shaped populations and regular circular shaped populations, to empirically ascertain the winner between different shapes of population spread, following manipulation of scales of genetic diversity (mixed vs clonal colonies) and scales of competition for limited resources (competition within and/or between colonies). Unfortunately, for two different selection regimes, our results show that repeated positive and negative selection of the shape of the colony has no clear, consistent, effect upon the pattern of spread.

Methods

In this study, we artificially selected for the shape of spread via two different selection regimes.

Experiment one: Selecting the whole outer edge of the colony

At the beginning of experiment one, we cultured five isogenic populations by propagating five samples of a *Ps. aeruginosa* PAO1 frozen stock population (kept at -80°C) in separate sealed plastic test tubes containing 5ml of King's B medium (10g/l glycerol, 20g/l proteose peptone No 3, 1.5g/l K₂HPO₄.3H₂O and 1.5g/l MgSO₄.7H₂O). We placed these tubes in an orbital shaker set at 37°C and left these to grow overnight.

We inoculated 2.5µl of the culture from each of the five test tubes onto the centre of five replicate King's agar plates containing 0.5% (wt./vol.) agar (0.5% agar was used in order to promote the development of tendrils – as shown in Chapter 3) before placing these agar plates in an incubator at 37°C for 24 hours. We made these agar plates the day before and allowed them to dry for 15-20 minutes under an airflow hood before leaving them overnight at room temperature (consistent with the protocol used in Chapter 3). The next day we allowed the plates to dry for a further 10 minutes before inoculation and for a further 15 minutes after inoculation.

From each set of five inoculated agar plates, we selected the colonies with the lowest and highest tendrill scores (i.e. how many tendrils a colony exhibits – discussed later in the methodology) to create a negative selection line and a positive selection line from each initial isogenic population respectively (figure 8.1). We isolated the bacteria from the chosen plates by using a sterilised pipette tip to sample the entire leading edge of the colony (figure 8.2). We then passaged these cells into a sterile 1.5ml eppendorf containing 1ml of King's B medium. We then thoroughly vortexed these eppendorfs before inoculating a 2.5µl sample from each eppendorf onto five fresh 0.5% (wt./vol.) King's agar plates. Finally, we placed these plates in an incubator at 37°C for 24 hours.

After initial selection lines were set up on the 1st transfer, we repeated the process with the exception that we only passaged cells from the plates with the lowest tendrill scores for the negative selection lines and we only passaged cells from the plates with the highest tendrill scores for the positive selection lines. We repeated this process for 20 transfers with assays conducted (discussed later in methodology) at the 10th and 20th transfer. Note that after the 10th transfer, we considered all plates of the assay when selecting the colony for the 11th transfer.

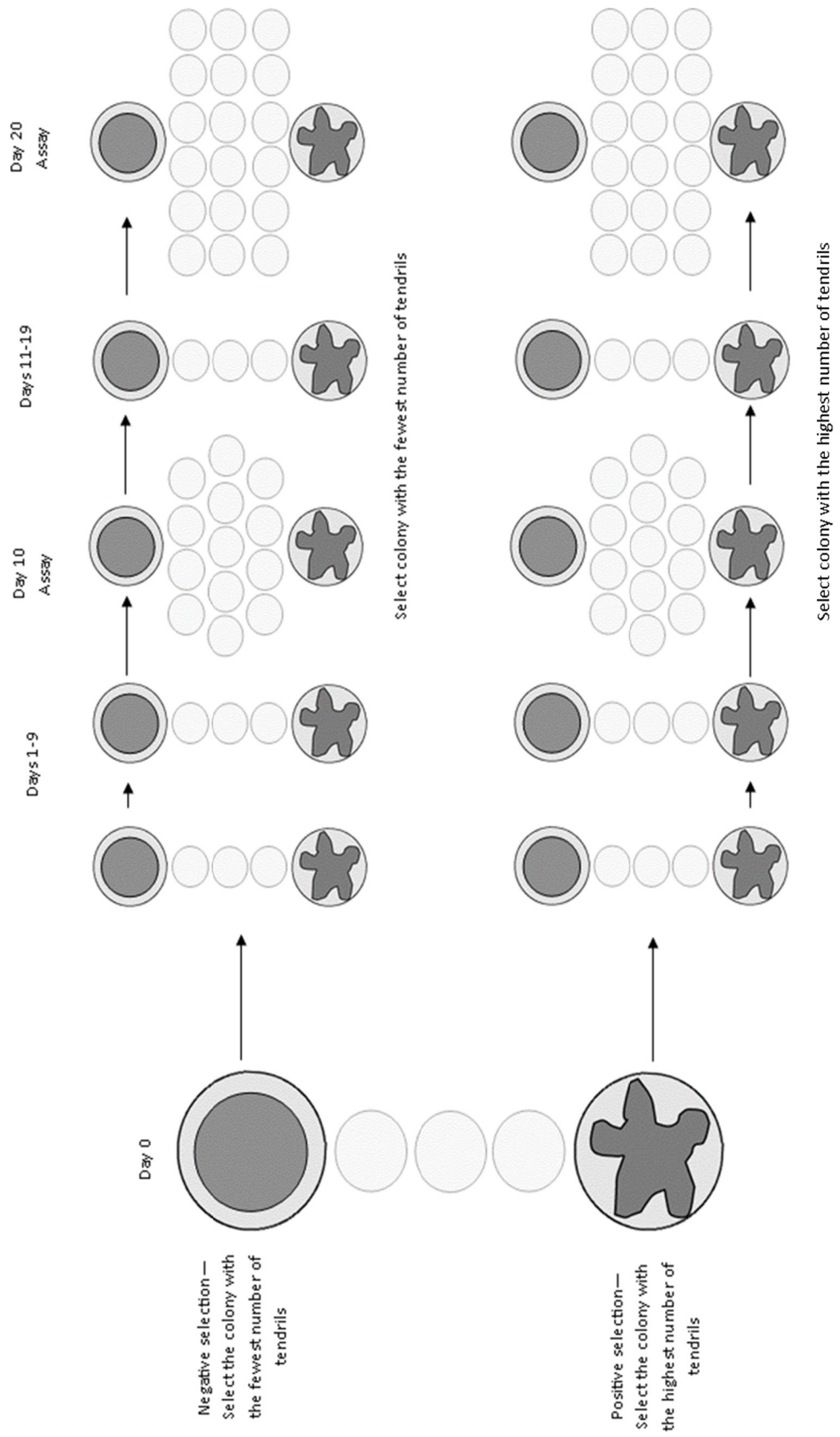


Figure 8.1: The experimental design used in experiment one. Five sets of artificial selection were setup in this experiment. Each set had a negative selection line against irregular shapes of spread and a positive selection line promoting irregular shapes of spread.

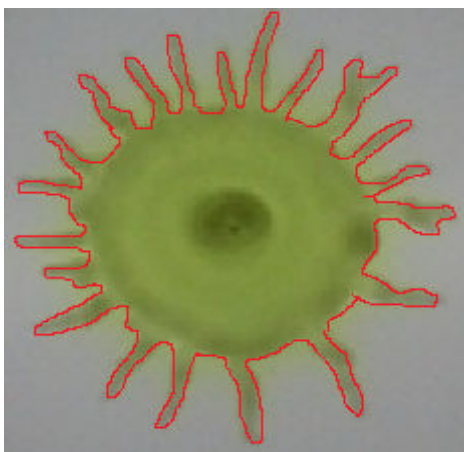


Figure 8.2: In experiment one, we sampled the area along the leading edge (as illustrated by the red line along the edge of the colony in this picture). We selected this region, as we believed those individuals situated along the leading edge of the colony are more likely to have evolved than their counterparts in the centre of the colony (Taylor and Buckling, 2011).

Experiment two: Selecting sections of the colony

As in experiment one, we cultured five isogenic populations by propagating five samples of a *Ps. aeruginosa* PAO1 frozen stock population (kept at -80°C) in separate sealed plastic test tubes containing 5ml of King's B medium (10g/l glycerol, 20g/l proteose peptone No 3, 1.5g/l $\text{K}_2\text{HPO}_4 \cdot 3\text{H}_2\text{O}$ and 1.5g/l $\text{MgSO}_4 \cdot 7\text{H}_2\text{O}$). We placed these tubes overnight in an orbital shaker set at 37°C . We inoculated $2.5\mu\text{l}$ of the culture from each of the five test tubes onto the centre of five replicate King's agar plates containing 0.5% (wt./vol.) agar (0.5% agar was used in order to promote the development of tendrils – Chapter 3) before placing them in an incubator at 37°C for 24 hours.

From each set of five inoculated agar plates, we selected the colonies with the lowest and highest tendril scores (typically how many tendrils a colony exhibits – discussed later in the methodology) to create a negative selection line and a positive selection line from each initial isogenic population respectively (figure 8.3). Instead of sampling the whole leading edge of the selected colony (as in experiment one), we took samples from four locations (figure 8.4):

1. The tip of a tendril – we defined the tip as the end of a tendril. If we observed no tendrils then we selected a point around the edge of the colony distinct from the knuckle. This was usually from a point of the

colony with the most irregularity (least circular) but not necessarily a tendril

2. The knuckle of a tendril – we defined the knuckle as a localised part of a tendril, which has higher population density than the rest of the tendril. Knuckles are observable to the naked eye by being a darker green colour than the remainder of the tendril. There may be more than one of them and they occur roughly halfway along the tendril. If no such knuckle region occurs, then we selected a point roughly halfway up a tendril. Furthermore, if we observed no tendrils, we chose the part of the leading edge of the colony with the highest observable density to represent the knuckle region.
3. The webbing between tendrils – this was defined as the area in-between either the stems of two tendrils or between the stem of one tendril and the main part of the colony. If no such point existed, then we sampled a point close to the site chosen for the tip.
4. The centre of the colony – we defined the centre as the point of inoculation

If there were multiple tendrils to select from, where possible, we chose a tendril consisting of all selection zones (tip, knuckle and webbing). We passaged each sample into a sterile 1.5ml eppendorf containing 500µl of King's B medium. We thoroughly vortexed eppendorfs before inoculating a 2.5µl sample of each eppendorf onto three fresh 0.5% (wt./vol.) King's agar plates. We then propagated these plates for 24 hours in an incubator at 37 °C.

We repeated this process for 10 transfers before conducting an assay. Note that after the 1st transfer, we only passaged cells from the plates with the lowest tendril scores for the negative selection lines and we only passaged cells from the plates with the highest tendril scores for the positive selection lines.

Because of laboratory constraints, we modified the protocol for the agar plates from experiment one. Rather than leaving the plates to rest overnight and drying them briefly the next day, we inoculated plates soon after they were poured and dried in a flow hood.

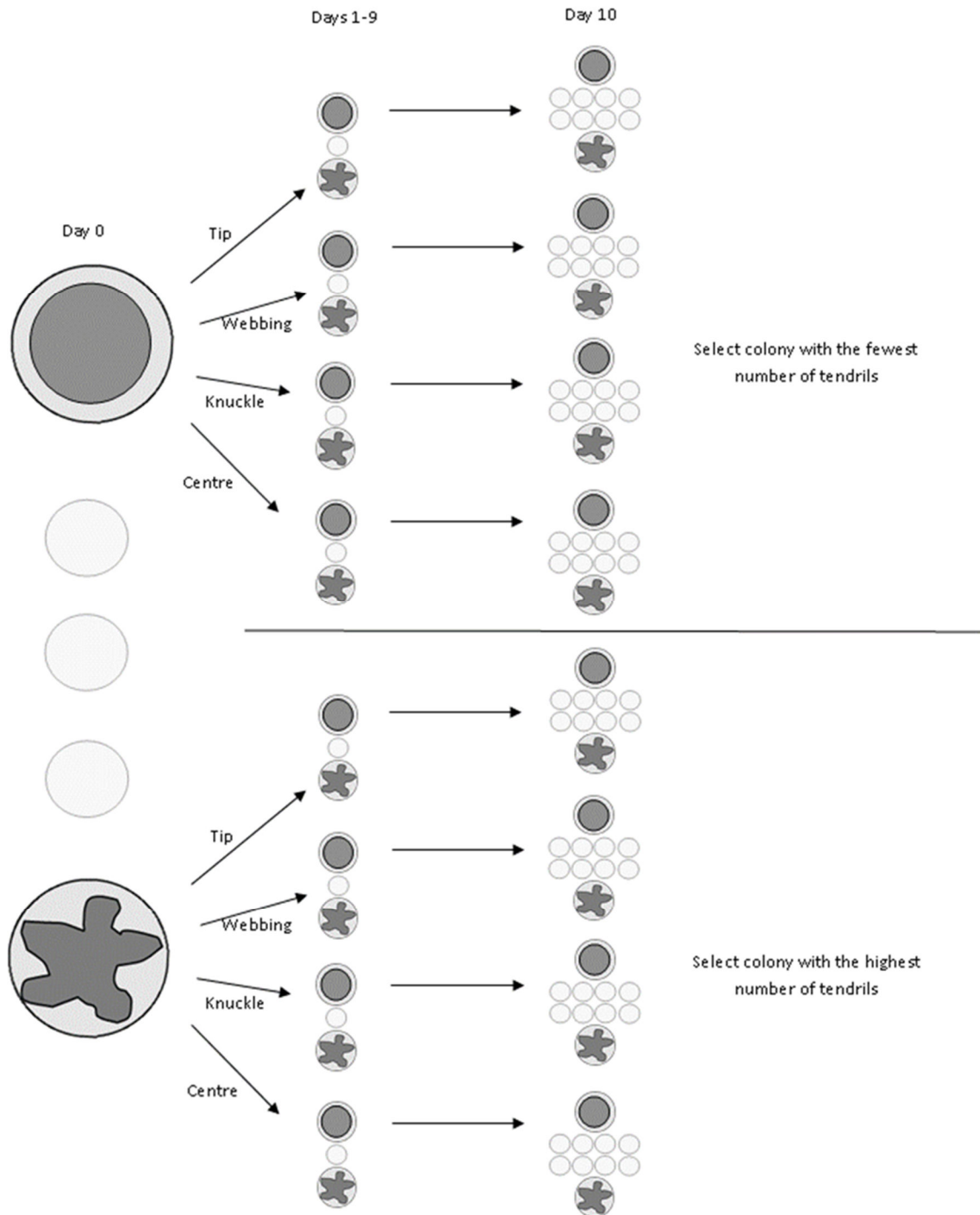


Figure 8.3: The experimental design used in experiment two. There were five sets of artificial selection in this experiment, with four sub sets of selection in each set representing the four areas sampled (webbing, tip, centre and knuckle). Each subset had a negative selection line set up against irregular shapes of spread and a positive selection line promoting irregular shapes of spread.

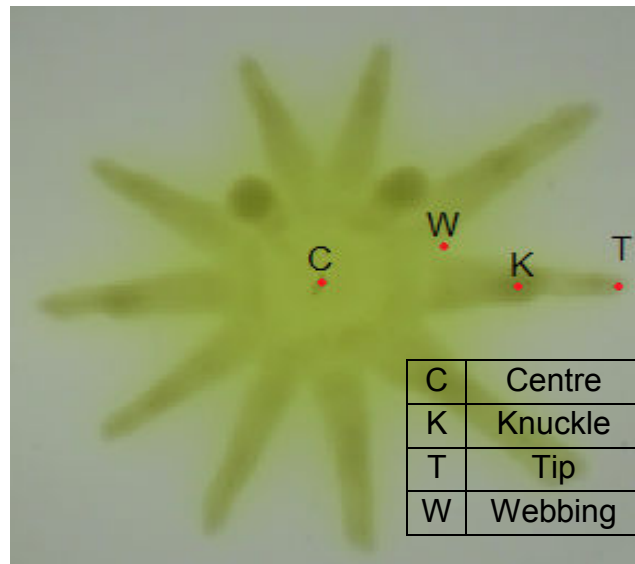


Figure 8.4: In experiment two, we sampled a chosen colony from four separate areas: the centre, a knuckle of the colony, the tip of a tendril and the webbing in-between tendrils.

Assay process

We conducted assays by inoculating 2.5µl of each sample onto multiple King's agar plates with the same protocol as that used in the experiment. For experiment one, we inoculated 15 King's agar plates for each selection line at the 10th transfer and we inoculated 20 King's agar plates for each selection line at the 20th transfer. For experiment two, we inoculated 10 King's agar plates for each selection line at the 10th transfer. We chose these numbers due to equipment and budget constraints.

Shape measurements

We used two quantifiers to measure the irregularity of a colony's spread:

1. Tendril score – This was a count of the tendrils exhibited by a colony 24 hours after inoculation. We defined tendrils as distinct formations outward from the otherwise circular leading edge of the colony. We used this measurement to decide which colony to select from at each transfer to avoid further computational processing.
2. Circularity – this was a normalised measurement using physical characteristics of the colony to quantify how irregular the shape of colony is. We calculated circularity by the following:

$$\text{Circularity} = \frac{4\pi A}{p^2}$$

Where A was the area occupied by the colony and p was the length of the colony's perimeter. We denoted a colony as a perfect circle when this value is 1 and not at all circular when this value was 0. The area and perimeter of a colonies shape of spread was calculated using the java based, standalone software ImageJ (Rasband, 2014.)

In theory, a link exists between the two measurements, with a decreased tendrill score corresponding to an increased circularity.

Results

Experiment one: Selecting the whole outer edge of the colony

Selection had no clear effect on the pattern of spread exhibited by a colony. This was true for both the tendril score measurement [Selection 10 assay: sign test, $p = 0.9688$, $n = 5$, (figures 8.5 and 8.6); Selection 20 assay: sign test, $p = 0.8125$, $n = 5$ (figures 8.5 and 8.6)] and for the circularity measurement [Selection 10 assay: Sign test, $p = 0.9688$, $n = 5$ (figures 8.5 and 8.6); Selection 20 assay: Sign test, $p = 1$, $n = 5$, (figures 8.5 and 8.6)]. We found a general decrease in circularity (and a consequential increase in tendril score) between the day 10 and day 20 assays but this was true for both negative and positive selection.

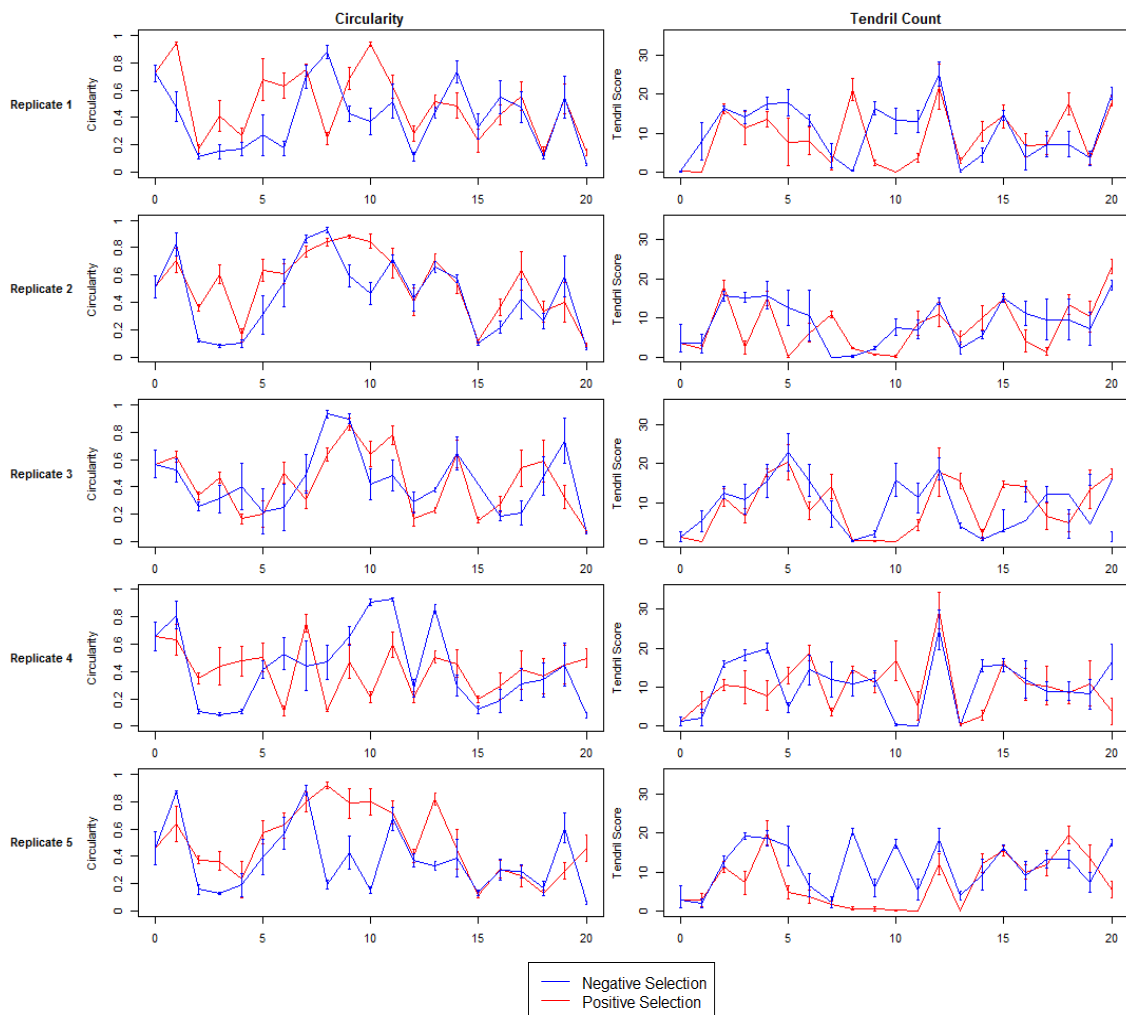


Figure 8.5: The circularity (left) and tendril score (right) measurement for each selection line through each selection point. Error bars show ± 1 SE. There was no clear pattern for those colonies undergoing either negative selection or positive selection.

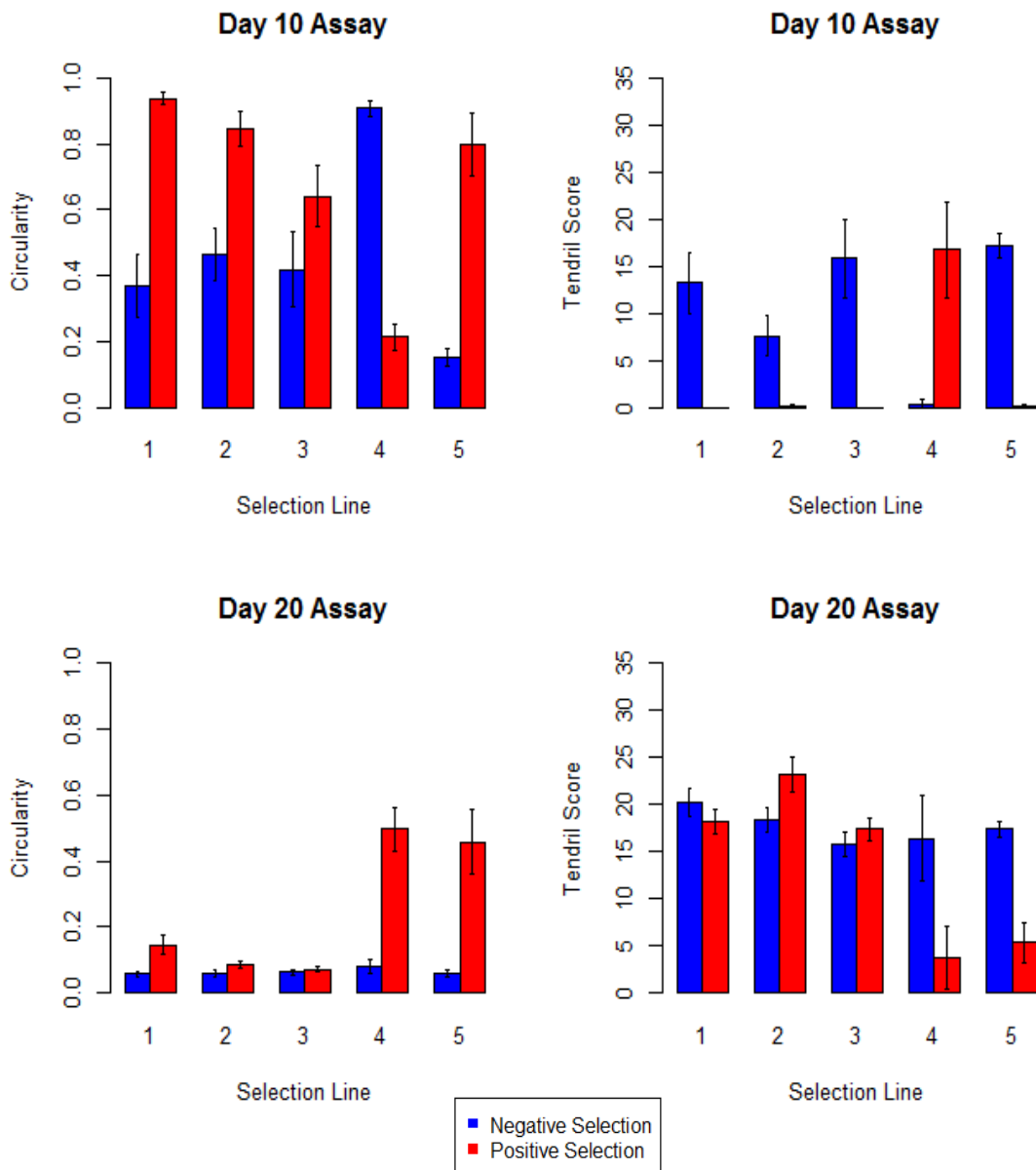


Figure 8.6: The results of the assays taken after 10 and 20 selection points for both the circularity (left) and tendril score (right) measurements. Error bars show ± 1 SE. There was no clear pattern for those colonies undergoing either negative selection or positive selection.

Experiment two: Selecting sections of the colony

For all four spatial sites, selection had no clear effect on the pattern of spread exhibited by a colony. This was true for both the tendrill score measurement [centre: sign test, $p = 0.96875$, $n = 5$ (figures 8.7 and 8.11); knuckle: sign test, $p = 0.5000$, $n = 5$ (figures 8.8 and 8.11); tip: sign test, $p = 0.5$, $n = 5$ (figures 8.9 and 8.11); webbing: sign test, $p = 0.1875$, $n = 5$, (figure 8.10 and 8.11)] and for the circularity measurement [centre: sign test, $p = 0.5$, $n = 5$ (figure 8.7 and 8.11); knuckle: sign test, $p = 0.8125$, $n = 5$ (figure 8.8 and 8.11); tip: sign test, $p = 0.1875$, $n = 5$ (figure 8.9 and 8.11); webbing: sign test, $p = 0.5$, $n = 5$ (figure 8.10 and 8.11)].

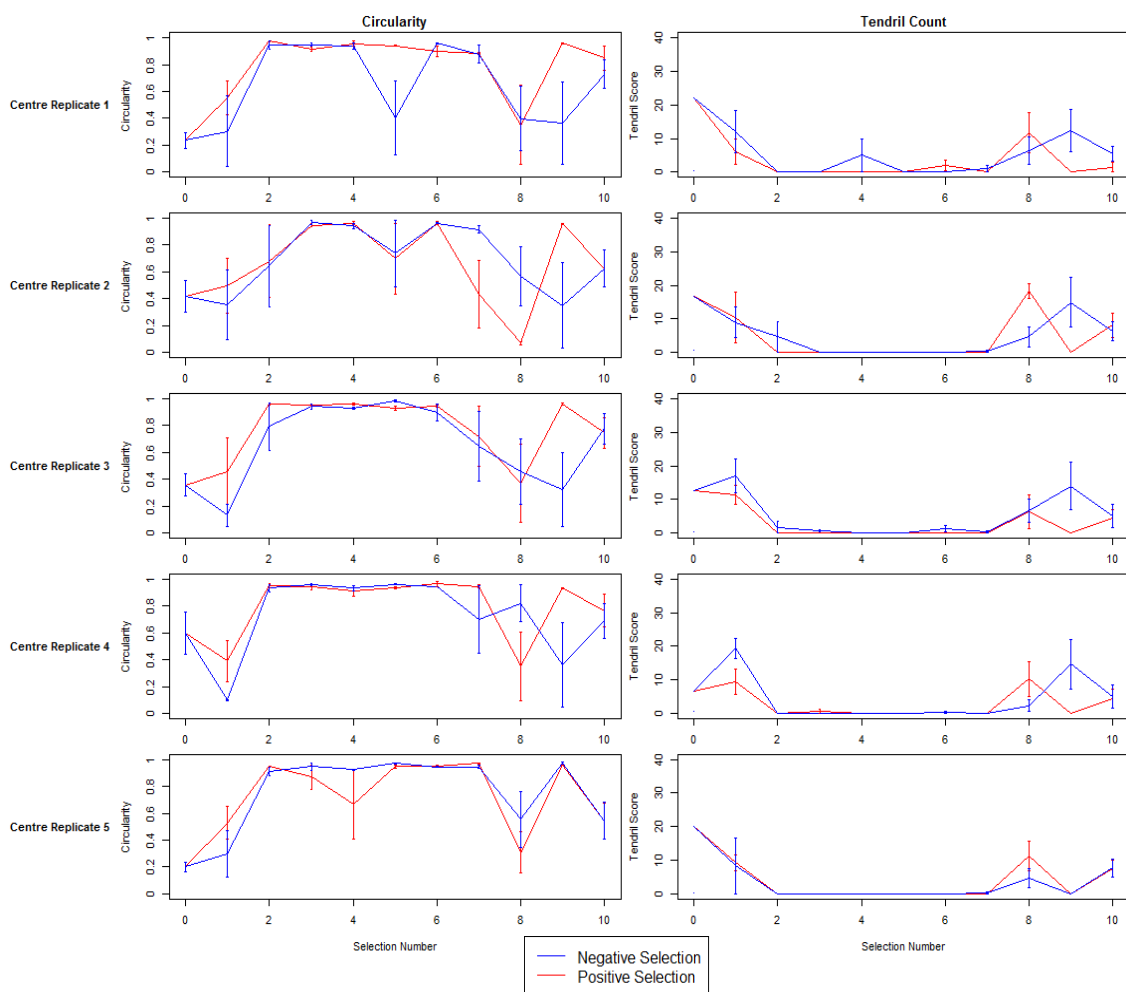


Figure 8.7: The circularity (left) and tendrill score (right) measurements at each selection point for those colonies sampled from the centre. Error bars show ± 1 SE. There was no clear pattern for those colonies undergoing either negative selection or positive selection.

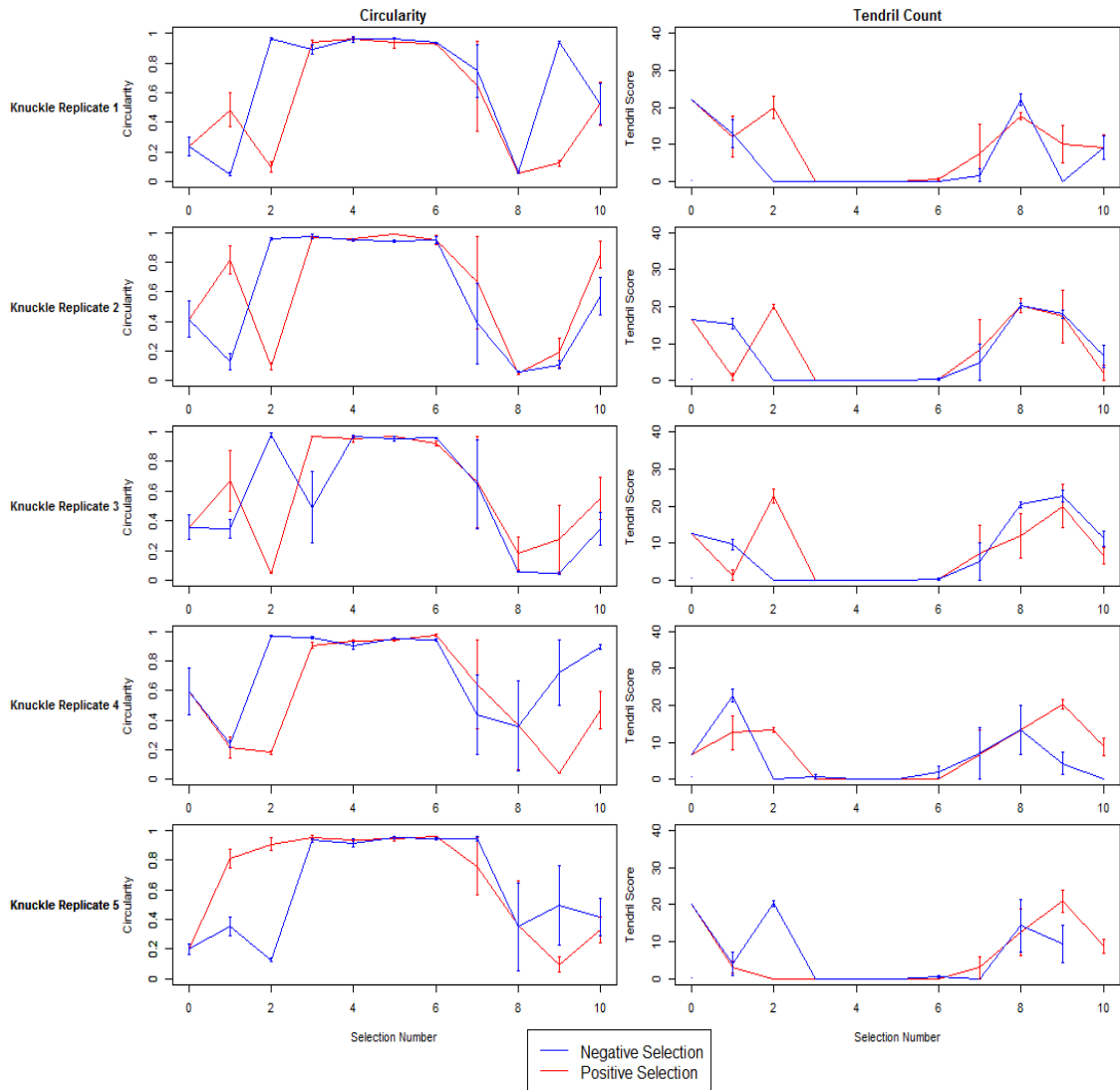


Figure 8.8: The circularity (left) and tendril score (right) measurements at each selection point for those colonies sampled from one of the knuckles of the colony. Error bars show ± 1 SE. There was no clear pattern for those colonies undergoing either negative selection or positive selection.

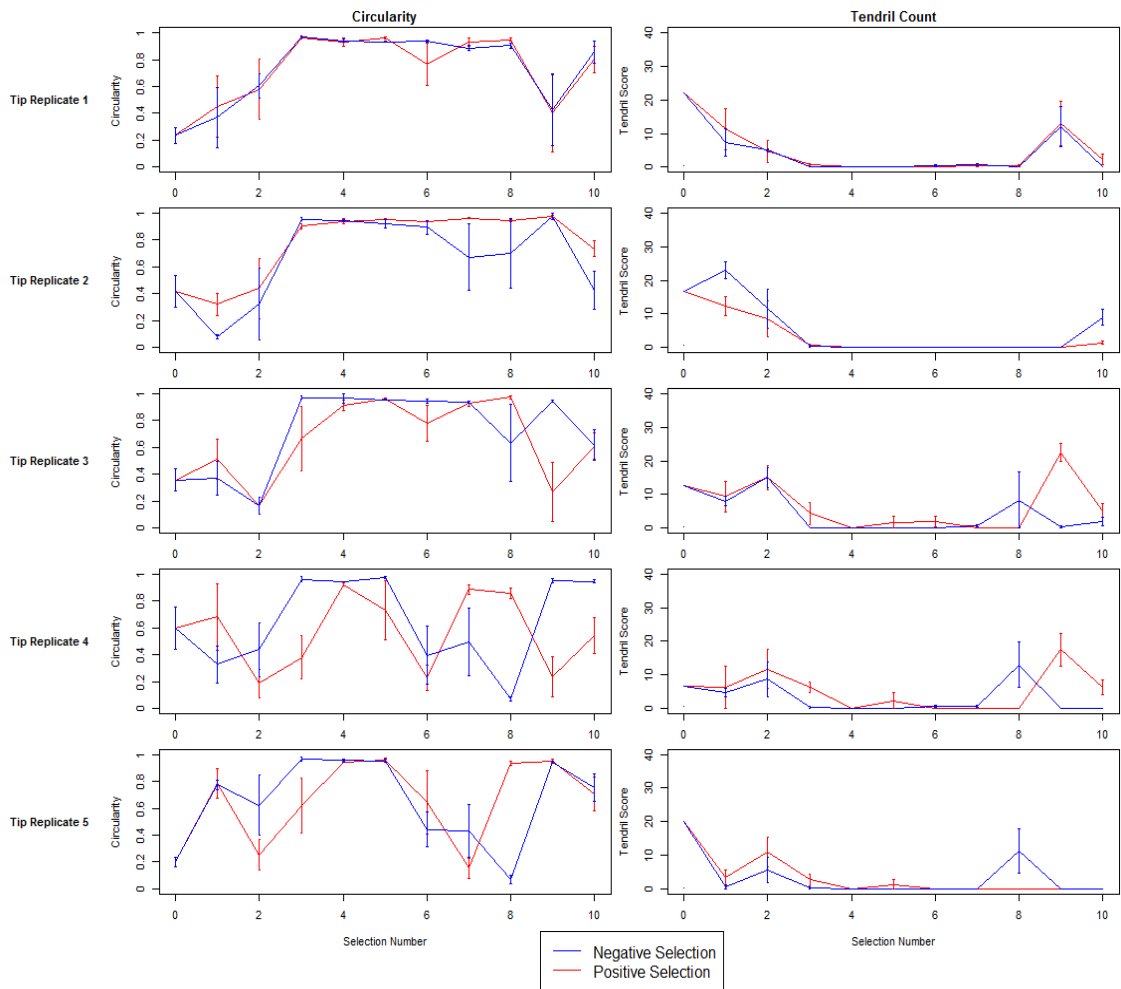


Figure 8.9: The circularity (left) and tendril score (right) measurements at each selection point for those colonies sampled from one of the tendril tips of the colony. Error bars show ± 1 SE. There was no clear pattern for those colonies undergoing either negative selection or positive selection.

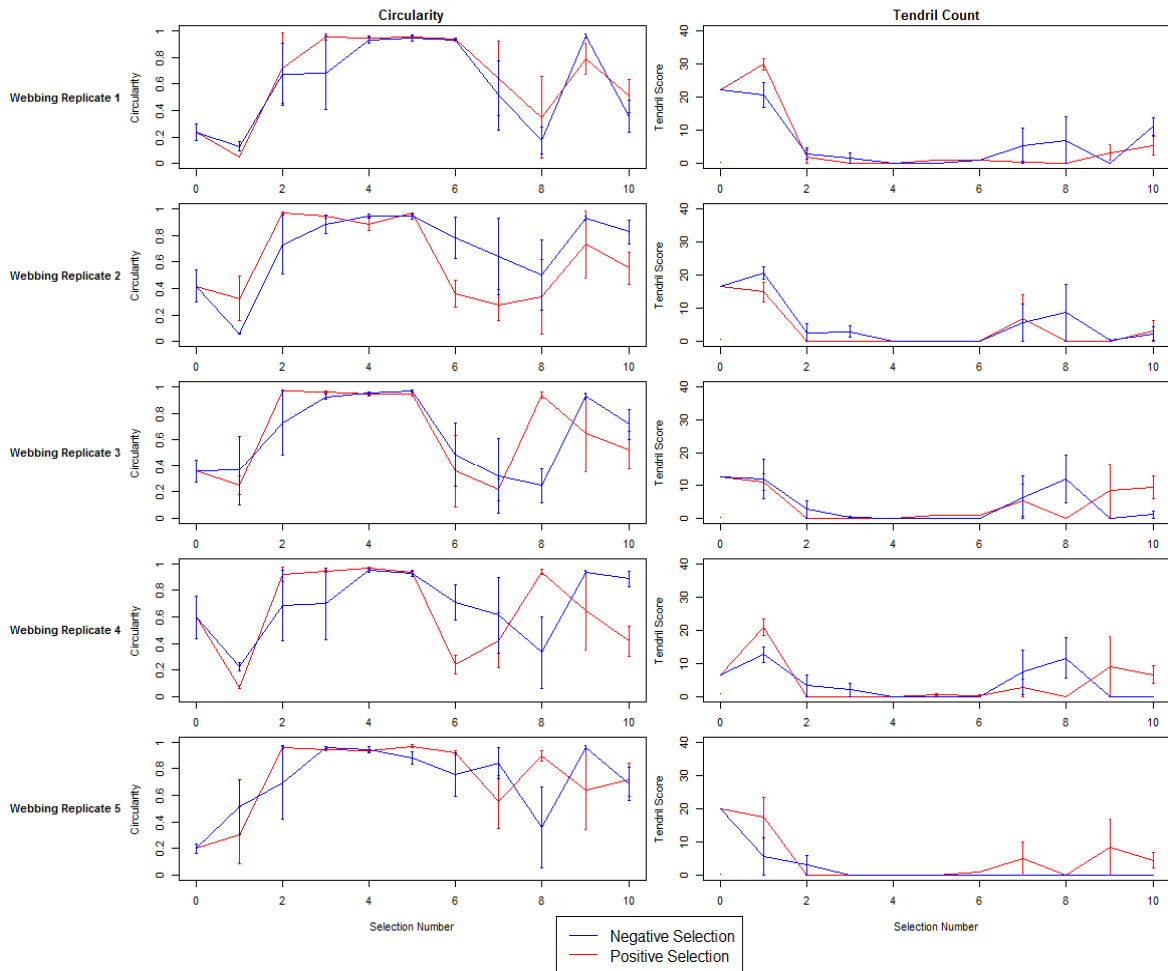


Figure 8.10: The circularity (left) and tendril score (right) measurements at each selection point for those colonies sampled from one of the webbing sites in-between tendrils of the colony. Error bars show ± 1 SE. There was no clear pattern for those colonies undergoing either negative selection or positive selection.

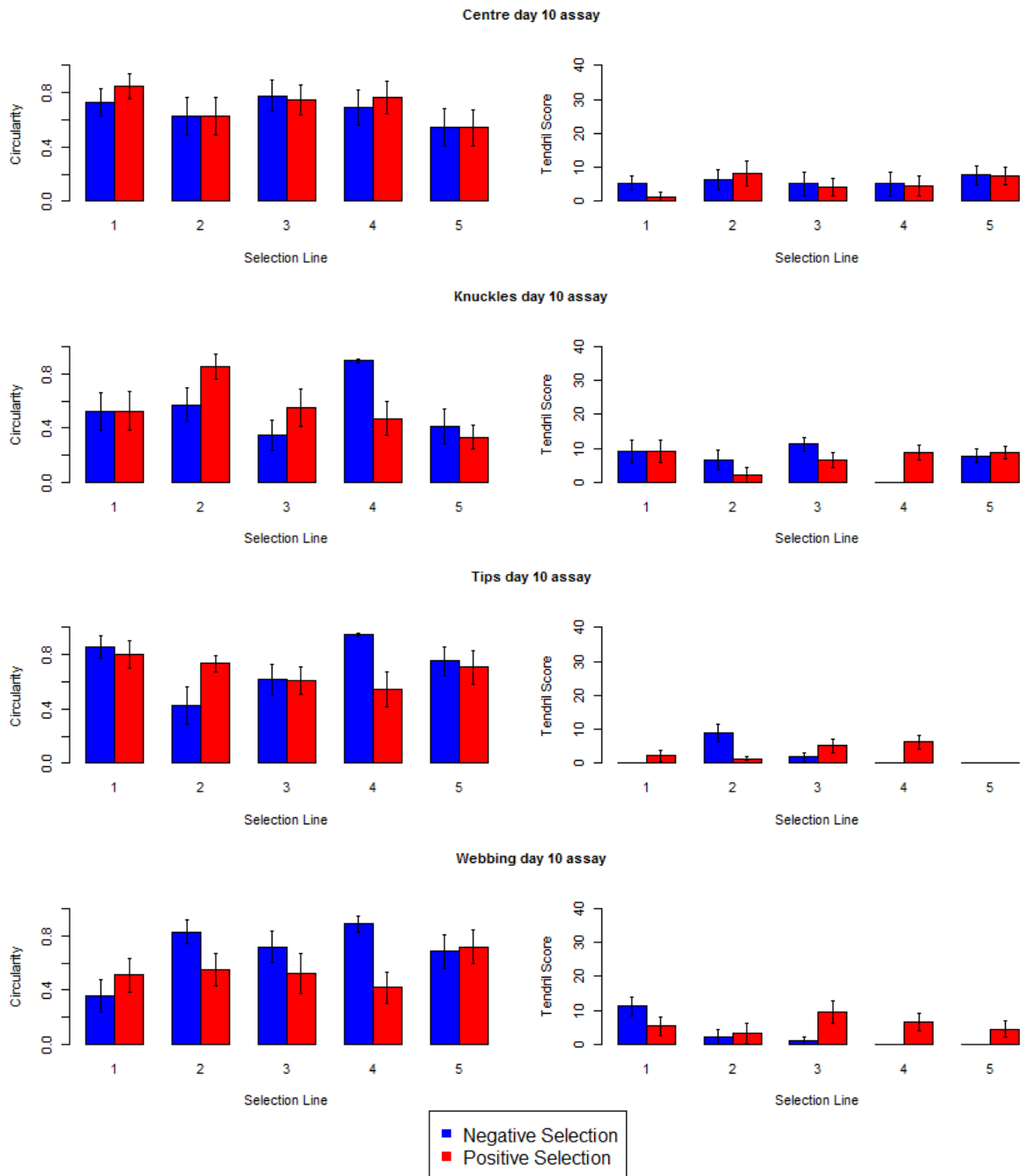


Figure 8.11: The circularity (left) and tendril score (right) measurements from the assay of the colonies after 10 selections points. Error bars show ± 1 SE. There was no clear pattern for those colonies either undergoing negative selection or positive selection.

Discussion

We have found that the pattern of spread was not amenable to artificial selection via the methodologies we have used. It was unfortunate that this experiment achieved negative results, as we intended to use the evolved strains in competition experiments. This would have allowed us to investigate whether colonies with a circular shape of spread or colonies with an irregular shape of spread achieved the higher total fitness following manipulation of scales of genetic diversity (mixed vs clonal colonies) and scales of competition for limited resources (competition within and/or between colonies), i.e. to test the results discussed in this thesis. Negative results are often difficult to interpret, but there are a number of possible explanations for these results.

First, the shape of spread may have a limited heritability between generations and/or it might be a relatively plastic trait i.e. has low stability. It is known that the swarming motility required for irregular patterns of spread is a complex process (Yeung et al., 2009, van Ditmarsch et al., 2013), requiring the individuals to exhibit both cooperative social behaviour to form rafts (Kearns, 2010) and to excrete rhamnolipids to expedite surface mobility (Taylor et al., 2013). This process requires ~200 transcriptional regulators (Yeung et al., 2009). How our methods of selection affects these transcription regulators is unknown. However, we believe our experimental design was sufficient to detect whether our methods of selection would lead to consistent evolution of these transcription regulators.

For each selection regime, we created five negative selection lines and five positive selection lines. We chose this number of selection lines such that if we had found a possible evolutionary effect, it would have been determined statistically significant whilst also staying within the strict budget of this experiment. In addition to this, we chose the length of each experiment (experiment 1 was run for 20 transfers and experiment 2 for 10 transfer) such that if selection had a clear effect, it would have been observable within the timeframe of this experiment whilst also staying within our budget. We believe this as the number of selections used in this study is similar to the number of selections used by other microbial evolution experiments (Taylor and Buckling, 2011). Indeed, a similar study conducted by (van Ditmarsch et al., 2013) since

this experiment was conducted passaged the entire colony for 10 selections (rather than distinct areas of the colony). Their study saw consistent evolution of dispersal ability within this period (although the shape of spread was not the focus of this study). Consequently, with these parameters of the experimental design in mind, we believe we would have observed a change in the shape of spread if it were selectable by the method used in this chapter. Future research could conduct genetic analysis to see which transcriptional regulators have changed in the selected strains of this study versus the ancestral strain.

An alternative explanation is that the region of each colony we selected from might not have been suitable for selection. In this study, we conducted two different selection experiments, each selecting different parts of the colony at each transfer. In the first experiment, we selected along the outer edge of the colony, as we assumed that these individuals have undergone more generations and therefore have had more time for mutations to accumulate (Taylor and Buckling, 2011). However, by selecting along the whole edge, we were assuming that all individuals along the outer edge of the colony have evolved the same mutations. With resource and population densities varying through space, this may not be the case, as the selection pressures for those individuals at the tip of the tendril are likely to be different from the selection pressures experienced by individuals situated in-between tendrils.

Consequently, at each transfer, by sampling the entire outer edge of the colony, we were possibly competing individuals with different mutations (i.e. those at the tip versus those in-between tendrils) against each other. Moreover, due to the higher density of individuals in-between tendrils than at the tips, it was likely that we selected more individuals from in-between tendrils than at the tips of tendrils. These confounding factors may have influenced our method of selection (e.g. by biasing the system towards individual-level fitness) and thus affecting the shape of spread (Chapter 4).

In the second experiment, we attempted to address these issues by selecting from certain spatial points of the colony, namely, the centre, the webbing, the knuckles and the tips of the tendrils. For each of these selection lines, we found negative results with no clear selection occurring. For all selection lines in this experiment, we noticed that between selection points 3 and 8, very few (if any) tendrils occurred. We suspect there are a number of reasons for this. First, in

comparison to the first experiment, we selected fewer individuals from the colony at each transfer. To compensate for this, we reduced the dilution each transfer, by reducing the amount of medium in the eppendorf. However, the rate of spread is explicitly linked to the cell density (Taylor and Buckling, 2011). Consequently, the 24 hours given to each colony to spread across the agar plate was maybe not sufficient enough for the colony to escape the bacterial growth lag phase (Kearns, 2010) and therefore not long enough for tendrill formation. Secondly, we altered the protocol used to produce the agar plates. Rather than allowing plates to settle overnight, we used the plates on the same day as they we made them. We made this modification to the protocol because of the increased production of agar plates required in experiment 2 and the limited resources available at the time of the experiment. However, (Tremblay and Deziel, 2008) show that swarm assay plates are highly dependent upon a range of factors including the drying time of the agar. In hindsight, we would not have adjusted the protocol but due to limitations in our budget, we are unable to conduct a repeat. Alternatively, the consistent lack of tendrills during the timescale of our experiment (i.e. between the 3rd and 8th selection point) might be indicative of the colony in the system evolving other characteristics (traits such as biofilm formation which is a crucial group-level trait offering protection from adverse circumstances (van Ditmarsch et al., 2013, López et al., 2010)) in reaction to the selection process, even if the number of tendrills was not necessarily a heritable trait. To ascertain whether this is the case, further research should look to repeat this experiment without the methodological issues discussed here and sequence the evolved strains to identify whether our selection regime affected any other traits of the population.

Future experiments may wish to diverge from the artificial selection experiments conducted here and focus upon genetic modifications to create colonies deficient in their pattern of spread. For instance, (Kearns and Losick, 2003) found laboratory strains had lost their ability to swarm (and thereby lost their ability to produce irregular patterns of spread) due to the accumulation of multiple genetic defects during their time growing in an environment void of their natural predators. Such an approach would enable researchers to conduct competition experiments between irregular and regular shaped colonies, in order to observe which shape of spread has the highest competitive ability.

However, this approach would need to quantify whether the effect on fitness is due to the shape or due to a defect in another attribute arising from the genetic modification.

In conclusion, our results suggest the shape of spread, an important foraging trait of a colony, is not an artificially selectable trait. However, due to the possible complications with the methodology used in these experiments, we require more research to rule out the evolution of traits at the group-level i.e. the shape of the colony. Furthermore, empirical research via competition experiments is required to empirically ascertain whether those colonies with an irregular shape of spread gain an ecological advantage over colonies with a circular shape of spread. Particularly as based on the previous results in this thesis, we believe it remains likely that the patterns of spatial spread exhibited by microbial population and the strategies responsible for them, have evolved over time and potentially will continue to evolve.

Chapter 9

General Discussion

The spread of invasive species is a key issue in ecology due to their potentially adverse effect upon the quality of habitats, the biodiversity of ecosystems and the services these ecosystems provide (D'Antonio et al., 2004). Indeed, ignoring the threat of invasive species can result in a severe impact on the long-term health of populations and lead to various socio-economic problems (Mack et al., 2000, Pimentel et al., 2000). For example, the accidental introduction and subsequent invasion of the venomous brown tree snake (*Boiga irregularis*) across Guam has led to significant declines in dozens of native bird, mammal and lizard populations. This has caused the extinction of 10 out of the 13 species of forest birds originally native to Guam (Pimentel et al., 2005).

Moreover, due to the power outages caused by these snakes, combined with the medical cost of dealing with snakebite victims and the cost of trying to control their spread, the cost to regional governments is in the region of \$12 million per year (Holt, 1998). Because of the severe impact of invasive species, their threat is widely acknowledged in society, to the extent that one of the UN's eight millennium goals aims to ensure the health of worldwide ecosystems via the control of invasive species (Pimentel et al., 2000). To help control invasive species within the confines of our limited resources, conservation managers and researchers recognise that we require a detailed understanding of the factors driving the spread of populations across environments (Mack et al., 2000, Pimentel et al., 2000).

Populations spread across environments to escape density/environmental dependent factors associated with low fitness i.e. factors such as scarce food availability, kin competition and habitat loss (Mack et al., 2000). However measuring the spread of populations is a difficult task, due to deficiencies with the methods used to capture spread data in macro-organism populations (Cumming, 2002, Kokko and Lopez-Sepulcre, 2006). Because of recent evidence showing that many of the ecological and evolutionary processes influencing the dynamics of microbial populations also influence macrobial populations, we speculate that many of the inherent processes driving the spatial spread of microorganism populations across agar plates scale up to be relevant to populations consisting of macroorganisms (Jessup et al., 2004,

Buckling et al., 2009). However, researchers have yet to fully exploit the microbial model system in spatial ecology for this purpose. Consequently, to help improve our understanding of how populations spread, the work in this thesis has attempted to examine the spread of microbial populations on two-dimensional agar plate surfaces in the context of the spatial ecology of general populations. Moreover, this work has aimed to highlight and promote microorganisms as a model system in spatial ecology, in order to help future research and to help inspire new ideas and questions. In order to achieve this, we have utilised a mixture of empirical, analytical and simulation approaches throughout this thesis. The following section discusses the overall findings of this thesis, synthesises the results of the thesis together with respect to current knowledge and discusses the implications of these results before highlighting areas for future research.

A general overview of our findings, their broader context and their contributions to our understanding

Mathematical models are key tools in ecology because of their ability to recreate the dynamics behind natural systems, subsequently allowing researchers to identify the key factors responsible for these dynamics. In classical spatial ecology, the modelling approaches used to represent the spread of a population traditionally involve the use of reaction-diffusion equations with relatively simple underlying assumptions (Kot et al., 1996). One of the main predictions of these classical reaction-diffusion models is a linear relationship between the radius of the population and time (i.e. a constant radial rate of spread) (Liebhold and Tobin, 2008). While this relationship agreed with the evidence available to researchers at the time of the conception of these models, recent empirical evidence has observed many populations spreading at a non-constant radial rate of spread. This casts doubt about the assumptions made by these classical reaction-diffusion models (Hastings et al., 2005, Clark et al., 2001). Ignoring the possibility of non-constant radial rates of spread (in particular accelerating radial rates of spread) in our predictive models can reduce the effectiveness of conservation methods reliant on these models, thus increasing the invasive species' likelihood of establishment (Liebhold et al., 1992, Andow et al., 1990, Neubert and Caswell, 2000, Kokko and Lopez-Sepulcre, 2006, Hastings et al., 2005). Consequently, in order to help improve

our predictive models, we established that we require more empirical studies to improve our understanding of the factors affecting the rate of population spread. However, this data can be difficult to collect at a high resolution for macro-organism populations (Kokko and Lopez-Sepulcre, 2006). These findings, combined with our speculation that many of the processes affecting the spread of microorganism populations also affect the spread of macroorganism populations, provided us with the motivation behind Chapter 2.

We used the *Pseudomonas fluorescens* microbial model system in Chapter 2 to conduct a novel large-scale investigation into the radial rate of spread of microbial populations on agar plate surfaces. This investigation aimed to test whether the measured rates of microbial spatial spread, across a number of microbial morphologies and types of surface environment, agreed with the constant radial rate of spread prediction of the classical reaction-diffusion equations. The key finding of this study was that whilst the constant radial rate of spread prediction was correct for many cases, it was not for many others, with both intrinsic (morphology) and extrinsic (agar concentration) factors significantly affecting the reliability of the constant rate of spread prediction for microbial *Ps. fluorescens* populations. This was a finding not reported in the microbiology literature. While there is some possibility that the experiment does not allow the colonies to reach their full rate of spread, these results highlight that non-constant rates of population spatial spread are a real phenomenon, adding to the current discourse found in other empirical studies (Hastings et al., 2005, Travis et al., 2009, Perkins et al., 2013, Perkins, 2012). Utilising the microbial model system in this novel way contributes further evidence that researchers should treat the assumptions made by the classical ecological models of spatial spread that exclusively predict constant rates of spatial spread with caution and highly scrutinise their justification before their application. This is to ensure the basis of our predictive models (which inform our conservation management strategies) is accurate and representative of the processes responsible for invasive population spread. This is particularly important in light of the increasing evidence suggesting the exhibition of non-constant rates of population spread by invasive populations (Hastings et al., 2005, Travis et al., 2009, Perkins et al., 2013, Perkins, 2012).

In Chapter 2, there was clear evidence of intrinsic and extrinsic factors affecting whether a *Ps. fluorescens* population exhibits a non-constant or constant radial rate of spread. We particularly noted the exhibition of an accelerating rate of spread by the *Ps. fluorescens* WS morphology when grown in a soft agar environment. We suspected this was due to the WS morphology colonies adapting their ecological traits (reproduction rates and thus dispersal rates) to improve their ability to persist on the agar plate environment (Spiers, 2007). Intrinsic and extrinsic factors are widely acknowledged to affect the rate of population spread, potentially leading to accelerating rates of spread (as in our results), but these can be difficult to clearly measure in macro-organism empirical systems without requiring researchers to account for uncontrollable factors such as seasonal climate heterogeneity and therefore evidence is still relatively limited (Travis et al., 2009, Perkins et al., 2013, Perkins, 2012, Phillips et al., 2008). Due to the clear effect of intrinsic and extrinsic factors on our results, we suggest that researchers should especially examine the assumptions made by the classic spatial ecology models relating to how intrinsic adaptation and extrinsic environmental factors affect these ecological traits and their subsequent consequences on the rate of spread. This is because in their formulation, these models assume intrinsic homogeneity in these ecological traits throughout the population with no ability for these parameters to adapt through time according to environmental conditions (Hastings et al., 2005, Clark et al., 2001). Moreover, our results in Chapter 2 highlight that the microbial model system might be an appropriate tool to test these assumptions, although we note that different organisms have been observed to respond in different ways to different combinations of intrinsic/extrinsic factors and therefore the links between micro- and macroorganisms will need to be established (Beale and Lennon, 2012, Phillips et al., 2010).

In the literature, an often-overlooked factor with regard to the spatial dynamics of populations is the shape of the population spread as it colonises the environment (Misevic et al., 2015). We speculate this is due to the difficulty of collecting the high-resolution data needed to accurately record the shape of population spread at a global level (Cumming, 2002, Kokko and Lopez-Sepulcre, 2006). Microbial populations can exhibit a wide array of readily

observable and capturable shapes of spread during their colonisation of agar plate environments (Kearns, 2010), thus making them a robust solution to the problem of collecting high resolution data for these shapes of spread. A relationship found in Chapter 2 was that those colonies of the *Ps. fluorescens* WS morphology which consistently exhibited accelerating radial rates of spread when grown on a soft agar plate environment also exhibited the largest decrease in its circularity from the point of inoculation (i.e. the shape of population spread became more irregular through time) compared to other colonies. This result is evidence of a possible link between the shape of spread and the rate of spread, with accelerating rates of spatial spread seemingly related to irregular shapes of spatial spread. Researchers to date have typically focused upon the ecological, evolutionary and human induced causes for accelerating rates of spread (Wilson et al., 2010, Travis et al., 2009, Phillips et al., 2010), thereby ignoring the possible effects stemming from the global shape of the population, which has only recently begun to be recognised (Misevic et al., 2015). Although we require more research to establish this link for a range of populations (as this could just be strain/organism dependent), our study is some of the first possible empirical evidence for this relationship. Because of the lack of appreciation for the shape of population spread in the literature, we used this unique observation to form the basis for the remainder of the thesis.

A number of microbial populations exhibit a wide variety of patterns (shapes) of spread as they colonise agar plate environments (Fujikawa and Matsushita, 1989, Ben-Jacob et al., 1998). Extrinsic environmental factors such as agar concentration (viscosity) and peptone (food) concentration are known to affect the shape of spatial spread exhibited by some microbial strains, e.g. the *Bacillus subtilis* microbial system (Fujikawa and Matsushita, 1989). But we recognised that there was a general lack of knowledge in the literature reporting the effect of these extrinsic factors upon the shape of spread exhibited by *Pseudomonas aeruginosa* strain PAO1 populations, in particular whether there was an interaction between these two parameters upon the shape of spread. To test whether the *Ps. aeruginosa* model system agreed with the observed effect of environmental factors seen in other microbial model systems, our investigation in Chapter 3 tested how agar concentration and peptone concentration affected the shape of *Ps. aeruginosa* strain PAO1 microbial

spread across agar plate surfaces. This was in order to improve our knowledge of the conditions affecting the shape of spread in *Ps. aeruginosa* populations as well as to ascertain whether there was consistency between the observations from the *Ps. aeruginosa* model system and the observations from these other microbial strains/species.

Our findings were that relatively low viscosity, relatively high food environments promoted the exhibition of irregular, non-circular patterns of spread in the *Ps. aeruginosa* strain PAO1 microbial model system. Moreover, we found an interaction between agar concentration (viscosity) and peptone (food) concentration, with populations in environments with increased viscosity, seemingly requiring more food to exhibit irregular patterns of spread. These results confirm the findings relating to environmental viscosity in studies of other microbial model systems, i.e. that relatively low agar concentration environments are required for the swarming motility responsible for the exhibition of irregular patterns of spread (Kearns, 2010). However, the results of this study highlight that the effect of food abundance on the spatial spread of a microbial population is specific to each strain or species of bacteria. Indeed, for *Ps. aeruginosa* strain PAO1 we found that irregular patterns of microbial spread best occurred in relatively high food environments in contrast to the relatively low food environments required for the exhibition of irregular patterns for other microbial species. Many of the models in the literature designed to recreate the patterns of microbial spread in these other microbial strains assume nutrient limited environments in order to recreate irregular patterns of spread (Golding et al., 1998, Marrocco et al., 2010). However, we challenge the general assumption that exotic shapes of spread only occur in food-limited environments: in *Ps. aeruginosa*, we found exotic shapes were more prevalent in relatively high-nutrient conditions.

Researchers have generally considered the shape of the population an emergent consequence of the landscape and the spatial distribution of resources (Nash et al., 1995, Agassiz et al., 1994). However, due to the diversity of patterns of spread exhibited by different microbial populations when spreading across different environmental conditions, the results of Chapter 3 suggest there is much more to the shape of spread than just the constraints of landscape topology and food availability in difficult environments. In

evolutionary ecology, there is growing interest of the possibility that evolutionary selection can act at various scales of organisation (Griffin et al., 2004, de Vargas Roditi et al., 2013). Given that expanding populations have different shapes of spread, and might compete for limited space with other invading populations, consisting of different genotypes or species, we believe there may be some role for optimal shapes of spread at the population (group) level. This is especially likely in bacteria, an ideal system to study evolutionary ecology (Buckling et al., 2009, Jessup et al., 2004), whose biofilms often arise from single founder cells and are therefore genetically quite uniform and highly related (West et al., 2007a). This forges a link between individual-level selection and group-level selection (Griffin et al., 2004). Thus, in order to understand the factors affecting and affected by the shape of spread, we believed the evolutionary implications across multiple-levels of selection of these shapes of spread was an important factor requiring further investigation.

We made the observation from Chapter 3 that during the spatial spread of *Ps. aeruginosa*, individuals within the population produce siderophores (a public good) which diffuse past the leading edge of the colony thereby enabling individuals within the population to sequester iron from the surrounding environment (Griffin et al., 2004). Based on this observation, we used a geometric model combined with a multi-level selection framework in Chapter 4 to discover that the shape of spread affects the ability of the colony to sequester resources across many scales, thereby affecting the balance of selection in the system. Specifically, an irregular pattern of spread maximised the group-level of fitness at the expense of the individual-level of fitness (individual-level of fitness was defined in this study as those individuals along the edge of the population). We found that this result occurred due to the perimeter of the colony (i.e. the number of individuals along the leading edge) increasing proportionally more than the area sequestered by the siderophore halo. We found the converse was also true, i.e. a circular pattern of spread maximised the individual-level of fitness at the expense of the group-level of fitness. This agrees with other findings which suggest that the swarming motility mechanism responsible for irregular shapes of spread in microbial populations (and its consequential spatial expansion and thus carrying capacity advantage due to covering more total area) is typically exhibited in systems favouring group-level fitness (de

Vargas Roditi et al., 2013). We also found that our results held in a variety of theoretical environments (albeit with limited heterogeneity). Consequently, we believe that when a colony is in the presence of other colonies, it should exhibit irregular shaped patterns to outcompete them via maximising group-level fitness, but in the absence of external competition, the colony should instead exhibit circular patterns in order to maximise individual-level fitness. The limited empirical evidence in the literature agrees with this key result, with some wild type *Ps. aeruginosa* microbial strains losing their distinctive tendrill patterns of spread as they became acclimatised to laboratory environments, which lack the competitors commonplace in their natural environment (van Ditmarsch et al., 2013, Kearns and Losick, 2003). However, this requires further investigation using competition experiments.

We speculate that this result could have implications with regard to the conservation effort against invasive species. For example, if a link exists between irregular shapes of spread and accelerating rates of spread, then in the absence of global competition, a population might be less likely to exhibit an accelerating rate of spread as they traverse across environments due to the lack of external fitness pressures promoting a regular circular shape of spread. Indeed, by manipulating the shape of spread through the usage of corridors, we suggest that conservation managers maybe be unintentionally affecting evolution of the population across multiple-levels of selection, which may have unexpected consequences (Resasco et al., 2014). Because of the increasing evidence that evolutionary processes are a cause of accelerating rates of spread (Travis et al., 2009, Perkins et al., 2013, Perkins, 2012, Phillips et al., 2008), our theoretical results suggest that the shape of spread is an aspect that should be investigated further to ascertain how it could affect the evolution of processes related to the rate of spread.

There is a growing recognition that the global structuring of populations can be an emergent property arising from localised interactions between individuals (Nadell et al., 2010). The finding in Chapter 4 that the shape of spread affected individual-level fitness along the leading edge, suggested that the shape of spread affects the interactions between these individuals (de Vargas Roditi et al., 2013). These interactions subsequently affect the competition between these individuals and so depending on the selective pressures in the system,

we theorised this might cause mechanisms and traits at the individual level to develop in response (Hibbing et al., 2010). We speculated that these developed traits might themselves then feedback upon the shape of spread i.e. localised interactions affecting the global structural shape of the population.

Consequently, we turned our attention towards this possibility and focused on individual-level selection along the population wave front in order to understand how this might give rise to different shapes of spread. We particularly focused on these individuals on the wave front due to their access to a unique spatial region without conspecifics (through which it can invade (Phillips, 2009)), and because of our thesis' focus on microbial populations, in which those individuals along the frontier are thought to be those most important for driving the shape of spread (Nadell et al., 2010, Du et al., 2011, Kearns, 2010).

As previously discussed, studies have frequently used reaction-diffusion equations to recreate the spread of populations. A factor known to affect the spatial spread predictions of these equations in two or more dimensions is the curvature of the travelling front of the population (Volpert and Petrovskii, 2009). By considering individual-level competition along the leading edge in a unique geometric model, Chapter 5 established that as an initially circular population expanded across an environment, the curvature of the population's leading edge decreased, matching the widely known mathematical relationship (Volpert and Petrovskii, 2009). Subsequently, this change in curvature increased the exposure of the feeding neighbourhoods of individuals along the leading edge to the feeding neighbourhoods of their neighbours, thereby causing competition to intensify between individuals for the non-sequestered resources outside of the confines of the population. Such a factor has ecological implications, with increased competition known to drive adaptation, resulting in the development of new mechanisms (such as dispersal) either to outcompete other individuals for resources or to alleviate competition with other nearby individuals (May and Hamilton, 1977, Ronce, 2007). We speculate that this observation may explain the delay before initially circular microbial populations exhibit irregular patterns of spread (Kearns, 2010).

Based on this novel observation in Chapter 5 and due to the association between increased dispersal and the irregular patterns of spread exhibited by microbial populations (i.e. these irregular patterns require investment into

dispersal (Hamze et al., 2011)), we explored what happens between individuals along the population's leading edge when mechanisms leading to increased dispersal develop in order to alleviate competition (Taylor and Buckling, 2010, Kubisch et al., 2013, Ronce, 2007). By integrating dispersal into the system formulated in Chapter 5, Chapter 6 showed that the process of dispersal affects the social behaviour between neighbouring individuals situated on the leading edge of the population, consequently leading to an evolutionary game between these individuals, with the evolutionary dilemma of whether to stay or to disperse. Whether this social behaviour was beneficial for the actively dispersing individual or its neighbours on the leading edge seemingly depended on the distance dispersed and the cost of dispersal, as well as the curvature of the leading edge (i.e. Chapter 5).

A key result from our analysis of the evolutionary game outlined in Chapter 6 was that for two neighbouring individuals along the population leading edge, their total combined fitness (our measurement of group fitness for individuals along the leading edge) peaked in situations where both individuals obtain a fitness benefit. From this, we found that when the population was small (i.e. populations during their initial stages of spread), the peak combined and individual fitness for these two individuals was obtained when the individuals both moved the same distance as each other, i.e. when dispersal strategies were uniform along the leading edge. As the population expanded and competition along the population frontier intensified due to curvature-driven competition (Chapter 5), at a critical point, peak combined (group) fitness was obtained when neighbouring individuals employed different strategies, such that they moved different dispersal distances from each other. We speculate that this situation encourages the development of irregular patterns of spatial spread (such as those observed in Chapter 3) and an increase to the rate of spread, due to the development of the dispersal mechanisms required for the differential phenotypes in this scenario. Because of the required investment into dispersal and the findings in the literature (described in Chapter 4), whether the parameters of these dispersal strategies in this evolutionary game maximise combined (group) fitness or individual fitness depends upon the relative strength of local (individual) versus global (group/colony) selection and the level of relatedness between individuals along the leading edge (Griffin et al., 2004,

West et al., 2006b). Subsequently, these results show that geometric characteristics of the population affect the interactions between individuals along the leading edge of the population, thereby influencing social behaviour between these individuals.

While studies have investigated the social behaviour within a population in a spatial context, either via the use of lattice models or relatively simple model organisms, these studies typically do not account for the population's shape of spread (Misevic et al., 2015, Van Dyken et al., 2013, Lion and Baalen, 2008). Our results in Chapters 5 and 6 are a unique report suggesting that the geometric characteristics of the shape of spread affect the social behaviour of individuals within a population, particularly those individuals situated along the leading edge. Consequently, we require further study to ascertain the extent these geometric factors affect this evolutionary game described in Chapter 6 and how this itself might feedback upon the shape of spread. Moreover, our results suggest that future models studying social behaviour in a spatial context should give more consideration towards the effect of the shape of the population.

To ascertain whether the evolutionary game described in Chapter 6 could give rise to irregular shapes of spread, we integrated the geometric framework of Chapters 5 and 6 into an individual-based model (IBM) in Chapter 7 with a number of simple life-cycle rules. The results of the IBM showed that irregular patterns of spread, such as those seen in microbial populations (Chapter 3), could indeed emerge seemingly because of curvature-driven, individual-level competition arising along the leading edge of a population and the resultant development of dispersal mechanisms. The results of the IBM highlighted the significance of the cost of dispersal parameter, with circular patterns of spread found at relatively low and high costs of dispersal (corresponding to those agar plate environments tested in Chapter 3) and irregular tendril patterns of spread found at intermediate costs of dispersal. In our model, we found that these tendrils occurred via a slipstream mechanism resulting from the stable polymorphism of dispersal phenotypes along the leading edge.

The illustration of a stable polymorphism of dispersal phenotypes resulting in tendrill dynamics was a key finding in Chapter 7. While other models have illustrated similar mechanisms responsible for these shapes of spread, these models have typically relied on nutrients becoming limiting in the environment, thereby assuming cells switch between a passive non-motile state and an active motile state according to food availability (Golding et al., 1998, Marrocco et al., 2010, Xue et al., 2011), which we had already showed was not always a suitable assumption for microbial populations (Chapter 3). Instead, our model's focus on individual-level competition and the evolution of dispersal phenotypes, showed that these tendrils could arise without the nutrient limiting basis of these other models. Indeed, through this approach, we found that those individuals at the tip of the tendrils, whom are driving the tendrill shaped spread, actually suffer a decrease in fitness compared to those individuals who colonise the area behind them. Whilst some theorise that tendrils are a consequence of a cooperative division of labour between those at the tendrill tip and those behind, our results suggest this cooperation is not actually required for tendrill dynamics, although we speculate this might be possible depending on the conditions of the system. Together, the results of this model provided further evidence that irregular shapes of spread are beneficial at the group-level (as the colony can sequester more resources from outside the population) but are perhaps at the trade-off of fitness at the individual-level for those individuals initiating the process. We note that polymorphisms of dispersal phenotypes are commonplace in invasive populations (Cain et al., 2000, Elliott and Cornell, 2012, Yamamura, 2002, Robinet and Liebhold, 2009), yet our knowledge of their effect is still relatively limited and often only focused upon the rate of spread, not the shape of spread (Misevic et al., 2015). Therefore, further research should investigate whether those populations that exhibit a stable polymorphism of dispersal strategies, particularly those populations consisting of invasive species, can spread in irregular patterns and whether these shapes of spread cause changes to the ecological characteristics of the population.

The studies of Chapters 4-7 have used a multi-level selection framework to study the link between natural selection and the pattern of microbial spatial spread i.e. the cases when selection should favour circular colonies or irregular shaped colonies. Throughout this thesis, we have shown how the shape of

spread is a trait of the colony with a number of evolutionary and ecological implications. In bacteria, selective fitness pressures are known to act both on the individual bacteria themselves and on the colony as a whole (de Vargas Roditi et al., 2013, Griffin et al., 2004). As discussed in Chapter 4, the relative intensity of these selective pressures depends on local vs global selection, within-population relatedness and variation through space and time (Griffin et al., 2004, West et al., 2006b). Hence, if a colony exists in isolation, then despite the asexuality of the cells in the colony, natural selection should be intense for selfish behaviour and therefore traits favouring individual-level selection (which could give rise to cheaters in the population, individuals who take advantage of the public goods produced by other individuals without contributing themselves) (West et al., 2006a). This factor would be possibly exaggerated if the colony was in fact multi-clonal (consisting of cells from two or more ancestries), although the effect of kin selection between individuals may influence the direction of selection in another way (Griffin et al., 2004). Thus, based on the results of Chapters 4-7, for a colony in isolation, we would expect selection to favour a circular shape of the spread, with the evolutionary dispersal games arising as the population expands (Chapter 6), favouring individual-level fitness as competition intensifies. However, if colonies are competing with each other in the same system for limited space or food, then multi-level selection should occur, with the system moving towards the group-level of selection. Consequently, in this situation, the evolutionary dispersal games arising as the population expands should begin to favour dispersal strategies which result in irregular shapes of spread when the winner in the system is the colony that sequesters the most food (Chapter 4). Thus, the shape of spread is a trait that in theory, should respond to the selective evolutionary parameters of the system, at both the cellular level and at the level of the colony itself. Learning more about the evolutionary factors affecting how populations spread across many levels of selection is important to our understanding of the spatial dynamics, especially in light of recent evidence establishing evolution as a key factor affecting the rate of a population's spread (Travis et al., 2009, Shine et al., 2011a, Travis and Dytham, 2002). We believe that the multi-level selection framework should be used more to understand how the traits (such as the shape of spread) driving the associated exhibited spatial dynamics evolve, particularly as evidence has increasingly observed group-level competition to be

as influential on the evolution of dispersal and other invasive traits as individual-level competition (De Meester et al., 2014).

Looking back to the results of Chapter 2, we note that only the WS morphology grown on 0.5% agar typically favoured irregular shapes of spread and accordingly an accelerating rate of spread. The results of Chapters 4-7 show that irregular shapes of spread are generally favoured in systems where selection favours group-level fitness. Subsequently, we suggest that the SM morphology is possibly less cooperative and therefore more inclined to favour traits increasing individual-level fitness over group-level fitness, when compared to the WS morphology (Griffin et al., 2004). This is in agreement with the fact that in the static microcosm, the WS morphology arises specifically to form a biofilm with other individuals across the air liquid interface such that it sequesters as much oxygen as possible from the static vial (Spiers, 2007). Biofilms are one of the most noticeable consequences of cooperation between individuals, with biofilm formation enabling unicellular organisms to act and behave like a multicellular organism i.e. biofilm formation is a group-level trait (López et al., 2010, Nadell et al., 2009, Kreft, 2004). The SM morphology on the other hand does not form a biofilm and instead stays isolated in the central part of the static microcosm, thereby suggesting it favours individual-level fitness (Spiers, 2007). Thus we presume that the SM morphology is less inclined to cooperate and therefore less likely to form irregular shapes of spread. This may be one possible explanation for why the SM morphology did not consistently develop an accelerating rate of spread (Chapter 2). With regard to conservation, this possibly demonstrates how understanding the evolutionary basis of a population and whether it's behaviour is favouring individual- or group-level traits (such as the shape of spread) may enable us to understand and predict the populations likely shape and possibly rate of spread. Thus, we highlight that conservation managers should look to understand more about these evolutionary factors and about how their conservation strategies might affect them.

The microbial model system has enabled observation of the rapid evolution of traits, thereby empowering us to discover how evolutionary factors affect the ecological processes within a population in a controlled laboratory environment; this makes the microbial model system a useful tool in evolutionary ecology

(Buckling et al., 2009, Jessup et al., 2004). The results of Chapter 4 suggested that the shape of population spread was a trait linked to selective pressures across multiple levels of selection. Accordingly, we speculated that the shape of spread could potentially adapt according to evolutionary pressures. Indeed, we believed that based on other results in the thesis, the strategies and parameters responsible for patterns of spatial spread have evolved (Deng et al., 2014) and will continue to evolve in order to improve the persistence of the population as whole. Focusing on the shape of spread at a group-level and through positive and negative artificial selection, we investigated in Chapter 8 whether the shape of spread could evolve through time. After two intensive efforts, each utilising slightly different selection regimes, the findings suggested that this was not the case, with the shape of spread not reliably selected for through time. Due to some problems with the experiments conducted, we outlined various improvements to the methodology within Chapter 8, which we recommended as future research to establish without doubt, the inability to select upon the shape of spread. If the shape of spread is in fact selectable, then we believe this would yield the opportunity for competition experiments to determine the outcome of selection on the shape of spread following manipulation of scales of genetic diversity (mixed vs clonal colonies) and scales of competition for limited resources (competition within and/or between colonies), as per our original intention. This would help us to uncover the evolutionary basis of these patterns of spread and thus help us to understand and potentially control the spread of populations.

One of the key aims of this thesis was to demonstrate the usefulness of the microbial model system for the study of spatial ecology. Historically, the microbial model system has been underutilised in ecology due to it being perceived as too simplistic a model system compared to those model systems utilising macroorganisms (Carpenter, 1996). However, a recent surge in the popularity of microbial ecology had shown the microbial model system to be an effective model system for the study of ecology across wide range of topics (Jessup et al., 2004, Buckling et al., 2009). For example, bacteria have recently been used to study senescence and the trade-off between reproduction and ageing, as well as the evolution of dispersal and the links between species diversity and community productivity, aspects known to affect the ecology of

macro-organisms (Ackermann et al., 2003, Buckling et al., 2009, Jessup et al., 2004, Hodgson et al., 2002, Taylor and Buckling, 2010). This thereby illustrates the wide range of traits microorganisms have in common with macroorganisms, many of which researchers have investigated via the microbial model system. Yet with regard to spatial ecology, we believed researchers had not fully exploited the microbial model system. Throughout this thesis, we have demonstrated the usefulness of the this system to spatial ecology by highlighting a number of ways researchers could study invasive populations via the microbial model system, both empirically and as a tool inspiring new questions. For example, Chapter 2 first demonstrated how the experimental control offered by the microbial model system enabled us to clearly distinguish the effect of intrinsic and extrinsic factors upon the rate of spatial population spread, without the effects from non-controllable extrinsic factors that often plague empirical spatial ecology studies (Urban et al., 2008, Buckling et al., 2009, Jessup et al., 2004). This illustrated one of the many advantages of the microbial model system compared to model systems. We also attempted to demonstrate the evolutionary properties of the microbial model system in Chapter 8, thereby studying theories that would be otherwise impossible to empirically test in macroorganism populations. Secondly, we showed in Chapter 2 that the shape of spread, an aspect often ignored in spatial ecology studies, could potentially affect ecological characteristics of the population such as the rate of spread. This observation formed the key inspiration for the remainder of the thesis, leading us to investigate a number of questions relating to spatial ecology via the topic of population shape. This thereby highlights how the microbial model system can inspire new ideas and questions. All of this together highlights the usefulness of the microbial model system and its ability to be a solution to many of the problems experienced in studies of spatial ecology, suggesting that future spatial ecology studies should look towards the microbial model system as an effective tool to investigate phenomena seen in macro-organism populations.

In summary, the key findings we make in this thesis and their main contributions to knowledge are:

1. The microbial model system is a useful tool in spatial ecology, with a number of highly advantageous characteristics that researchers should

- take advantage of to study the spatial spread of populations (Chapters 2 and 8).
2. Depending on the intrinsic/extrinsic properties of the system, the *Pseudomonas fluorescens* strain SBW25 microbial model system can exhibit non-constant (accelerating/decelerating) rates of spread. This is in contrast to the constant rate of spread prediction made by the classical reaction-diffusion equation models in spatial ecology (Chapter 2). This adds to the discourse from other macroorganism studies, which suggest the assumptions responsible for this prediction (in particular the constant population growth rate and dispersal speed) need to be closely scrutinised before their use in predictive models of population spread.
 3. The shape of spatial population spread has potentially important ecological and evolutionary implications for the population. Our results in Chapter 2, suggest a link between the shape of spatial spread and the rate of spread, while our results in Chapter 4 illustrate that irregular patterns of spread benefit group-level fitness at the expense of the individual-level fitness and vice versa for regular shapes of spread. Overall, our results highlight there is more to the shape of spread than just landscape topology and food availability in different environments, as previously assumed, with evolutionary factors possibly playing a significant role. Indeed, throughout the thesis, we have tried to highlight the shape of spread to raise its profile as an influential trait of a population.
 4. Extrinsic factors of the agar plate environment affect the pattern of spatial spread of *Ps. aeruginosa* strain PAO1 populations across agar plate surfaces but differently to that reported for other microbial strains (Chapter 3). Specifically, we found that relatively low viscosity (agar concentration), relatively high nutrient (peptone) concentration agar plates promoted tendril (irregular) patterns of spatial spread in *Ps. aeruginosa* strain PAO1. Hence, modellers need to be aware of the non-universal effect of environmental factors of the agar plate environment upon microbial spread.
 5. Curvature-driven, individual-level competition between individuals along the leading edge increases during the expansion of the population (Chapter 5). We predict this culminates in the development of dispersal

mechanisms, leading to unique social behaviour between individuals along the leading edge and the associated evolutionary fitness games between individuals described in Chapter 6.

6. The same curvature-driven, individual-level evolutionary competition between individuals along the leading edge of a population can result in the emergence of irregular patterns of spread, such as those exhibited by microbial populations (Chapter 7). In particular, tendrils can develop because of a slipstream mechanism arising along the leading edge resulting from the existence of a stable polymorphism of dispersal phenotypes.
7. The shape of spread is seemingly not a selectable trait but more research is required to rule this out (Chapter 8).

Taken together, the results show how the shape of a population during its spatial expansion across an environment is a consequence of various intrinsic and extrinsic factors, with implications for the ecological and evolutionary outcome of the population. Regarding conservation, our results highlight that a true integrated approach to conservation management needs to account for the shape of spread, as this factor in isolation can influence both the selective pressures faced by the population and the ecological characteristics of the population. In particular, these results have potential importance for conservation measures which influence the shape of spread (such as the introduction of environmental corridors), as we suggest they may lead to unexpected and undesirable consequences, such as an increase to the rate of invasive spread (Resasco et al., 2014), due to neglecting the potential effect of the shape of spread. However, in order to develop this integrated approach, more work needs to be done in order to understand the whole effect that the shape of the population has on various ecological and evolutionary characteristics. This thesis demonstrates that the microbial model system is and will be an ideal tool to help develop our understanding in this area.

Our broad recommendations for future research

The discussion sections of each data chapter in this thesis raise a number of detailed avenues for further research. Subsequently, here we list a number of broad recommendations for future research.

The links between the spatial ecology of microorganisms and macroorganisms need to be established

Recent research has debunked the historic opinion of microbial populations as relatively simple organisms with little in common with macroorganism populations (Jessup et al., 2004, Buckling et al., 2009). This is due to the increasing recognition that many of the evolutionary and ecological pressures influencing macroorganism populations also influence microorganism populations, thus enabling us to use microorganisms as a tool to understand phenomena in evolutionary ecology (Buckling et al., 2009). However to date, the field of spatial ecology has not yet fully utilised the microbial model system to study the spatial spread of populations. Whilst one of the aims of this thesis was to demonstrate some of the possible benefits that the microbial model system could offer to spatial ecology, we have assumed that the processes affecting the spatial distribution of microbial species were similar to those processes affecting the spatial distribution of populations of larger, multicellular species. Future research should look to verify this assumption, so that researchers can unequivocally say that the underlying processes dictating the spatial spread of microorganisms are the same or similar as those seen in macroorganisms and thus encourage the utilisation of the microbial model system to study spatial ecology.

Increased usage of the microbial model system in spatial ecology studies

While there is still work to do on analysing the links between the processes driving the spatial spread of microorganisms and the spatial spread of macroorganisms, future studies in spatial ecology should look to the microbial model system to help answer questions that are difficult to answer with macro-organism populations. This is due to the many advantages associated with the microbial model system (Buckling et al., 2009). For example, the spread of the microbial populations is easily capturable, they spread in relatively short timescales and evolution in the microbial model system occurs in relatively short timescales (Jessup et al., 2004). One broad topic primed for future experiments is to use the microbial model system to establish how the process of evolution affects processes in spatial ecology, an aspect that is difficult to measure in macro-organism populations. Such knowledge could have application both in

conservation (Mack et al., 2000) and in medicine (de Bentzmann and Plésiat, 2011, Ehrlich et al., 2005, Korolev et al., 2014).

A greater appreciation of how the shape of spread influences the characteristics of the population

Investigations studying the spread of a population have focused on both the rate of spread and on predicting where the population will likely spread as it traverses an environment (Hastings et al., 2005). We suggest that the shape of spread is an overlooked factor in spatial ecology that deserves more attention due to the significant implications it could potentially have for the evolutionary and ecological properties of the population and its members (de Vargas Roditi et al., 2013, Nadell et al., 2010, Misevic et al., 2015). For instance, the findings in this thesis suggest the shape of spatial spread influences the individual-level and group-level fitness of the population, thereby affecting the social behaviour between individuals in the population. Investigating the feedback between the shape of spread and social behaviour, and incorporating this knowledge into our predictive models will help to improve our predictions of population spatial spread, which to date have generally been focused on the mechanistic processes driving the spread of populations. Empirical and computational studies involving the microbial model system will help to investigate this.

Detailed analysis of the ecological game along the leading edge of the population.

In Chapters 5 and 6, we found that as the radial spread of a circular population increased, individuals situated along the frontier of the population suffered increased competition. Consequently, we assumed individuals were more likely to disperse in order to alleviate this competition. By initiating dispersal, we found that an evolutionary game occurred between neighbouring individuals, with different types of social behaviour arising depending upon the cost of dispersal, the distance of dispersal and the curvature parameters of the leading edge. Whilst we showed that such a game occurred, we limited the analysis of this game to a number of geometric calculations and theoretical strategies. However, to realise the impact of this scenario, we require a thorough game theory analysis of this evolutionary game to understand the various strategies in more detail and to find out whether there exists an optimum stable strategy in

this game. Moreover, this analysis should look to investigate how the parameters of selective pressures at the individual/group levels and how relatedness affects the resultant strategies individuals use in this game.

Further knowledge is required about the microbial system itself

We are increasingly learning more about the mechanisms used by microbes to survive and thrive. For instance researchers have established how microbes move, how they interact with each other and how they acquire resources from the surrounding environment (Shapiro, 1998, Kearns, 2010). However, there is still more to learn about these mechanisms, in particular how these survival strategies may have evolved through time (Deng et al., 2014). Indeed, whilst the research in this thesis has investigated how and why the spatial patterns of spread may have arisen for some ecological and evolutionary reasons, it was still not entirely clear what drives the evolution of the different patterns of spread i.e. why does one strain of bacteria exhibit a different pattern of spread to another strain of bacteria. Consequently, more knowledge about the environmental, ecological and evolutionary drivers behind these patterns of spread is required.

Studying the shape of microbial spatial spread in competition experiments according to a multi-level selection framework

Whilst classical microbiology has perceived microbes as relatively simple organisms, a recent shift in perspective has revealed that microbes are social organisms, living in communities with traits seemingly both at the individual-level and at the group-level (de Vargas Roditi et al., 2013). With regard to spatial ecology, a future research programme should continue to study the patterns of spatial spread exhibited by populations according to a multi-level selection framework.

We propose that continuation of this research could be by conducting competition experiments based on the classic experimental design of Griffin (2004). For instance, these competition experiments could examine how relatedness between individuals in the colony and/or manipulating the local/global competition of the system affects the resultant spatial patterns of spread, where we assume the winner to be the colony that sequesters the most environment and therefore the most resources. We predict that competition

experiments with multiple colonies in the same agar plate environment would show that small colonies, initially favouring individual level-selection and therefore circular spread with evolutionary dispersal games as the population spreads, would begin to favour traits according to group-level selection pressures (such as tendril development) in order to combat other colonies for the non-sequestered environment. The degree of relatedness of the colony and the degree of global competition vs local competition would affect this resultant outcome. These competition experiments could include analysis of the geometric shape of the colony i.e. measuring whether the tendrils are optimally distributed as well as the number of tendrils. Competition experiments such as these would help us to understand the evolutionary pressures responsible for the spatial spread of populations, an area that still has much to uncover. In particular, it would help researchers to understand the reasons why populations might spread in patterns deviating from typical circles, thereby helping to improve our ability to predict the resultant outcome of a spreading population. Such findings would help to inform new bio-control strategies that could be utilised to control the spread of invasive populations (Misevic et al., 2015).

Concluding remarks

Using a mixture of evolutionary ecology theory and the microbial model system, we have demonstrated that the shape of population spread has genotypic, phenotypic and environmental drivers, and that the resulting shapes of population spread feedback on selection at both individual- and group-levels, with significant ecological consequences. What is apparent is the spatial invasion process is not simply just ecological, but a process involving evolution as well, with organisms constantly evolving according to selective processes across multiple levels, either to adapt to niches in the environment, to help escape negative ecological effects and/or because of evolutionary spatial sorting mechanisms. The wide range of factors affecting the spatial dynamics of invasive spread, the evolutionary pressures on these factors and the feedbacks these spatial dynamics can have on these factors mean that predicting the evolutionary and ecological dynamics of invasive species is a fundamentally difficult problem, more difficult than that suggested by the classical models of spatial spread. However, our findings suggest that an appreciation of these feedbacks and the effect of multi-level selection, in the form of game theory

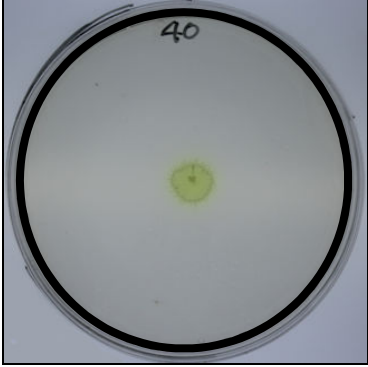
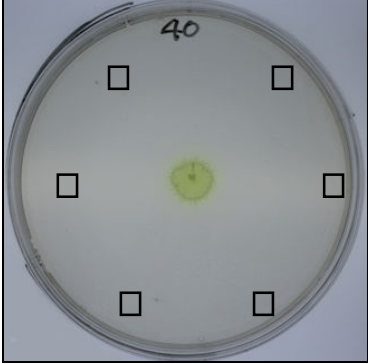
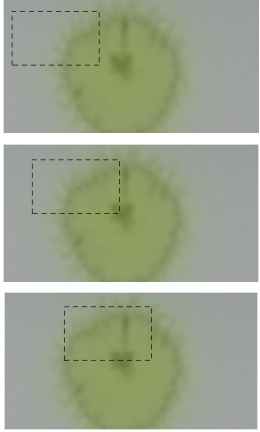
scenarios, is a possible solution in order to help us control current invasions and prevent future invasions from occurring. This thesis only scratches the surface of this topic, a topic that could have important implications, and we are intrigued to see how others take these results on further.

Appendix A: Image analysis protocol used in Chapter 2

In this study, we utilised an automated threshold algorithm to differentiate the spread of the colony from the agar background. We did this by applying pixel intensity thresholds to create a binary image (as in Chapter 2 – figure 2.3) such that, if the pixel intensity of a pixel is above the threshold, the pixel equals 1 (i.e. white in Chapter 2- figure 2.3), else the pixel is made equal to 0 (i.e. black in Chapter 2 – figure 2.3).

To distinguish the agar plate background from the overall picture background, we first applied a threshold to detect the edge of the agar plate and removed any part of the picture, which lay outside of this region. Upon the remaining region, we then applied six different thresholds (table A-1), each slightly different to increase the likelihood that a threshold could isolate the microbial biofilm from the agar plate background. We investigated a range of commonly used threshold methods ranging from histogram shape-based methods to Otsu's method (Sezgin, 2004). However, we found these were rarely successful. Instead, we used thresholds based upon the pixel intensities of certain regions of the picture due to their relatively high success rate in pilot experiments. In cases where the image analysis could not differentiate the microbial growth from the agar plate background, we manually conducted image differentiation using Adobe Photoshop CS6.

Table A.1: A description of the six different thresholds used in the image-analysis algorithm.

	Threshold Description	Image of Threshold
Threshold 1	The mean of the pixel intensities of the whole agar plate was taken and used as a threshold value	
Thresholds 2 and 3	<p>We selected six quadrats around the edge of the agar plate. For threshold 2, we took the pixel intensities of the pixels within these regions and used their average as a threshold.</p> <p>Similarly for threshold 3, but instead we took the pixel intensities of the pixels within these regions and used their average plus one standard deviation as a threshold.</p>	
Thresholds 4,5 and 6	<p>The inbuilt threshold method in EImage utilises a localised adaptive threshold. This adaptive threshold works by scanning the picture, region by region (i.e. the box in the picture) and applying a threshold according to the mean of the values within the searchable region and a user supplied offset parameter.</p> <p>Threshold 5 was the same but with a smaller search box whilst threshold 6 also uses this smaller search box but with a smaller, stricter offset parameter.</p>	

Appendix B – Sensitivity analysis of the numeric model used in Chapter 4

In Chapter 4, we used equation B.1 to create shapes in polar coordinates representing the microbial colony spread.

$$r = \alpha + b \sin(k\theta), \theta = 0, \dots, 2\pi \quad (\text{Equation B.1})$$

The following appendix briefly describes the effect of changing the default parameters (as provided in table B.1) for the static model in Chapter 4. We found that whilst the quantitative results change, the qualitative behaviour of the model did not change, thereby strengthening our results.

Table B.1: The parameters used in this appendix for shapes in both the matching area and matching perimeter scenarios

Parameter name and description	Values used in matching area scenario	Values used in matching perimeter scenario
α = Radius of circle with zero tendrils	2,3,4	
b = Tendril length	0.5,1,2	
k = number of tendrils	0 , 5, 10, ..., 295,300	0 , (6,8,...,30,32)
h = halo length surrounding shape	0.1, 0.2, 0.3	

Changing the length of the halo surrounding the shape

The halo length affected the proportional advantage/disadvantage achieved by an irregular shape when compared to the characteristics of a circle. First, in the scenario where the area of the colony is equal for all shapes, we noticed that an increased halo length reduces the possible proportional group-level fitness benefit achieved by an irregular shape compared to a circular shape (figure B.1). This occurs because irregular shapes are more circular as the halo length increases. Second, as the halo length increases, the rate at which the fitness of individuals along the leading edge declines increases (figure B.1). A similar result occurs in the scenario where the perimeter of the colony is equal for all shapes i.e. the group-level fitness of the colony declines faster as the length of the halo increases (figure B.1).

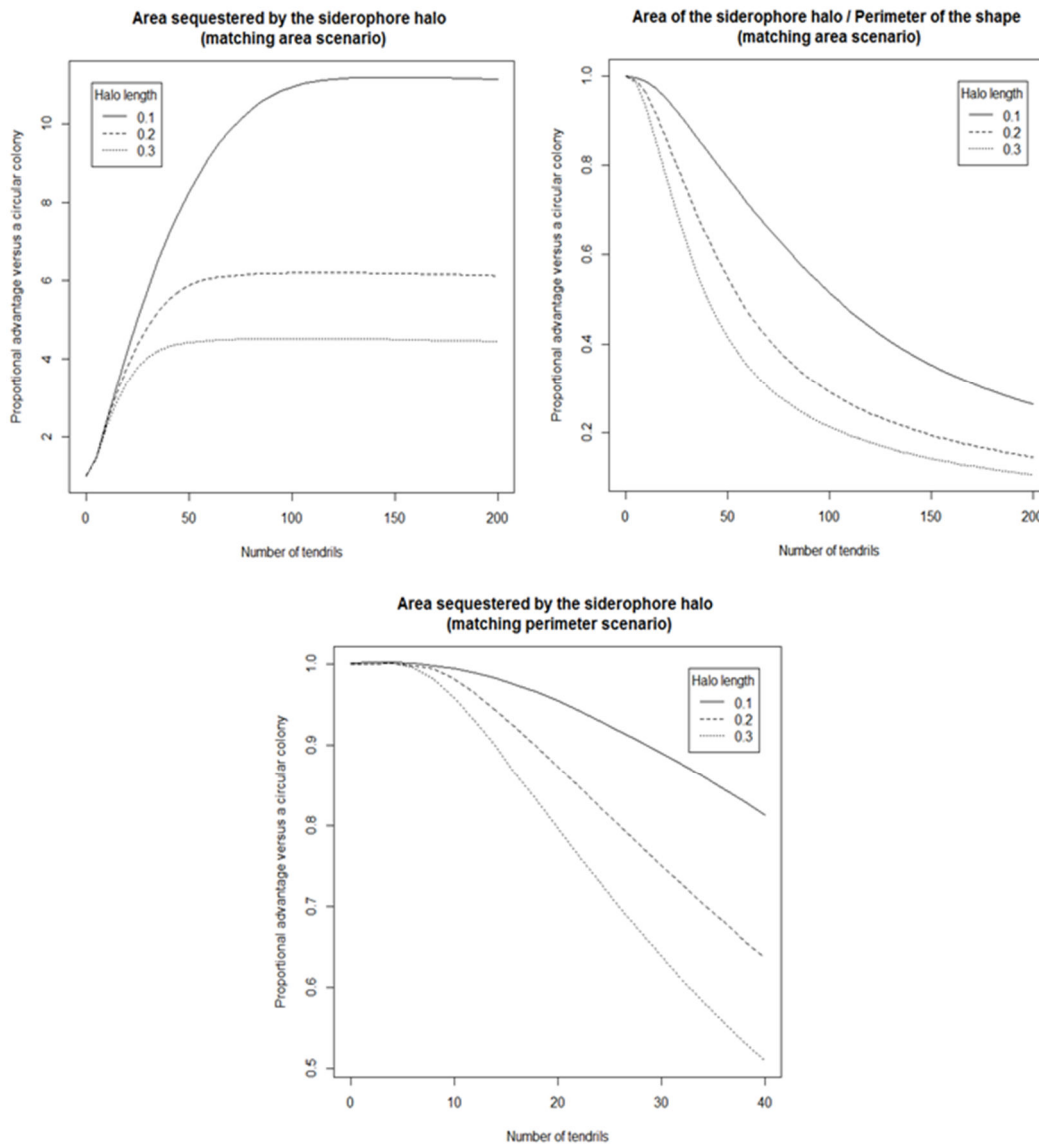


Figure B.1: These plots show the effect of the halo length parameter upon the various fitness measurements used in Chapter 4. (Top left) The area sequestered by the siderophore halo surrounding a colony shape proportional to the area sequestered by the siderophore halo surrounding a circle with the same area as the colony shape. (Top right) The area sequestered by a siderophore halo of a colony divided by the perimeter of the colony, proportional to the same measurement of a circle with the same area as the colony shape. (Bottom) The area sequestered by the siderophore halo surrounding a colony shape proportional to the area sequestered by the siderophore halo surrounding a circle with the same perimeter as the colony shape.

Changing the length of the tendrils

As in the case of the halo length, the tendril length affects the proportional advantage/disadvantage achieved by an irregular shape when compared to the characteristics of a circle. First, in the scenario where the area of the colony is equal for all shapes, we notice that an increased tendril length increases the proportional group-level fitness benefit achieved by an irregular shape compared to a circular shape (figure B.2). This occurs because irregular shapes are less circular as the tendril length increases. Second, as the tendril length increases, the rate at which the fitness of individuals along the leading edge declines increases (figure B.2). A similar result occurs in the scenario where the perimeter of the colony is equal for all shapes, i.e. the group-level fitness of the colony declines faster as the length of the halo increases (figure B.2).

Changing the radius of the circular colony

As in the case of the other parameters, the initial radius of the circular colony affects the proportional advantage or disadvantage achieved by an irregular shape when compared to the characteristics of a circle. First, in the scenario where the area of the colony is equal for all shapes, we notice that an increase to the initial radius of the circular colony leads to a decreased maximum proportional group-level fitness benefit for an irregular shape compared to a circular shape when the number of tendrils is low (figure B.3). However, by increasing the initial radius of the circular colony, there is a less rapid decline in fitness as the number of tendrils increases. Second, as the initial radius of the circular colony increases, the rate at which the fitness of individuals along the leading edge declines decreases (figure B.3). A similar result occurs in the scenario where the perimeter of the colony is equal for all shapes; the group-level fitness of the colony declines slower as the initial radius of the circular colony increases (figure B.3).

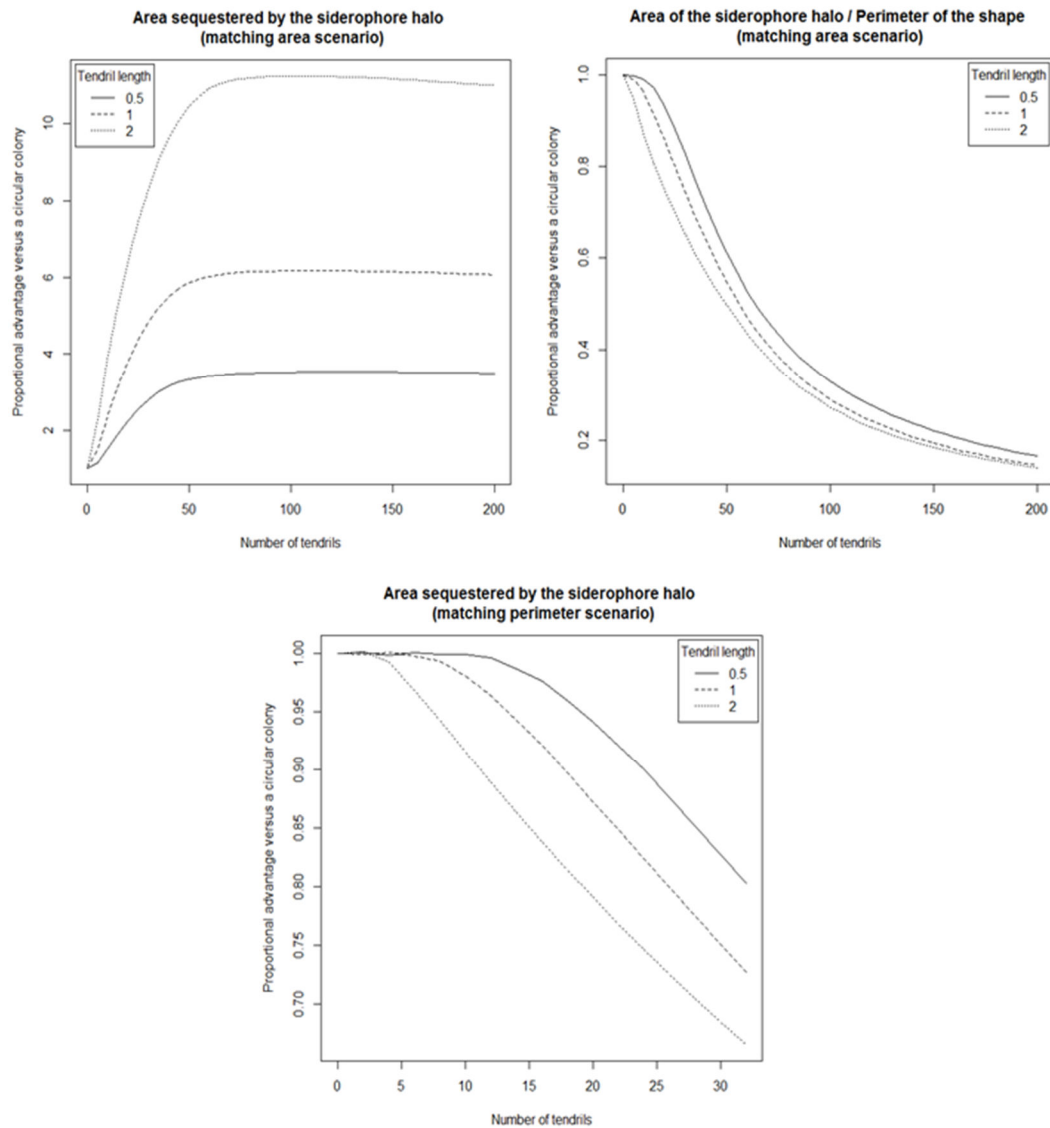


Figure B.2: These plots show the effect of the tendril length parameter upon the various fitness measurements used in Chapter 4. (Top left) The area sequestered by the siderophore halo surrounding a colony shape proportional to the area sequestered by the siderophore halo surrounding a circle with the same area as the colony shape. (Top right) The area sequestered by a siderophore halo of a colony divided by the perimeter of the colony, proportional to the same measurement of a circle with the same area as the colony shape. (Bottom) The area sequestered by the siderophore halo surrounding a colony shape proportional to the area sequestered by the siderophore halo surrounding a circle with the same perimeter as the colony shape.

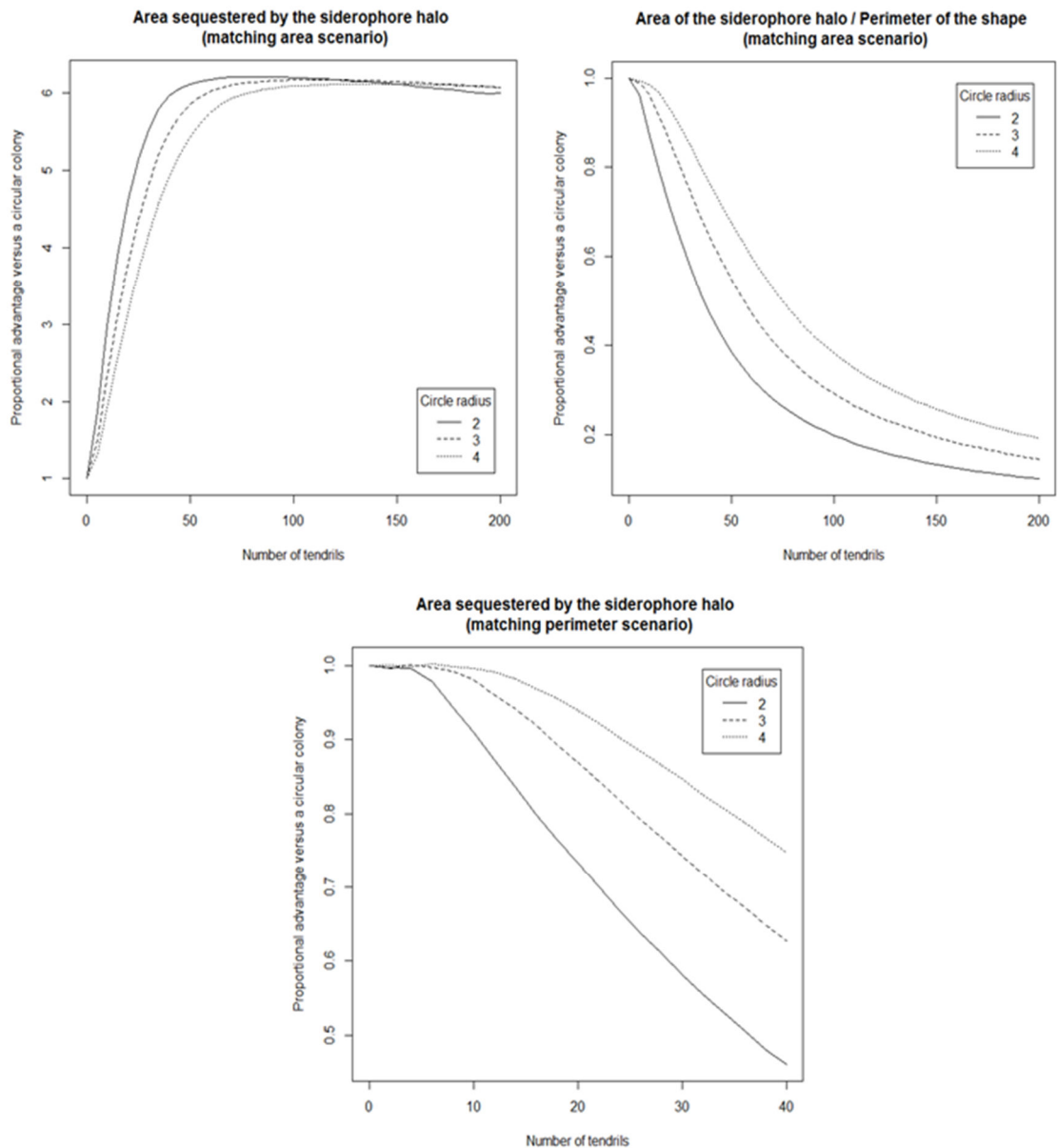


Figure B.3: These plots show the effect of the circle radius parameter upon the various fitness measurements used in Chapter 4. (Top left) The area sequestered by the siderophore halo surrounding a colony shape proportional to the area sequestered by the siderophore halo surrounding a circle with the same area as the colony shape. (Top right) The area sequestered by a siderophore halo of a colony divided by the perimeter of the colony, proportional to the same measurement of a circle with the same area as the colony shape. (Bottom) The area sequestered by the siderophore halo surrounding a colony shape proportional to the area sequestered by the siderophore halo surrounding a circle with the same perimeter as the colony shape.

Appendix C: Calculating the overlap between two circles

Theorem C.1: The lens-shaped area of intersection between two circles of radii, r and R , centred at $(0,0)$ and $(d,0)$ is calculated by:

$$A = r^2 \cos^{-1} \left(\frac{d^2 + r^2 - R^2}{2dr} \right) + R^2 \cos^{-1} \left(\frac{d^2 + R^2 - r^2}{2dR} \right) - \frac{1}{2} \sqrt{(-d + r + R)(d - r + R)(d + r - R)(d + r + R)}$$

Where d is the distance between the origins of both circles (Figure C.1).

Note: the following proof is from (Weisstein, 2010).

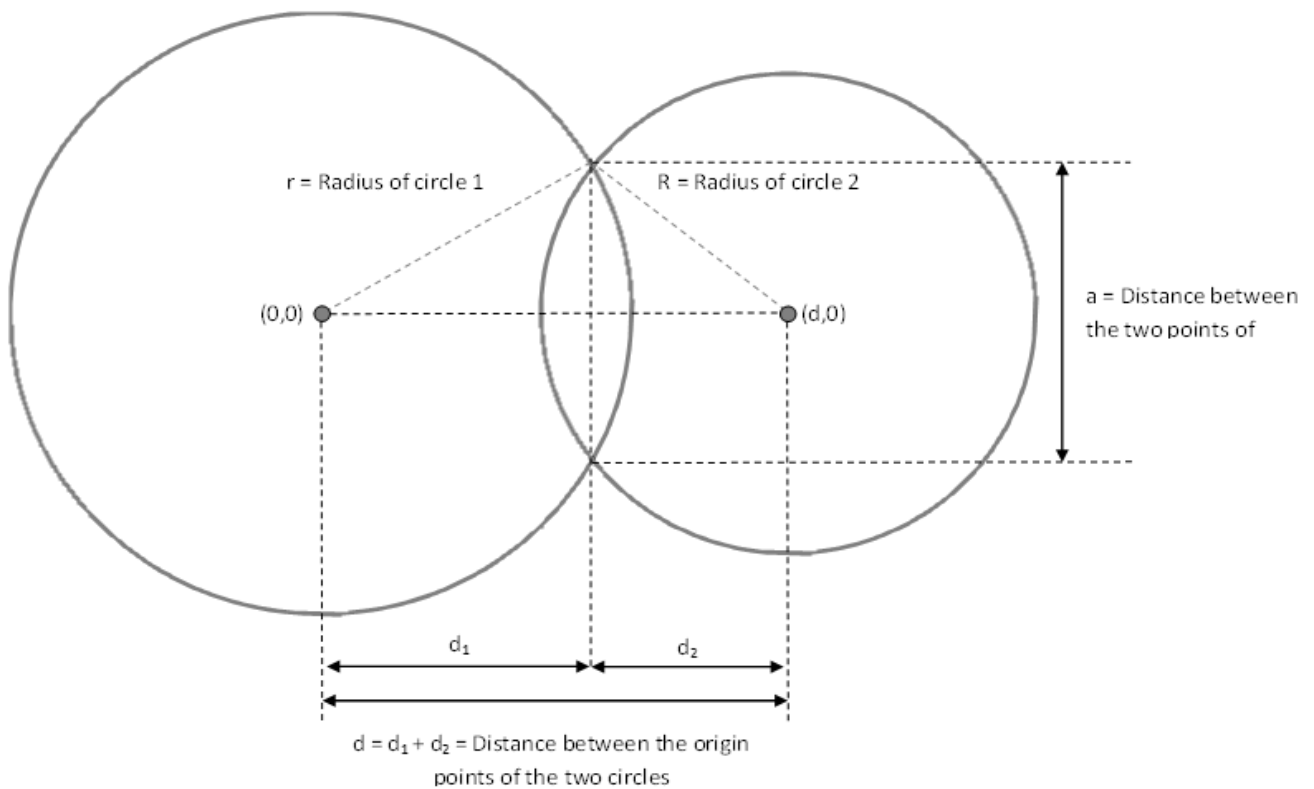


Figure C.1: An illustration of two circles of radii, r and R , situated a distance d from each other such that they intersect. This results in a region of intersection shaped as an asymmetric lens.

Proof: To find the area of the lens shaped area of intersection, split the lens into two circular sectors according to the chord at the axis, $x = d_1$. Call these intersection segments A_1 and A_2 (figure C.2). The area of A_1 and A_2 is found by calculating the area of the circular sector formed by the points of intersection

between the two circles on the circumference of the circle and subtracting the triangle formed by lines connecting the radius of the circle to the intersection points and the line $x = d_1$ (equation C.1).

$$Area_{intersection\ segment} = Area_{circular\ sector} - Area_{triangle} \quad (C.1)$$

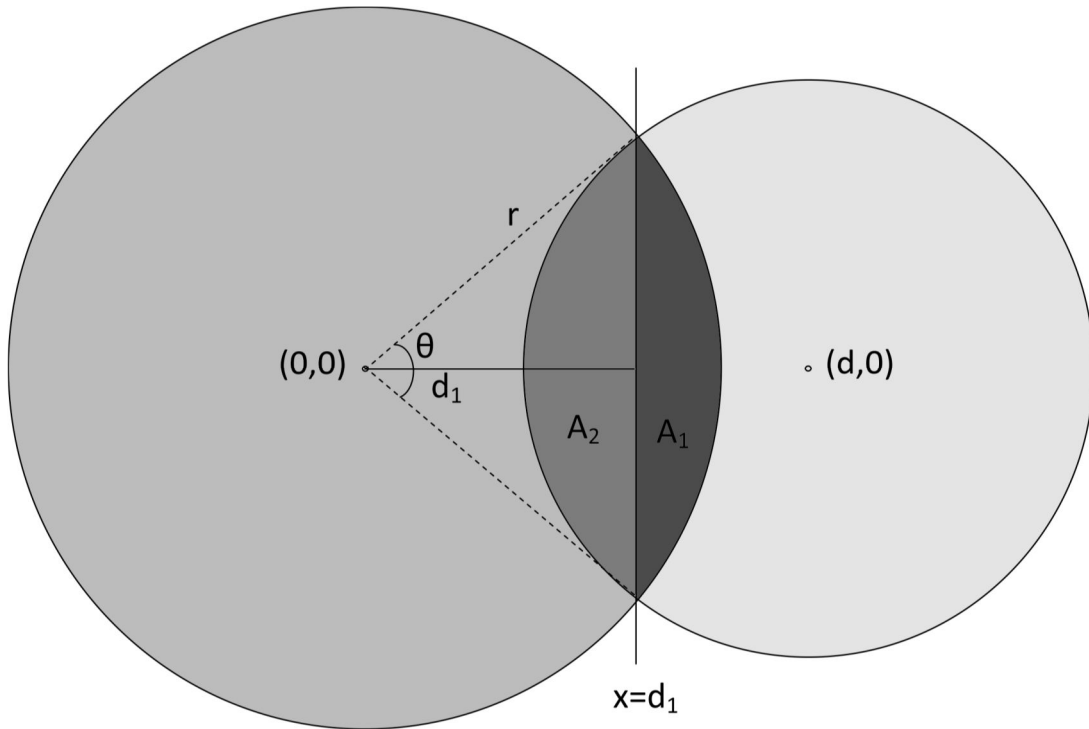


Figure C.2: We split the region of intersection into two regions A_1 and A_2 according to the line $x = d_1$. This forms a triangle between the intersection points and the origin.

First, we begin by finding the points of intersection between the two circles. The equations of the two circles are:

$$x^2 + y^2 = R^2 \quad (C.2)$$

$$(x - d)^2 + y^2 = r^2 \quad (C.3)$$

Combining (C.2) and (C.3) gives:

$$(x - d)^2 + (R^2 - x^2) = r^2$$

Multiplying through and rearranging gives:

$$x^2 - 2dx + d^2 - x^2 = r^2 - R^2$$

And then solving for x :

$$x = \frac{d^2 - r^2 + R^2}{2d}$$

Plugging x into (C.2) and rearranging gives us

$$y^2 = \frac{4d^2R^2 - (d^2 - r^2 + R^2)^2}{4d^2}$$

Therefore intersection points between the two circles is

$$\left(\frac{d^2 - r^2 + R^2}{2d}, \pm \sqrt{\frac{4d^2R^2 - (d^2 - r^2 + R^2)^2}{4d^2}} \right) \quad (\text{C.4})$$

From this, we can calculate the chord length between the two points of intersection, a , as $a = 2y$.

$$\begin{aligned} a &= 2 \sqrt{\frac{4d^2R^2 - (d^2 - r^2 + R^2)^2}{4d^2}} = \frac{1}{d} \sqrt{4d^2R^2 - (d^2 - r^2 + R^2)^2} \\ &= \frac{1}{d} \sqrt{(-d + r - R)(-d - r + R)(-d + r + R)(d + r + R)} \end{aligned} \quad (\text{C.5})$$

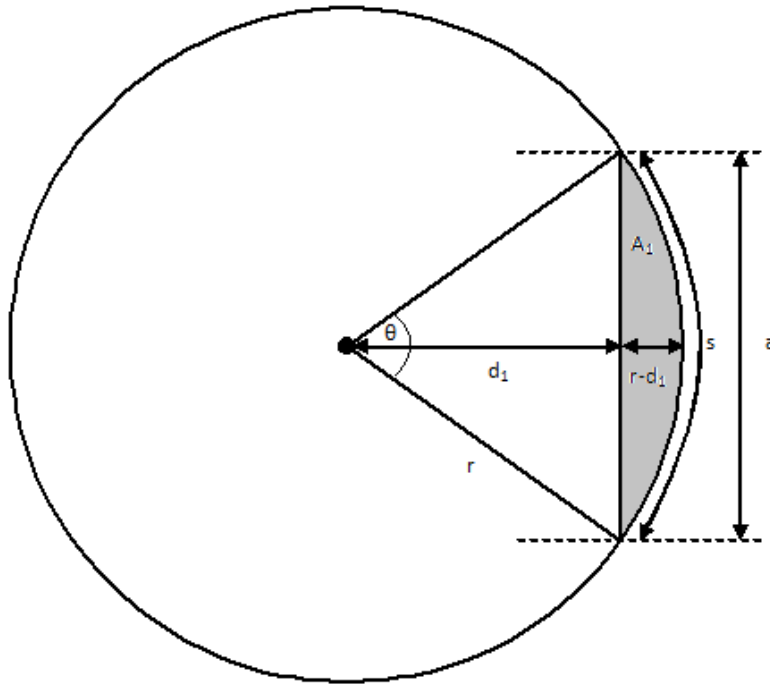


Figure C.3: Consider the intersection circular segment A_1 . Let r be the radius of the circle, a be the chord length between the two intersection points, $x = d_1$ be the height of the arced portion of the circular segment, d_1 be the height of the triangular portion, θ be the angle between the two lines connection the centre of the centre to the two points of intersection.

To find the area of the circular segment (shaded area of figure C.3) for the circle of radius r , we require the area of the circular sector defined by the angle made between the two intersection points, θ , and the area of the triangle formed between the points of intersection and the origin. The area of the circular sector is defined as:

$$Area_{circular\ sector} = \frac{1}{2}r^2\theta \quad (C.6)$$

Which via the trigonometric relationship $\theta = 2\cos^{-1}\left(\frac{d_1}{r}\right)$ can be represented in terms of the circle radius and the height of the triangular portion of the sector, d_1 (figure C.3).

$$Area_{circular\ sector} = r^2\cos^{-1}\left(\frac{d_1}{r}\right) \quad (C.7)$$

To find the area of the isosceles triangle, we use the fact that the height of the triangle is equal to d_1 (from C.4) and the base is equal to a (equation C.5).

$$Area_{isosceles\ triangle} = \frac{1}{2} \times base \times height \quad (C.8)$$

By using the trigonometric fact that the height = $r \cos\left(\frac{\theta}{2}\right)$ and the base = $2r \sin\left(\frac{\theta}{2}\right)$, equation (C.8) becomes:

$$Area_{isosceles\ triangle} = r^2 \cos\left(\frac{\theta}{2}\right) \sin\left(\frac{\theta}{2}\right)$$

By double angle formula, this becomes

$$Area_{isosceles\ triangle} = \frac{r^2}{2} \sin(\theta)$$

Which via the trigonometric relationship $\theta = 2 \sin^{-1}\left(\frac{a}{2r}\right)$ and the relationship

by Pythagoras Theorem, $a = 2\sqrt{r^2 - d_1^2}$, becomes: (C.9)

$$Area_{isosceles\ triangle} = \frac{r^2}{2} \sin(\theta) = \frac{1}{2} ar = r\sqrt{r^2 - d_1^2}$$

Therefore the area of the circular segment becomes

$$Area_{circular\ segment} = Area_{circular\ sector} - Area_{isosceles\ triangle} \quad (C.10)$$

$$Area_{circular\ segment\ i} = r_i^2 \cos^{-1}\left(\frac{d_i}{r_i}\right) - r_i \sqrt{r_i^2 - d_i^2}$$

Where r_i is the radius of the circle and d_i is the height of the isosceles triangle.

- For circular segment A_1 , $r_1 = r$ and $d_1 = \frac{d^2 + R^2 - r^2}{2dR}$
- For circular segment A_2 , $r_2 = R$ and $d_2 = \frac{d^2 + r^2 - R^2}{2dr}$

Therefore:

$$\begin{aligned} Area_{A_1} + Area_{A_2} &= r^2 \cos^{-1}\left(\frac{d_1}{r}\right) - d_1 \sqrt{r^2 - d_1^2} + R^2 \cos^{-1}\left(\frac{d_2}{R}\right) - d_2 \sqrt{R^2 - d_2^2} \\ &= r^2 \cos^{-1}\left(\frac{d^2 + r^2 - R^2}{2dr}\right) + R^2 \cos^{-1}\left(\frac{d^2 + R^2 - r^2}{2dR}\right) \\ &\quad - \frac{1}{2} \sqrt{4d^2 r^2 - (d^2 - R^2 + r^2)^2} \\ &= r^2 \cos^{-1}\left(\frac{d^2 + r^2 - R^2}{2dr}\right) + R^2 \cos^{-1}\left(\frac{d^2 + R^2 - r^2}{2dR}\right) \\ &\quad - \frac{1}{2} \sqrt{(-d + r + R)(d - r + R)(d + r - R)(d + r + R)} \end{aligned}$$

Appendix D: Calculating the overlap between 3 circles

Note: the following proof is from (Fewell, 2006).

When three circles are positioned such that there is a common area of overlap between all three, a circular triangle is formed (the dark grey region of figure D.1).

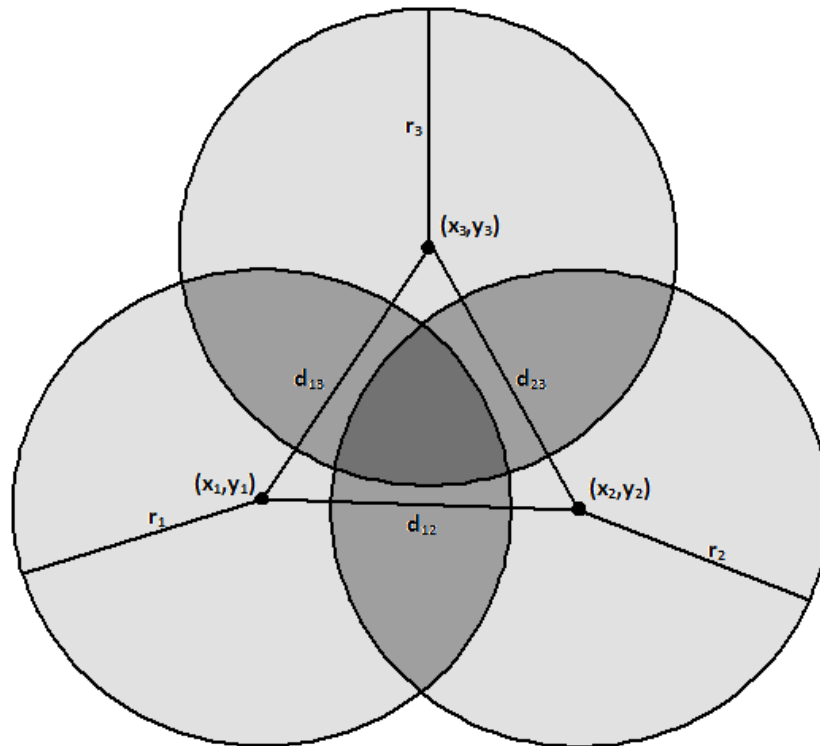


Figure D.1: Example of three circles with radii r_1, r_2 and r_3 respectively overlapping such that a circular triangle is formed (area shaded dark grey).

The distance d_{ij} is calculated by:

$$d_{ij} = \sqrt{(x_i - x_j)^2 + (y_i - y_j)^2}$$

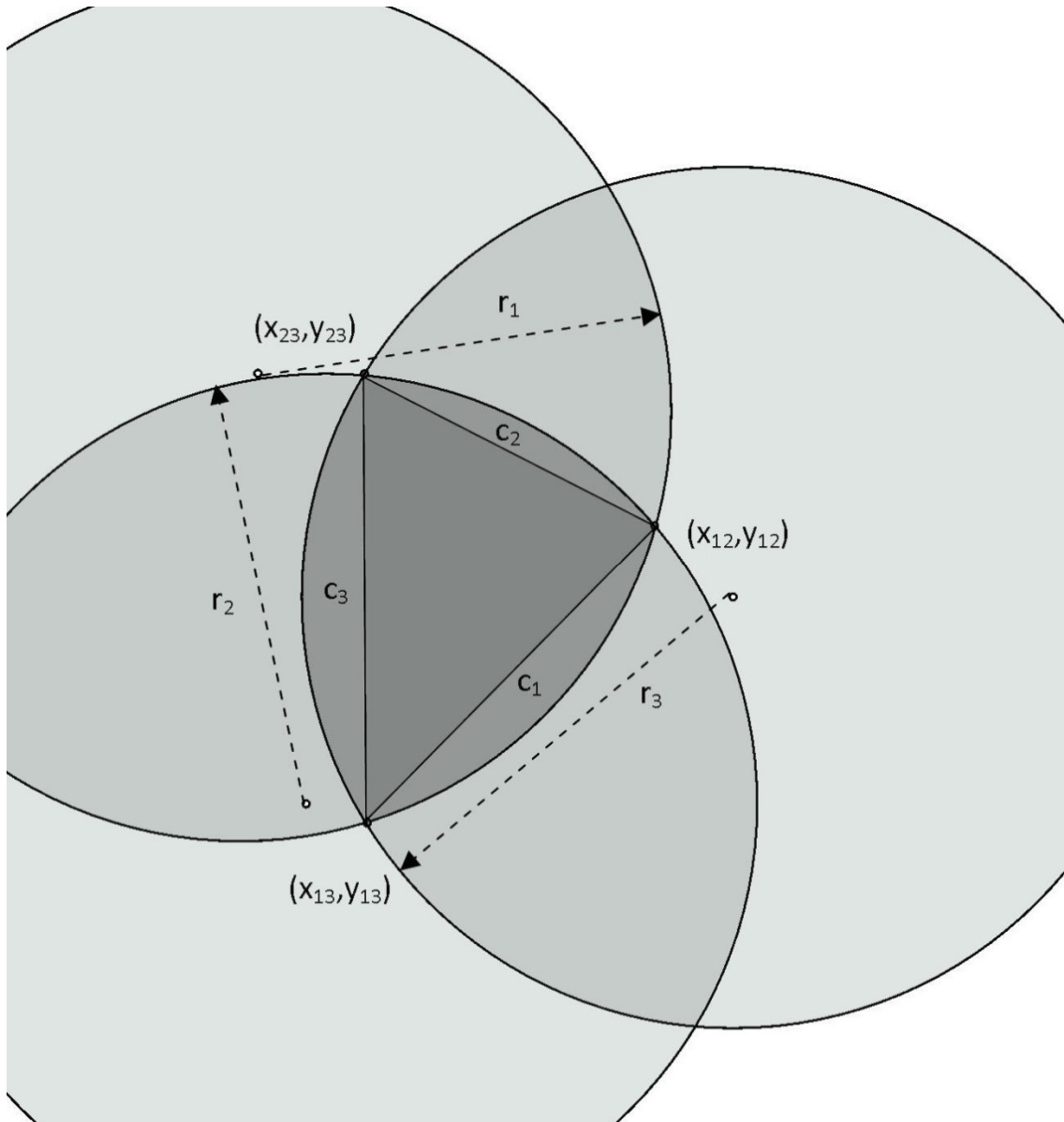


Figure D.2: The circular triangle formed by the intersection of three circles.

The chord length c_i is calculated by:

$$c_i = \sqrt{(x_{ij} - x_{ik})^2 + (y_{ij} - y_{ik})^2}$$

Theorem D.2: The area of a circular triangle (i.e. the area of overlap between three circles) is:

$$\begin{aligned}
Area_{circular\ triangle} &= \frac{1}{4} \sqrt{(c_1 + c_2 + c_3)(c_2 + c_3 - c_1)(c_1 + c_3 - c_2)(c_1 + c_2 - c_3)} \\
&+ \sum_{k=1}^3 \left(r_k^2 \arcsin \frac{c_k}{2r_k} - \frac{c_k}{4} \sqrt{4r_k^2 - c_k^2} \right)
\end{aligned}$$

where r_k and c_k are the three radii and chord lengths shown in figure D.1 and figure D.2.

Proof: We can consider the circular triangle to be the sum of the area of a normal triangle and the area of the three circular segments as shown in figure D.2.

$$Area_{circular\ triangle} = Area_{triangle} + \sum_{n=1}^3 Area_{circular\ segment\ n} \quad (D.1)$$

First, by using the chord lengths, we can use Heron's formula to calculate the area of the normal triangle.

$$Area_{triangle} = \frac{1}{4} \sqrt{(c_1 + c_2 + c_3)(c_2 + c_3 - c_1)(c_1 + c_3 - c_2)(c_1 + c_2 - c_3)} \quad (D.2)$$

The area of a circular segment can be calculated in a similar way to the intersection area between two circles.

$$Area_{circular\ segments} = \frac{1}{2} r^2 (\theta - \sin \theta) \quad (D.3)$$

In this calculation however, due to the formulation of the area of the triangle in terms of chord lengths, we define the area of the circular segments also in chord lengths. Substituting the trigonometry identity:

$$\theta = 2 \sin^{-1} \left(\frac{c}{2r} \right)$$

Into equation D.3 gives:

$$\frac{1}{2} r^2 \theta = r^2 \sin^{-1} \left(\frac{c}{2r} \right)$$

and

$$\begin{aligned} \frac{1}{2}r^2 \sin \theta &= \frac{1}{2}r^2 \sin \left(2\sin^{-1} \left(\frac{c}{2r} \right) \right) = \frac{1}{2}r^2 \left(2 \sin \left(\sin^{-1} \left(\frac{c}{2r} \right) \right) \cos \left(\sin^{-1} \left(\frac{c}{2r} \right) \right) \right) \\ &= r^2 \left(\frac{c}{2r} \right) \sqrt{1 - \left(\frac{c}{2r} \right)^2} = \frac{c}{4} \sqrt{4r^2 - c^2} \end{aligned}$$

Together this equates to:

$$Area_{circular\ section} = r^2 \sin^{-1} \left(\frac{c}{2r} \right) - \frac{c}{4} \sqrt{4r^2 - c^2} \quad (D.4)$$

Inserting equations D.2 and D.4 into equation D.1 gives us the desired result

$$\begin{aligned} Area_{circular\ triangle} &= \frac{1}{4} \sqrt{(c_1 + c_2 + c_3)(c_2 + c_3 - c_1)(c_1 + c_3 - c_2)(c_1 + c_2 - c_3)} \\ &+ \sum_{k=1}^3 \left(r_k^2 \sin^{-1} \left(\frac{c_k}{2r_k} \right) - \frac{c_k}{4} \sqrt{4r_k^2 - c_k^2} \right) \end{aligned}$$

(Fewell, 2006) notes that this straightforward equation only works for calculating the area in the case we show in figure D.1. Other configurations of three overlapping circles may exist (figure D.3 gives one example), however the equation seen in theorem D.2 will give incorrect values.

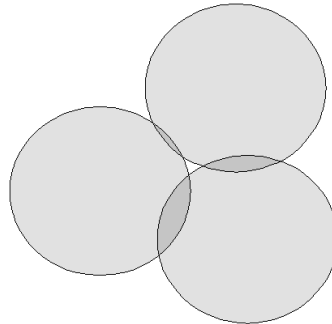


Figure D.3: A situation with three overlapping circles which do not form a compatible circular triangle.

To ensure that the area of overlap between three circles is only calculated when circles overlap in the case shown in figure D.1, the situation must satisfy two requirements:

1. The circles must intersect with each other. We did this by making sure the following inequality holds:

$$r_i - r_j < d_{ij} < r_i + r_j \text{ for } i,j = 1,2,3 \text{ such that } r_1 \geq r_2 \geq r_3$$

2. The case shown in figure D.1 differs from that in figure D.3 by two properties: the point (x_{12}, y_{12}) lies inside circle 3 and the point $(x_{12}, -y_{12})$ does not. Hence, if equations D.6 and D.7 hold then we can calculate the area of a circular triangle.

$$(x_{12} - x_3)^2 + (y_{12} - y_3)^2 < r_3^2 \quad (\text{B-6})$$

$$(x_{12} - x_3)^2 + (y_{12} + y_3)^2 > r_3^2 \quad (\text{B-7})$$

Appendix E: Proof of the asymptotic fitness of individuals in Chapter 5

We define the fitness, ω , of an individual of radius r , situated beside two neighbouring individual along the leading edge of the colony of radius R as the following approximation:

$$\begin{aligned} \lim_{R \rightarrow \infty} (\omega) \approx & \pi r^2 - \frac{1}{2} \pi r^2 \\ & - \left(\frac{1}{4} \sqrt{(r^4(2+h)(2-h)^3)} + 2r^2 \sin \left(\frac{\sqrt{(2-h)r^2}}{2r} \right) \right. \\ & \left. - \frac{1}{2} \sqrt{r^2(2-h)} \sqrt{r^2(2+h)} \right) \end{aligned}$$

Proof

We begin with the observation that as $R \rightarrow \infty$, the radius of curvature tends towards 0. Consequently, for three individuals situated along the leading edge of the population, we consider that the leading edge can be approximated as a straight line as $R \rightarrow \infty$ (figure E.1).

Considering this, without loss of generality, assume that the main population is represented by a circle of Radius R with origin $(0, -R)$ and three non-dispersing individuals along the leading edge are represented by circles of radius r , situated at the three origins $(0,0)$, $(hr, 0)$ and $(-hr, 0)$ respectively. We define these circles as circle 1, 2, 3 and 4 respectively (figure E.1).

We begin by finding the points of intersection between the three circles; circle 1 representing the main population, circles 2 representing the focal individual and circle 3 representing a neighbouring individual. The equations representing the circles are:

$$\text{Equation of circle 1:} \quad x^2 + (y + R)^2 = R^2 \quad (\text{E.1})$$

$$\text{Equation of circle 2:} \quad x^2 + y^2 = r^2 \quad (\text{E.2})$$

$$\text{Equation of circle 3:} \quad (x - hr)^2 + y^2 = r^2 \quad (\text{E.3})$$

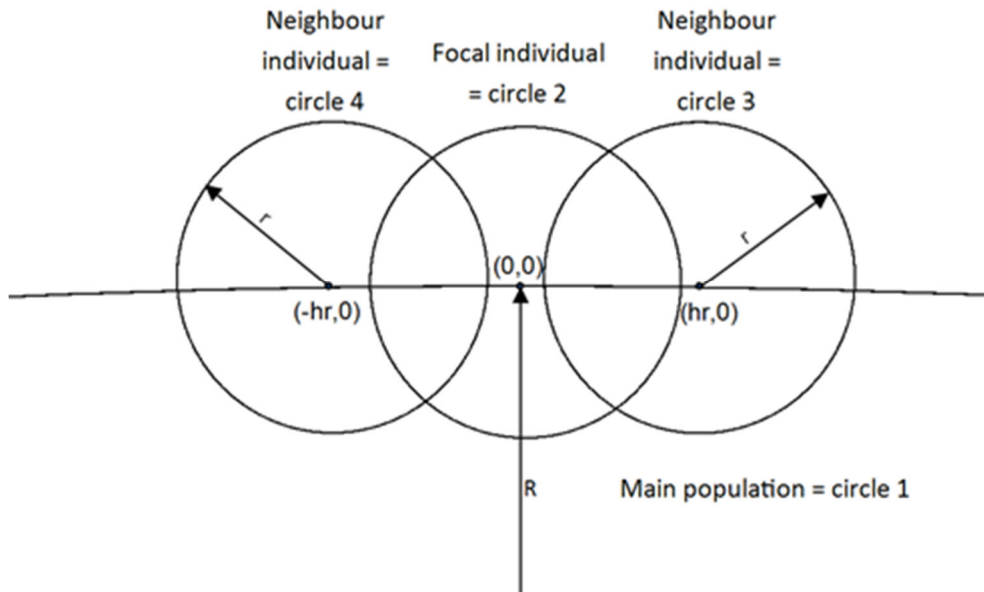


Figure E.1: For 3 individuals along the leading edge of the population, the leading edge connecting their origins can be approximated as a straight line as $R \rightarrow \infty$.

The intersection between circle 1 and circle 2 is found as follows:

Rearranging (E.1) and (E.2) gives:

$$r^2 - y^2 = R^2 - (y + R)^2$$

Hence

$$y = \frac{r^2}{-2R}$$

Which due to $R \rightarrow \infty$

$$\lim_{R \rightarrow \infty} y = 0$$

Plugging into (E.1) gives us:

$$x = r$$

Therefore intersection point between circles 1 and 2 is

$$(r, 0)$$

The intersection between circle 1 and circle 3 is found as follows:

Rearranging (E.1) gives:

$$y^2 + 2Ry + x^2 = 0$$

Using the quadratic equation in terms of y gives:

$$y = \frac{-2R \pm \sqrt{(2R)^2 - 4x^2}}{2}$$

Which

$$\lim_{R \rightarrow \infty} y = \frac{-2R \pm \sqrt{(2R)^2}}{2} = 0$$

Therefore by assuming $y \approx 0$ and plugging into (E.3) and rearranging gives:

$$x^2 + 2xhr + h^2r^2 - r^2 = 0$$

Which can be factorised as:

$$(-x + r + hr)(-x - r + hr) = 0$$

Hence

$$x = (h \pm 1)r$$

As we know that the point of intersection between circle 1 and circle 3 is on the left side of circle 3, x must equal: $(h - 1)r$

Therefore intersection point between circles 1 and 3 is

$$((h - 1)r, 0)$$

The intersection between circle 2 and circle 3 is found as follows:

Rearranging (E.2) gives:

$$r^2 - x^2 = y^2$$

Substituting this into (E.3) and rearranging gives

$$x = \frac{hr}{2}$$

Plugging x into (E.2) and rearranging gives us

$$y = \frac{r}{2} \sqrt{(4 - h^2)}$$

Therefore intersection point between circles 2 and 3 is

$$\left(\frac{hr}{2}, \frac{r}{2} \sqrt{(4 - h^2)} \right)$$

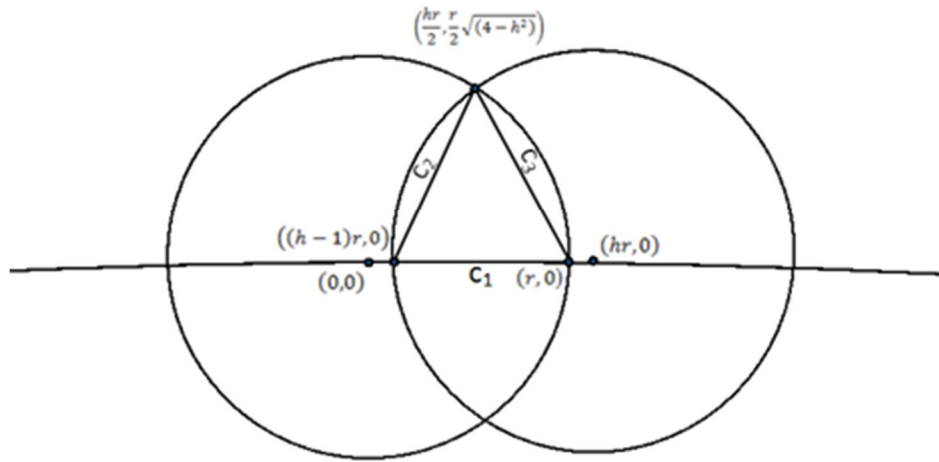


Figure E.2: An illustration of the chords and intersection points for the overlapping area between two circles.

From these intersection points, we calculate by Pythagoras the length of the chords as shown in figure E.1 intersection points:

$$c_1 = \sqrt{(r - (h-1)r)^2 + (0 - 0)^2} = (2-h)r$$

$$c_2 = \sqrt{\left(\frac{hr}{2} - r\right)^2 + \left(\frac{r}{2}\sqrt{4-h^2} - 0\right)^2} = \sqrt{2r^2 - hr^2} = \sqrt{(2-h)r^2}$$

$$c_3 = \sqrt{\left(\frac{hr}{2} - (h-1)r\right)^2 + \left(\frac{r}{2}\sqrt{4-h^2} - 0\right)^2} = \sqrt{2r^2 - hr^2} = \sqrt{(2-h)r^2}$$

We conceptually approximate the asymptotic overlap of circle 2 with circle 1; we first consider that by taking into account the limit as $R \rightarrow \infty$, and thereby assuring $R \gg r$, the line connecting the two neighbouring individuals is assumed to be as close to a straight line as possible. As circle 2 lies along the circumference of the circle 1, the area of overlap can be assumed to be approximately half the area covered by the focal individual.

$$\lim_{R \rightarrow \infty} Area_{overlap} \approx \frac{\pi}{2} r^2$$

Using the chord lengths above, the asymptotic overlap between two neighbouring individuals can be found by plugging into theorem E.2:

$$\begin{aligned}
Area_{overlap\ between\ neighbours} &= Area_{triangle} + \sum_{k=1}^3 (Area_{circular\ section\ k}) \\
&= \frac{1}{4} \sqrt{(c_1 + c_2 + c_3)(c_2 + c_3 - c_1)(c_1 + c_3 - c_2)(c_1 + c_2 - c_3)} \\
&\quad + \sum_{k=1}^3 \left(r_k^2 \arcsin \frac{c_k}{2r_k} - \frac{c_k}{4} \sqrt{4r_k^2 - c_k^2} \right)
\end{aligned}$$

The first part we calculate is the central triangle section of the circular triangle:

$$Area_{triangle} = \frac{1}{4} \sqrt{(c_1 + c_2 + c_3)(c_2 + c_3 - c_1)(c_1 + c_3 - c_2)(c_1 + c_2 - c_3)}$$

Plugging in c_1, c_2 and c_3 , this becomes:

$$\frac{1}{4} \sqrt{-r^4(h+2)(h-2)^3}$$

The second part we calculate are the three lens shaped circular sections between the central triangle and the edge of the circular triangle:

$$Area_{circular\ section\ k} = \sum_{k=1}^3 \left(r_k^2 \arcsin \frac{c_k}{2r_k} - \frac{c_k}{4} \sqrt{4r_k^2 - c_k^2} \right)$$

For circle 1 (i.e. $k=1$), due to the assumption of the leading edge being suitably approximated by a straight line between the origins of three individuals along the leading edge, we can assume that equation $Area_{circular\ section\ 1}$ is ≈ 0 . For circles 2 and 3, we know that both r_2 and r_3 are the same; similarly both c_2 and c_3 are the same length.

Consequently, we only need to consider the case for $k=2$.

$$\begin{aligned}
Area_{circular\ section\ 2} &= \left(r_2^2 \arcsin \frac{c_2}{2r_2} - \frac{c_2}{4} \sqrt{4r_2^2 - c_2^2} \right) \\
&= \left(r^2 \arcsin \left(\frac{\sqrt{(2-h)r^2}}{2r} \right) - \frac{\sqrt{(2-h)r^2}}{4} \sqrt{4r^2 - (2-h)r^2} \right) \\
&= r^2 \arcsin \left(\frac{\sqrt{(2-h)}}{2} \right) - \frac{1}{4} \sqrt{(2-h)r^2} \sqrt{(2+h)r^2}
\end{aligned}$$

Therefore, the circular triangle of overlap between two neighbouring individuals along the leading edge is given by:

$Area_{circular\ triangle}$

$$= Area_{triangle} + Area_{circular\ section\ 1} + Area_{circular\ section\ 2} \\ + Area_{circular\ section\ 3}$$

$$= \frac{1}{4}\sqrt{-r^4(h+2)(h-2)^3} + 2r^2 \arcsin\left(\frac{\sqrt{(2-h)}}{2}\right) - \frac{1}{2}\sqrt{(2-h)r^2}\sqrt{(2+h)r^2}$$

Together, by equation (E.1), this gives the asymptotic fitness of individuals along the leading edge as:

$$\lim_{R \rightarrow \infty} (\omega) \approx \pi r^2 - \frac{1}{2}\pi r^2 \\ - \left(\frac{1}{4}\sqrt{(r^4(2+h)(2-h)^3)} + 2r^2 \sin^{-1}\left(\frac{\sqrt{(2-h)}}{2}\right) \right. \\ \left. - \frac{1}{2}\sqrt{r^2(2-h)}\sqrt{(2+h)r^2} \right)$$

Appendix F: Proof of values in table 6.2

First, we set up the problem as follows: consider a population centred at $(0, 0)$ with a circular shape of spread of radius R . We consider individuals and their circle of influence to be represented by circles of radius r along the leading edge such that they overlap with each other. Without loss of generality, we consider the cases of two individuals, who may or may not be actively dispersing, originally situated at points $(R, 0)$ and $(R\cos(\theta), R\sin(\theta))$. Note $\theta = \frac{2\pi}{n}$, where $n = \frac{2\pi R}{hr}$. Therefore θ may also be equal to $\frac{hr}{R}$.

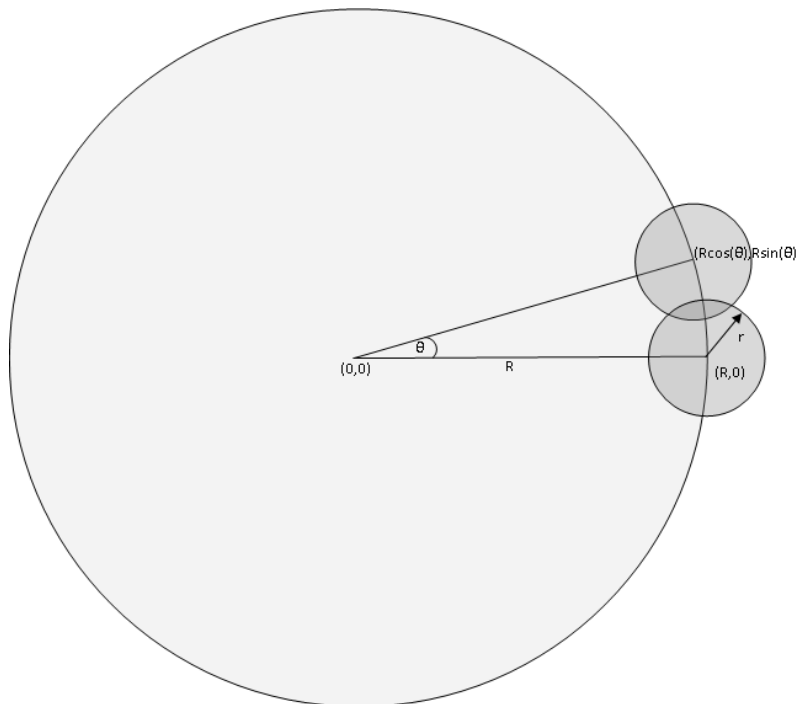


Figure F.1: The main population of radius R with two individuals of radius r , situated along the leading edge.

For each of the following proofs, values are substituted into theorem F.1 from the previous chapter unless otherwise stated.

Theorem F.1: The area of the lens-shaped intersection between two circles of different radii r_i, r_j , is calculated as:

*Area*_{intersection between two circles}

$$= r_i^2 \cos^{-1} \left(\frac{d^2 + r_i^2 - r_j^2}{2dr_i} \right) + r_j^2 \cos^{-1} \left(\frac{d^2 + r_j^2 - r_i^2}{2dr_j} \right) - \frac{1}{2} \sqrt{(-d + r_i + r_j)(d - r_i + r_j)(d + r_i - r_j)(d + r_i + r_j)}$$

Where d is the distance between the centres of the two circles. Note that for an intersection to exist the following must hold $0 \leq d \leq r_i + r_j$.

Corollary F.2: Overlap between dispersing individual and main population equals zero when $m = r$.

Proof F.2: For this situation, circle 1 represents the main population and circle 2 represents an individual along the leading edge. Consequently, $r_1 = R$, $r_2 = r$ and the distance between the origins of the two circles is represented by $d = R + m$, where m is the extra movement of the disperser. Substituting into theorem F.1 gives:

*Area*_{intersection between two circles}

$$= R^2 \cos^{-1} \left(\frac{(R + m)^2 + R^2 - r^2}{2(R + m)R} \right) + r^2 \cos^{-1} \left(\frac{(R + m)^2 + r^2 - R^2}{2(R + m)r} \right) - \frac{1}{2} \sqrt{(m + 2R + r)(m + 2R - r)(r + m)(r - m)}$$

By substituting $m = r$, this becomes:

$$= R^2 \cos^{-1} \left(\frac{2R^2 + 2rR}{2(R + r)R} \right) + r^2 \cos^{-1} \left(\frac{2r^2 + 2rR}{2(R + r)r} \right) = R^2 \cos^{-1} \left(\frac{R + r}{(R + r)} \right) + r^2 \cos^{-1} \left(\frac{R + r}{(R + r)} \right) = 0$$

Therefore, if $m \geq r$, there is no overlap between the individual and the main population.

Corollary F.3: Overlap between a dispersing individual and a neighbour non-dispersing individual:

$$m = R \cos \left(\frac{rh}{R} \right) - R + \sqrt{R^2 \cos \left(\frac{hr}{R} \right) - R^2 + 4r^2}$$

Proof F.3: Using the fact that the Cartesian coordinates of the two individuals $(R,0)$ and $(R\cos(\theta),R\sin(\theta))$ can be transformed into the polar coordinates, $(R,0)$ and (R, θ) respectively. By assuming the circle with origin $(r,0)$ represents a dispersing individual, we can represent it's positive with movement as $(R + m, 0)$. Consequently, the distance between the two points, d , can be represented with Pythagoras as:

$$d = \sqrt{R^2 + (R + m)^2 - 2R(R + m) \cos\left(\frac{hr}{R}\right)}$$

With $r_1 = r_2 = r$

Substituting r_1 and r_2 into theorem F.1 gives:

$$2r^2 \cos^{-1}\left(\frac{d}{2r}\right) - \frac{1}{2}\sqrt{(d + 2r)(d^2)(2r - d)}$$

Then plugging in d gives:

$$\begin{aligned} & 2r^2 \cos^{-1}\left(\frac{\sqrt{R^2 + (R + m)^2 - 2R(R + m) \cos\left(\frac{hr}{R}\right)}}{2r}\right) \\ & - \frac{1}{2}\left(\left(2R^2 + 2Rm + m^2 - 2R^2 \cos\left(\frac{hr}{R}\right) - 2R \cos\left(\frac{hr}{R}\right)\right)\right. \\ & \left. \times \left(2Rm \cos\left(\frac{hr}{R}\right) + 2R^2 \cos\left(\frac{hr}{R}\right) - 2R^2 - 2Rm - m^2 + 4r^2\right)\right)^{\frac{1}{2}} \end{aligned}$$

Isolating the first part of this equation and solving for m gives the solutions:

$$R\cos\left(\frac{hr}{R}\right) - R \pm \sqrt{R^2 \cos^2\left(\frac{hr}{R}\right) - R^2 + 4r^2}$$

which we assume the plus/minus sign is a plus sign, as m must be positive in order to move radially outwards in the way we have structured the problem. Substituting this into the second part of the equation, we find that it can simplify to:

$$2\sqrt{-r^2(\sqrt{r^2+r})(\sqrt{r^2-r})}$$

which equals zero, therefore:

$$m = R \cos\left(\frac{rh}{R}\right) - R + \sqrt{R^2 \cos\left(\frac{hr}{R}\right) - R^2 + 4r^2}$$

is a solution of the problem whereby if movement is greater or equal to m , the overlap is eliminated. We now find a general proof for two dispersing individuals.

Corollary F.4: Overlap between 2 dispersing individuals moving different distances

$$m = R \cos\left(\frac{hr}{R}\right) + M \cos\left(\frac{hr}{R}\right) - R \pm \sqrt{(R+M)^2 \cos\left(\frac{hr}{R}\right)^2 - (R+M)^2 - M^2 + 4r^2}$$

Moreover, the overlap between two dispersing individuals moving same distance as each other

$$m = \frac{R \cos\left(\frac{rh}{R}\right) - R + \sqrt{2r^2 - 2r^2 \cos\left(\frac{hr}{R}\right)}}{1 - \cos\left(\frac{rh}{R}\right)}$$

Proof F.4: We approach this the same way as in proof F.3; the circle representing individual one is centred at $(R+m, 0)$, Where m represents the dispersal of individual one and the circle representing individual two is centred at $(R+M, \theta)$, Where M represents the dispersal of individual two. Consequently, the distance between the two at any one time can be represented as

$$d = \sqrt{(R+m)^2 + (R+M)^2 - 2(R+m)(R+M) \cos\left(\frac{hr}{R}\right)}$$

Similar to proof F.3, substituting $r_1 = r_2 = r$ and d into theorem F.1 gives:

$$\begin{aligned}
&= 2r^2 \cos^{-1} \left(\frac{\sqrt{(R+m)^2 + (R+M)^2 - 2(R+m)(R+M) \cos\left(\frac{hr}{R}\right)}}{2r} \right) - \\
&\frac{1}{2} \left(- \left(2R^2 + 2Rm + m^2 + 2RM + M^2 - 2R^2 \cos\left(\frac{hr}{R}\right) \right. \right. \\
&\quad \left. \left. - 2RM \cos\left(\frac{hr}{R}\right) - 2Rm \cos\left(\frac{hr}{R}\right) - 2mM \cos\left(\frac{hr}{R}\right) \right) \right. \\
&\quad \left. \times \left(2R^2 + 2Rm + m^2 + 2RM + M^2 - 2R^2 \cos\left(\frac{hr}{R}\right) \right. \right. \\
&\quad \left. \left. - 2RM \cos\left(\frac{hr}{R}\right) - 2Rm \cos\left(\frac{hr}{R}\right) - 2mM \cos\left(\frac{hr}{R}\right) - 4r^2 \right) \right)^{\frac{1}{2}}
\end{aligned}$$

Isolating the first part of this equation and solving for m gives the solutions,

$$m = R \cos\left(\frac{hr}{R}\right) + M \cos\left(\frac{hr}{R}\right) - R \pm \sqrt{(R+M)^2 \cos\left(\frac{hr}{R}\right)^2 - (R+M)^2 - M^2 + 4r^2}$$

which we assume the plus/minus sign is a plus sign, as m must be positive in order to move radially outwards in the way we have structured the problem.

Substituting this into the second part of the equation, we find that it equals 0, therefore,

$$m = R \cos\left(\frac{hr}{R}\right) + M \cos\left(\frac{hr}{R}\right) - R + \sqrt{(R+M)^2 \cos\left(\frac{hr}{R}\right)^2 - (R+M)^2 - M^2 + 4r^2}$$

Special case: Consequently the overlap between 2 dispersing individuals moving same distance as each other is the special case when $M = m$.

Substituting this into m above gives:

$$m = R \cos\left(\frac{hr}{R}\right) + m \cos\left(\frac{hr}{R}\right) - R + \sqrt{(R+m)^2 \cos\left(\frac{hr}{R}\right)^2 - (R+m)^2 - m^2 + 4r^2}$$

This can be rearranged as:

$$m = \frac{R \cos\left(\frac{rh}{R}\right) - R + \sqrt{2r^2 - 2r^2 \cos\left(\frac{hr}{R}\right)}}{1 - \cos\left(\frac{rh}{R}\right)}$$

Appendix G - Collision detection for IBM model used in Chapter 7

Assuming individuals move at a constant velocity, in a straight line and do not change the radius of their circle of influence, we can detect if collision occurs between two individuals as follows (note we use halo to describe the radius of a circle of influence):

For individuals p and q , let p_0 and q_0 be their initial position and p_f and q_f be their position after movement assuming no collision occurs. We can represent the linear trajectory of each individual as a pair of linear parametric functions p_t and q_t :

$$p_t = p_0 + t(p_f - p_0)$$

$$q_t = q_0 + t(q_f - q_0)$$

Where t represents the time at which collision occurs. If collision occurs, then $0 < t < 1$.

We calculate the distance between the two trajectories at time t by calculating the Euclidean distance between p_t and q_t minus the sum of the halo radii (We assume each individual has a halo size, r).

$$d(t) = |p_t - q_t| - (2r)$$

If collision occurs then $\exists t \mid d(t)=0$, i.e. $|p_t - q_t| = (2r)$. Therefore:

$$0 = \sqrt{(p(t) - q(t))^2} - 2r$$

$$2r^2 = (p(t) - q(t))^2$$

$$2r^2 = (p_0 + t(p_f - p_0) - q_0 + t(q_f - q_0))^2$$

$$2r^2 = \left((p_0 - q_0) + t \left((p_f - p_0) - (q_f - q_0) \right) \right)^2$$

Let $\Delta p = p_f - p_0$ and $\Delta q = q_f - q_0$

$$2r^2 = \left((p_0 - q_0) + t(\Delta p - \Delta q) \right)^2$$

$$0 = t^2(\Delta p - \Delta q) \cdot (\Delta p - \Delta q) + (2t(p_0 - q_0) \cdot (\Delta p - \Delta q)) + (p_0 - q_0) \cdot (p_0 - q_0) - 2r^2$$

Solving for t:

$$t = \frac{-b \pm \sqrt{b^2 - 4ac}}{2a}$$

Where:

$$a = (\Delta p - \Delta q) \cdot (\Delta p - \Delta q)$$

$$b = 2(p_0 - q_0) \cdot (\Delta p - \Delta q)$$

$$c = (p_0 - q_0) \cdot (p_0 - q_0) - 2r^2$$

Collision occurs when $b^2 - 4ac \geq 0$ and t is between 0 and 1. If there exists more than one root of t between 0 and 1, then the lower one is taken to be the point of collision.

Appendix H – Sensitivity analysis of proposed IBM model in Chapter 7

The following Appendix describes the effect of changing the default parameters for the IBM model in Chapter 7 (i.e. the sensitivity of results upon initial parameters of the system). We list the parameters used in this section in table H.1. We found that whilst the quantitative results changed (i.e. the number of individuals or the range of dispersal costs at which different patterns are produced), the qualitative behaviour of the model did not change according to the parameters of the system. Note that all results are for the averaged values after five runs of the model with the probability of mutation = 0.1.

Table H.1: The parameters used in this appendix to examine the sensitivity of results produced by the individual based model shown in Chapter 7 on initial parameters

Parameter set	Circle of influence radius	Initial radius of population	Dispersal distance by active dispersers	Dispersal distance of non-active dispersers	Allowed overlap between individuals
Default	0.0025	0.01	0.0002	0.0001	1.2
A1	0.0017	0.01	0.0002	0.0001	1.2
B1	0.0037	0.01	0.0002	0.0001	1.2
A2	0.0025	0.05	0.0002	0.0001	1.2
B2	0.0025	0.005	0.0002	0.0001	1.2
A3	0.0025	0.01	0.00015	0.0001	1.2
B3	0.0025	0.01	0.0003	0.0001	1.2
A4	0.0025	0.01	0.0002	0.00004	1.2
B4	0.0025	0.01	0.0002	0.0001	1.2
A5	0.0025	0.01	0.0002	0.0001	1.5

Changing the radius of each individual's circle of influence

Compared to the results of the system based on the default parameters, we first found that decreasing the radius of each individual's circle of influence, increased the number of individuals situated along the leading edge of the main population due to each individual occupying less space along the leading edge of the population (Figure H.1). Secondly, by decreasing the radius of each individual's circle of influence, we found that our derived fitness measurement (see Chapter 7) decreased across all dispersal costs. This was presumably because of either each individual being able to sequester less of the area outside of the confines of the population without competition or because curvature had a larger effect on individuals with smaller radii (Figure H.1).

However, the models still exhibited the same patterns of spread as those produced by the default parameters. The same patterns also emerged as the circle of influence's radius increases, however the number of individuals decreased and the derived measure of fitness increased (Figure H.1). We notice that there was only a small change to the proportion of actively vs non-actively dispersing individuals situated along the leading edge of the population (with this change possibly as a result of the model only being run 5 times rather than the 25 times for the original parameters), suggesting results were consistent regardless of the radius of the circle of influence.

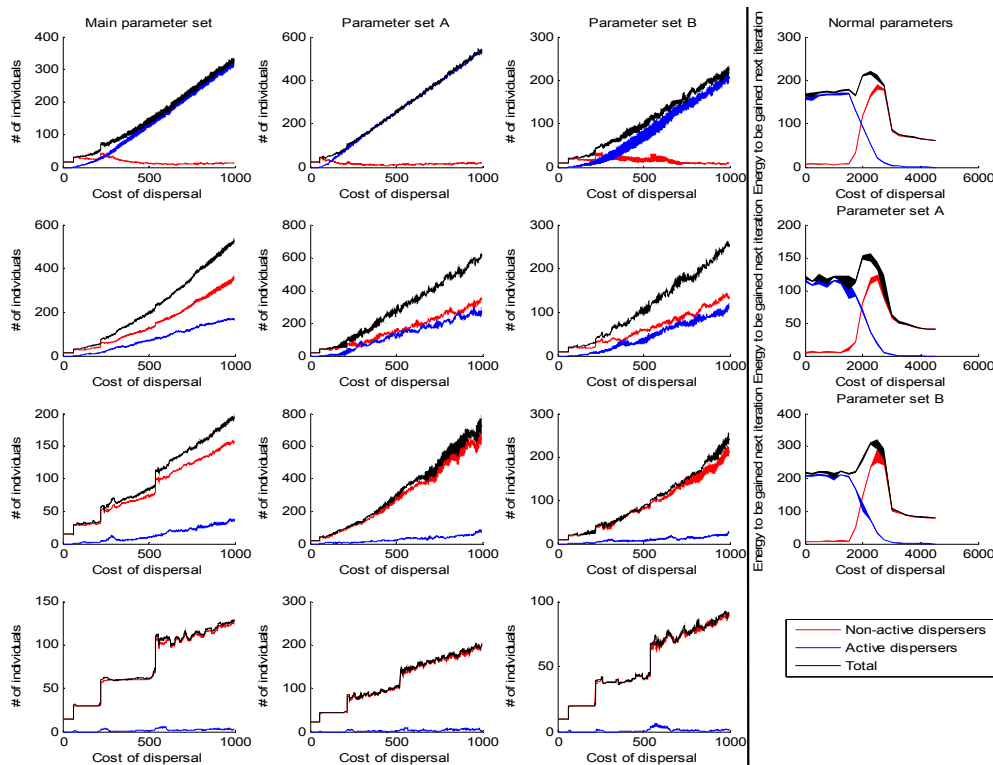


Figure H.1: Left side of black line - The total number of individuals, the number of non-actively and the number actively dispersing individuals situated along leading edge across 1000 iterations for dispersal cost coefficient = 500 (1st row), 2000 (2nd row), 2500 (3rd row) and 3500 (4th row). This is for the original circle of influence radius parameter value used in Chapter 7 (1st column), a smaller radius (2nd column) and a larger radius (3rd column). Right side of figure – The total energy/fitness obtained by individuals in the next iteration as well as the energy/fitness obtained by individuals with the non-actively and actively dispersing phenotype. This is for dispersal costs ranging between 0 and 4500. On the top row is the energy obtainable for the normal circle of influence radius, 2nd row is the energy obtainable for a smaller radius and the 3rd row is the energy obtainable for a larger radius.

Changing the starting radius of the main population

Compared to the results of the system based on the default parameters, we first found that by changing the radius of the population, the initial number of individuals along the leading edge changes (Figure H.2). Specifically as the starting radius of the population increased, the initial number of individual increased and vice versa as the starting radius of the population decreased. A consequence of this is that as the initial radius of the main population increased, the number of iterations required before a deterministic reproduction event occurred also increased because of the decreased curvature of the main population resulting in it taking longer for space to open up along the leading edge of the population. This meant it took longer for the system to reach the eventual asymptotic proportion between non-actively and actively dispersing individuals. The derived fitness measure showed a small increase in fitness as the initial radius increased and a decrease as the initial radius decreased (Figure H.2). We theorised this result occurred due to the increased initial radius resulting in typically more individuals. This factor had a small effect upon the pattern of spread in the short term, but in the long term, we found that the patterns of spread corresponding to the cost of dispersal were consistent with those seen in the default case. We note a difference in the 3rd row between the default parameters and the new parameters, notably an increase in the long-term number of individuals. Further investigation suggested this occurred due to the stochasticity of the system and the relatively low number of repeats conducted for this appendix.

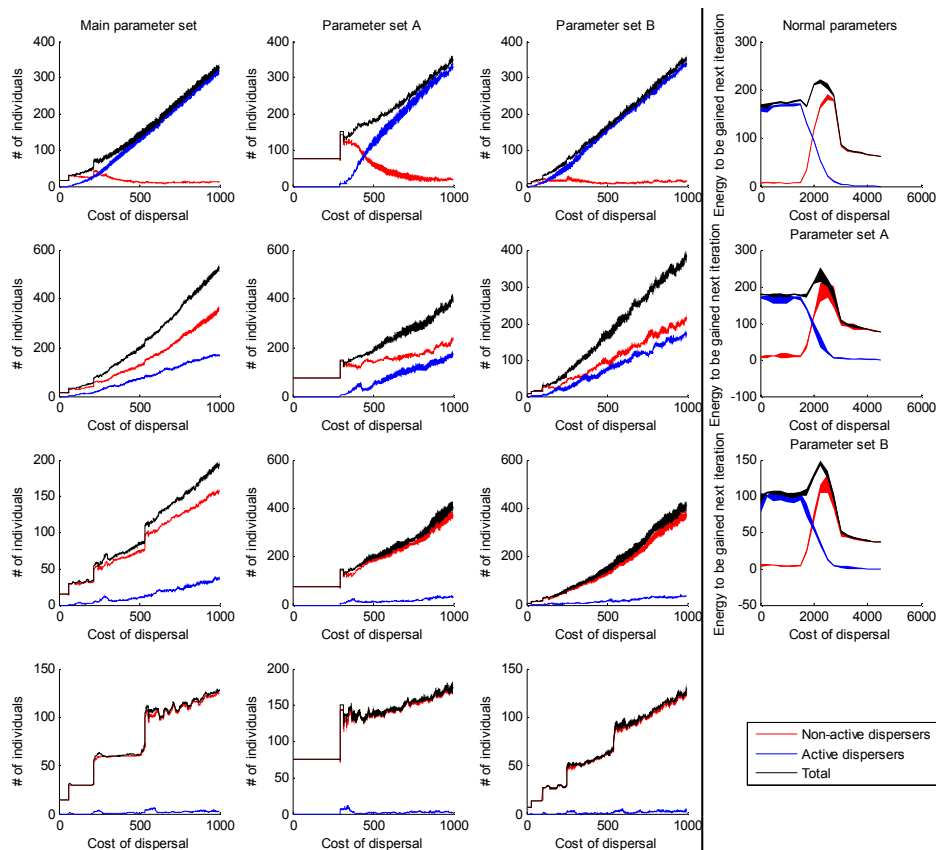


Figure H.2: Same as figure H.1 but for the initial population radius parameter value used in Chapter 7 (1st column), a larger radius (2nd column) and a smaller radius (3rd column).

Changing the movement distance of active dispersers only

Compared to the results of the system based on the default parameters, we found that changing the distance moved by actively dispersing individuals affected the range of dispersal costs at which different patterns of spread occurred. For instance, as the movement distance of actively dispersing individuals increased, the range of intermediate dispersal cost values for which tendrill patterns were exhibited, decreased (and vice versa when the movement distance decreased), as did the range at which circular patterns with a leading edge consisting of active dispersers. Alternatively, the range at which the model exhibited circular patterns with a leading edge consisting of non-active dispersers increased (the converse was also true for when the active dispersal distance decreased). This was because of the increased dispersal costs experienced by actively dispersing individuals, combined with an increased cost of reproduction. This increased reproduction cost was due to an increased number of reproduction events resulting from the increased dispersal distance

(such an effect meant that as the distance increased, it was quicker for the system to reach the asymptotic proportions of dispersers and non-dispersers compared to default parameters and conversely slower as the dispersal distance decreased). Consequently, as the distance of the active disperser increased, the active disperser was more advantageous for a smaller range of dispersal costs (and more advantageous for a larger range of dispersal costs as the distance of the active disperser decreased). Additional observations are that our derived measure of fitness had a higher peak as the distance moved by active dispersers increased (presumably due to the increased number of individuals) and the total number of individuals peaked at lower dispersal costs as the distance increased due to the change at where different spatial patterns are produced (Figure H-3). The converse was true for when the distance decreased.

Changing the movement distance of non-actively and actively dispersing individuals.

Compared to the results of the system based on the default parameters, we found that changing the distance moved by non-actively dispersing individuals led to results similar to those for when only the distance moved by actively dispersing individuals changed. The main observable difference between these results was the distinct change in dispersal costs at which the model exhibits certain spatial patterns. For instance, if the distance moved by non-actively dispersing individuals increased, then non-actively dispersing individuals suffered a decreased fitness compared to those in a system with default parameters (the converse was true for non-actively dispersing individuals moving a decreased distance). Due to the non-actively dispersing phenotype acting as the default phenotype in the system, as it became less viable as the dispersal distance increased, the peak value of our derived fitness value occurred at a lower cost of dispersal compared to the default parameters (Figure H.4) and vice versa as the distance of dispersal decreased. As a result, the region of dispersal costs for each type of pattern arising was significantly lowered as the non-active dispersal distance increased (and vice versa), including the point at which all individuals along the leading edge died out. Consequently, in Figure H.4, for the cost of dispersal = 3500, the model fails and all individuals died out.

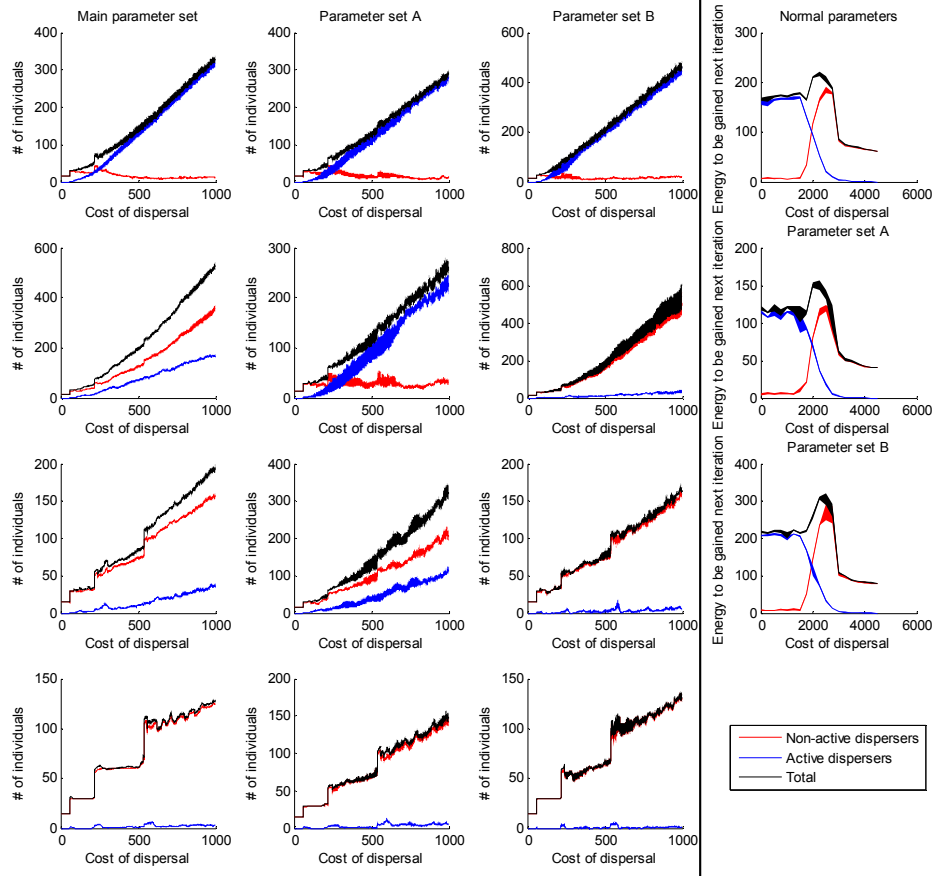


Figure H.3: Same as figure H.1 but for the parameter representing the distance moved by an active disperser value used in Chapter 7 (1st column), a smaller distance (2nd column) and a larger distance (3rd column).

Changing the allowed distance between individuals along leading edge

We found that the number of individuals changed (as the amount of overlap tolerate decreased, the number of individuals also decreased) but there was otherwise no major change to the characteristics of the system i.e. our derived fitness measurement and proportion of active dispersers vs non-active dispersers (Figure H.5). We note there was a slight change between the transition points between circular patterns at low costs of dispersal and tendrill patterns at intermediate costs of dispersal. Similarly, there was a slight change between the transition points between tendrill patterns at intermediate costs of dispersal and circular patterns at high costs of dispersal.

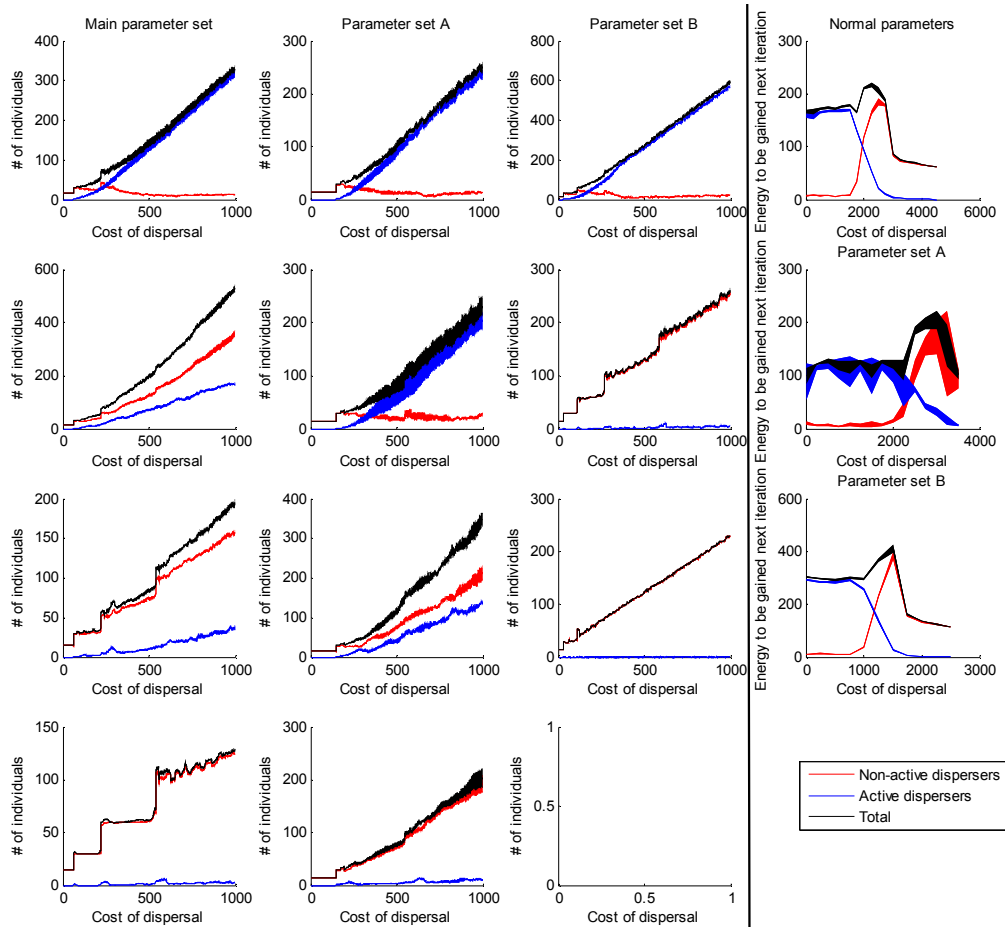


Figure H.4: Same as figure H.1 but for the system parameter representing the distance moved by a non- active disperser value used in Chapter 7 (1st column), a smaller distance (2nd column) and a larger distance (3rd column).

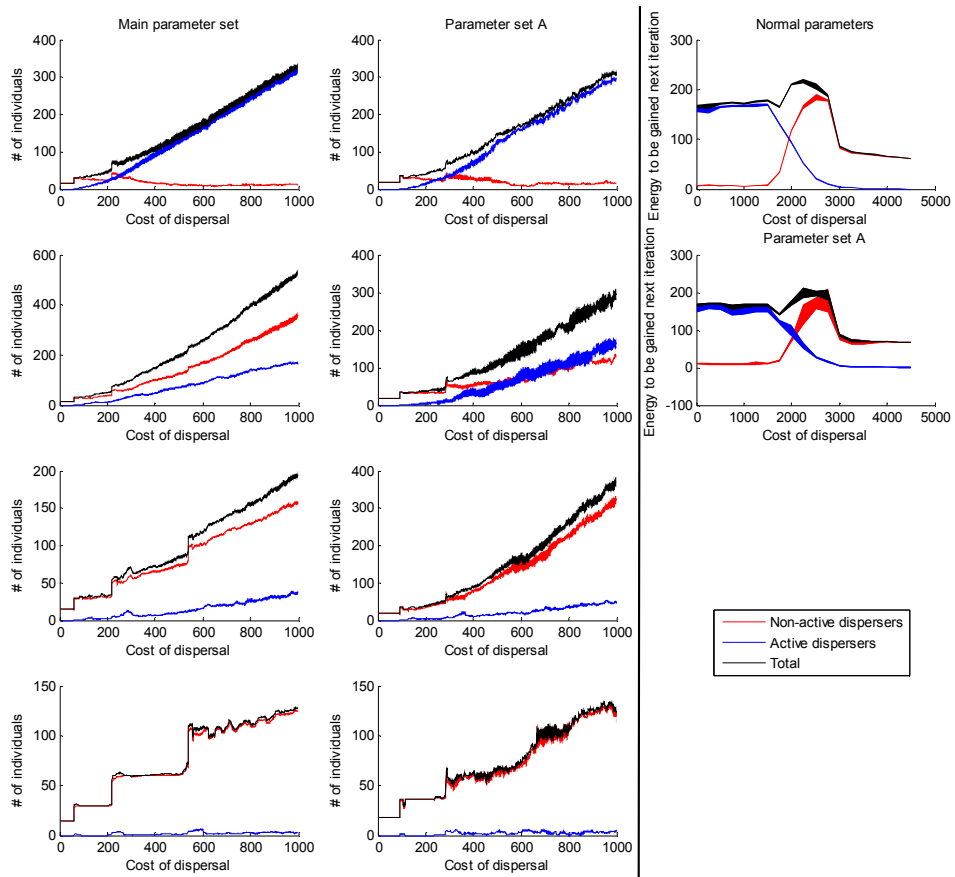


Figure H.5: Same as figure H.1 but for the allowed overlap parameter value used in Chapter 7 (1st column) and a smaller amount of allowed overlap (2nd column).

Appendix I – Classification algorithm/criteria in Chapter 7

We used the following criteria to classify the patterns produced by the null and proposed models in Chapter 7.

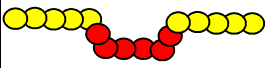
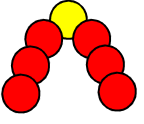
Shape

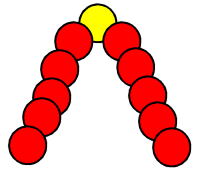
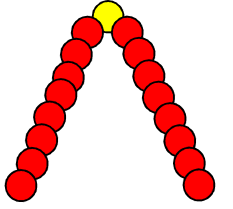
To classify the shape according to table 7.3, we used the ratio of individuals along the leading edge with an actively dispersing phenotype to individuals along the leading edge with a non-actively dispersing phenotype at iteration 1000 (Table I.1). We further clarified the pattern classification by checking whether the pattern met certain visual criteria such as the length of the tendril in terms of the number of individuals (as specified in table I.1).

Wrinkles

To classify the wrinkles of the shape according to table 7.4, we counted the number of wrinkles by eye. We defined wrinkles as the number of lines of individuals going from the leading edge of the colony towards the centre, whereby lines of individuals consist of three or more trapped individuals.

Table I.1: The first part of the pattern categorisation describing the spatial pattern of spread for those scenarios involving mutation.

Code	Classification	Percentage of individuals that are active $\alpha = P(\text{mutation in } \%)$		Visual observation that must be met for classification	Example picture
		Minimum % of active individuals	Maximum % of active individuals		
Cn	Circle	0 %	0 %	No mutations survive and edge consists purely of non-dispersers	See table 7.3
Fc	Flowery Circle	100%	100%	Active dispersal phenotype takes hold and occupies whole leading edge.	See table 7.3
FwG	Flowery circle with intermittent gaps	$(\alpha + 5)\%$	$(100 - (\alpha + 5))\%$	There must exist at least two gaps of such a length that the leading edge can consist of at least 4 individuals with one phenotype, followed by at least 4 individuals with the other phenotype, followed again by at least 4 individuals with the original phenotype	
Mn	Mostly non-dispersing	0%	$(\alpha + 5)\%$	Apart from occasional mutations, edge consists of almost entirely non-dispersers	See table 7.3
Md	Mostly dispersing	$(100 - (\alpha + 5))\%$	100%	Apart from occasional mutations, edge consists of almost entirely dispersers	See table 7.3
I	Irregular/no clear majority	$(\alpha + 5)\%$	$(100 - (\alpha + 5))\%$	Seemingly a mix of both dispersers and non-dispersers	See table 7.3
vST	Very small tendrils	0%	$(\alpha + 15)\%$	Exhibits at least 3 tendrils whereby a dispersing individual has 3 non-actively dispersing individuals either side of it along the leading edge	

ST	Small tendrils	0%	$(\alpha + 15)\%$	Exhibits at least 3 tendrils whereby a dispersing individual has 5 non-actively dispersing individuals either side of it along the leading edge	
LT	Large tendrils	0%	$(\alpha + 15)\%$	Exhibits at least 3 tendrils whereby a dispersing individual has 8 non-actively dispersing individuals either side of it along the leading edge	
D	Death		N/A	No Individuals exist	

References

- ACKERMANN, M., STEARNS, S. C. & JENAL, U. 2003. Senescence in a bacterium with asymmetric division. *Science*, 300, 1920-1920.
- AKÇAKAYA, H. R., MILLS, G. & DONCASTER, C. P. 2007. The role of metapopulations in conservation. *Key topics in conservation biology*, 64-84.
- ALFORD, R. A., BROWN, G. P., SCHWARZKOPF, L., PHILLIPS, B. L. & SHINE, R. 2009. Comparisons through time and space suggest rapid evolution of dispersal behaviour in an invasive species. *Wildlife Research*, 36, 23-28.
- ALLSTADT, A., CARACO, T. & KORNISS, G. 2007. Ecological invasion: spatial clustering and the critical radius. *Evolutionary Ecology Research*, 9, 375-394.
- ANDOW, D. A., KAREIVA, P. M., LEVIN, S. A. & OKUBO, A. 1990. Spread of invading organisms. *Landscape Ecology*, 4, 177-188.
- ANDOW, D. A., KAREIVA, P. M., LEVIN, S. A. & OKUBO, A. 1993. Spread of invading organisms: patterns of spread. In: KIM KC, M. B. (ed.) *Evolution of insect pests: patterns of variation*. New York: Wiley.
- ARIM, M., ABADES, S. R., NEILL, P. E., LIMA, M. & MARQUET, P. A. 2006. Spread dynamics of invasive species. *Proceedings of the National Academy of Science*, 103, 374-8.
- AYATI, B. P. 2006. A structured-population model of *Proteus mirabilis* swarm-colony development. *Journal of Mathematical Biology*, 52, 93-114.
- BAILEY, S. F., DETTMAN, J. R., RAINEY, P. B. & KASSEN, R. 2013. Competition both drives and impedes diversification in a model adaptive radiation. *Proceedings of the Royal Society of London B: Biological Sciences*, 280, 20131253.
- BARBER, S. & MACKAY, A. 1986. Root growth and phosphorus and potassium uptake by two corn genotypes in the field. *Fertilizer research*, 10, 217-230.
- BARRAQUAND, F. & MURRELL, D. J. 2012. Intense or Spatially Heterogeneous Predation Can Select against Prey Dispersal. *PLoS One*, 7, e28924.
- BE'ER, A., SMITH, R. S., ZHANG, H. P., FLORIN, E. L., PAYNE, S. M. & SWINNEY, H. L. 2009. Paenibacillus dendritiformis Bacterial Colony Growth Depends on Surfactant but Not on Bacterial Motion. *Journal of Bacteriology*, 191, 5758-5764.
- BEALE, C. M. & LENNON, J. J. 2012. Incorporating uncertainty in predictive species distribution modelling. *Philosophical Transactions of the Royal Society B: Biological Sciences*, 367, 247-258.
- BEEES, M. A., ANDRESEN, P., MOSEKILDE, E. & GIVSKOV, M. 2002. Quantitative effects of medium hardness and nutrient availability on the swarming motility of *Serratia liquefaciens*. *Bulletin of Mathematical Biology*, 64, 565-587.
- BEN-JACOB, E., COHEN, I. & GUTNICK, D. L. 1998. Cooperative organization of bacterial colonies: From genotype to morphotype. *Annual Review of Microbiology*, 52, 779-806.
- BEN-JACOB, E., COHEN, I. & LEVINE, H. 2000. Cooperative self-organization of microorganisms. *Advances in Physics*, 49, 395-554.
- BEN-JACOB, E. & LEVINE, H. 2006. Self-engineering capabilities of bacteria. *Journal of the Royal Society Interface*, 3, 197-214.

- BEN-JACOB, E., SCHOCHET, O., TENENBAUM, A., COHEN, I., CZIROK, A. & VICSEK, T. 1994. Generic modeling of cooperative growth-patterns in bacterial colonies. *Nature*, 368, 46-49.
- BERTHOULY-SALAZAR, C., VAN RENSBURG, B. J., LE ROUX, J. J., VAN VUUREN, B. J. & HUI, C. 2012. Spatial Sorting Drives Morphological Variation in the Invasive Bird, *Acridotheris tristis*. *PLoS One*, 7.
- BEYENAL, H., TANYOLAÇ, A. & LEWANDOWSKI, Z. 1998. Measurement of local effective diffusivity in heterogeneous biofilms. *Water Science and Technology*, 38, 171-178.
- BONABEAU, E. 2002. Agent-based modeling: Methods and techniques for simulating human systems. *Proceedings of the National Academy of Sciences of the United States of America*, 99, 7280-7287.
- BONTE, D., VAN DYCK, H., BULLOCK, J. M., COULON, A., DELGADO, M., GIBBS, M., LEHOUCQ, V., MATTHYSEN, E., MUSTIN, K. & SAASTAMOINEN, M. 2012. Costs of dispersal. *Biological reviews*, 87, 290-312.
- BOWLER, D. E. & BENTON, T. G. 2005. Causes and consequences of animal dispersal strategies: relating individual behaviour to spatial dynamics. *Biological Reviews*, 80, 205-225.
- BRADING, M. G., BOYLE, J. & LAPPINSCOTT, H. M. 1995. Biofilm formation in laminar-flow using *Pseudomonas Fluorescens* EX101. *Journal of Industrial Microbiology*, 15, 297-304.
- BRAMSON, M. 1983. Convergence of solutions of the Kolmogorow equation to traveling waves. *Memoirs of the American Mathematical Society*, 44, 1-190.
- BROWN, G. P., SHILTON, C., PHILLIPS, B. L. & SHINE, R. 2007. Invasion, stress, and spinal arthritis in cane toads. *Proceedings of the National Academy of Sciences of the United States of America*, 104, 17698-17700.
- BUCKLING, A., CRAIG MACLEAN, R., BROCKHURST, M. A. & COLEGRAVE, N. 2009. The Beagle in a bottle. *Nature*, 457, 824-9.
- BUDRENE, E. O. & BERG, H. C. 1991. Complex patterns formed by motile cells of *Escherichia coli*. *Nature*, 349, 630.
- CAIAZZA, N. C., SHANKS, R. M. Q. & O'TOOLE, G. A. 2005. Rhamnolipids modulate swarming motility patterns of *Pseudomonas aeruginosa*. *Journal of Bacteriology*, 187, 7351-7361.
- CAIN, M. L., MILLIGAN, B. G. & STRAND, A. E. 2000. Long-distance seed dispersal in plant populations. *American Journal of Botany*, 87, 1217-1227.
- CAREY, J. R. 1991. Establishment of the Mediterranean fruit fly in California. *Science*, 253, 1369-1373.
- CARPENTER, S. R. 1996. Microcosm experiments have limited relevance for community and ecosystem ecology. *Ecology*, 77, 677-680.
- CASELLAS, E., GAUTRAIS, J., FOURNIER, R., BLANCO, S., COMBE, M., FOURCASSIÉ, V., THERAULAZ, G. & JOST, C. 2008. From individual to collective displacements in heterogeneous environments. *Journal of Theoretical Biology*, 250, 424-434.
- CASPER, B. B. & JACKSON, R. B. 1997. Plant competition underground. *Annual Review of Ecology and Systematics*, 545-570.
- CASWELL, H., LENSINK, R. & NEUBERT, M. G. 2003. Demography and dispersal: life table response experiments for invasion speed. *Ecology*, 84, 1968-1978.

- CERRETI, F., PERTHAME, B., SCHMEISER, C., TANG, M. & VAUCHELET, N. 2011. Waves for a hyperbolic Keller–Segel model and branching instabilities. *Mathematical Models and Methods in Applied Sciences*, 21, 825-842.
- CHAPMAN, D. S., DYTHAM, C. & OXFORD, G. S. 2007. Modelling population redistribution in a leaf beetle: an evaluation of alternative dispersal functions. *Journal of Animal Ecology*, 76, 36-44.
- CHETEHOUNA, K., ER-RIANI, M. & SERO-GUILLAUME, O. 2004. On the rate of spread for some reaction-diffusion models of forest fire propagation. *Numerical Heat Transfer: Part A-Applications*, 46, 765-784.
- CIOSI, M., MILLER, N., TOEPFER, S., ESTOUP, A. & GUILLEMAUD, T. 2011. Stratified dispersal and increasing genetic variation during the invasion of Central Europe by the western corn rootworm, *Diabrotica virgifera virgifera*. *Evolutionary Applications*, 4, 54-70.
- CLARK, J. S. 1998. Why trees migrate so fast: Confronting theory with dispersal biology and the paleorecord. *American Naturalist*, 152, 204-224.
- CLARK, J. S., LEWIS, M. & HORVATH, L. 2001. Invasion by extremes: Population spread with variation in dispersal and reproduction. *American Naturalist*, 157, 537-554.
- CLAVERO, M. & GARCIA-BERTHOUE, E. 2005. Invasive species are a leading cause of animal extinctions. *Trends in Ecology & Evolution*, 20, 110-110.
- COMINS, H. N., HAMILTON, W. D. & MAY, R. M. 1980. Evolutionarily stable dispersal strategies. *Journal of Theoretical Biology*, 82, 205-230.
- COOMBS, E. M. C., J. K. AND PIPER, G. L. 2004. *Biological Control of Invasive Plants in the United States*, Oregon, Oregon State University Press.
- COOPER, A., DEAN, A. & HINSHELWOOD, C. 1968. Factors affecting the growth of bacterial colonies on agar plates. *Proceedings of the Royal Society of London. Series B. Biological Sciences*, 171, 175-199.
- CREED JR, R. & MILLER, J. 1990. Interpreting animal wall-following behavior. *Experientia*, 46, 758-761.
- CRESPI, B. J. 2001. The evolution of social behavior in microorganisms. *Trends in Ecology & Evolution*, 16, 178-183.
- CROOKS, J. A. 2005. Lag times and exotic species: the ecology and management of biological invasions in slow-motion. *Ecoscience*, 12, 316-329.
- CROOKS, J. A., SOULÉ, M. E., SANDLUND, O., SCHEI, P. & VIKEN, A. 1999. Lag times in population explosions of invasive species: causes and implications. *Invasive species and biodiversity management*, 103-125.
- CUMMING, G. 2002. Habitat shape, species invasions, and reserve design: Insights from simple models. *Conservation Ecology*, 6.
- CWYNAR, L. C. & MACDONALD, G. M. 1987. Geographical variation of lodgepole pine in relation to population history. *American Naturalist*, 129, 463-469.
- D'ANTONIO, C. M., JACKSON, N. E., HORVITZ, C. C. & HEDBERG, R. 2004. Invasive plants in wildland ecosystems: merging the study of invasion processes with management needs. *Frontiers in Ecology and the Environment*, 2, 513-521.
- DANELL, K. 1996. Introductions of aquatic rodents: lessons of the muskrat *Ondatra zibethicus* invasion. *Wildlife Biology*, 2, 213-220.
- DARWIN, C. 1859. *The Origin of Species*, London, John Murray.

- DAVEY, M. E. & O'TOOLE, G. A. 2000. Microbial biofilms: from ecology to molecular genetics. *Microbiology and Molecular Biology Reviews*, 64, 847-+.
- DAWKINS, R. 1976. *The Selfish Gene*, Oxford University Press.
- DAY, K. J., JOHN, E. A. & HUTCHINGS, M. J. 2003. The effects of spatially heterogeneous nutrient supply on yield, intensity of competition and root placement patterns in *Briza media* and *Festuca ovina*. *Functional Ecology*, 17, 454-463.
- DE BENTZMANN, S. & PLÉSIAT, P. 2011. The *Pseudomonas aeruginosa* opportunistic pathogen and human infections. *Environmental Microbiology*, 13, 1655-1665.
- DE DORLODOT, S., FORSTER, B., PAGÈS, L., PRICE, A., TUBEROSA, R. & DRAYE, X. 2007. Root system architecture: opportunities and constraints for genetic improvement of crops. *Trends in Plant Science*, 12, 474-481.
- DE MEESTER, N., DERYCKE, S., RIGAUX, A. & MOENS, T. 2014. Active dispersal is differentially affected by inter- and intraspecific competition in closely related nematode species. *Oikos*.
- DE VARGAS RODITI, L., BOYLE, K. E. & XAVIER, J. B. 2013. Multilevel selection analysis of a microbial social trait. *Molecular Systems Biology*, 9.
- DEANGELIS, D. L. & MOOIJ, W. M. 2005. Individual-based modeling of ecological and evolutionary processes. *Annual Review of Ecology, Evolution, and Systematics*, 147-168.
- DÉBARRE, F., HAUERT, C. & DOEBELI, M. 2014. Social evolution in structured populations. *Nature Communications*, 5.
- DECHESNE, A. & SMETS, B. F. 2012. *Pseudomonas* swarming motility is restricted to a narrow range of high matric water potentials. *Applied and Environmental Microbiology*, 78, 2936-2940.
- DENG, P., DE VARGAS RODITI, L., VAN DITMARSCH, D. & XAVIER, J. B. 2014. The ecological basis of morphogenesis: branching patterns in swarming colonies of bacteria. *New Journal of Physics*, 16, 015006.
- DÉZIEL, E., COMEAU, Y. & VILLEMUR, R. 2001. Initiation of biofilm formation by *Pseudomonas aeruginosa* 57RP correlates with emergence of hyperpilated and highly adherent phenotypic variants deficient in swimming, swarming, and twitching motilities. *Journal of Bacteriology*, 183, 1195-1204.
- DOEBELI, M. 1995. Dispersal and dynamics. *Theoretical Population Biology*, 47, 82-106.
- DOEBELI, M. & HAUERT, C. 2005. Models of cooperation based on the Prisoner's Dilemma and the Snowdrift game. *Ecology Letters*, 8, 748-766.
- DU, H., XU, Z., SHROUT, J. D. & ALBER, M. 2011. Multiscale modeling of *Pseudomonas aeruginosa* swarming. *Mathematical Models and Methods in Applied Sciences*, 21, 939-954.
- DUNGAN, J. L., PERRY, J. N., DALE, M. R. T., LEGENDRE, P., CITRON-POUSTY, S., FORTIN, M. J., JAKOMULSKA, A., MIRITI, M. & ROSENBERG, M. S. 2002. A balanced view of scale in spatial statistical analysis. *Ecography*, 25, 626-640.
- DYKHUIZEN, D. E. & DEAN, A. M. 1990. Enzyme activity and fitness: evolution in solution. *Trends in Ecology & Evolution*, 5, 257-262.
- EHRlich, G. D., STOODLEY, P., KATHJU, S., ZHAO, Y., MCLEOD, B. R., BALABAN, N., HU, F. Z., SOTEREANOS, N. G., COSTERTON, J. W. &

- STEWART, P. S. 2005. Engineering approaches for the detection and control of orthopaedic biofilm infections. *Clinical Orthopaedics and Related Research*, 59.
- EL MOUDEN, C. & GARDNER, A. 2008. Nice natives and mean migrants: the evolution of dispersal-dependent social behaviour in viscous populations. *Journal of Evolutionary Biology*, 21, 1480-1491.
- ELLIOTT, E. C. & CORNELL, S. J. 2012. Dispersal polymorphism and the speed of biological invasions. *PLoS One*, 7, e40496.
- ELLNER, S. P. & SCHREIBER, S. J. 2012. Temporally variable dispersal and demography can accelerate the spread of invading species. *Theoretical Population Biology*, 82, 283-298.
- ESIPOV, S. E. & SHAPIRO, J. A. 1998. Kinetic model of *Proteus mirabilis* swarm colony development. *Journal of Mathematical Biology*, 36, 249-268.
- FACON, B. & DAVID, P. 2006. Metapopulation dynamics and biological invasions: a spatially explicit model applied to a freshwater snail. *The American Naturalist*, 168, 769-783.
- FEWELL, M. 2006. Area of common overlap of three circles. DTIC Document.
- FISHER, R. A. 1930. *The genetical theory of natural selection*. , Oxford Oxford University Press.
- FISHER, R. A. 1937. The wave of advance of advantageous genes. *Annual of Eugenics*, 7, 353-369.
- FOSTER, K. R., SHAULSKY, G., STRASSMANN, J. E., QUELLER, D. C. & THOMPSON, C. R. 2004. Pleiotropy as a mechanism to stabilize cooperation. *Nature*, 431, 693-696.
- FRANSEN, B., DE KROON, H. & BERENDSE, F. 2001. Soil nutrient heterogeneity alters competition between two perennial grass species. *Ecology*, 82, 2534-2546.
- FRANZÉN, M. & NILSSON, S. G. 2010. Both population size and patch quality affect local extinctions and colonizations. *Proceedings of the Royal Society B: Biological Sciences*, 277, 79-85.
- FRONHOFER, E. A., KUBISCH, A., HILKER, F. M., HOVESTADT, T. & POETHKE, H. J. 2012. Why are metapopulations so rare? *Ecology*, 93, 1967-1978.
- FUJIKAWA, H. & MATSUSHITA, M. 1989. Fractal growth of *Bacillus-subtilis* on agar plates. *Journal of the Physical Society of Japan*, 58, 3875-3878.
- FUNK, J. L. 2008. Differences in plasticity between invasive and native plants from a low resource environment. *Journal of Ecology*, 96, 1162-1173.
- GANDON, S. 1999. Kin competition, the cost of inbreeding and the evolution of dispersal. *Journal of Theoretical Biology*, 200, 345-364.
- GANDON, S. & MICHALAKIS, Y. 1999. Evolutionarily stable dispersal rate in a metapopulation with extinctions and kin competition. *Journal of Theoretical Biology*, 199, 275-290.
- GARDNER, A., WEST, S. A. & BARTON, N. H. 2007. The relation between multilocus population genetics and social evolution theory. *The American Naturalist*, 169, 207-226.
- GILBERT, M. & LIEBHOLD, A. 2010. Comparing methods for measuring the rate of spread of invading populations. *Ecography*, 33, 809-817.
- GILPIN, M. 1990. Biological Invasions - A global perspective. *Science*, 248, 88-89.

- GLEN, A. S., PECH, R. P. & BYROM, A. E. 2013. Connectivity and invasive species management: towards an integrated landscape approach. *Biological Invasions*, 15, 2127-2138.
- GNEITING, T., KLEIBER, W. & SCHLATHER, M. 2010. Matern Cross-Covariance Functions for Multivariate Random Fields. *Journal of the American Statistical Association*, 105, 1167-1177.
- GODFRAY, H. C. J. & REES, M. 2002. Population growth rates: issues and an application. *Philosophical Transactions of the Royal Society of London Series B-Biological Sciences*, 357, 1307-1319.
- GOLDING, I., KOZLOVSKY, Y., COHEN, I. & BEN-JACOB, E. 1998. Studies of bacterial branching growth using reaction-diffusion models for colonial development. *Physica A-Statistical Mechanics and Its Applications*, 260, 510-554.
- GOROCHOWSKI, T. E., MATYJASZKIEWICZ, A., TODD, T., OAK, N., KOWALSKA, K., REID, S., TSANEVA-ATANASOVA, K. T., SAVERY, N. J., GRIERSON, C. S. & DI BERNARDO, M. 2012. BSim: an agent-based tool for modeling bacterial populations in systems and synthetic biology. *Plos One*, 7, e42790.
- GRIFFIN, A. S., WEST, S. A. & BUCKLING, A. 2004. Cooperation and competition in pathogenic bacteria. *Nature*, 430, 1024-1027.
- GRIMM, V. 1999. Ten years of individual-based modelling in ecology: what have we learned and what could we learn in the future? *Ecological Modelling*, 115, 129-148.
- GRIMM, V., BERGER, U., BASTIANSEN, F., ELIASSEN, S., GINOT, V., GISKE, J., GOSS-CUSTARD, J., GRAND, T., HEINZ, S. K. & HUSE, G. 2006. A standard protocol for describing individual-based and agent-based models. *Ecological Modelling*, 198, 115-126.
- GRIMM, V., BERGER, U., DEANGELIS, D. L., POLHILL, J. G., GISKE, J. & RAILSBACK, S. F. 2010. The ODD protocol: a review and first update. *Ecological Modelling*, 221, 2760-2768.
- GRIMM, V. & RAILSBACK, S. F. 2013. *Individual-based modeling and ecology*, Princeton university press.
- GROSHOLZ, E. D. & RUIZ, G. M. 1996. Predicting the impact of introduced marine species: Lessons from the multiple invasions of the European green crab *Carcinus maenas*. *Biological Conservation*, 78, 59-66.
- GUREVITCH, J. & PADILLA, D. K. 2004. Are invasive species a major cause of extinctions? *Trends in Ecology & Evolution*, 19, 470-474.
- HAMILTON, W. D. 1964. Genetical Evolution of Social Behaviour I. *Journal of Theoretical Biology*, 7.
- HAMZE, K., AUTRET, S., HINC, K., LAALAMI, S., JULKOWSKA, D., BRIANDET, R., RENAULT, M., ABSALON, C., HOLLAND, I. B. & PUTZER, H. 2011. Single-cell analysis in situ in a *Bacillus subtilis* swarming community identifies distinct spatially separated subpopulations differentially expressing hag (flagellin), including specialized swimmers. *Microbiology*, 157, 2456-2469.
- HANERT, E. 2012. Front dynamics in a two-species competition model driven by Lévy flights. *Journal of Theoretical Biology*, 300, 134-142.
- HANFLING, B. & KOLLMANN, J. 2002. An evolutionary perspective of biological invasions. *Trends in Ecology and Evolution*, 17, 545-546.
- HANSKI, I. 1994. A practical model of metapopulation dynamics. *Journal of Animal Ecology*, 151-162.
- HANSKI, I. 1998. Metapopulation dynamics. *Nature*, 396, 41-49.

- HANSKI, I. & GILPIN, M. 1991. Metapopulation dynamics: brief history and conceptual domain. *Biological journal of the Linnean Society*, 42, 3-16.
- HANSKI, I., PAKKALA, T., KUUSSAARI, M. & LEI, G. 1995. Metapopulation persistence of an endangered butterfly in a fragmented landscape. *Oikos*, 21-28.
- HARRISON, S. 1991. Local extinction in a metapopulation context: an empirical evaluation. *Biological journal of the Linnean Society*, 42, 73-88.
- HARSHEY, R. M. 2003. Bacterial motility on a surface: Many ways to a common goal. *Annual Review of Microbiology*, 57, 249-273.
- HASTINGS, A. 1996. Models of spatial spread: Is the theory complete? *Ecology*, 77, 1675-1679.
- HASTINGS, A., CUDDINGTON, K., DAVIES, K. F., DUGAW, C. J., ELMENDORF, S., FREESTONE, A., HARRISON, S., HOLLAND, M., LAMBRINOS, J., MALVADKAR, U., MELBOURNE, B. A., MOORE, K., TAYLOR, C. & THOMSON, D. 2005. The spatial spread of invasions: new developments in theory and evidence. *Ecology Letters*, 8, 91-101.
- HAUERT, C., HOLMES, M. & DOEBELI, M. 2006. Evolutionary games and population dynamics: maintenance of cooperation in public goods games. *Proceedings of the Royal Society B: Biological Sciences*, 273, 2565-2571.
- HECTOR, A., JOSHI, J., LAWLER, S. P., SPEHN, E. M. & WILBY, A. 2001. Conservation implications of the link between biodiversity and ecosystem functioning. *Oecologia*, 129, 624-628.
- HEMINGWAY, J., FIELD, L. & VONTAS, J. 2002. An overview of insecticide resistance. *Science*, 298, 96-97.
- HENGEVELD, R. 1989. *Dynamics of biological invasions*.
- HENRICH, J. 1972. Bacterial surface translocation - Survey and a classification. *Bacteriological Reviews*, 36, 478-503.
- HIBBING, M. E., FUQUA, C., PARSEK, M. R. & PETERSON, S. B. 2010. Bacterial competition: surviving and thriving in the microbial jungle. *Nature Reviews Microbiology*, 8, 15-25.
- HIGGINS, S. & RICHARDSON, D. 1996. A review of models of alien plant spread. *Ecological modelling*, 87, 249-265.
- HIRAMATSU, F., WAKITA, J.-I., KOBAYASHI, N., YAMAZAKI, Y., MATSUSHITA, M. & MATSUYAMA, T. 2005. Patterns of Expansion produced by a Structured Cell Population of *Serratia marcescens* in Response to Different Media. *Microbes and Environments*, 20, 120-125.
- HOCHBERG, M. S. & FOLKMAN, J. 1972. Mechanism of size limitation of bacterial colonies. *Journal of Infectious Diseases*, 126, 629-635.
- HODGSON, D. J., RAINEY, P. B. & BUCKLING, A. 2002. Mechanisms linking diversity, productivity and invasibility in experimental bacterial communities. *Proceedings of the Royal Society B-Biological Sciences*, 269, 2277-2283.
- HODGSON, J. A., THOMAS, C. D., DYTHAM, C., TRAVIS, J. M. & CORNELL, S. J. 2012. The speed of range shifts in fragmented landscapes. *PLoS One*, 7, e47141.
- HOLT, A. 1998. Hawaii's reptilian nightmare. *World conservation*, 31.
- HOLT, R. D., M. BARFIELD, AND R. GOMULKIEWICZ 2005. Theories of niche conservatism and evolution. In: D. F. SAX, J. J. S., AND S. D. GAINES (ed.) *Species invasions: insights into ecology, evolution, and biogeography*. Sunderland, MA.: Sinauer.

- HOOPER, D. U., CHAPIN, F. S., EWEL, J. J., HECTOR, A., INCHAUSTI, P., LAVOREL, S., LAWTON, J. H., LODGE, D. M., LOREAU, M., NAEEM, S., SCHMID, B., SETALA, H., SYMSTAD, A. J., VANDERMEER, J. & WARDLE, D. A. 2005. Effects of biodiversity on ecosystem functioning: A consensus of current knowledge. *Ecological Monographs*, 75, 3-35.
- HORVÁTH, D., PETROV, V., SCOTT, S. K. & SHOWALTER, K. 1993. Instabilities in propagating reaction-diffusion fronts. *The Journal of Chemical Physics*, 98, 6332-6343.
- HOURY, A., BRIANDET, R., AYMERICH, S. & GOHAR, M. 2010. Involvement of motility and flagella in *Bacillus cereus* biofilm formation. *Microbiology*, 156, 1009-1018.
- HUGHES, T. P., BAIRD, A. H., BELLWOOD, D. R., CARD, M., CONNOLLY, S. R., FOLKE, C., GROSBERG, R., HOEGH-GULDBERG, O., JACKSON, J. B. C., KLEYPAS, J., LOUGH, J. M., MARSHALL, P., NYSTROM, M., PALUMBI, S. R., PANDOLFI, J. M., ROSEN, B. & ROUGHGARDEN, J. 2003. Climate change, human impacts, and the resilience of coral reefs. *Science*, 301, 929-933.
- HÜLS, J. 2005. *Populationsbiologische Untersuchung von *Heracleum mantegazzianum* Somm. et Lev. in Subpopulationen unterschiedlicher Individuendichte*. Universitätsbibliothek Giessen.
- HUTCHINGS, J. A. 1991. Fitness consequences of variation in egg size and food abundance in brook trout *Salvelinus fontinalis*. *Evolution*, 1162-1168.
- INNOCENT, T., ABE, J., WEST, S. & REECE, S. 2010. Competition between relatives and the evolution of dispersal in a parasitoid wasp. *Journal of evolutionary biology*, 23, 1374-1385.
- JACKSON, L. J., TREBITZ, A. S. & COTTINGHAM, K. L. 2000. An introduction to the practice of ecological modeling. *Bioscience*, 50, 694-706.
- JESSUP, C. M., KASSEN, R., FORDE, S. E., KERR, B., BUCKLING, A., RAINEY, P. B. & BOHANNAN, B. J. M. 2004. Big questions, small worlds: microbial model systems in ecology. *Trends in Ecology & Evolution*, 19, 189-197.
- JOHNSEN, K. & NIELSEN, P. 1999. Diversity of *Pseudomonas* strains isolated with King's B and Gould's S1 agar determined by repetitive extragenic palindromic polymerase chain reaction, 16S rDNA sequencing and Fourier transform infrared spectroscopy characterisation. *Fems Microbiology Letters*, 173, 155-162.
- JOHNSON, M. L. & GAINES, M. S. 1990. Evolution of dispersal: theoretical models and empirical tests using birds and mammals. *Annual review of ecology and systematics*, 449-480.
- JOHNSON, M. T. & STINCHCOMBE, J. R. 2007. An emerging synthesis between community ecology and evolutionary biology. *Trends in Ecology & Evolution*, 22, 250-257.
- JULKOWSKA, D., OBUCHOWSKI, M., HOLLAND, I. B. & SEROR, S. J. 2005. Comparative analysis of the development of swarming communities of *Bacillus subtilis* 168 and a natural wild type: Critical effects of surfactin and the composition of the medium. *Journal of Bacteriology*, 187, 65-76.
- JULKOWSKA, D., OBUCHOWSKI, M., HOLLAND, I. B. & SÉROR, S. J. 2004. Branched swarming patterns on a synthetic medium formed by wild-type *Bacillus subtilis* strain 3610: detection of different cellular morphologies and constellations of cells as the complex architecture develops. *Microbiology*, 150, 1839-1849.

- KAMATKAR, N. G., SARNA, M. J. & SHROUT, J. D. 2011. Population dynamics during swarming of *Pseudomonas aeruginosa*. *Communicative & Integrative Biology*, 4, 689.
- KAMATKAR, N. G. & SHROUT, J. D. 2011. Surface hardness impairment of quorum sensing and swarming for *Pseudomonas aeruginosa*. *PLoS One*, 6, e20888.
- KASSEN, R., BUCKLING, A., BELL, G. & RAINEY, P. B. 2000. Diversity peaks at intermediate productivity in a laboratory microcosm. *Nature*, 406, 508-512.
- KAWASAKI, K., MOCHIZUKI, A., MATSUSHITA, M., UMEDA, T. & SHIGESADA, N. 1997. Modeling spatio-temporal patterns generated by *Bacillus subtilis*. *Journal of Theoretical Biology*, 188, 177-185.
- KEARNS, D. B. 2010. A field guide to bacterial swarming motility. *Nature Reviews Microbiology*, 8, 634-644.
- KEARNS, D. B. & LOSICK, R. 2003. Swarming motility in undomesticated *Bacillus subtilis*. *Molecular Microbiology*, 49, 581-590.
- KELLER, E. F. & SEGEL, L. A. 1970. Initiation of slime mold aggregation viewed as an instability. *Journal of Theoretical Biology*, 26, 399-415.
- KELLER, R. P., LODGE, D. M. & FINNOFF, D. C. 2007. Risk assessment for invasive species produces net bioeconomic benefits. *Proceedings of the National Academy of Sciences of the United States of America*, 104, 203-207.
- KENDALL, B. E. & FOX, G. A. 1998. Spatial structure, environmental heterogeneity, and population dynamics: analysis of the coupled logistic map. *Theoretical population biology*, 54, 11-37.
- KERR, B., RILEY, M. A., FELDMAN, M. W. & BOHANNAN, B. J. M. 2002. Local dispersal promotes biodiversity in a real-life game of rock-paper-scissors. *Nature*, 418, 171-174.
- KESSLER, D. A. & LEVINE, H. 1998. Fluctuation-induced diffusive instabilities. *Nature*, 394, 556-558.
- KILLINGBACK, T. & DOEBELI, M. 1996. Spatial evolutionary game theory: Hawks and Doves revisited. *Proceedings of the Royal Society of London. Series B: Biological Sciences*, 263, 1135-1144.
- KIM, W., KILLAM, T., SOOD, V. & SURETTE, M. G. 2003. Swarm-cell differentiation in *Salmonella enterica serovar Typhimurium* results in elevated resistance to multiple antibiotics. *Journal of Bacteriology*, 185, 3111-3117.
- KIM, W., RACIMO, F., SCHLUTER, J., LEVY, S. B. & FOSTER, K. R. 2014. Importance of positioning for microbial evolution. *Proceedings of the National Academy of Sciences*, 111, E1639-E1647.
- KING, E. O., WARD, M. K. & RANEY, D. E. 1954. Simple media for the demonstration of pyocyanin and fluorescin. *Journal of Laboratory and Clinical Medicine*, 44, 301-307.
- KITSUNEZAKI, S. 1997. Interface dynamics for bacterial colony formation. *Journal of the Physical Society of Japan*, 66, 1544-1550.
- KOKKO, H. & LOPEZ-SEPULCRE, A. 2006. From individual dispersal to species ranges: Perspectives for a changing world. *Science*, 313, 789-791.
- KOLAR, C. S. & LODGE, D. M. 2001. Progress in invasion biology: predicting invaders. *Trends in Ecology & Evolution*, 16, 199-204.
- KOLMOGOROV, A., PETROVSKII, I. & PISCOUNOV, N. 1937. A study of the diffusion equation with increase in the amount of substance, and its

- application to a biological problem. *Byulleten Moskovskogo Universitet*, 1, 1-25.
- KOROLEV, K. S., XAVIER, J. B. & GORE, J. 2014. Turning ecology and evolution against cancer. *Nature Reviews Cancer*, 14, 371-380.
- KOT, M., LEWIS, M. A. & VANDENDRIESSCHE, P. 1996. Dispersal data and the spread of invading organisms. *Ecology*, 77, 2027-2042.
- KOZLOVSKY, Y., COHEN, I., GOLDING, I. & BEN-JACOB, E. 1999. Lubricating bacteria model for branching growth of bacterial colonies. *Physical Review E*, 59, 7025-7035.
- KREFT, J.-U. 2004. Biofilms promote altruism. *Microbiology*, 150, 2751-2760.
- KREFT, J. U., PICIOREANU, C., WIMPENNY, J. W. T. & VAN LOOSDRECHT, M. C. M. 2001. Individual-based modelling of biofilms. *Microbiology-Sgm*, 147, 2897-2912.
- KUBISCH, A., FRONHOFER, E. A., POETHKE, H. J. & HOVESTADT, T. 2013. Kin competition as a major driving force for invasions. *The American Naturalist*, 181, 700-706.
- KÜMMERLI, R. & BROWN, S. P. 2010. Molecular and regulatory properties of a public good shape the evolution of cooperation. *Proceedings of the National Academy of Sciences*, 107, 18921-18926.
- LAWTON, J. H. 1995. Ecological experiments with model systems. *Science*, 269, 328-331.
- LEE, K. A. & KLASING, K. C. 2004. A role for immunology in invasion biology. *Trends in Ecology & Evolution*, 19, 523-529.
- LEGETT, H. C., BENMAYOR, R., HODGSON, D. J. & BUCKLING, A. 2013. Experimental evolution of adaptive phenotypic plasticity in a parasite. *Current Biology*, 23, 139-142.
- LEHMANN, L., KELLER, L., WEST, S. & ROZE, D. 2007. Group selection and kin selection: two concepts but one process. *Proceedings of the National Academy of Sciences*, 104, 6736-6739.
- LENDA, M., ZAGALSKA-NEUBAUER, M., NEUBAUER, G. & SKÓRKA, P. 2010. Do invasive species undergo metapopulation dynamics? A case study of the invasive Caspian gull, *Larus cachinnans*, in Poland. *Journal of Biogeography*, 37, 1824-1834.
- LEOTARD, G., DEBOUT, G., DALECKY, A., GUILLOT, S., GAUME, L., MCKEY, D. & KJELLBERG, F. 2009. Range Expansion Drives Dispersal Evolution In An Equatorial Three-Species Symbiosis. *PLoS One*, 4.
- LEVIN, B. R., STEWART, F. M. & CHAO, L. 1977. Resource-limited growth, competition, and predation: a model and experimental studies with bacteria and bacteriophage. *American Naturalist*, 3-24.
- LEVIN, S. A., MULLER-LANDAU, H. C., NATHAN, R. & CHAVE, J. 2003. The ecology and evolution of seed dispersal: a theoretical perspective. *Annual Review of Ecology, Evolution, and Systematics*, 575-604.
- LEVIN, S. A. A. S., L. A. . 2013. Pattern Generation in Space and Aspect *Society for Industrial and Applied Mathematics* 27, 45-67.
- LEVINE, J. M. 2000. Species diversity and biological invasions: Relating local process to community pattern. *Science*, 288, 852-854.
- LEVINS, R. 1969. Some demographic and genetic consequences of environmental heterogeneity for biological control. *Bulletin of the ESA*, 15, 237-240.
- LEVINS, R. 1970. Complex systems. *Towards a theoretical biology*, 3, 73-88.
- LEWIS, M. & KAREIVA, P. 1993. Allee dynamics and the spread of invading organisms. *Theoretical Population Biology*, 43, 141-158.

- LEWIS, M. & PACALA, S. 2000. Modeling and analysis of stochastic invasion processes. *Journal of Mathematical Biology*, 41, 387-429.
- LEYVA, J., MÁLAGA, C. & PLAZA, R. G. 2013. The effects of nutrient chemotaxis on bacterial aggregation patterns with non-linear degenerate cross diffusion. *Physica A: Statistical Mechanics and its Applications*, 392, 5644-5662.
- LIEBHOLD, A. M. & GUREVITCH, J. 2002. Integrating the statistical analysis of spatial data in ecology. *Ecography*, 25, 553-557.
- LIEBHOLD, A. M., HALVERSON, J. A. & ELMES, G. A. 1992. Gypsy moth invasion in North America: a quantitative analysis. *Journal of biogeography*, 513-520.
- LIEBHOLD, A. M. & TOBIN, P. C. 2008. Population ecology of insect invasions and their management. *Annual Review of Entomology*.
- LION, S. & BAALEN, M. V. 2008. Self-structuring in spatial evolutionary ecology. *Ecology letters*, 11, 277-95.
- LION, S., JANSEN, V. A. & DAY, T. 2011. Evolution in structured populations: beyond the kin versus group debate. *Trends in Ecology & Evolution*, 26, 193-201.
- LIU, S., LI, Y., WU, J., HUANG, D., SU, Y. & WEI, W. 2010. Spatial variability of soil microbial biomass carbon, nitrogen and phosphorus in a hilly red soil landscape in subtropical China. *Soil Science and Plant Nutrition*, 56, 693-704.
- LOCKWOOD, J. L., CASSEY, P. & BLACKBURN, T. 2005. The role of propagule pressure in explaining species invasions. *Trends in Ecology & Evolution*, 20, 223-228.
- LÓPEZ, D., VLAMAKIS, H. & KOLTER, R. 2010. Biofilms. *Cold Spring Harbor Perspectives in Biology*, 2, 398.
- LUBINA, J. A. & LEVIN, S. A. 1988. The spread of a reinvading species - range expansion in the california sea otter. *American Naturalist*, 131, 526-543.
- LYNCH, J. 1995. Root architecture and plant productivity. *Plant Physiology*, 109, 7.
- MACK, R. N., SIMBERLOFF, D., LONSDALE, W. M., EVANS, H., CLOUT, M. & BAZZAZ, F. A. 2000. Biotic invasions: Causes, epidemiology, global consequences, and control. *Ecological Applications*, 10, 689-710.
- MAGALHÃES, R. J. S., CLEMENTS, A. C., PATIL, A. P., GETHING, P. W. & BROOKER, S. 2011. The applications of model-based geostatistics in helminth epidemiology and control. *Advances in Parasitology*, 74, 267.
- MALMQVIST, B. & RUNDLE, S. 2002. Threats to the running water ecosystems of the world. *Environmental Conservation*, 29, 134-153.
- MARROCCO, A., HENRY, H., HOLLAND, I. B., PLAPP, M., SEROR, S. J. & PERTHAME, B. 2010. Models of Self-Organizing Bacterial Communities and Comparisons with Experimental Observations. *Mathematical Modelling of Natural Phenomena*, 5, 148-162.
- MARSHALL, J. A. 2011. Group selection and kin selection: formally equivalent approaches. *Trends in Ecology & Evolution*, 26, 325-332.
- MATSUSHITA, M. & FUJIKAWA, H. 1990. Diffusion-limited growth in bacterial colony formation. *Physica A*, 168, 498-506.
- MATSUSHITA, M., WAKITA, J., ITOH, H., WATANABE, K., ARAI, T., MATSUYAMA, T., SAKAGUCHI, H. & MIMURA, M. 1999. Formation of colony patterns by a bacterial cell population. *Physica A: Statistical Mechanics and its Applications*, 274, 190-199.

- MATSUYAMA, T. & MATSUSHITA, M. 1993. Fractal morphogenesis by a bacterial-cell population. *Critical Reviews in Microbiology*, 19, 117-135.
- MAY, R. M. & HAMILTON, W. D. 1977. Dispersal in stable habitats. *Nature*, 269, 578-581.
- MIGNOT, T., SHAEVITZ, J. W., HARTZELL, P. L. & ZUSMAN, D. R. 2007. Evidence that focal adhesion complexes power bacterial gliding motility. *Science*, 315, 853-856.
- MILLER, J. R. 2010. Survival of mutations arising during invasions. *Evolutionary Applications*, 3, 109-121.
- MILLER, T. E. & INOUE, B. D. 2013. Sex and stochasticity affect range expansion of experimental invasions. *Ecology letters*, 16, 354-361.
- MIMURA, M., SAKAGUCHI, H. & MATSUSHITA, M. 2000. Reaction-diffusion modelling of bacterial colony patterns. *Physica A: Statistical Mechanics and its Applications*, 282, 283-303.
- MINASNY, B. & MCBRATNEY, A. B. 2007. Spatial prediction of soil properties using EBLUP with the Matern covariance function. *Geoderma*, 140, 324-336.
- MISEVIC, D., FRÉNOY, A., LINDNER, A. B. & TADDEI, F. 2015. Shape matters: Lifecycle of cooperative patches promotes cooperation in bulky populations. *Evolution*, 69, 788-802.
- MITCHELL, A. & WIMPENNY, J. 1997. The effects of agar concentration on the growth and morphology of submerged colonies of motile and non-motile bacteria. *Journal of Applied Microbiology*, 83, 76-84.
- MONDS, R. D. & O'TOOLE, G. A. 2009. The developmental model of microbial biofilms: ten years of a paradigm up for review. *Trends in Microbiology*, 17, 73-87.
- MOTOIKE, I. N. 2007. Simple modeling of branching pattern formation in a reaction diffusion system with cellular automaton. *Journal of the Physical Society of Japan*, 76, 034002.
- MOYLE, P. B. & MARCHETTI, M. P. 2006. Predicting invasion success: freshwater fishes in California as a model. *Bioscience*, 56, 515-524.
- MURRAY, J. D. 1993. *Mathematical Biology*, Springer
- MURRAY, T. S. & KAZMIERCZAK, B. I. 2008. *Pseudomonas aeruginosa* exhibits sliding motility in the absence of type IV pili and flagella. *Journal of Bacteriology*, 190, 2700-2708.
- NADELL, C. D., FOSTER, K. R. & XAVIER, J. B. 2010. Emergence of spatial structure in cell groups and the evolution of cooperation. *PLoS computational biology*, 6, e1000716.
- NADELL, C. D., XAVIER, J. B. & FOSTER, K. R. 2009. The sociobiology of biofilms. *FEMS Microbiology Reviews*, 33, 206-224.
- NATHAN, R. 2006. Long-distance dispersal of plants. *Science*, 313, 786-788.
- NEHRBASS, N. & WINKLER, E. 2007. Is the Giant Hogweed still a threat? An individual-based modelling approach for local invasion dynamics of *Heracleum mantegazzianum*. *Ecological modelling*, 201, 377-384.
- NEILANDS, J. B. 1982. Microbial envelope proteins related to iron. *Annual Review of Microbiology*, 36, 285-309.
- NELDER, J. A. A. W., R. W. M. 1972. Generalized Linear Models. *Journal of the Royal Statistical Society. Series A (General)*, 135, 370-384.
- NEUBERT, M. G. & CASWELL, H. 2000. DEMOGRAPHY AND DISPERSAL: CALCULATION AND SENSITIVITY ANALYSIS OF INVASION SPEED FOR STRUCTURED POPULATIONS. *Ecology*, 81, 1613-1628.

- NISBET, R. M. A. G., W.S.C. 1998. *Ecological Dynamics*, Oxford Oxford University Press.
- NONAKA, E. & HOLME, P. 2007. Agent-based model approach to optimal foraging in heterogeneous landscapes: effects of patch clumpiness. *Ecography*, 30, 777-788.
- NOWAK, M. A. & MAY, R. M. 1993. The spatial dilemmas of evolution. *International Journal of bifurcation and chaos*, 3, 35-78.
- NUR, N., PAGE, G. W. & STENZEL, L. E. 1999. Population viability analysis for Pacific coast snowy plovers. *Point Reyes Bird Observatory, Stinson Beach, California*.
- O'MAY, C. & TUFENKJI, N. 2011. The swarming motility of *Pseudomonas aeruginosa* is blocked by cranberry proanthocyanidins and other tannin-containing materials. *Applied and Environmental Microbiology*, 77, 3061-3067.
- OCHSNER, U. A. & REISER, J. 1995. Autoinducer-mediated regulation of rhamnolipid biosurfactant synthesis in *Pseudomonas aeruginosa*. *Proceedings of the National Academy of Sciences of the United States of America*, 92, 6424-6428.
- OKASHA, S. 2010. Altruism researchers must cooperate. *Nature*, 467, 653-655.
- OKKOTSU, Y., TIEKU, P., FITZSIMMONS, L. F., CHURCHILL, M. E. & SCHURR, M. J. 2013. *Pseudomonas aeruginosa* AlgR phosphorylation modulates rhamnolipid production and motility. *Journal of Bacteriology*, 195, 5499-5515.
- OKUBO, A. Diffusion-type models for avian range expansion. In: CONGRESS., P. T. I. O., ed. Henri Queslet 1988. Ottawa. 1038-1049.
- OLIVER, A., CANTÓN, R., CAMPO, P., BAQUERO, F. & BLÁZQUEZ, J. 2000. High frequency of hypermutable *Pseudomonas aeruginosa* in cystic fibrosis lung infection. *Science*, 288, 1251-1253.
- OPDAM, P. & WASCHER, D. 2004. Climate change meets habitat fragmentation: linking landscape and biogeographical scale levels in research and conservation. *Biological Conservation*, 117, 285-297.
- OVASKAINEN, O. & CORNELL, S. J. 2003. Biased movement at a boundary and conditional occupancy times for diffusion processes. *Journal of Applied Probability*, 557-580.
- PEARSON, R. G. & DAWSON, T. P. 2005. Long-distance plant dispersal and habitat fragmentation: identifying conservation targets for spatial landscape planning under climate change. *Biological Conservation*, 123, 389-401.
- PECHY-TARR, M., BOTTIGLIERI, M., MATHYS, S., LEJBOLLE, K. B., SCHNIDER-KEEL, U., MAURHOFER, M. & KEEL, C. 2005. RpoN (σ^{54}) controls production of antifungal compounds and biocontrol activity in *Pseudomonas fluorescens* CHA0. *Molecular Plant-Microbe Interactions*, 18, 260-272.
- PENNEKAMP, F. & SCHANTZELLE, N. 2013. Implementing image analysis in laboratory-based experimental systems for ecology and evolution: a hands-on guide. *Methods in Ecology and Evolution*, 4, 483-492.
- PERGL, J., HÜLS, J., PERGLOVA, I., ECKSTEIN, R. L., PYŠEK, P. & OTTE, A. 2007. Population dynamics of *Heracleum mantegazzianum*. *Ecology and Management of Giant Hogweed*, 92-111.
- PERKINS, A. T., PHILLIPS, B. L., BASKETT, M. L. & HASTINGS, A. 2013. Evolution of dispersal and life history interact to drive accelerating spread of an invasive species. *Ecology Letters*, 16, 1079-1087.

- PERKINS, T. A. 2012. Evolutionarily labile species interactions and spatial spread of invasive species. *The American Naturalist*, 179, E37-E54.
- PHILLIPS, B., BROWN, G. & SHINE, R. 2010. Evolutionarily accelerated invasions: the rate of dispersal evolves upwards during the range advance of cane toads. *Journal of evolutionary biology*, 23, 2595-2601.
- PHILLIPS, B. L. 2009. The evolution of growth rates on an expanding range edge. *Biology Letters*, rsbl20090367.
- PHILLIPS, B. L., BROWN, G. P., TRAVIS, J. M. J. & SHINE, R. 2008. Reid's paradox revisited: The evolution of dispersal kernels during range expansion. *American Naturalist*, 172, S34-S48.
- PHILLIPS, B. L., BROWN, G. P., WEBB, J. K. & SHINE, R. 2006. Invasion and the evolution of speed in toads. *Nature*, 439, 803-803.
- PICHANCOURT, J.-B. & VAN KLINKEN, R. D. 2012. Phenotypic plasticity influences the size, shape and dynamics of the geographic distribution of an invasive plant. *PLoS One*, 7, e32323.
- PIMENTEL, D., LACH, L., ZUNIGA, R. & MORRISON, D. 2000. Environmental and economic costs of nonindigenous species in the United States. *Bioscience*, 50, 53-65.
- PIMENTEL, D., ZUNIGA, R. & MORRISON, D. 2005. Update on the environmental and economic costs associated with alien-invasive species in the United States. *Ecological Economics*, 52, 273-288.
- PITT-FRANCIS, J., PATHMANATHAN, P., BERNABEU, M. O., BORDAS, R., COOPER, J., FLETCHER, A. G., MIRAMS, G. R., MURRAY, P., OSBORNE, J. M. & WALTER, A. 2009. Chaste: a test-driven approach to software development for biological modelling. *Computer Physics Communications*, 180, 2452-2471.
- PRICE, G. R. 1970. Selection and covariance. *Nature*, 227, 520-21.
- PROSSER, J. I., BOHANNAN, B. J., CURTIS, T. P., ELLIS, R. J., FIRESTONE, M. K., FRECKLETON, R. P., GREEN, J. L., GREEN, L. E., KILLHAM, K. & LENNON, J. J. 2007. The role of ecological theory in microbial ecology. *Nature Reviews Microbiology*, 5, 384-392.
- PURVIS, A., GITTLEMAN, J. L., COWLISHAW, G. & MACE, G. M. 2000. Predicting extinction risk in declining species. *Proceedings of the Royal Society B-Biological Sciences*, 267, 1947-1952.
- PUTH, L. M. & POST, D. M. 2005. Studying invasion: have we missed the boat? *Ecology Letters*, 8, 715-721.
- PYKE, G. H. 1984. Optimal foraging theory: a critical review. *Annual Review of Ecology and Systematics*, 523-575.
- QUELLER, D. C. 1992. Quantitative genetics, inclusive fitness, and group selection. *American Naturalist*, 540-558.
- R DEVELOPMENT CORE TEAM 2014. R: A Language and Environment for Statistical Computing. Vienna, Austria: R Foundation for Statistical Computing.
- RAINEY, P. B. & TRAVISANO, M. 1998. Adaptive radiation in a heterogeneous environment. *Nature*, 394, 69-72.
- RAMANKUTTY, N. & FOLEY, J. A. 1999. Estimating historical changes in global land cover: Croplands from 1700 to 1992. *Global Biogeochemical Cycles*, 13, 997-1027.
- RAMSAYER, J., FELLOUS, S., COHEN, J. E. & HOCHBERG, M. E. 2012. Taylor's Law holds in experimental bacterial populations but competition does not influence the slope. *Biology Letters*, 316-319.

- RAPOPORT, A. 1965. *Prisoner's dilemma: A study in conflict and cooperation*, University of Michigan Press.
- RASBAND, W. S. 2014. ImageJ. Version 1.49a ed. Bethesda, Maryland, USA: U. S. National Institutes of Health.
- RASHID, M. H. & KORNBERG, A. 2000. Inorganic polyphosphate is needed for swimming, swarming, and twitching motilities of *Pseudomonas aeruginosa*. *Proceedings of the National Academy of Sciences of the United States of America*, 97, 4885-90.
- RAUPRICH, O., MATSUSHITA, M., WEIJER, C. J., SIEGERT, F., ESIPOV, S. E. & SHAPIRO, J. A. 1996. Periodic phenomena in *Proteus mirabilis* swarm colony development. *Journal of Bacteriology*, 178, 6525-6538.
- REISE, K., OLENIN, S. & THIELTGES, D. W. 2006. Are aliens threatening European aquatic coastal ecosystems? *Helgoland Marine Research*, 60, 77-83.
- RESASCO, J., HADDAD, N. M., ORROCK, J. L., SHOEMAKER, D., BRUDVIG, L. A., DAMSCHEN, E. I., TEWKSBURY, J. J. & LEVEY, D. J. 2014. Landscape corridors can increase invasion by an exotic species and reduce diversity of native species. *Ecology*, 95, 2033-2039.
- RICHARDSON, D. M. & PYŠEK, P. 2008. Fifty years of invasion ecology—the legacy of Charles Elton. *Diversity and Distributions*, 14, 161-168.
- RICHARDSON, D. M. & REJMANEK, M. 2004. Conifers as invasive aliens: a global survey and predictive framework. *Diversity and Distributions*, 10, 321-331.
- RICKLEFS, R. E. 2005. Historical and ecological dimensions of global patterns in plant diversity. *Kongelige Danske Videnskabernes Selskab Biologiske Skrifter*, 55, 583-603.
- ROBINET, C. & LIEBHOLD, A. M. 2009. Dispersal polymorphism in an invasive forest pest affects its ability to establish. *Ecological Applications*, 19, 1935-1943.
- RODITI, L. D. V., BOYLE, K. E. & XAVIER, J. B. 2013. Multilevel selection analysis of a microbial social trait. *Molecular Systems Biology*, 9.
- ROFF, D. A. 1992. *Evolution of life histories: theory and analysis*, Springer.
- RONCE, O. 2007. How does it feel to be like a rolling stone? Ten questions about dispersal evolution. *Annual Review of Ecology, Evolution, and Systematics*, 231-253.
- ROQUES, L., HAMEL, F., FAYARD, J., FADY, B. & KLEIN, E. 2010. Recolonisation by diffusion can generate increasing rates of spread. *Theoretical Population Biology*, 77, 205-212.
- SANCHEZ-CONTRERAS, M., MARTIN, M., VILLACIEROS, M., O'GARA, F., BONILLA, I. & RIVILLA, R. 2002. Phenotypic selection and phase variation occur during alfalfa root colonization by *Pseudomonas fluorescens* F113. *Journal of Bacteriology*, 184, 1587-1596.
- SANDERS, N. J., GOTELLI, N. J., HELLER, N. E. & GORDON, D. M. 2003. Community disassembly by an invasive species. *Proceedings of the National Academy of Sciences of the United States of America*, 100, 2474-2477.
- SANTOS, A. S., SAMPAIO, A. P. W., VASQUEZ, G. S., SANTA ANNA, L. M., PEREIRA JR, N. & FREIRE, D. M. 2002. Evaluation of different carbon and nitrogen sources in production of rhamnolipids by a strain of *Pseudomonas aeruginosa*. *Biotechnology for Fuels and Chemicals*. Springer.

- SAX, D. F., STACHOWICZ, J. J. & GAINES, S. D. 2005. *Species invasions: insights into ecology, evolution and biogeography*, Sinauer Associates Incorporated.
- SCHREIBER, S. J. & LLOYD-SMITH, J. O. 2009. Invasion dynamics in spatially heterogeneous environments. *The American Naturalist*, 174, 490-505.
- SEGER, J. 1985. Intraspecific resource competition as a cause of sympatric speciation. *Evolution: Essays in Honour of John Maynard Smith*, 43-53.
- SEMMLER, A. B., WHITCHURCH, C. B. & MATTICK, J. S. 1999. A re-examination of twitching motility in *Pseudomonas aeruginosa*. *Microbiology*, 145, 2863-2873.
- SENNET, R. 2009. London's Urban Sprawl (available at <https://www.flickr.com/photos/richardsennett/3961555659/in/photostream/>, accessed 14th December 2014).
- SEZGIN, M. 2004. Survey over image thresholding techniques and quantitative performance evaluation. *Journal of Electronic imaging*, 13, 146-168.
- SHAPIRO, J. A. 1998. Thinking about bacterial populations as multicellular organisms. *Annual Reviews in Microbiology*, 52, 81-104.
- SHAROV, A. A., LEONARD, D., LIEBHOLD, A. M. & CLEMENS, N. S. 2002. Evaluation of preventive treatments in low-density gypsy moth populations using pheromone traps. *Journal of Economic Entomology*, 95, 1205-1215.
- SHIGESADA, N. & KAWASAKI, K. 1997. *Biological invasions: theory and practice*, Oxford University Press.
- SHIGESADA, N. & KAWASAKI, K. 2002. *Invasion and the range expansion of species: effects of long-distance dispersal*.
- SHIGESADA, N., KAWASAKI, K. & TAKEDA, Y. 1995. Modeling stratified diffusion in biological invasions. *American Naturalist*, 146, 229-251.
- SHIGESADA, N., KAWASAKI, K. 1997. *Biological Invasions: Theory and Practice*, Oxford, Oxford University Press.
- SHILTON, C. M., BROWN, G. P., BENEDICT, S. & SHINE, R. 2008. Spinal arthropathy associated with *Ochrobactrum anthropi* in free-ranging cane toads (*Chaunus Bufo marinus*) in Australia. *Veterinary Pathology*, 45, 85-94.
- SHINE, R. 2010. The ecological impact of invasive cane toads (*Bufo marinus*) in Australia. *The Quarterly review of biology*, 85, 253-291.
- SHINE, R., BROWN, G. P. & PHILLIPS, B. L. 2011a. An evolutionary process that assembles phenotypes through space rather than through time. *Proceedings of the National Academy of Sciences of the United States of America*, 108, 5708-5711.
- SHINE, R., BROWN, G. P. & PHILLIPS, B. L. 2011b. Reply to Lee: Spatial sorting, assortative mating, and natural selection. *Proceedings of the National Academy of Sciences of the United States of America*, 108, E348-E348.
- SILVA, T., REINO, L. M. & BORRALHO, R. 2002. A model for range expansion of an introduced species: the common waxbill *Estrilda astrild* in Portugal. *Diversity and Distributions*, 8, 319-326.
- SIMMONS, A. D. & THOMAS, C. D. 2004. Changes in dispersal during species' range expansions. *The American Naturalist*, 164, 378-395.
- SIMOES, M., PEREIRA, M. O. & VIEIRA, M. J. 2005. Action of a cationic surfactant on the activity and removal of bacterial biofilms formed under different flow regimes. *Water Research*, 39, 478-486.

- SKELLAM, J. G. 1951. Random dispersal in theoretical populations. *Biometrika*, 38, 196-218.
- SKLYAR, O., PAU, G., SMITH, M. & HUBER, W. 2014. EBImage: Image processing toolbox for R. . R package version 3.12.0. ed.
- SMITH, S. M. 1996. Biological control with Trichogramma: advances, successes, and potential of their use. *Annual review of entomology*, 41, 375-406.
- SOBER, E. & WILSON, D. S. 1998. *Unto Others The Evolution and Psychology of Unselfish Behavior*, Cambridge, Harvard University Press.
- SOULÉ, M. E. & ORIAN, G. 2001. *Conservation biology: research priorities for the next decade*, Island Press.
- SPELLBERG, B., GUIDOS, R., GILBERT, D., BRADLEY, J., BOUCHER, H. W., SCHELD, W. M., BARTLETT, J. G., EDWARDS, J., JR. & INFECT DIS SOC, A. 2008. The epidemic of antibiotic-resistant infections: A call to action for the medical community from the Infectious Diseases Society of America. *Clinical Infectious Diseases*, 46, 155-164.
- SPIERS, A. J. 2007. Wrinkly-Spreader Fitness in the Two-Dimensional Agar Plate Microcosm: Maladaptation, Compensation and Ecological Success. *PLoS One*, 2.
- SPIERS, A. J., BOHANNON, J., GEHRIG, S. M. & RAINEY, P. B. 2003. Biofilm formation at the air-liquid interface by the *Pseudomonas fluorescens* SBW25 wrinkly spreader requires an acetylated form of cellulose. *Molecular Microbiology*, 50, 15-27.
- SPIERS, A. J. & RAINEY, P. B. 2005. The *Pseudomonas fluorescens* SBW25 wrinkly spreader biofilm requires attachment factor, cellulose fibre and LIPS interactions to maintain strength and integrity. *Microbiology*, 151, 2829-2839.
- STARRFELT, J. & KOKKO, H. 2010. Parent-Offspring Conflict and the Evolution of Dispersal Distance. *The American Naturalist*, 175, 38-49.
- STEIN, A., GERSTNER, K. & KREFT, H. 2014. Environmental heterogeneity as a universal driver of species richness across taxa, biomes and spatial scales. *Ecology Letters*, 17, 866-880.
- STOTT, I., FRANCO, M., CARSLAKE, D., TOWNLEY, S. & HODGSON, D. 2010. Boom or bust? A comparative analysis of transient population dynamics in plants. *Journal of Ecology*, 98, 302-311.
- SUAREZ, A. V., HOLWAY, D. A. & CASE, T. J. 2001. Patterns of spread in biological invasions dominated by long-distance jump dispersal: Insights from Argentine ants. *Proceedings of the National Academy of Sciences of the United States of America*, 98, 1095-1100.
- TAYLOR, C. M. & HASTINGS, A. 2005. Allee effects in biological invasions. *Ecology Letters*, 8, 895-908.
- TAYLOR, T. B. & BUCKLING, A. 2010. Competition and Dispersal in *Pseudomonas aeruginosa*. *American Naturalist*, 176, 83-89.
- TAYLOR, T. B. & BUCKLING, A. 2011. Selection experiments reveal trade-offs between swimming and twitching motilities in *Pseudomonas aeruginosa*. *Evolution*, 65, 3060-3069.
- TAYLOR, T. B., RODRIGUES, A. M. M., GARDNER, A. & BUCKLING, A. 2013. The social evolution of dispersal with public goods cooperation. *Journal of Evolutionary Biology*, 26, 2644-2653.
- THE MATHWORKS, I. 2014. MATLAB. Release 2014a ed. Natick, Massachusetts, United States.

- THOMAS, C. S. 1983. The relationships between breeding experience, egg volume and reproductive success of the kittiwake *Rissa tridactyla*. *Ibis*, 125, 567-574.
- TILMAN, D. 1994. Competition and biodiversity in spatially structured habitats. *Ecology*, 75, 2-16.
- TILMAN, D. 2004. Niche tradeoffs, neutrality, and community structure: a stochastic theory of resource competition, invasion, and community assembly. *Proceedings of the National Academy of Sciences of the United States of America*, 101, 10854-10861.
- TILMAN, D., FARGIONE, J., WOLFF, B., D'ANTONIO, C., DOBSON, A., HOWARTH, R., SCHINDLER, D., SCHLESINGER, W. H., SIMBERLOFF, D. & SWACKHAMER, D. 2001. Forecasting agriculturally driven global environmental change. *Science*, 292, 281-284.
- TILMAN, D. & LEHMAN, C. 2001. Human-caused environmental change: impacts on plant diversity and evolution. *Proceedings of the National Academy of Sciences*, 98, 5433-5440.
- TINGLEY, R., PHILLIPS, B. L., LETNIC, M., BROWN, G. P., SHINE, R. & BAIRD, S. J. E. 2013. Identifying optimal barriers to halt the invasion of cane toads *Rhinella marina* in arid Australia. *Journal of Applied Ecology*, 50, 129-137.
- TISUE, S. & WILENSKY, U. NetLogo: Design and implementation of a multi-agent modeling environment. *Proceedings of agent*, 2004. 7-9.
- TOBIN, P. C., SHAROV, A. A., LIEBHOLD, A. A., LEONARD, D. S., ROBERTS, E. A. & LEARN, M. R. 2004. Management of the gypsy moth through a decision algorithm under the STS project. *American Entomologist*, 50, 200-209.
- TORSVIK, V. & OVREAS, L. 2002. Microbial diversity and function in soil: from genes to ecosystems. *Current Opinion in Microbiology*, 5, 240-245.
- TOUHAMI, A., JERICHO, M. H., BOYD, J. M. & BEVERIDGE, T. J. 2006. Nanoscale characterization and determination of adhesion forces of *Pseudomonas aeruginosa* pili by using atomic force microscopy. *Journal of Bacteriology*, 188, 370-377.
- TRAVIS, J. M. & DYTHAM, C. 2002. Dispersal evolution during invasions. *Evolutionary Ecology Research*, 4, 1119-1129.
- TRAVIS, J. M., HARRIS, C. M., PARK, K. J. & BULLOCK, J. M. 2011. Improving prediction and management of range expansions by combining analytical and individual-based modelling approaches. *Methods in Ecology and Evolution*, 2, 477-488.
- TRAVIS, J. M., MUSTIN, K., BARTOŃ, K. A., BENTON, T. G., CLOBERT, J., DELGADO, M. M., DYTHAM, C., HOVESTADT, T., PALMER, S. C. & VAN DYCK, H. 2012. Modelling dispersal: an eco-evolutionary framework incorporating emigration, movement, settlement behaviour and the multiple costs involved. *Methods in Ecology and Evolution*, 3, 628-641.
- TRAVIS, J. M. J., MUSTIN, K., BENTON, T. G. & DYTHAM, C. 2009. Accelerating invasion rates result from the evolution of density-dependent dispersal. *Journal of Theoretical Biology*, 259, 151-158.
- TREMBLAY, J. & DEZIEL, E. 2008. Improving the reproducibility of *Pseudomonas aeruginosa* swarming motility assays. *Journal of Basic Microbiology*, 48, 509-515.

- TREMBLAY, J., RICHARDSON, A.-P., LEPINE, F. & DEZIEL, E. 2007. Self-produced extracellular stimuli modulate the *Pseudomonas aeruginosa* swarming motility behaviour. *Environmental Microbiology*, 9, 2622-2630.
- TSIMRING, L., LEVINE, H., ARANSON, I., BEN-JACOB, E., COHEN, I., SHOCHET, O. & REYNOLDS, W. N. 1995. Aggregation patterns in stressed bacteria. *Physical Review Letters*, 75, 1859.
- TURING, A. M. 1952. The Chemical Basis of Morphogenesis 237, 37-72.
- URBAN, M. C., PHILLIPS, B. L., SKELLY, D. K. & SHINE, R. 2007. The cane toad's (*Chaunus Bufo marinus*) increasing ability to invade Australia is revealed by a dynamically updated range model. *Proceedings of the Royal Society B-Biological Sciences*, 274, 1413-1419.
- URBAN, M. C., PHILLIPS, B. L., SKELLY, D. K. & SHINE, R. 2008. A toad more traveled: The heterogeneous invasion dynamics of cane toads in Australia. *American Naturalist*, 171, E134-E148.
- VAN DITMARSCH, D., BOYLE, K. E., SAKHTAH, H., OYLER, J. E., NADELL, C. D., DÉZIEL, É., DIETRICH, L. E. & XAVIER, J. B. 2013. Convergent evolution of hyperswarming leads to impaired biofilm formation in pathogenic bacteria. *Cell Reports*, 4, 697-708.
- VAN DYKEN, J. D., MÜLLER, M. J., MACK, K. M. & DESAI, M. M. 2013. Spatial population expansion promotes the evolution of cooperation in an experimental Prisoner's Dilemma. *Current Biology*, 23, 919-923.
- VEIT, R. R. & LEWIS, M. A. 1996. Dispersal, population growth, and the Allee effect: Dynamics of the house finch invasion of eastern North America. *American Naturalist*, 148, 255-274.
- VENTURI, V., BERTANI, I., KERENYI, A., NETOTEA, S. & PONGOR, S. 2010. Co-Swarming and Local Collapse: Quorum Sensing Conveys Resilience to Bacterial Communities by Localizing Cheater Mutants in *Pseudomonas aeruginosa*. *PLoS One*, 5.
- VERHULST, S., PERRINS, C. M. & RIDDINGTON, R. 1997. Natal dispersal of Great Tits in a patchy environment. *Ecology*, 78, 864-872.
- VERSTEIRT, V., DE CLERCQ, E., FONSECA, D., PECOR, J., SCHAFFNER, F., COOSEMANS, M. & VAN BORTEL, W. 2012. Bionomics of the established exotic mosquito species *Aedes koreicus* in Belgium, Europe. *Journal of Medical Entomology*, 49, 1226-1232.
- VINATIER, F., LESCOURET, F., DUYCK, P.-F., MARTIN, O., SENOUSSE, R. & TIXIER, P. 2011. Should I stay or should I go? A habitat-dependent dispersal kernel improves prediction of movement. *PLoS One*, 6, e21115.
- VOLPERT, V. & PETROVSKII, S. 2009. Reaction–diffusion waves in biology. *Physics of Life Reviews*, 6, 267-310.
- WADE, M. J. 1985. Soft selection, hard selection, kin selection, and group selection. *American Naturalist*, 61-73.
- WAJNBERG, E., COQUILLARD, P., VET, L. E. & HOFFMEISTER, T. 2012. Optimal resource allocation to survival and reproduction in parasitic wasps foraging in fragmented habitats. *PLoS One*, 7, e38227.
- WALTHER, G.-R., ROQUES, A., HULME, P. E., SYKES, M. T., PYSEK, P., KUEHN, I., ZOBEL, M., BACHER, S., BOTTA-DUKAT, Z., BUGMANN, H., CZUCZ, B., DAUBER, J., HICKLER, T., JAROSIK, V., KENIS, M., KLOTZ, S., MINCHIN, D., MOORA, M., NENTWIG, W., OTT, J., PANOV, V. E., REINEKING, B., ROBINET, C., SEMENCHENKO, V., SOLARZ, W., THUILLER, W., VILA, M., VOHLAND, K. & SETTELE, J. 2009. Alien

- species in a warmer world: risks and opportunities. *Trends in Ecology & Evolution*, 24, 686-693.
- WANG, P., LEI, J.-P., LI, M.-H. & YU, F.-H. 2012. Spatial heterogeneity in light supply affects intraspecific competition of a stoloniferous clonal plant. *PLoS One*, 7, e39105.
- WATNICK, P. & KOLTER, R. 2000. Biofilm, city of microbes. *Journal of Bacteriology*, 182, 2675-2679.
- WEBB, J. S., THOMPSON, L. S., JAMES, S., CHARLTON, T., TOLKER-NIELSEN, T., KOCH, B., GIVSKOV, M. & KJELLEBERG, S. 2003. Cell death in *Pseudomonas aeruginosa* biofilm development. *Journal of Bacteriology*, 185, 4585-4592.
- WEISSTEIN, E. W. 2010. *CRC concise encyclopedia of mathematics*, CRC press.
- WENNY, D. G. 2001. Advantages of seed dispersal: A re-evaluation of directed dispersal. *Evolutionary Ecology Research*, 3, 51-74.
- WENSING, A., BRAUN, S. D., BUETTNER, P., EXPERT, D., VOELKSCH, B., ULLRICH, M. S. & WEINGART, H. 2010. Impact of Siderophore Production by *Pseudomonas* on Epiphytic Fitness and Biocontrol Activity against *Pseudomonas syringae*. *Applied and Environmental Microbiology*, 76, 2704-2711.
- WEST, S. A. & BUCKLING, A. 2003. Cooperation, virulence and siderophore production in bacterial parasites. *Proceedings of the Royal Society B-Biological Sciences*, 270, 37-44.
- WEST, S. A., DIGGLE, S. P., BUCKLING, A., GARDNER, A. & GRIFFINS, A. S. 2007a. The social lives of microbes. *Annual Review of Ecology Evolution and Systematics*.
- WEST, S. A., GARDNER, A. & GRIFFIN, A. S. 2006a. Altruism. *Current Biology*, 16, R482-R483.
- WEST, S. A., GRIFFIN, A. S. & GARDNER, A. 2007b. Social semantics: altruism, cooperation, mutualism, strong reciprocity and group selection. *Journal of Evolutionary Biology*, 20, 415-432.
- WEST, S. A., GRIFFIN, A. S. & GARDNER, A. 2008. Social semantics: how useful has group selection been? *Journal of Evolutionary Biology*, 21, 374-385.
- WEST, S. A., GRIFFIN, A. S., GARDNER, A. & DIGGLE, S. P. 2006b. Social evolution theory for microorganisms. *Nature Reviews Microbiology*, 4, 597-607.
- WEST, S. A., PEN, I. & GRIFFIN, A. S. 2002. Conflict and cooperation - Cooperation and competition between relatives. *Science*, 296, 72-75.
- WHITE, T. A., LUNDY, M. G., MONTGOMERY, W. I., MONTGOMERY, S., PERKINS, S. E., LAWTON, C., MEEHAN, J. M., HAYDEN, T. J., HECKEL, G., REID, N. & SEARLE, J. B. 2012. Range expansion in an invasive small mammal: influence of life-history and habitat quality. *Biological Invasions*, 14, 2203-2215.
- WHITLOCK, M., DAVIS, B. & YEAMAN, S. 2007. The costs and benefits of resource sharing: reciprocity requires resource heterogeneity. *Journal of evolutionary biology*, 20, 1772-1782.
- WILLIAMSON, M. 1996. *Biological Invasions*, London, UK, Chapman and Hall.
- WILLIAMSON, M. H. & FITTER, A. 1996. The characters of successful invaders. *Biological Conservation*, 78, 163-170.
- WILSON, D. S. & SOBER, E. 1994. Reintroducing group selection to the human behavioral sciences. *Behavioral and Brain Sciences*, 17, 585-608.

- WILSON, R. J., DAVIES, Z. G. & THOMAS, C. D. 2010. Linking habitat use to range expansion rates in fragmented landscapes: a metapopulation approach. *Ecography*, 33, 73-82.
- WITTENBERG, R. A. M. J. W. C. 2001. *Invasive alien species. How to address one of the greatest threats to biodiversity: A toolkit of best prevention and management practices.*, Wallingford, Oxon, UK., , CAB International.
- WOLGEMUTH, C. W. & OSTER, G. 2004. The junctional pore complex and the propulsion of bacterial cells. *Journal of Molecular Microbiology and Biotechnology*, 7, 72-77.
- WOODWARD, D., TYSON, R., MYERSCOUGH, M., MURRAY, J., BUDRENE, E. & BERG, H. 1995. Spatio-temporal patterns generated by *Salmonella typhimurium*. *Biophysical journal*, 68, 2181-2189.
- WORLD TRADE ORGANISATION 6 December 1951. International plant protection convention. *In: ORGANISATION, W. T. (ed.)*. Rome.
- XAVIER, J. B. & FOSTER, K. R. 2007. Cooperation and conflict in microbial biofilms. *Proceedings of the National Academy of Sciences of the United States of America*, 104, 876-881.
- XAVIER, J. B., MARTINEZ-GARCIA, E. & FOSTER, K. R. 2009. Social evolution of spatial patterns in bacterial biofilms: when conflict drives disorder. *The American Naturalist*, 174, 1-12.
- XAVIER, J. B., PICIOREANU, C. & VAN LOOSDRECHT, M. 2005. A framework for multidimensional modelling of activity and structure of multispecies biofilms. *Environmental Microbiology*, 7, 1085-1103.
- XUE, C., BUDRENE, E. O. & OTHMER, H. G. 2011. Radial and spiral stream formation in *Proteus mirabilis* colonies.
- YAMAMURA, K. 2002. Dispersal distance of heterogeneous populations. *Population Ecology*, 44, 93-101.
- YEUNG, A. T., TORFS, E. C., JAMSHIDI, F., BAINS, M., WIEGAND, I., HANCOCK, R. E. & OVERHAGE, J. 2009. Swarming of *Pseudomonas aeruginosa* is controlled by a broad spectrum of transcriptional regulators, including MetR. *Journal of Bacteriology*, 191, 5592-5602.
- YOSHIDA, T., JONES, L. E., ELLNER, S. P., FUSSMANN, G. F. & HAIRSTON, N. G. 2003. Rapid evolution drives ecological dynamics in a predator-prey system. *Nature*, 424, 303-306.